Retromer deficiency in amyotrophic lateral sclerosis

Eduardo J Pérez-Torres

Submitted in partial fulfillment of the
requirements for the degree of
Doctor of Philosophy
under the Executive Committee
of the Graduate School of Arts and Sciences

COLUMBIA UNIVERSITY

2020

ABSTRACT

RETROMER DEFICIENCY IN AMYOTROPHIC LATERAL SCLEROSIS

Eduardo J Pérez-Torres

The retromer is a protein complex whose function is to mediate the recycling of proteins from the endosome to either the plasma membrane or the trans-Golgi network. A deficit in retromer function has been associated with multiple neurodegenerative disorders, including Alzheimer's disease (AD) and Parkinson's disease (PD). In both AD and PD, deficiencies have been found in retromer expression both in patient tissues and in animal models of disease. Furthermore, mutations in the retromer and in retromer-associated genes have been strongly linked with both diseases. Despite ample evidence of the link between the retromer and neurodegeneration, little is known about the retromer in the context of amyotrophic lateral sclerosis (ALS), another common neurodegenerative disorder. ALS is an adult-onset neurodegenerative disorder of the upper and lower motor neurons (MNs) characterized by muscle wasting and weakness leading to death within 3-5 years after diagnosis. To date, the most commonly used model of ALS is a transgenic (Tg) mouse that overexpresses an ALS-causing G93A mutation in the human superoxide dismutase 1 (SOD1) gene. In this study, I first establish a link between the retromer and ALS by showing that cells from ALS patients as well as tissues and cells from $SOD1^{G93A}$-Tg mice express lower protein levels of the retromer core components—vacuolar protein sorting 35 (Vps35), Vps26a, and Vps29. I then establish that deficiencies in retromer core proteins have functional consequences in an *in vitro* model of ALS. Having found significant deficiencies in the retromer in $SOD1^{G93A}$-Tg mice, I then followed the model of studies performed in mouse models of other neurodegenerative disorders by investigating whether repletion of retromer levels, either virally or pharmacologically, in $SOD1^{G93A}$-Tg mice confers a therapeutic benefit. Surprisingly, I find that rather than

ameliorating disease, repletion of retromer levels in SOD1^{G93A}-Tg mice exacerbates it, resulting in a faster decline in motor performance, earlier mortality, and a decrease in MNs in the spinal cord. Finally, since retromer repletion causes deleterious effects on SOD1^{G93A}-Tg mouse disease progression, I study the effect of a single allele deletion of Vps35 in SOD1^{G93A}-Tg mice and find that this depletion of the retromer results in amelioration of disease, including delayed onset of symptomatology, slower decline of motor deficits, delayed mortality, and an increase in MNs in the spinal cord. Altogether, the findings reported herein, support the notion that a mild defect in retromer develops over the course of the disease, which, rather than being deleterious may be therapeutic in mutant SOD1-induced MN degeneration. Perhaps this unexpected outcome may be explained by the fact that the observed mild nature of the defect is not sufficient to kill MNs but enough to alter the trafficking of specific cargos such as AMPA receptors, allowing MNs to better withstand the neurodegenerative process.

TABLE OF CONTENTS

LIST OF FIGURES AND TABLES

Chapter 1

Chapter 2

Chapter 3

Chapter 4

Chapter 5

Chapter 7

ACKNOWLEDGEMENTS

During my graduate studies, I had the privilege of working with a number of talented and passionate scientists without whom this work would not be possible.

First, I would like to thank Serge Przedborski for his willingness and eagerness to mentor me throughout my education as a scientist. His unwavering support and enthusiasm for both my work and myself were critical to my success in this program. I thank him for his uncanny ability to have made every unexpected twist and turn of my graduate work feel like yet another opportunity for intellectual advancement. Furthermore, I would like to specifically express my admiration for his skill as a critical mind and his deep love for statistics, a love that I share and has been a wonderful source of connection between us.

I would also like to express my thanks to the leaders of the ALS team during my time in the lab, Diane Re and Francesco Lotti. Diane's enthusiasm, like her laugh, was infectious and provided encouragement as I started my work in the lab. Francesco provided me with constant guidance, helped me sort through many of the experiments that ultimately led to my thesis work, and taught me how to perform ICV injections for my work in Chapter 4.

Next, I would like to deeply thank the members of the Przedborski lab during my time there, who both directly and indirectly, and both through science and through friendship, made this work possible. I thank the Przedborski lab manager during my entire time there, Norma Romero, for her assistance maintaining mouse colonies as well as all the last-minute product orders and laboratory upkeep that she undertook with a constant smile. I thank James Caceido for his assistance with the generation and maintenance of astrocyte cultures used in this work. I thank Vartika Mishra for her help with learning multiple techniques used in this project, including viral

work and human astrocyte culture, as well as for being an excellent collaborator to work with. I thank Kristin Politi for being my trailblazer and teaching me what it was to be a graduate student in this lab. I thank Mariàngels “Nini” de Planell-Saguer for her help in the differentiation of ES-derived motor neurons. I thank Paola Rinchetti and Peter Barbuti for their help in generating iPSC-derived motor neurons. I thank Cristina Guardia-Laguarta for her help teaching me confocal microscopy. Every member of the lab was a joy to work with and helped me during my studies, so I would also like to thank Vernice Jackson-Lewis, Georgia Ntermentzaki, Virginia LeVerche, Sudarshan Phani, Takaaki Kuwajima, Irene Faravelli, Irina Utkina-Sosunova, Giulietta Riboldi, Yuhui Liu, Radhika Pradhan, and my BRAINYAC program summer student Savannah Harcum. I also thank Jennifer Fernandez, Jessenia Guzman, and Mary Thomas for their administrative support.

I would also like to thank Scott Small and the members of his lab for their collaborative contributions to these studies, including Sabrina Alves Simoes Spassov and Milankumar Kothiya for running the ELISA in Chapter 3, Yasir Qureshi for providing plasmids used in the viruses in Chapter 3 and for his advice on reagents and antibodies to use for this work, and Diego Berman for providing the Vps35 conditional knockout mice used in Chapter 5.

I would also like to thank Hemali Phatnani and the members of her lab for their collaborative contributions to these studies, including the RNAseq analysis of human astrocytes shown in Chapter 2.

I also appreciate the Columbia Stem Cell Core, particularly Barbara Corneo, and the lab of Michael Boland, particularly Andrew Ressler, for creating, validating, and providing the iPSCs used in this work.

I would also like to take this space to thank the de-identified patients who agreed to donate their tissues and cells for use in this work.

I also thank the members of the labs of the Motor Neuron and Merritt Centers who provided a wonderful work and collaborative environment, including the Shneider, Pellizzoni, Schon, Zhang, Wichterle, Monani, Harms, Area, and Mentis labs. In particular, I would like to thank Benjamin Hoover, Rishi Agrawal, Nicole Vo, and Marina Triplett.

I would also like to thank the program coordinator of the Neurobiology and Behavior program, Alla Kerzhner, and the directors, Darcy Kelley, Wesley Grueber, Kenneth Mille, and Ai Yamamoto, for facilitating my journey through the program.

I also thank the leadership of the MD/PhD program, director Steven Reiner and associate directors Michael Shelanski, Ronald Liem, Ira Tabas, and particularly Patrice Spitalnik for their constant support and for making the journey through medical and graduate school possible. I would also like to thank the program coordinators Kate Matthews, Becky Spurr, and Jeffrey Brandt for their amazing abilities in coordinating the program.

I would also like to thank the previous mentors I have worked with during both my undergraduate and graduate studies who contributed to my growth as a scientist: Ole Isacson at Harvard University, and David Sulzer and Karen Duff at Columbia University.

Importantly, I owe my immense gratitude to the members serving on my thesis committee for their thoughtfulness and contributions to this work: Neil Shneider, Scott Small, and Clarissa Waites. I also thank Carol Troy for her willingness to serve as a fourth examiner in my defense.

My graduate work is supported by an F31 Individual National Research Service Award for Diverse PhD Students (NS101966) from the NIH National Institute of Neurological Disorders and Stroke (NINDS) as well as an NIH T32 institutional training grant (GM007367).

Finally, I would like to thank my friends and family, who supported me throughout my studies. I especially thank the members of the Bard Hall Players, who provided camaraderie and encouragement throughout my education.

CHAPTER 1

GENERAL INTRODUCTION

1.1 Endosomal trafficking

If the mitochondrion is the powerhouse of the cell, and the Golgi is the post office, then the endosome can best be characterized as the warehouse of the cell. While some enzymatic reactions do occur in the endosome, the majority of the materials that are brought into the endosome are ultimately meant for either another compartment of the cell or degradation by the lysosome. As such, the trafficking to and from the endosome is paramount to its function. What is a warehouse if nothing is ever added to or taken from it?

The endosomal compartment can be broadly subdivided into three types of endosome: the early endosome (EE), the late endosome (LE), and the recycling endosome (RE). While it is perhaps sometimes useful to speak of these as three discrete classes of endosome, it is important to keep in mind that evidence suggests that these are not physically easily distinguished and that the continuous flow of materials and membranes among them suggests more of a continuum. That said, EEs, LEs, and REs are often distinguished via specific marker proteins and lipids found on their surfaces.

Broadly, there are three major axes whereby endosomal trafficking takes place: endosomal maturation--that is, the process whereby an EE becomes an LE--, exchange with the trans-Golgi network (TGN), and exchange with the plasma membrane (PM). Here, I will discuss how proteins are processed and trafficked along these axes.

1.1.1 Endocytosis

Endocytosis is perhaps one of the most versatile forms of cellular trafficking, as it shuttles, not only the PM's own membrane and membrane-bound proteins, but also extracellular materials into the intracellular space. Thus, it can have an equally wide range of purposes in various cell types including regulation of synaptic and developmental signaling, hormone signaling, and delivery of nutrients into the cell. With only a few exceptions, the vesicles formed via endocytosis are ultimately delivered to the endosome. There are many forms of endocytosis, and how such different forms are subdivided, defined, and elucidated is hotly debated in the field. It is generally understood, however, that all endocytosis can be broadly divided into two forms: clathrin-dependent and clathrin-independent. Of these, clathrin-dependent endocytosis (CDE) is the most deeply studied and the most widely understood.

CDE can be incited by numerous processes including simply random chance (Ehrlich et al. 2004), but whatever the inciting incident, CDE begins with the recruitment of the proteins that make up the CDE pioneer module to the PM. First, F-BAR domain only protein 1 (FCHO1), FCHO2, and the adaptor protein 2 complex (AP2), bind to the PM (Henne et al. 2010; Cocucci et al. 2012; Taylor, Perrais, and Merrifield 2011; Umasankar et al. 2012). These adaptor proteins are recruited to the PM via their recognition of the specific phosphoinositide (PIP) found in the lipid bilayer of the plasma membrane, $PI(4,5)P_2$ (Antonescu et al. 2011; Zoncu et al. 2007; Di Paolo and De Camilli 2006). Once at the PM, the adaptor proteins recruit the scaffold proteins, epidermal growth factor receptor substrate 15 (EPS15), EPS15-like 1 (EPS15L1), and intersectins 1 and 2, which cluster the adaptor proteins, forming the pioneer module (Stimpson et al. 2009; Umasankar et al. 2012; Ma et al. 2016; Taylor, Perrais, and Merrifield 2011; Cocucci et al. 2012; Henne et al. 2010; Brach et al. 2014). Finally, clathrin and other associated coat proteins are recruited to the

pioneer module to form a clathrin-coated pit (CCP). It has been shown that one of the mechanisms that induces this recruitment involves the binding of $PI(4,5)P_2$ and cargo proteins to AP2, which causes a conformational change in AP2 that exposes its clathrin-binding site (Traub 2009; Kadlecova et al. 2017; Kelly et al. 2014; Jackson et al. 2010).

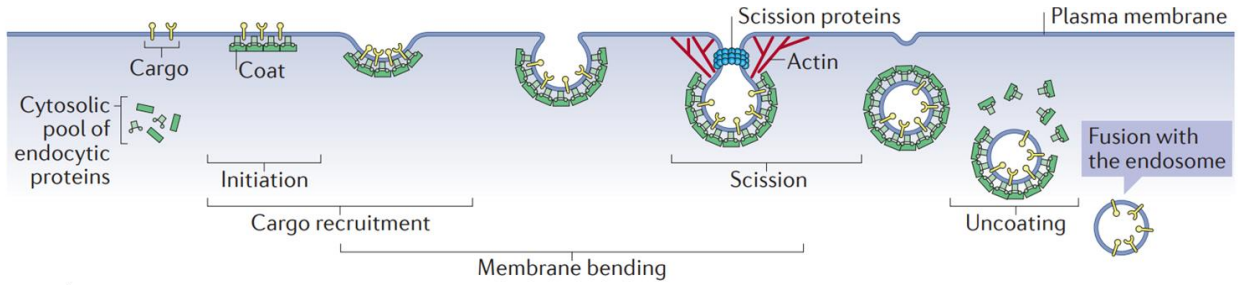

Figure 1.1 Stages of Clathrin-Dependent Endocytosis

Reproduced from (Kaksonen and Roux 2018)

At this point, studies have pointed to a possible cargo checkpoint in which, if a certain amount of cargo is not present in a given CCP, the vesicle-forming process is either aborted or delayed, assuring that any endocytosed vesicles contain a sufficient amount of cargo to be transported (Mettlen et al. 2010; Mettlen et al. 2009; Carroll et al. 2012; Ehrlich et al. 2004; Loerke et al. 2009; Henry et al. 2012). The mechanism for this checkpoint is not well understood, but is hypothesized to involve the interaction between dynamin and the CCP coat (Loerke et al. 2009). Upon further maturation of the CCP, the molecular conformation of the clathrin coat causes the membrane to bend, and the vesicle undergoes dynamin-mediated scission from the PM (Kirchhausen and Harrison 1981; Pearse 1975; Heuser 1980).

On the way to the endosome, the vesicle loses its clathrin coat. First, the $PI(4,5)P_2$ in the vesicle is dephosphorylated to PI4P by an inositol 5-phosphatase (McPherson et al. 1996; Cremona et al. 1999; Varnai et al. 2006; Zoncu et al. 2007; Erdmann et al. 2007; Nandez et al. 2014). An

inositol 3-kinase then converts PI4P to $PI(3,4)P_2$, which can be dephosphorylated further to PI3P (the PIP found in the endosome) (Posor et al. 2013; Zoncu et al. 2009). Auxilin can bind specifically to $PI(3,4)P_2$ or PI3P, and once it does, it recruits heat shock cognate 71 kDa protein (HSC70), which consumes ATP to actively cause a steric hindrance that disrupts the clathrin coat (Massol et al. 2006; Schlossman et al. 1984; Braell et al. 1984; Ungewickell 1985; Barouch et al. 1994). Once uncoated, and with an endosomal-identified lipid bilayer, the vesicle is then free to fuse with the endosome via a Rab5-mediated mechanism. Thus, cargo from the extracellular space and from the PM enter the luminal space and the lipid bilayer of the endosome, respectively.

1.1.2 Golgi-to-Endosome Transport

Once a protein has been synthesized in the rough endoplasmic reticulum and processed through the Golgi apparatus to the TGN, it may be localized to the endosomal compartment of the cell. Perhaps the best-characterized way this can happen is through a mannose-6-phosphate (M6P) modification which is then recognized by one of two M6P receptors (MPRs). These can be either cation dependent (CD-MPR) or cation independent (CI-MPR), referring to whether or not the M6P residue needs to be bound to a divalent cation in order to be recognized by the MPR. Once the MPR is bound to its cargo, it is, in turn, recognized by the adaptor protein 1 complex (AP1) and a family of proteins known as Golgi-localized, gamma-ear-containing, ADP-ribosylation-factor binding proteins (GGA) (Doray et al. 2002). These proteins recruit the MPR-cargo complex to endosome-fated clathrin-coated vesicles. These vesicles then undergo a process similar to those involved in CDE until they arrive at the endosome.

Once the cargo vesicle is delivered to the endosome, the relatively low pH of the endosome causes the MPR to release its cargo. When this cargo is a lysosomal enzyme, the enzyme remains inactive in the endosome until it is activated by the even lower pH of the lysosome.

It is important to note that other cargo-recognizing proteins act in a similar way to MPRs, but do not require a M6P modification on the cargo protein. Indeed, in patients with I-cell disease, in which a deficiency in UDP-N-acetylglucoseamine-1-phosphotransferase prevents proteins from acquiring the M6P modification, cells still have some measure of TGN-to-endosome transport, with some cells not being affected at all (Kollmann et al. 2010). The VPS10 family of proteins is another group of cargo-recognizing proteins in the TGN-to-endosomal pathway, and includes sortilin and other proteins named after it: sortilin related VPS10 domain containing receptors 1, 2, and 3 (SORCS1, SORCS2, SORCS3), and sortilin related receptor 1 (SORL1) (Burda et al. 2002; Willnow, Petersen, and Nykjaer 2008; Marcusson et al. 1994). Indeed, sortilin and SORL1 are known to have cytoplasmic tails closely resembling that of CI-MPR, and are sorted into the same vesicles as CI-MPR by AP1 and the GGA (Canuel et al. 2008; Coutinho, Prata, and Alves 2012; Nielsen et al. 2001; Mari et al. 2008).

1.1.3 Endosomal Maturation

A protein that arrives to the EE and remains within the endosomal compartment without being recycled elsewhere will ultimately either be degraded or take part in degradation. This will occur when the endosome fuses with a lysosome, creating the endolysosome where the intraluminal pH is significantly lowered, and enzymes are activated such that degradation can take place. For this to happen, the EE must first acquire the proteins to be degraded and mature into the LE.

1.1.3.1 Multivesicular Bodies

Besides being transported to the endosome from the PM or the TGN, proteins can enter the endosome directly from the cytosol through the formation of intraluminal vesicles (ILV). This process results in a multivesicular body (MVB), a round matured endosome which is a highly distinct organelle in that it contains vesicles within its lumen derived from the more tubular system of the early endosome. The molecular process of MVB formation is mediated via a series of complexes known as the endosomal sorting complex required for transport (ESCRT) system. The ESCRT system involves 4 complexes, ESCRT-0, -I, -II, and -III, and the process by which the interaction of these complexes with protein cargoes results in the formation of ILVs has only recently been better understood and is currently heavily studied.

A protein, either in the cytosol or bound to a membrane, is targeted to the MVB via the addition of ubiquitin moieties, which are recognized by several proteins in the early acting ESCRT complexes (Raiborg and Stenmark 2009). The first of these, ESCRT-0, is made up of two proteins--Hrs and STAM--, each of which has two low-affinity ubiquitin-binding motifs (Hofmann and Falquet 2001; McCullough et al. 2006; Mayers et al. 2011; Mizuno et al. 2003; Ren and Hurley 2010). Hrs also has a PI3P-binding motif, thus tethering ubiquitinated proteins to the endosomal membrane (Gaullier et al. 1998; Burd and Emr 1998; Raiborg et al. 2001). Finally, ESCRT-0 can multimerize, both by binding directly to other ESCRT-0 complexes and by binding to clathrin, which can form a flat lattice (Mayers et al. 2011; Takahashi et al. 2015; Sachse et al. 2002; Raiborg et al. 2001; Raiborg et al. 2002). All this together makes it so that ESCRT-0 creates an area with a high concentration of ubiquitin-binding motifs that recruit ubiquitin-tagged proteins to one area of the endosomal membrane.

In contrast to that of ESCRT-0, the mechanisms of ESCRT-I and ESCRT-II are far less understood. It is known that ESCRT-0 can bind ESCRT-I, which, in turn, can bind ESCRT-II, which itself recruits ESCRT-III (Bache et al. 2003; Katzmann et al. 2003; Lu et al. 2003; Kostelansky et al. 2007; Teo et al. 2004; Teo et al. 2006). Furthermore, proteins in both ESCRT-I and ESCRT-II contain ubiquitin binding domains that display a much higher binding affinity for ubiquitin than for ESCRT-0, but each ESCRT-I or ESCRT-II complex only contains one ubiquitin binding domain (Garrus et al. 2001; Agromayor et al. 2012; Slagsvold et al. 2005; Hirano et al. 2006; Alam et al. 2006). Thus, it is thought that the purpose of ESCRT-0 is to create a local area of relatively high concentration of ubiquitinated proteins which are then passed more discriminatingly to ESCRT-I and ESCRT-II. However, whether these complexes serve some sort of discriminatory function or how they would do that is an area of active investigation.

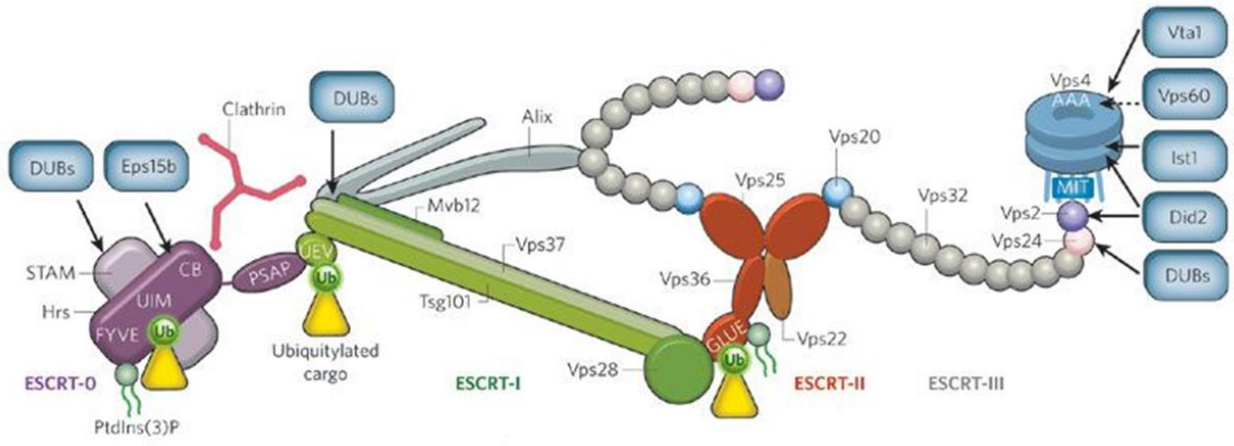

Figure 1.2 Interactions Within the ESCRT Machinery

Reproduced from (Raiborg and Stenmark 2009)

Once ESCRT-0, ESCRT-I, and ESCRT-II have been sequentially recruited, ESCRT-II recruits ESCRT-III to the endosomal membrane. The ESCRT-III complex is made up of at least

four essential subunits in yeast: Vps2, Vps20, Vps24, and Vps32, termed charged multivesicular body proteins (CHMP) 2, 6, 3, and 4 respectively in mammals (Teis, Saksena, and Emr 2008). ESCRT-II recruits ESCRT-III via the direct binding of its Vps25 subunit to Vps20 (Teo et al. 2004). This binding causes a nucleation event that activates inactive Vps32 subunits in the cytosol, which then polymerize in a coiled filamentous chain from the Vps20 base (Saksena et al. 2009; Teis, Saksena, and Emr 2008). Bro1--termed ALIX in mammals--binds both the Tsg101 subunit of ESCRT-I and Vps32, helping stabilize this oligomerization event (von Schwedler et al. 2003; McCullough et al. 2008; Katoh et al. 2003; Pires et al. 2009; Pashkova et al. 2013). Finally, this chain is capped by Vps24 and Vps2 (Teis, Saksena, and Emr 2008; Saksena et al. 2009).

The coiled chain of ESCRT-III serves two purposes. First, it allows for the deubiquitination of cargoes. Once the early ESCRT complexes have gathered the cargoes to be engulfed into the MVB via association with the ubiquitin modification, they need to be deubiquitinated to recycle and avoid the quick depletion of cell reserves of ubiquitin. To this end, ESCRT-III along with ALIX and the STAM subunit of ESCRT-0 recruit deubiquitinating enzymes (Amerik et al. 2000; Swaminathan, Amerik, and Hochstrasser 1999; Row et al. 2006; Mizuno et al. 2006; McCullough et al. 2006). The tight coil of ESCRT-III keeps the newly deubiquitinated cargo from diffusing away from the bud (Nickerson, Russell, and Odorizzi 2007; Teis et al. 2010). The second and arguably most important purpose of ESCRT-III is membrane abscission. While in CME, dynamin creates a tight coil around the stalk that brings membranes together and cuts a vesicle off, ESCRT-III does the same thing, but from the inside of the stalk. It has been shown that once the Vps32 coil has been capped by Vps24 and Vps2, this cap recruits Vps4, an ATPase that can force the disassembly of the coil (Lata et al. 2008; Ghazi-Tabatabai et al. 2008; Saksena et al. 2009). How

exactly this disassembly results in vesicular budding, and how ESCRT machinery manages to not be trapped within the vesicle are not fully understood and are areas of active investigation.

It is important to note that while the loading of ubiquitinated proteins into the ILVs is best understood, this is not the only method whereby cargo enters the ILVs. Indeed, these vesicles contain not just proteins, but also often RNA, which may enter the vesicles via association to RNA-binding proteins or even simply random loading of cytoplasm into the vesicle (Shurtleff et al. 2016; Yang et al. 2004; Yamashita et al. 2008; Wurmser and Emr 1998).

Once the MVB has been formed from an EE, it can have one of multiple fates: fusion with the PM, fusion with an autophagosome to create an amphisome, or terminal maturation into a late endosome, and ultimately an endolysosome. The mechanism by which an MVB fuses with the PM is poorly understood, but, nonetheless, it results in the release of its ILVs into the extracellular space as exosomes which can have a variety of functions depending on cell type, environment, and the cargo released in the exosomes (Raposo and Stoorvogel 2013).

1.1.3.2 Maturation of the Endosomal Membrane

Above, I briefly mentioned that certain proteins and lipids can be found on the surfaces of different types of endosomes, differentiating them from each other. These markers often play an essential role in trafficking and defining the molecular composition of the endosome. In this section, I will outline some of the ways in which the markers on endosomal membranes aid the function of the endosome and how the markers found on EEs change as the endosome matures into a LE in preparation to form the degradative endolysosome.

Perhaps the most important and well-known marker of EEs and LEs are the Rab GTPases (hereafter referred to as just Rabs) found on their surfaces. A Rab is a class of peripheral membrane

proteins which direct protein machinery to specific organelles, which is crucial for the correct sorting of trafficked vesicles to particular organelles (Wandinger-Ness and Zerial 2014). Rabs exist in one of two states: the GTP-bound form is active while GDP-bound form is inactive. In order to switch between these two states, they require two regulatory proteins: the guanine nucleotide exchange factor (GEF) replaces the Rab-bound GDP for GTP, activating the Rab, while the GTPase activating protein (GAP) activates the GTPase activity of the Rab, hydrolyzing its bound GTP to GDP, inactivating it. The specificity of localization of Rab proteins to their membranes is controlled by a combination of their activation state and binding by GDP dissociation inhibitor (GDI). Rab proteins have a hydrophobic prenyl group modification which anchors them to the lipid bilayer. In their inactive state, GDIs bind the prenyl group, making the Rab soluble, and detaching it from the membrane (Goody, Muller, and Wu 2017). Thus, Rabs are only localized and associated to membranes in their activated state, making the localization of GEFs one of the main ways in which Rabs are targeted to specific organelles (Kummel and Ungermann 2014; Yu and Hughson 2010). Membrane-tethered active Rabs can then recruit other proteins, termed effectors to serve any of a number of functions in vesicle trafficking (Vetter and Wittinghofer 2001). While many different Rabs are expressed on the membranes along the endosomal-lysosomal pathway, the primary Rabs that direct vesicular transport and fusion on the membranes of EEs and LEs are Rab5 and Rab7, respectively (Rink et al. 2005; Poteryaev et al. 2010).

The first step in the formation of the EE involves the identification of a cargo to be trafficked to the EE. A membrane cargo that has been endocytosed is ubiquitinated by any of a host of ubiquitin ligases; the ubiquitin moiety is recognized by Rabex5, the Rab5 GEF, which consequently activates Rab5, recruiting it to the membrane (Lee et al. 2006; Mattera et al. 2006). Activated Rab5 can then recruit a number of effectors, among them Rabaptin5, which itself can

then recruit Rabex5 (Horiuchi et al. 1997). This creates a positive feedback loop which results in a high concentration of Rab5 at the membrane of the vesicle carrying the cargo, making it an EE-identified membrane which can be fused with the EE. Of the effectors Rab5 recruits, early endosome antigen 1 (EEA1) and the class C core vacuole/endosome tethering (CORVET) complex are essential to the tethering and fusion of vesicles to be incorporated into the EE, as they coordinate the activity of proteins called soluble N-ethylmaleimide-sensitive factor attachment protein receptors (SNARE) (de Renzis, Sonnichsen, and Zerial 2002; Perini et al. 2014; Lachmann et al. 2014; Balderhaar et al. 2013; Ohya et al. 2009). SNAREs are long membrane-bound proteins that induce membrane fusion between vesicles and organelles by coiling together tightly, bringing the membranes close enough together to fuse (Jahn and Scheller 2006; Sudhof and Rothman 2009). While SNAREs can induce lipid bilayer fusion independently *in vitro*, at physiological conditions, EEA1 and the CORVET complex are needed to coordinate SNARE activity between vesicles and the EE (Starai, Jun, and Wickner 2007). Another important Rab5 effector is the class III phosphatidylinositol 3-kinase (PI3K) complex, which phosphorylates phosphatidylinositol (PI) to PI 3-phosphate (PI3P) (Shin et al. 2005). The synthesis of PI3P at the EE membrane is crucial, as PI3P is heavily involved in the to the identity of the EE membrane and in the binding of EE-specific proteins to the EE membrane. Indeed, EEA1 is localized to the EE via its binding of both Rab5 and PI3P (Stenmark et al. 1996; Lawe et al. 2002).

The process of the maturation of an EE to a LE involves a process called Rab conversion whereby Rab5 is stripped from the endosomal membrane and is replaced by Rab7 (Rink et al. 2005). Rab conversion takes place on the surface of an MVB, and is started when Rab5 and PI3P recruit the Mon1-Ccz1 complex to the membrane of the EE (Poteryaev et al. 2010; Lawrence et al. 2014; Cabrera et al. 2014). The Mon1 of the complex displaces Rabex5 from the membrane,

preventing further recruitment of Rab5 to the endosomal membrane, while the Ccz1 of the complex functions as a Rab7 GEF, recruiting Rab7 to the membrane (Poteryaev et al. 2010; Nordmann et al. 2010; Poteryaev et al. 2007; Cabrera et al. 2014). Rab7 then recruits TBC2, the Rab5 GAP, which actively inactivates and detaches Rab5 from the endosomal membrane (Haas et al. 2005).

Once the endosomal membrane is marked with Rab7 rather than Rab5, it is termed the LE. In the LE, Rab7 recruits its own effector proteins to coordinate trafficking and membrane fusion. The Rab7 effector complex homotypic fusion and protein sorting (HOPS) is the LE corollary to CORVET, and, in fact, shares four of its subunits with CORVET (Spang 2016; Balderhaar et al. 2013). Like CORVET in the EE, HOPS mediates vesicle tethering and fusion at the membrane of the LE. The process of maturation to the LE also involves the exchange of PI3P at the membrane for $PI(3,5)P_2$, the PIP that typifies LE membranes, which occurs via three axes: PI3P is directly phosphorylated to $PI(3,5)P_2$ by the kinase PIKfyve; excess PI3P is dephosphorylated to PI by a class of proteins called myotubularins; and the Rab7 effectors, suppressor of organelle fusion (SORF), inhibit the catalytic activity of PI3K, preventing the synthesis of more PI3P (Zolov et al. 2012; Cao et al. 2008; Liu et al. 2016; Poteryaev et al. 2010; Robinson and Dixon 2006; Gary et al. 1998). Finally, while EEs are relatively acidic compared to the cytosol and TGN, as they mature into LEs, and finally endolysosomes, the pH of endosomes gradually decreases. This is mediated by vacuolar ATPase (V-ATPase), a proton pump that acidifies the lumen. While V-ATPase is found on the membrane of many organelles, LEs and lysosomes actively recruit it via the Rab7 effector, Rab interacting lysosomal protein (RILP) (De Luca et al. 2014; Gary et al. 1998).

1.1.4 Macroautophagy

Macroautophagy is the process by which the cell, as the name would suggest, eats large parts of itself. Macroautophagy (hereafter referred to as just autophagy) is generally induced by different forms of cellular stress. It can therefore serve multiple functions including clearance of abnormal protein aggregates, clearance of old or damaged organelles, and breaking down of cellular proteins and structures for the recycling of nutrients during cellular starvation. Autophagy can broadly be said to have 4 steps: initiation via nucleation of a membranous structure known as the phagophore, elongation of the phagophore, envelopment of material to be degraded by the phagophore to form the autophagosome, and fusion of the autophagosome with either the endosome or the lysosome to form either an amphisome or an autolysosome, respectively.

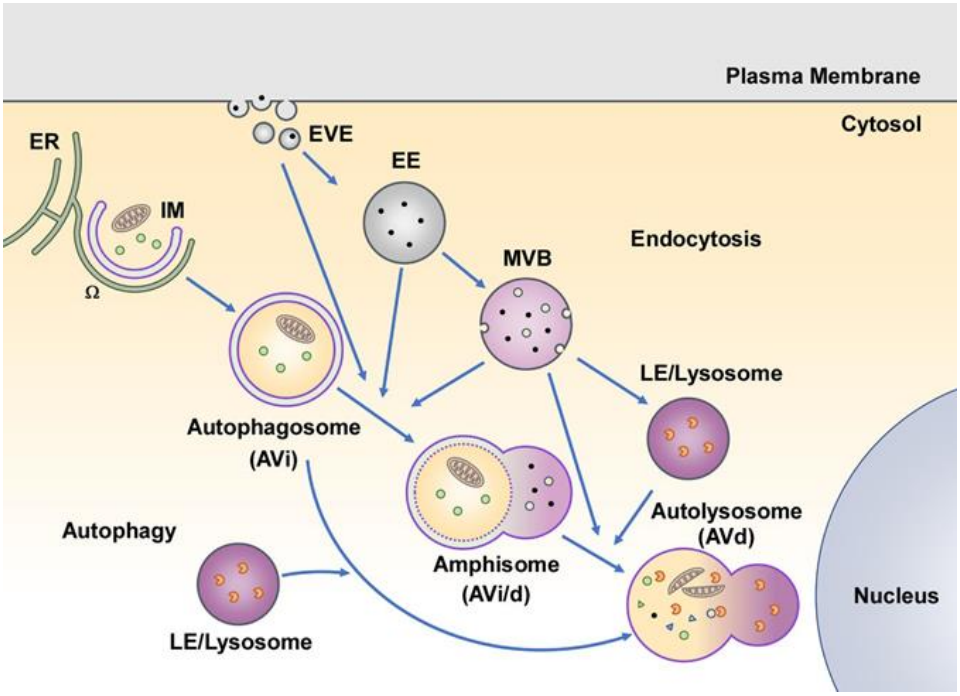

Figure 1.3 Overview of Autophagy

Reproduced from (Zhao and Zhang 2019)

Initiation of autophagy can occur via any of a number of pathways, but these all converge into a common pathway that begins with the inactivation of mammalian target of rapamycin complex 1 (mTORC1) (Kim et al. 2002; Noda and Ohsumi 1998). mTORC1 normally inhibits the unc-51-like kinase (ULK) complex formation via the phosphorylation of its components ULK1 and ULK2 (Hosokawa et al. 2009). No longer inhibited, the ULK complex can form, recruited to the endoplasmic reticulum (ER) by resident proteins VAPA and VAPB (Karanasios et al. 2016; Zhao, Liu, et al. 2018). At the ER membrane, ULK recruits the PI3K complex to make a PI3P-dense region known as the omegasome, which serves as the platform for the nucleation and elongation of the phagophore (Itakura and Mizushima 2010; Zhao and Zhang 2018; Axe et al. 2008).

The origin of the membrane that forms the phagophore adjacent to the omegasome has proven to be elusive. It is known that ATG9-tagged vesicles, which are normally involved in trafficking between the TGN and the endosome, are incorporated in the phagophore, but evidence exists that points to multiple organelles possibly contributing membrane to the phagophore, including the PM, mitochondria, ER, endosomes, and Golgi (Lamb, Yoshimori, and Tooze 2013; Karanasios et al. 2016; Hailey et al. 2010; Ravikumar et al. 2010; Orsi et al. 2012; Ge et al. 2013; Graef et al. 2013; Puri et al. 2013). Whatever its origin, the phagophore membrane needs to be modified to include a family of proteins known as light chain 3 (LC3) which are membrane markers vital to the function of the autophagosome. Proteins at the membrane of the phagophore including the PI3K complex recruit the ATG12-ATG5:ATG16L complex, which conjugates LC3 to phosphatidylethanolamine (PE), a lipid that anchors the normally soluble LC3 to the phagophore membrane (Kabeya et al. 2000; Mizushima et al. 2003; Mizushima et al. 1998; Nakatogawa et al. 2009; Itoh et al. 2008).

When the phagophore has been successfully formed, MTMs in the membrane decrease levels of PI3P, inducing dissociation of the machinery used to create the phagophore, and the ER protein VMP1 mediates detachment of phagophore from the ER (Vergne et al. 2009; Cebollero et al. 2012; Zhao et al. 2017). Once detached from the ER, the phagophore can envelop cytosolic material and organelles, forming a double membraned structure known as the autophagosome. The closing of the autophagosome is mediated by ESCRT machinery similar to the formation of the MVB (Takahashi et al. 2018; Rusten and Stenmark 2009; Yu and Melia 2017).

The fusion of the autophagosome and the endosome or lysosome begins with the tethering of their membranes by dedicated tether proteins which bind to markers of each membrane, often, but not always Rab7 and an LC3. Such tether proteins include EPG5, PLEKHM1, BRUCE, and GRASP55 to name a few (Wang, Miao, et al. 2016; McEwan et al. 2015; Ebner et al. 2018; Zhang, Wang, et al. 2018). Once the autophagosome has been tethered to the endosome or lysosome, HOPS machinery at the autophagosome mediates the fusion of the membranes (Jiang, Nishimura, et al. 2014; Takats et al. 2014). This machinery is recruited by UVRAG, which itself is recruited by protein associated with UVRAG as autophagy enhancer (Pacer), a protein bound to the autophagosome via interaction with the autophagosome-specific SNARE, STX17, and with the autophagosome's PIPs (Cheng et al. 2017; Liang et al. 2008).

Once the outer membrane of the autophagosome has fused with the endosome or lysosome, the resultant amphisome or autolysosome, respectively, contains an ILV composed of the autophagosome's inner membrane and the material within it that was phagocytosed. This ILV is reminiscent of a much larger version of those found in MVBs, and can be trafficked and degraded similarly.

1.1.5 Recycling

I have thus far discussed the processes whereby a protein cargo can enter the endosomal compartment and how such cargoes can be degraded. However, many proteins that enter the endosome are not meant to be immediately degraded. If that were the case, it would make the endosome an ultimately useless organelle that only became useful on merging with a lysosome. Moreover, it would increase the rate of degradation of many proteins to the point of extreme inefficiency. A receptor at the PM would only be able to be stimulated and endocytosed once before being destroyed. Any given MPR would only be able to deliver a single cargo before being stuck in the endosome and degraded. Finally, it would create the absurd situation where the PM and the TGN quickly depleted their membrane lipids by transporting them to the endosome. Indeed, it is essential that the endosome transport lipids and cargoes back to the PM and TGN at a highly coordinated rate.

The process by which a protein is exported from the endosome to either the PM or the TGN is called recycling. There are myriad ways in which recycling can occur, and of the endosomal trafficking pathways, recycling is perhaps the least well understood. However, in recent years, great strides have been made in the study of endosomal recycling. Endosomal recycling is broadly subdivided into two categories: the fast recycling pathway, which involves the direct recycling from the EE or LE to the PM or TGN; and the slow recycling pathway, which involves trafficking through the RE as an intermediate compartment. Here, I will discuss some of the better understood mechanisms in these categories of endocytic recycling.

1.1.5.1 Slow Recycling

Above, I discussed the subdivision of endosomes into early endosomes, late endosomes, and recycling endosomes. While I have thus far discussed EEs and LEs in detail, I have yet to address the RE. This is in part due to its specialized role in recycling, a pathway distinct from the ones mentioned above, but it is at least also partly due to its significantly more murky definition. The defining of the RE is significantly more recent than that of the EE or LE, and the structure we now call the RE was previously indistinguishable from the EE. However, while the RE remains a relative mystery, certain molecular markers and morphological peculiarities have helped to shed some light on what it is and how it functions.

The RE is an endosomal compartment dedicated to the recycling of proteins to the cell surface. Particularly, endocytosed PM receptors, when brought to the EE, may be trafficked to the RE to then be released back to the PM (Marsh et al. 1995). In most cells, REs seem to be localized to the endocytic recycling compartment (ERC), a tubulovesicular compartment located perinuclearly at the microtubule-organizing center (MTOC) (Ghosh et al. 1998; Burkhardt et al. 1997; Soldati and Schliwa 2006). However in some cell types--such as neurons--, REs can be more spread out throughout the cell (Joensuu et al. 2017).

The Rab that has been historically used to define REs is Rab11, which seems to be an important moderator of ERC structure and of trafficking to and from REs (Pasqualato et al. 2004; Ren et al. 1998; Baetz and Goldenring 2013). However, whether Rab11 is as cohesive a moderator and definer of REs as Rab5 and Rab7 are of EEs and LEs is unknown, as Rab8 has also proven an important regulator in RE function. Indeed, it is uncertain whether Rab11 and Rab8 are localized to the same membrane or to distinct subcompartments of the ERC (Roland et al. 2007). While Rab8 and Rab11 have distinct effectors that contribute to RE function and structure, both share

some effectors, and Rab11 can interact with the Rab8 GEF, Rabin8 (Knodler et al. 2010). However, the actual mechanisms whereby Rab8, Rab11, and their various effectors contribute to ERC structure and protein recycling remain elusory.

1.1.5.2 Rapid Recycling

While the nature of the RE has made the mechanisms of slow endosomal recycling somewhat of an enigma, some of the more direct mechanisms of rapid recycling from the EE or LE to the PM or TGN are better understood, particularly through recent years' studies.

1.1.5.2.1 Retromer

The retromer complex is perhaps the best characterized form of endosomal recycling, at least in part due to its known involvement in multiple diseases, particularly neurodegenerative diseases, a connection that I will explore in a later section (Small and Petsko 2015). The retromer is an ancient recycling pathway vital to the proper trafficking of a diverse set of cargoes in all eukaryotes (Burd and Cullen 2014). Here, I will discuss the function of the retromer in direct trafficking from the endosome to both the PM and the TGN.

The retromer is composed of a number of subcomplexes and associated machinery, but is generally understood to be defined by its core, which is composed of a trimer of vacuolar protein sorting-associated protein 26 (Vps26), Vps29, and Vps35 (Seaman 2005; Hierro et al. 2007; Haft et al. 2000). In mammals, Vps26 has two paralogues, Vps26a and Vps26b, which, while having mostly redundant functions, have been shown to behave in some distinct ways (Kerr et al. 2005; Collins et al. 2008; Gallon et al. 2014). Specifically, the retromer with Vps26b has been shown to be less able to recycle CI-MPR, and the two paralogs are found differentially expressed both in

different tissues and in different subcellular localization with Vps26a being expressed in a more broad selection of tissues and more commonly found associated to the endosome (Bugarcic et al. 2011; Kim et al. 2010).

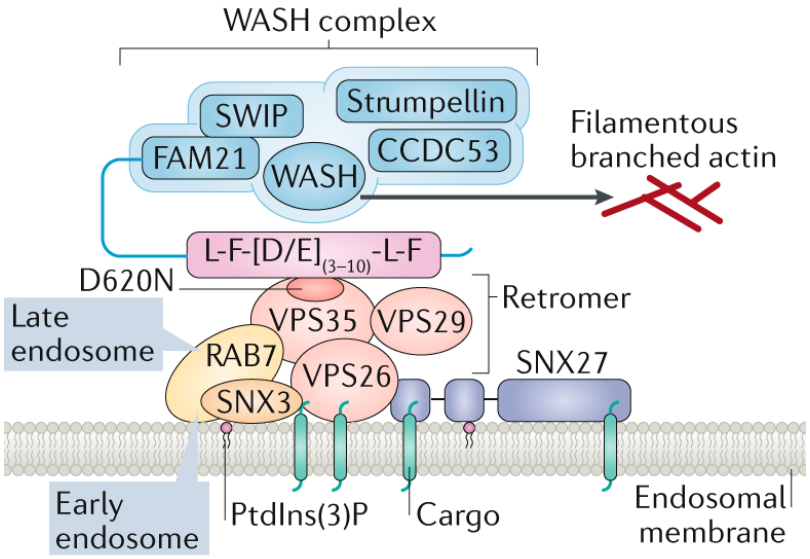

Figure 1.4 Composition of the Retromer Complex

Reproduced from (Cullen and Steinberg 2018)

In yeast, where the retromer was first described, the retromer core subcomplex is crucially associated to Vps5 and Vps17, two members of a family of proteins known as sorting nexins (SNX) (Seaman et al. 1997; Horazdovsky et al. 1997). SNX proteins are defined by the inclusion of a phox-homology (PX) domain, an inositol- and protein-binding domain crucial to SNX protein function (Chandra and Collins 2018; Teasdale and Collins 2012). In mammals, the function of Vps5 can be performed by one of a few different SNX proteins, which can lead to differential retromer functions from different associated SNX proteins. The best-established retromer-associated SNX proteins in mammals are SNX3 and SNX27, with a close homologue of SNX3, SNX12, being proposed as another possibility (Simonetti et al. 2017; Priya et al. 2017; Harterink

et al. 2011; Temkin et al. 2011; Steinberg et al. 2013). Another SNX complex, known as the SNX-BAR heterodimer, was originally thought to also fill this function in mammals, but this has recently been put into question. Here, I will first describe the function of the retromer and its interactions with SNX proteins, and later discuss why the SNX-BAR heterodimer may work independently of the retromer.

As a first step of retromer function, a number of subunits of the retromer complex are recruited to the endosome through a combination of endosomal markers and recognition of membrane-associated cargoes to be transported. Evidence suggests that the core complex is recruited via the direct interaction between Vps35 and Rab7 (Priya et al. 2015; Rojas et al. 2008; Seaman et al. 2009; Harrison et al. 2014). One study has suggested that this interaction occurs specifically during the process of Rab conversion in endosomal maturation (Rojas et al. 2008). The bond between SNX proteins and the core complex is also crucial in the recruitment of retromer to the endosome. SNX3 and SNX27 have been shown to bind PI3P via their PX domain, thus recruiting them to the endosomal membrane (Xu et al. 2001; Ghai et al. 2011; Ghai et al. 2015). They can then influence the structure and binding of the core complex by binding Vps26, with SNX3 having a second lower-affinity interaction with Vps35 (Gallon et al. 2014; Steinberg et al. 2013; Lucas et al. 2016).

The retromer machinery has the ability to recognize cargo to be recycled, usually via motifs on the cytosolic side of a transmembrane protein. This not only serves to recruit retromer machinery to the endosome, but also to ensure that the correct cargoes are being specifically recycled by the retromer. In both the SNX27- and SNX3-retromer, it has been shown that direct binding of the SNX protein to Vps26 promotes recognition of the cargo. Specifically, the point of direct interaction between SNX3 and Vps26 creates a binding surface which can recognize cargo

proteins, and the interaction between SNX27 and Vps26 causes a conformational change in SNX27 such that its protein-binding psd95/dlg/zo-1 (PDZ) domain binds cargoes with a significantly higher affinity (Lucas et al. 2016; Gallon et al. 2014). Furthermore, it has been shown that the modification of the cargoes can cause them to be specifically targeted to be recycled by the SNX27-retromer. A kinase, such as G protein-coupled receptor kinase 5 (GRK5), may phosphorylate a cargo on its PDZ-binding surface either increasing or decreasing the affinity of the surface for the PDZ domain of SNX27 (Cao et al. 1999; Clairfeuille et al. 2016). This has been shown to be the case for a number of retromer cargoes including the β2-adrenergic receptor, and N-methyl-D-aspartate (NMDA) and α-amino-3-hydroxy-5-methyl-4-isoxazole propionic acid (AMPA) glutamate receptors (Clairfeuille et al. 2016).

At the endosome, the retromer machinery disrupts the membrane to form a tubule where cargoes are concentrated. How this tubulation occurs in mammals is currently an open question, and studies have pointed to a number of proteins associated with the retromer machinery, including EH domain-containing protein 1 (EHD1), that may be involved (Cai et al. 2013; Caplan et al. 2002). In yeast, Vps5 and Vps17, besides containing a PX domain, also contain a bin/amphiphysin/rvs (BAR) domain, which has a curved shape that can cause membrane tubulation (Teasdale and Collins 2012; Horazdovsky et al. 1997; Seaman et al. 1997). The mammalian proteins SNX1, SNX2, SNX5, and SNX6 also containing BAR domains and form a heterodimer of SNX1 or SNX2 with SNX5 or SNX6, the aforementioned SNX-BAR heterodimer (Carlton et al. 2004). SNX1 and SNX2 are homologues of Vps5, and SNX5 and SNX6 are homologues of Vps17. Due to a combination of this homology and the fact that the SNX-BAR is localized to the same endosome as the retromer, it has long been understood that the SNX-BAR heterodimer performed the same function in mammals as Vps5 and Vps17 do in yeast (Carlton et

al. 2005; Kvainickas et al. 2017; Rojas et al. 2007). However, recent studies have shown that this is unlikely to be the case. While the heterodimer can interact with the retromer core, the affinity is relatively weak compared to that between the core and SNX3 or SNX27 (Simonetti et al. 2017; Steinberg et al. 2013; McGough et al. 2018). Also, while both the retromer and SNX-BAR complexes occupy the endosomal membrane, it has been shown through super-resolved stimulated emission depletion (STED) microscopy that retromer and SNX1 occupy distinct sublocations of said membrane (Kvainickas et al. 2017). Finally, studies have shown that the SNX-BAR heterodimer can, independently from the retromer, recycle CI-MPR to the TGN (Kvainickas et al. 2017). Thus, while it seems that the retromer and the SNX-BAR heterodimer perform similar functions, and have some ability to interact, it is becoming more and more apparent that they are not as functionally close as was previously assumed.

Once recruited to the endosomal membrane, the retromer recruits a number of accessory proteins. Among these are Tre-2/Bub2/Cdc16 1 domain-containing 5 (TBC1D5) and Vps9-ankyrin repeat protein (VARP) (Jimenez-Orgaz et al. 2018; Hesketh et al. 2014). TBC1D5 binds to Vps29 and is a Rab7 GAP whose Rab7-inactivating activity is crucial to the coordination of endosomal maturation with retromer recycling (Borg Distefano et al. 2018; Seaman, Mukadam, and Breusegem 2018; Jimenez-Orgaz et al. 2018; Jia et al. 2016). The inactivation of Rab7 delays the maturation of the endosome as long as there are retromer complexes attached to the endosomal membrane, so that only once the retromer has removed the cargoes to be recycled can Rab conversion be completed. VARP also binds Vps29 and serves a similar function in that VARP binds vesicle-associated membrane protein 7 (VAMP7), a SNARE protein crucial to the fusion of the endosome with the lysosome (Hesketh et al. 2014; Schafer et al. 2012). Thus until the retromer

has gathered its cargoes and VAMP7 is no longer sequestered by retromer-bound VARP, the endosome cannot fuse with a lysosome and begin the process of protein degradation.

FAM21 is recruited by Vps35 and is the largest protein in a pentamer known as the Wiskott–Aldrich Syndrome protein and scar homology (WASH) complex, the other members of which are WASH1, CCDC53, strumpellin, and SWIP (Harbour, Breusegem, and Seaman 2012; Jia et al. 2012). The WASH complex is crucial in the recruitment and initiation of the actin-related protein 2/3 (Arp2/3) complex (Derivery et al. 2009; Gomez and Billadeau 2009; Jia et al. 2010). Arp2/3 serves as a nucleation site for actin polymerization and branching, which is essential to the stabilization and eventual scission of the recycling tubule from the endosome (Gomez et al. 2012; Derivery et al. 2012). Much like with the formation of the recycling tubule, the scission of the tubule from the endosome is still largely not understood, and multiple retromer-associated proteins have been thought to be involved, including EHD1 (Simunovic et al. 2017).

The retromer recycling tubule, once excised from the endosome, gets transported either to the TGN or to the PM. Due to the interaction of SNX27 with a functional domain most commonly found on PM proteins, it is thought that the SNX27-retromer specifically mediates recycling to the PM, though the precise mechanism for this is not currently understood. Indeed, due to the recent revelation that the SNX-BAR heterodimer may not be directly involved in retromer function, much of what was previously understood about the transport of retromer-coated vesicles has been put to question. It has been previously shown that SNX6 interacts directly with the dynein/dynactin motor complex, which mediates retrograde transport along microtubules in the cell (Wassmer et al. 2009; Hong et al. 2009). And indeed, dynein dysfunction and retromer dysfunction show similar effects in endosomal missorting (Kimura et al. 2016). Thus, while it is possible, and even likely that retromer-coated vesicles are trafficked by the dynein/dynactin motor complex, how exactly

this interaction occurs may not be as clear as once thought. Similarly, the independence of the SNX-RAB heterodimer from the retromer has also led some to believe that despite previous study, the retromer may not even be involved in the trafficking of what was once considered its main model cargo, CI-MPR. However, recent studies have quelled that theory with an apparent middle ground. CI-MPR is indeed trafficked by a number of different, apparently redundant mechanisms including the retromer complex. However, the TGN receives these cargoes via three different golgins, golgin-97, golgin-245 and GCC88, depending on the vesicle's mechanism of origin. Retromer-coated vesicles are docked to the TGN via interaction with GCC88, the SNX-BAR heterodimer uses golgin-245, and an as yet unknown mechanism uses golgin-97 (Cui et al. 2019). Meanwhile docking of retromer-coated vesicles to the PM remains somewhat of a mystery.

1.1.5.2.2 COMMander

A much more recently discovered endosomal recycling system involves the COMMander complex. While it is not nearly as well characterized as the retromer complex, certain structural and functional similarities to the retromer have eased the process of unravelling the mechanism of the COMMander complex. The COMMander is mainly identified through two subcomplexes: the retriever heterotrimer and the COMMD/CCDC22/CCDC93 (CCC) (Mallam and Marcotte 2017; McNally et al. 2017; Bartuzi et al. 2016). However, before either of these subcomplexes had been found, what had been established was that there was an unknown link between SNX17 and the WASH complex that recycled certain cargoes from the endosome independently of the retromer (Lee et al. 2008; Steinberg et al. 2012; McNally et al. 2017). Here, I will describe what is currently known of the COMMander complex.

The similarities between the retromer and the COMMander start with SNX17, which is a homologue of SNX27. As a SNX protein, SNX17 has a PX domain that can recognize PI3P, recruiting it to the endosome (Ghai et al. 2011). Unlike SNX27, SNX17 does not have a PDZ domain, but rather can recognize cargoes directly through its 4.1/ezrin/radixin/moesin (FERM) domain, which it has in common with SNX27 (Ghai et al. 2013; McNally et al. 2017). SNX17 has also been shown to directly bind the retriever complex (McNally et al. 2017).

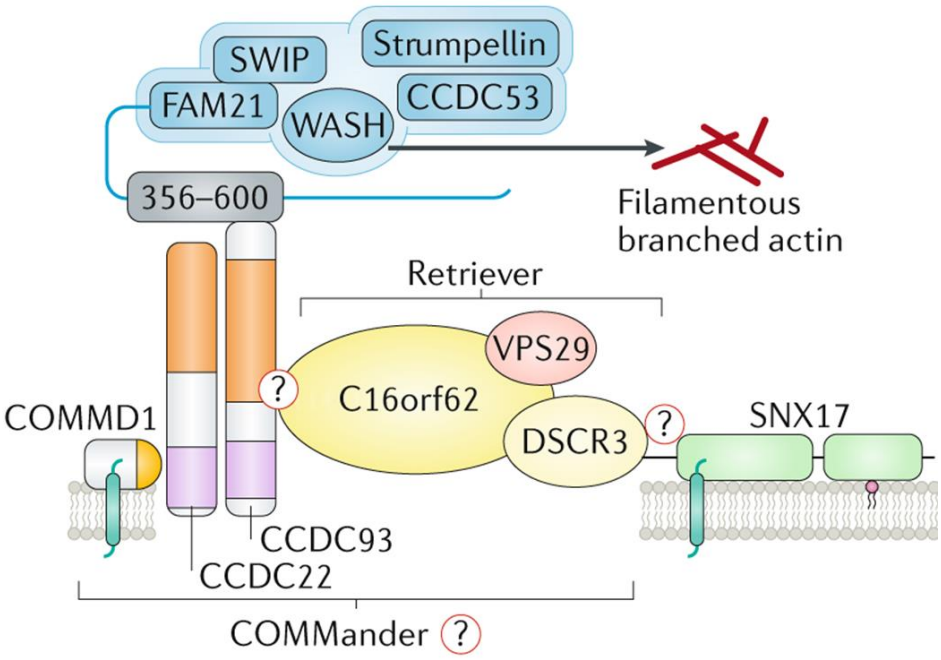

Figure 1.5 Composition of the COMMander Complex

Reproduced from (Cullen and Steinberg 2018)

The retriever complex, is highly similar to the retromer complex in that of its three component proteins, one, Vps29, is shared, and the other two are so closely homologous in structure (though not sequence), that they have been renamed from chromosome 16 open reading frame 62 (C16orf62) and Down syndrome critical region protein 3 (DSCR3) to Vps35l and Vps26c, respectively (McNally et al. 2017). Again, similar to the retromer and its associated SNX

proteins, the assembled retriever complex seems to be recruited to the endosome via the direct interaction between SNX17 and Vps26c (McNally et al. 2017; Gallon et al. 2014). Importantly, while a direct interaction between the retromer and its cargoes has been shown, there is currently no evidence that the retriever complex interacts with cargoes directly rather than through common association to SNX17.

While both the retromer and retriever require the recruitment of the WASH complex for the formation of recycling tubules, retriever requires an intermediary whereas retromer does not (Harbour, Breusegem, and Seaman 2012; Phillips-Krawczak et al. 2015). To form the entire COMMander complex, retriever must bind the CCC complex, which is composed of coiled-coil domain-containing protein 22 (CCDC22), CCDC93, and 10 members of the copper metabolism mouse U2af1-rs1 region 1 domain (COMMD) family (Wan et al. 2015; Mallam and Marcotte 2017). It is currently unclear how many or what combination of the COMMD1 - COMMD10 proteins are necessary for the formation of the CCC complex, and indeed, it is possible that different combinations of them can form functionally distinct CCC complexes. Various COMMD proteins have been shown to bind known COMMander cargoes, which provides evidence for this possibility (Li et al. 2015; Bartuzi et al. 2016; Phillips-Krawczak et al. 2015). However, while the function of the COMMD proteins is not well understood, it is known that the CCDC22 and CCDC93 proteins can bind both the retriever complex and FAM21, providing the basis for the recruitment of WASH, which likely leads to a tubulation cascade similar to the one that occurs in the retromer, though the study of the COMMander complex-associated WASH complex has not been as robust as the retromer-associated WASH complex (Phillips-Krawczak et al. 2015).

1.2 Retromer in Neurodegenerative Disease

Given the retromer's central role in endosomal trafficking, it makes sense that the dysfunction of the retromer would cause significant cellular dysfunction and disease pathology. Indeed, the knocking out of Vps35 or Vps26a has proven to be embryonically lethal in mice, though the knockout of Vps26b causes no overt pathology (Wen et al. 2011; Lee et al. 1992; Kim et al. 2010). Further studies have shown an important role for the retromer in multiple diseases, particularly neurodegenerative diseases, which is currently the subject of widespread study. In this section, I will review the studies that have been performed on how the retromer is connected to such diseases.

1.2.1 Alzheimer's Disease

Alzheimer's disease (AD) is both the most common neurodegenerative disease and the most common cause of dementia (Ballard et al. 2011). While usually sporadic in origin, AD has been shown to be associated with a number of genetic mutations (Nikolac Perkovic and Pivac 2019). AD is characterized pathologically by the accumulation in the brain of intracellular neurofibrillary tangles (NFTs) and plaques of toxic β-amyloid (Aβ) peptide (De Strooper 2010; Zheng and Koo 2011). NFTs are formed by the microtubule-associated protein tau, while Aβ is the product of the successive cleavage of amyloid precursor protein (APP) through β- (BACE1) and ϒ-secretase (Citron et al. 1992; Cai, Golde, and Younkin 1993; De Strooper 2010; Gendron and Petrucelli 2009). The cleavage of APP by BACE1 occurs predominantly in the EE, whereas the alternative non-toxic cleavage of APP to APPα by α-secretase occurs at the PM, thus the sequestering of APP to the endosome promotes the production of toxic Aβ (Sisodia 1992; Jiang, Li, et al. 2014; Checler 1995; Parvathy et al. 1999; Komano et al. 1998).

AD was the first disease to be associated to retromer dysfunction when a microarray study performed on the AD-affected entorhinal cortex from patients showed a decrease in the expression of VPS35, and a follow-up protein analysis showed a decrease in both VPS35 and VPS26A (Small et al. 2005). This retromer deficiency has since been replicated in an AD mouse model which overexpresses the AD-associated human KM670/671NL Swedish APP variant (Chu and Pratico 2017). Further genetic analyses have shown links between AD and retromer-associated proteins, particularly WASHC4, SNX1, SNX3, and RAB7A (Vardarajan et al. 2012). Variants in the retromer cargoes SORCS1, SORCS2, SORCS3, and particularly SORL1—which I have previously mentioned are important cargo-recognizing proteins in the TGN-to-endosomal pathway—have also been linked to AD (Reitz et al. 2013; Vardarajan et al. 2015; Fjorback et al. 2012). Importantly, SORL1 is known to traffic APP, and a disruption of SORL1 increases Aβ production whereas SORL1 overexpression decreases it (Dodson et al. 2008; Andersen et al. 2005; Offe et al. 2006; Rogaeva et al. 2007). Similar changes in Aβ occurs with the disruption or overexpression of Vps35 and Vps26a (Small et al. 2005; Bhalla et al. 2012; Muhammad et al. 2008; Wen et al. 2011; Ansell-Schultz et al. 2018). Indeed, the viral overexpression of VPS35 in a triple transgenic (3xTg) mouse model of AD has shown to effect not only a decrease in Aβ production, but also the amelioration of AD-associated behavioral deficits (Li, Chiu, and Pratico 2019). Given the involvement of retromer dysfunction in AD, pharmacological chaperones have been made that stabilize the retromer complex, aiding its function and preventing the degradation of its components (Berman et al. 2015; Mecozzi et al. 2014). As with viral overexpression, these chaperones have been shown to decrease the production of Aβ in neuronal cultures (Mecozzi et al. 2014; Chu and Pratico 2017). Thus, a model has arisen whereby under physiological conditions, the retromer traffics APP-bound SORL1 away from the endosome, preventing toxic Aβ

production, but disruption of this pathway leaves APP sequestered in the endosome, where BACE1 can cleave it. Furthermore, BACE1 itself has also been shown to be trafficked by the retromer, and disruption of the retromer core results in the sequestration of BACE1 to the endosome, where the acidity levels allow for optimal APP β-secretase cleavage, so higher Aβ levels are produced (He et al. 2005; Wen et al. 2011; Wang et al. 2012).

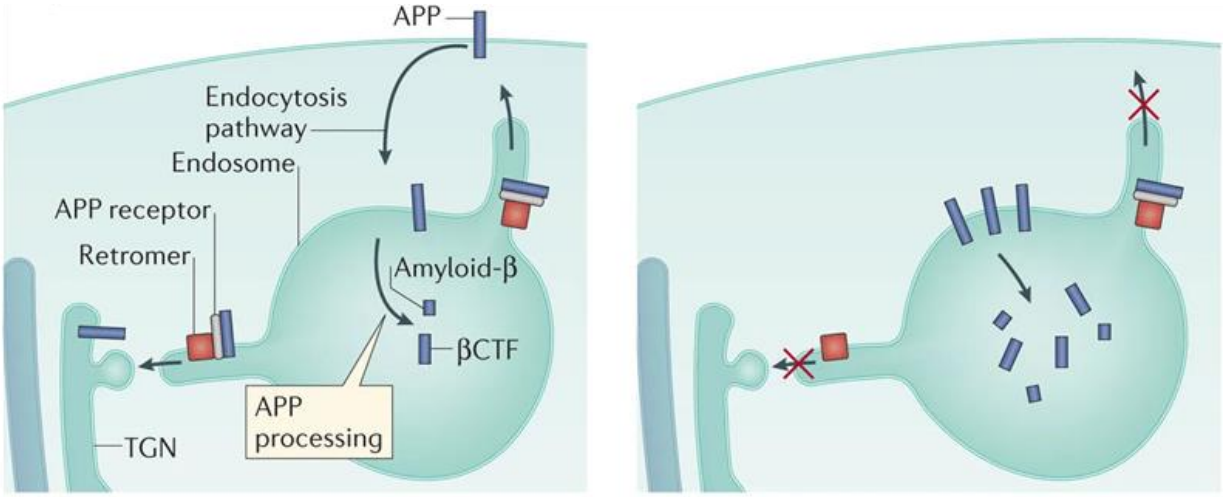

Figure 1.6 Effect of Retromer Dysfunction on APP Trafficking

Reproduced from (Small and Petsko 2015)

Under physiological conditions, the retromer has an important role in microglia in the recycling of phagocytic and cell signaling receptors to the cell surface (Lucin et al. 2013; Yin et al. 2016). However, AD patient microglia have been shown to have a cell-specific decrease in retromer components, resulting in a decrease in the transport of various receptors to the PM (Lucin et al. 2013). One particularly notable such receptor is triggering receptor expressed on myeloid cells 2 (TREM2), which mediates the sensing and phagocytosis of Aβ (Wang, Cella, et al. 2015; Choy et al. 2014). AD-associated TREM2 mutations have been shown to impede its association to

the retromer and its transport to the PM, thus decreasing the clearance of Aβ by microglia (Guerreiro et al. 2013; Kleinberger et al. 2014; Yin et al. 2016; Rojas et al. 2008; Choy et al. 2014).

Finally, a less well-defined method of retromer deficiency resulting in AD pathogenesis has been proposed involving the NFTs formed in AD (Small and Petsko 2015). NFTs are formed when neurons endocytose extracellular tau to the endosome where the pathogenic processing of tau (Wu et al. 2013; Michel et al. 2014). Microglia normally participate in the clearance of extracellular tau, preventing its delivery to neurons (Majerova et al. 2014; Bolos et al. 2017; Luo et al. 2015). Furthermore, it has been shown that a deficiency in cathepsin D (CathD), a protease trafficked by CI-MPR, can increase the pathogenic processing of tau (Khurana et al. 2010). Thus, two possibilities arise as to how retromer dysfunction may enhance NFT formation. First, much like with TREM2, if a decrease in tau-recognizing phagocytic receptors on the surface of microglia prevents them from clearing extracellular tau, more will be available for endocytosis by neurons. Second, since retromer deficiency causes CathD to fail to be delivered to the endosome, replicating a CathD deficiency, which, as mentioned above, increases the pathogenic processing of tau. This is supported by the fact that a study has shown that human induced pluripotent stem cell (iPSC)-derived neurons show a reduction in pathogenic tau phosphorylation upon the stabilization of the retromer (Young et al. 2018). Furthermore, the viral delivery of VPS35 to 3xTg mice has shown to decrease cortical NFT formation (Li, Chiu, and Pratico 2019). Finally, a study in two other diseases that result in the accumulation of tau—known as tauopathies, which will be discussed further below—have shown that retromer rescue can reduce tau accumulation (Vagnozzi et al. 2019).

1.2.2 Parkinson's Disease

Parkinson's disease (PD) is the second most common neurodegenerative disorder, and results in the degeneration of dopaminergic neurons in the substantia nigra of the midbrain, which causes a number of motor deficits in patients (Postuma et al. 2015; Forsaa et al. 2010). It is important to note that while PD is viewed as a primarily motor system disorder, there are a number of other neurological symptoms associated with PD such as cognitive dysfunction, psychosis, and mood disorders (Lim, Fox, and Lang 2009; Barone et al. 2009; Hussl, Seppi, and Poewe 2013; Chou, Koeppe, and Bohnen 2011). PD pathology is accompanied by the accumulation of toxic protein aggregates containing α-synuclein (SNCA) (Burre, Sharma, and Sudhof 2018). While usually sporadic in nature, PD has been shown to be linked to heritable mutations in roughly 10% of cases (Simon, Tanner, and Brundin 2020; Hernandez, Reed, and Singleton 2016; Lesage and Brice 2009).

The link between PD and the retromer was first established by exome sequencing of patients, which established an autosomal dominant missense D620N mutation in VPS35 as causative of PD (Vilarino-Guell et al. 2011; Zimprich et al. 2011). More recently, an increasing number of mutations in VPS35 have been tentatively linked to PD (Nuytemans et al. 2013; Vilarino-Guell et al. 2011; Bandres-Ciga et al. 2016; Verstraeten et al. 2012; Sharma et al. 2012; Gustavsson et al. 2015; Zimprich et al. 2011; Lesage et al. 2012; Chen et al. 2013). However, since the D620N mutation was the first found and has shown the most robust association to PD, much of the study of the link between the retromer and PD has centered around the effects of this mutation. Though a few studies have indicated that it may cause a toxic gain of function, it is generally understood that the D620N mutation results in a loss of function in the retromer (Mir et al. 2018; Tsika et al. 2014). While the mutation does not cause a defect in the formation of the

retromer core, it has been shown that it results in a deficiency in the recruitment of FAM21, and therefore, the WASH complex, ultimately impairing the ability of the retromer to function (Zavodszky et al. 2014; McGough et al. 2014; Seaman and Freeman 2014; Vilarino-Guell et al. 2011; Follett et al. 2014). The study of the downstream effects of this dysfunction have shown numerous possible mechanisms whereby it results in PD pathology.

First, as with most retromer dysfunction, the VPS35 D620N mutation results in the mislocalization of CI-MPR, which then leads to decreased delivery of CathD to the lysosome (MacLeod et al. 2013; Follett et al. 2014; McGough et al. 2014; Miura et al. 2014). Since CathD is the main protease involved in the degradation of SNCA at the lysosome, this results in the decreased clearance of SNCA, and thus the accumulation of SNCA aggregates (Miura et al. 2014; Follett et al. 2014; Sevlever, Jiang, and Yen 2008; Cullen et al. 2009). A study showed that in both a heterozygous Vps35 knockout mouse and a mouse virally overexpressing the VPS35 D620N mutant, the dysfunction of the retromer resulted in the mislocalization of lysosome-associated membrane glycoprotein 2a (Lamp2a), a protein involved in the lysosomal degradation of SNCA (Tang, Erion, et al. 2015). A final study proposed a third mechanism whereby the dysfunction of the retromer in PD may contribute to the reduced clearance of SNCA, involving the disruption of autophagy (Zavodszky et al. 2014). Namely, it showed that, through a poorly understood mechanism, the VPS35 D620N mutation leads to the mislocalization of ATG9A, a protein associated to membranes involved in the formation of the phagophore (Zavodszky et al. 2014; Karanasios et al. 2016; Orsi et al. 2012).

Mitochondrial dynamics have also long been proven to be crucial to the pathogenesis of PD (Winklhofer 2014; Winklhofer and Haass 2010; Trancikova, Tsika, and Moore 2012). Interestingly, in a poorly understood mechanism, the retromer has been shown to contribute to the

formation of mitochondria-derived vesicles (MDV), though whether this process is disrupted by PD-linked VPS35 mutations is unknown (Braschi et al. 2010; Sugiura et al. 2014). However, studies in mice both *in vitro* and *in vivo* as well as in fibroblasts from patients with the VPS35 D620N mutation have shown that the VPS35 D620N mutation results in increased mitochondrial fission and decreased mitochondrial function, both of which could be reversed by the pharmacological inhibition of mitochondrial fission (Wang, Wang, Fujioka, et al. 2016; Zhou et al. 2017; Tang, Liu, et al. 2015).

Another effect of retromer deficiency that the VPS35 D620N mutation has been shown to recapitulate involves the trafficking of neurotransmitter receptors. First, both the depletion of Vps35 and the overexpression of VPS35 D620N have been shown to cause the mislocalization of the AMPA glutamate receptors GluR1 and GluR2, resulting in impaired dendritic spine maturation and synaptic transmission (Tian et al. 2015; Munsie et al. 2015; Temkin et al. 2017). Furthermore, this mislocalization results in the impairment of long-term potentiation (LTP) in the mouse hippocampus (Temkin et al. 2017). The retromer also traffics dopamine receptor D1 (DRD1), which is depleted at the cell surface upon the depletion of VPS35 and increased upon overexpression of VPS35 (Wang, Niu, et al. 2016). Notably, the overexpression of VPS35 D620N has no effect on DRD1 cell surface expression, which may indicate that the deficiencies in dopamine signaling, and resulting cognitive symptoms involved in PD may at least in part be due to the dysfunction of the retromer (Wang, Niu, et al. 2016; Narayanan, Rodnitzky, and Uc 2013).

Besides the mutation of VPS35, retromer deficiency has also been linked to other PD-associated mutations, most notably SNCA and leucine-rich repeat kinase 2 (LRRK2). Mutations in LRRK2 and either mutations or multiplications of SNCA are causative of PD (Hernandez, Reed, and Singleton 2016; Stefanis 2012; Paisan-Ruiz, Lewis, and Singleton 2013). I already described

above much of what has been discovered about how retromer deficiency interacts with SNCA accumulation. One more study showed that the overexpression of VPS35 could rescue the hippocampal neuron loss found in a transgenic (Tg) mouse which overexpresses human SNCA (Dhungel et al. 2015). Similarly, studies in LRRK2 mutant drosophila models have shown that the neurotoxicity and behavioural deficits that these mutations elicit are rescued by the overexpression of VPS35 (Linhart et al. 2014; MacLeod et al. 2013). Interestingly, brain tissue analysis from both mouse models of LRRK2 mutations and post-mortem PD patients with mutations in the LRRK2 gene show a decrease in VPS35 as well as CI-MPR expression (Zhao, Perera, et al. 2018; MacLeod et al. 2013).

1.2.3 Other Neurological Disorders

The retromer has mostly been studied in the context of AD and PD, partly due to the strong association that retromer dysfunction has with those diseases, and partly due to the large prevalence of these diseases. However, further study has shown connections of the retromer with several other neurological disorders, which I will describe here.

Down syndrome (DS) is a chromosomal abnormality that is caused by a trisomy in chromosome 21, and results in a variety of symptoms including developmental impairment and intellectual disability (Bull 2011; Roizen and Patterson 2003; Brown et al. 1990). Tissue analysis from the Ts65Dn mouse model of DS and well as post-mortem analysis of brains from DS patients has shown a decrease in the expression of SNX27 (Wang, Zhao, et al. 2013). The overexpression of SNX27 in the Ts65Dn mouse has proven to correct abnormalities found in these mice, including cognitive and LTP deficits, and reduced levels of AMPA glutamate receptors at neuronal synapses (Wang, Zhao, et al. 2013). Further study has shown that this deficiency results in the

mislocalization of G protein-coupled receptor 17 (GPR17) at the cell surface of oligodendrocytes, which leads to aberrant oligodendrocyte maturation and deficient myelination, effects which have been associated with DS pathology (Meraviglia et al. 2016; Olmos-Serrano et al. 2016). Patients with DS develop early-onset AD, likely at least partly due to the presence of the APP gene on chromosome 21 and its resultant multiplication (Lai and Williams 1989). However, further evidence shows that the deficiency in SNX27 in DS may also contribute to this development, as a decrease in SNX27 has been shown to increase Aβ production, specifically via an increase in ϒ-secretase activity as well as in the delivery of APP to the cell surface (Wang et al. 2014; Huang et al. 2016).

Progressive supranuclear palsy (PSP) is a disease that results in PD-like symptoms, though its pathology is more similar to AD in that it involves tau-positive aggregates in several areas of the brain (Forrest, Kril, and Halliday 2019; Takahashi et al. 2002; Steele, Richardson, and Olszewski 1964). Pick's disease, a subclass of frontotemporal dementia (FTD), is a disease that, like AD, results in dementia and tau-positive aggregates, however, these are not accompanied by Aβ plaques (Hodges 2001; Forrest, Kril, and Halliday 2019). Recently, a study implicated the retromer in the pathogenesis of these two tauopathies (Vagnozzi et al. 2019). This study first showed that retromer levels are reduced in the brains of patients with these tauopathies. It also showed that the silencing and overexpression of VPS35 cultured neuroblastoma cells resulted in the overproduction and reduction of pathogenic forms of tau protein, respectively. Finally, it showed that the pathological and behavioural defects found in a mouse model of tauopathy were made more severe by the genetic downregulation of Vps35.

Neuronal ceroid lipofuscinosis (NCL) is a subgroup of a family of lysosomal storage disorders (LSD). NCL is characterized by the accumulation of lysosomal lipopigments in cells,

which results in a number of motor and psychological symptoms (Williams and Mole 2012; Kauss, Dambrova, and Medina 2019). Currently there are at least 13 genes whose mutation is known to cause NCL, including some that are connected to trafficking in the endosomal compartment (Butz et al. 2019). Namely, CLN3 is involved in the trafficking of CI-MPR between the TGN and the endosome (Metcalf et al. 2008). CLN5 is also involved in trafficking, and indeed is known to recruit the retromer to the endosome, such that a depletion in CLN5 results in the degradation of CI-MPR and sortilin due to decreased endosomal recruitment of the retromer (Mamo et al. 2012). Furthermore, CathD—whose function is, as I have described above, dependent on the retromer—is another gene whose mutation causes NCL (Jalanko and Braulke 2009).

Hereditary spastic paraplegias (HSP) are a groups of genetic disorders which result in lower limb spasticity and weakness (Harding 1983). Currently there are over 70 known genes that can cause HSP, a number which continually grows (Novarino et al. 2014; 'OMIM Phenotypic Series - PS303350' ; de Souza et al. 2017). Many of these genes are known to be involved in membrane trafficking, including the WASH complex protein strumpellin (Blackstone, O'Kane, and Reid 2011; Valdmanis et al. 2007; Freeman, Seaman, and Reid 2013). However, the mechanistic effect of this mutation on the development of HSP is unknown.

Similarly, a mutation in the WASH complex protein SWIP has been found to cause autosomal recessive intellectual disability (ARID) by significantly reducing the expression levels of SWIP and destabilizing the WASH complex (Ropers et al. 2011).

Mutations in the retromer-recruiting RAB7 have been shown to cause Charcot-Marie-Tooth (CMT) hereditary neuropathy, a disease characterized by the weakness and wasting of the distal limbs (Verhoeven et al. 2003).

Finally, mutations in the retromer-binding SORCS2 have been shown to be associated with schizophrenia and bipolar disorder (Ollila et al. 2009; Christoforou et al. 2011).

1.3 Amyotrophic Lateral Sclerosis

Amyotrophic lateral sclerosis (ALS), also known as Lou Gherig's disease, is the most common adult-onset paralytic disorder, with a mean age of onset of roughly 65 years (Chio et al. 2013; Rowland and Shneider 2001). ALS results in the axonal retraction and degeneration of both upper and lower motor neurons (MN), located in the brain and spinal cord (SC), which control skeletal muscle movement (Rowland and Shneider 2001). This results in patients suffering from progressive muscle weakness, paralysis, and finally death from respiratory failure within a median of 3-5 years after diagnosis (Rowland and Shneider 2001; Mizutani et al. 1992). Affecting roughly two out of every 100,000 people every year, ALS is the third most common neurodegenerative disorder after AD and PD, and due to the high mortality of the disease, the total amount of people affected by ALS is not much higher with about 5 people per 100,000 living with the disease (Mehta et al. 2016).

Particularly given the lethality of the disease, treatments for ALS have been aggressively pursued in the medical field, but thus far, no cure for the disease has been found. The only FDA-approved drugs to treat ALS are riluzole and edaravone (Miller et al. 2007; 'Safety and efficacy of edaravone in well defined patients with amyotrophic lateral sclerosis: a randomised, double-blind, placebo-controlled trial' 2017). However, the effects of these treatments are fairly modest with riluzole extending life expectancy by merely two months and edaravone slightly slowing the progression of disease symptoms, but showing no clear extension of life expectancy (Miller et al. 2007; 'Safety and efficacy of edaravone in well defined patients with amyotrophic lateral sclerosis:

a randomised, double-blind, placebo-controlled trial' 2017; Ito et al. 2008). While uncommon in the United States, mechanical ventilation has also been used to extend the life of ALS patients up to 6 years, but this does not result in any modification of the disease pathology (Dybwik et al. 2010; Tagami et al. 2014).

1.3.1 Clinical features of ALS

1.3.1.1 Symptoms and diagnosis of ALS

The symptoms of ALS are multiple, and are generally split into those caused by upper MN degeneration and those caused by lower MN degeneration. In general, these can be distinguished as symptoms that result from an inability to control the muscle of the muscle as opposed to those caused by an inherent weakness, respectively. Some common examples of upper MN symptoms include exaggerated reflexes, spasticity, and the presence of inappropriate, sudden, and uncontrollable laughing or crying, a syndrome known as pseudobulbar affect. Two tests that show degeneration of upper MNs include the lower limb Babinski sign—the reflexive extension as opposed to the normal flexion of the toe upon plantar stimulation of the foot—and the corresponding upper limb Hoffman sign—the reflexive flexion of the thumb and index fingers upon the flicking of the fingernail of the middle finger. Some of the more common lower MN symptoms include muscle weakness, muscle atrophy, and small, involuntary twitching of the muscle known as a fasciculation. The most common initial presentation of ALS is asymmetric weakness of the limbs, often found due to an inability to perform an ordinary task involving fine motor skills of the finger (Swinnen and Robberecht 2014).

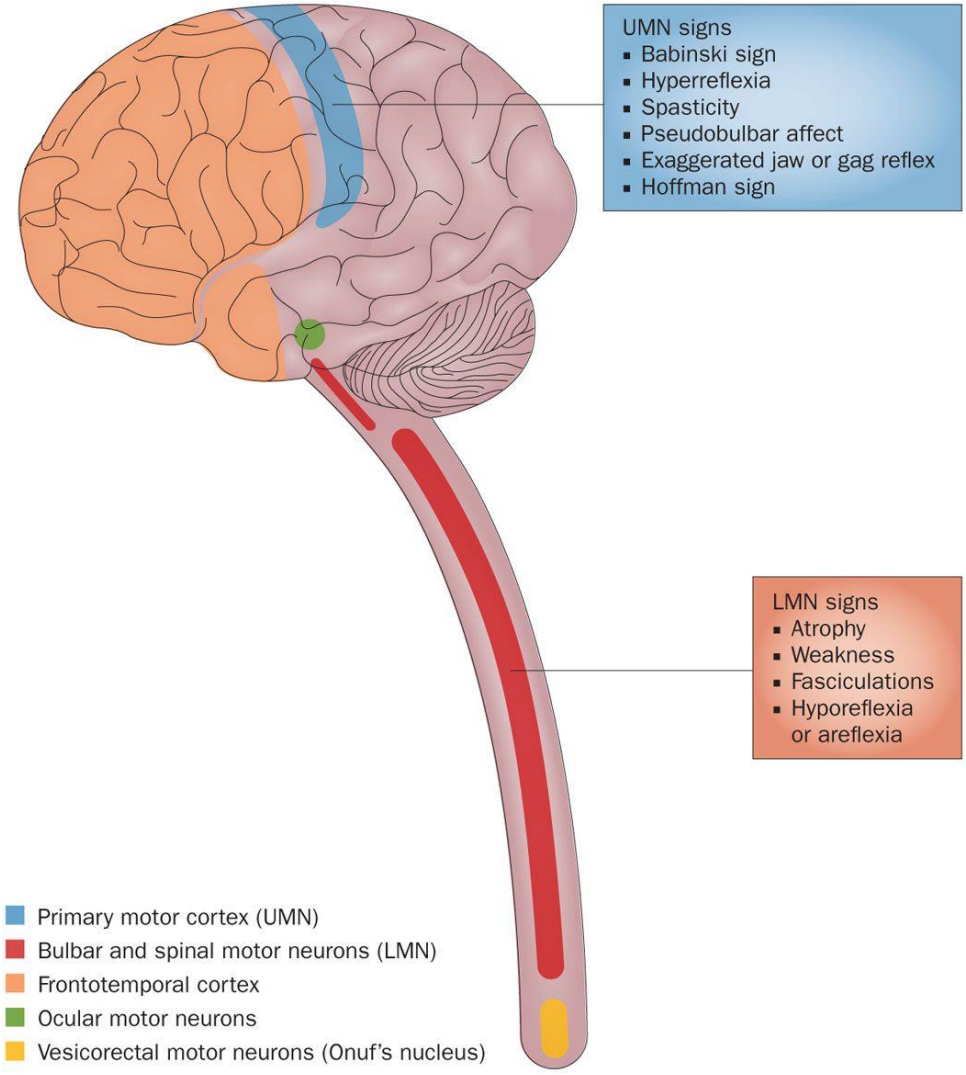

Figure 1.7 Symptoms of ALS by Origin of Degeneration

Reproduced from (Swinnen and Robberecht 2014)

The symptoms of ALS can be further divided by which segment of the body, and thus which group of neurons are affected. Namely, these are the bulbar region, which is innervated by a subset of cranial nerves, and the cervical, thoracic, and lumbrosacral regions, which are innervated by the respective sections of the SC. The diagnosis of ALS is dependent on evidence of the degeneration of both upper and lower MNs, through either symptomatic or

electrophysiologic evidence, which progresses over the course of months or years to multiple segments of the body (de Carvalho et al. 2008; Costa, Swash, and de Carvalho 2012; Brooks 1994). As there is no diagnostic test that can definitively confirm or exclude the diagnosis of ALS, diagnosis also requires the exclusion of other diseases that may cause similar symptomatology via neuroimaging, laboratory testing, and electromyography, among other tests.

The presence of certain symptoms not associated to ALS may also help to exclude it. Some such symptoms include, sensory loss, involuntary movement, cerebellar ataxia, autonomic dysfunction, and the involvement of the ocular or anal sphincter muscles, the only skeletal muscles that are not affected by ALS except in rare cases of ventilator-supported longstanding disease (Swinnen and Robberecht 2014). However, the presence of one or more of these symptoms in the context of what would otherwise be diagnosed as ALS is considered to indicate what is known as an ALS-plus syndrome.

Cognitive and psychiatric symptoms do not exclude the diagnosis of ALS, as FTD, a disease that results in behavioural and cognitive changes, co-occurs in about 10% of ALS patients (ALS-FTD) (Lomen-Hoerth 2004; Ferrari et al. 2011). This association has lead to the re-thinking of ALS and FTD not as distinct diseases, but rather as a spectrum of disease. Indeed genetic mutations that are associated with ALS—a topic that I will expand on in a later section—are often also associated with FTD (Guerreiro, Bras, and Hardy 2015).

1.3.1.2 Motor neuron disease and clinical variants of ALS

While ALS is often used interchangeably with the term “motor neuron disease” (MND), it is important to note that ALS is actually one of a set of MNDs. MNDs are characterized by the degeneration of a combination of upper and/or lower MNs, resulting in a combination of upper

and/or lower MN symptoms. ALS is distinguished as involving both upper and lower MNs which innervate muscles in the entire body. While other MNDs often progress to true ALS, this is not always the case, and a patient with an MND may never develop ALS. When conversion to ALS does happen, the case is given a designation as a particular clinical variant of ALS.

MND patients that present with only lower MN symptoms are diagnosed with progressive muscular atrophy (PMA). These patients have a higher median survival than patients with ALS by about 1 year (Kim et al. 2009; Visser et al. 2007). While most patients with PMA never develop upper MN symptoms, roughly 20% of patients do, and those that do not often present with upper MN pathology on post-mortem analysis identical to that found in ALS (Kim et al. 2009; Ince et al. 2003; Tsuchiya et al. 2004). When a patient with PMA develops upper MN symptoms, they are re-diagnosed as having lower motor neuron-onset ALS.

The converse of PMA is primary lateral sclerosis (PLS), which presents with symptoms of upper, but not lower MN degeneration. Patients with PLS have a significantly higher life expectancy than those with ALS by about 7 years, but unlike with PMA, the majority of patients diagnosed with PMA eventually progress to ALS (Gordon et al. 2006; Tartaglia et al. 2007). When this occurs, the patient is said to have upper motor neuron-onset ALS, which has a life expectancy between that of PLS and classic ALS (Gordon et al. 2006).

Unlike with PMA and PLS, patients with the MND known as progressive bulbar palsy (PBP) show symptoms of both upper and lower MN degeneration. However, in these patients, these symptoms are confined to muscles innervated by the cranial nerves, such as those that control chewing, swallowing, speaking, and facial expression. While patients occasionally do not progress to ALS from PBP, almost all do, so studies in pure PBP are scant (Karam, Scelsa, and Macgowan 2010). ALS that develops from patients with PBP is known as bulbar-onset ALS. While bulbar-

onset ALS is significantly less common than spinal-onset ALS—where symptoms begin in the arms and legs—, it results in a faster and more severe progression of the disease (Al-Chalabi et al. 2016; Swinnen and Robberecht 2014).

1.3.2 Neuropathology of ALS

1.3.2.1 Gross neuronal degeneration and gliosis

As mentioned above, the primary finding in the neuropathology of ALS is the loss of upper MN in the motor cortex and lower MN in the SC. These degenerated neurons are replaced by glial scar tissue from reactive astrocytes and microglia: the sclerosis referred to in "amyotrophic lateral sclerosis" (Ekblom et al. 1994; Schiffer et al. 1996; Murayama et al. 1991; Saberi et al. 2015; McGeer and McGeer 2002). Degenerating neurons in ALS that have not yet been lost are seen to display a reduction in size as well as vacuolization and fragmentation of the Golgi apparatus (Saberi et al. 2015; Gonatas, Stieber, and Gonatas 2006; Gonatas, Gonatas, and Stieber 1998; Okamoto et al. 1990).

As upper MNs in the motor cortex are lost, so too, on pathological analysis, can the atrophy and subsequent gliosis of the corticospinal tract along which their axons travel be seen. These changes in white matter are sometimes visible in the magnetic resonance imaging (MRI) of patients (Rajagopalan et al. 2013; Kassubek et al. 2005; Roccatagliata et al. 2009). Similarly, as lower MNs in the ventral horn of the SC are lost, so too do the motor nerves along which their axons travel atrophy with the loss of the MN fibers (Sobue et al. 1981; Nodera et al. 2014). Interestingly, an approximately 30% decrease in the density of sensory neuronal fibers that travel along the SC white matter has also been seen, though this does not seem to result in any noticeable clinical pathology (Bradley et al. 1983).

Interestingly, in ALS patients that exhibit symptoms of dementia, gross atrophy of the frontal and/or temporal cortex can be seen, which is particularly pronounced in patients that have been diagnosed with ALS-FTD (Chang et al. 2005; Murphy et al. 2007)

1.3.2.2 Inclusion bodies

As with most neurodegenerative diseases, one of the hallmarks of the neuropathology of ALS, besides the actual degeneration of neurons, is the presence of protein aggregates, termed inclusion bodies due to their presence within the degenerating neurons and the surrounding reactive astrocytes (Barbeito et al. 2004; Saberi et al. 2015). There are a number of different types of inclusions classified by their morphology, reactions to histologic stains, and particularly, their immunoreactivity for several given proteins (Saberi et al. 2015).

Bunina bodies are ubiquitin-negative inclusions found in the cell bodies of lower MN in the majority of ALS cases, and only rarely in upper MN. They are seen on hematoxylin and eosin (H&E) staining as small (3–6 μm), rounded, eosinophilic bodies found either independently or in chain-like formations (Piao et al. 2003). Immunostaining of Bunina bodies shows the inclusion of cystatin C, transferrin, and sometimes, the intermediate filament peripherin and SORCS2 (Mizuno et al. 2011; Okamoto et al. 1993; Mori et al. 2015). Bunina bodies are notable for being exclusively associated with ALS, though their role in the pathophysiology of the disease is unknown (Okamoto, Mizuno, and Fujita 2008).

Skein-like inclusions are cytoplasmic inclusions that take the form of loose filamentous bundles that are roughly 15-20nm in diameter (Robinson et al. 2013). They are the most commonly found inclusions in ALS most often seen in both upper and lower MNs, though frequently also found in glial cells (Arai et al. 2003). Skein-like inclusions are mainly characterized by their

immunoreactivity to ubiquitin and transactivation response DNA protein-43 (TDP-43), though they may also contain aggregated fused in sarcoma protein (FUS), superoxide dismutase 1 (SOD1), and p62 (Robinson et al. 2013; Arai et al. 2003; Sumi et al. 2009; Deng et al. 2010). Interestingly, TDP-43- and FUS- positive inclusions are also often found in FTD, further providing evidence for the connection between ALS and FTD (Geser, Lee, and Trojanowski 2010). However, it is important to note that TDP-43-positive inclusions are not unique to ALS and FTD, as they have also been found in a number of other neurodegenerative disorders (Amador-Ortiz et al. 2007; Higashi et al. 2007; Nakashima-Yasuda et al. 2007; Hasegawa et al. 2007; McKee et al. 2010).

1.3.3 Familial ALS and associated mutations

While ALS is mainly sporadic in origin (sALS), it presents in a familial (fALS) form in about 10% of patients as a result of inherited gene mutations (Byrne et al. 2011; Taylor, Brown, and Cleveland 2016). Despite the tendency for patients with fALS to display a relatively earlier onset of disease and a faster course, fALS and sALS are clinically indistinguishable and share or overlap in most neuropathological findings. Namely, post-mortem neuropathology has found SOD1- and TDP-43-positive inclusion in tissues from both fALS and sALS patients (Arai et al. 2006; Bosco et al. 2010; Forsberg et al. 2010; Kato et al. 2000; Shibata et al. 1994). Thus, it is expected that they share pathogenic mechanisms.

fALS is usually inherited in an autosomal dominant fashion, though some mutations display an autosomal recessive or X-linked inheritance pattern (Ince et al. 2011). The mutation of a growing number of genes—currently over 25—have been linked to ALS (Nguyen, Van Broeckhoven, and van der Zee 2018). However, these account for only about two thirds of fALS cases (Renton, Chio, and Traynor 2014). Interestingly, de novo mutations in these genes—mostly

the repeat expansion mutation in chromosome 9 open reading frame 72 (C9orf72)—also account for over 10% of non-inherited sALS cases (Renton, Chio, and Traynor 2014; Taylor, Brown, and Cleveland 2016; Alsultan et al. 2016). The genes currently known to be involved in ALS have been outlined in Table1.1. In later sections, I will discuss the functions and possible contributions to ALS pathology of some of these. However, it is worth noting that of these ALS-associated genes, those whose mutations cause the highest percentage of fALS cases are C9orf72 (~30%), SOD1 (~20%), the TDP-43-encoding TARDBP (~5%), and FUS (~5%) (Taylor, Brown, and Cleveland 2016; Alsultan et al. 2016). Of note, the expansion mutation of C9orf72 is also the mutation most frequently associated not only to ALS, but also to FTD (DeJesus-Hernandez et al. 2011; Renton et al. 2011).

Table 1.1: ALS-associated genes

Gene Locus	Chromosomal Location	Gene	Onset	Inheritance Pattern	Reference(s)
ALS1	21q22.11	*SOD1*	Adult	AD, AR	(Rosen et al. 1993; Andersen 2006)
ALS2	2q33.1	*ALS2*	Juvenile	AR	(Hadano et al. 2001; Yang et al. 2001)
ALS3	18q21	Unknown	Adult	AD	(Hand et al. 2002)
ALS4	9q34.13	*SETX*	Juvenile	AD	(Chen et al. 2004)
ALS5	15q21.1	*SPG11*	Juvenile	AR	(Orlacchio et al. 2010)
ALS6	16p11.2	*FUS*	Adult	AD, AR	(Vance et al. 2009; Kwiatkowski et al. 2009)
ALS7	20p13	Unknown	Adult	AD	(Sapp et al. 2003)
ALS8	20q13. 32	*VAPB*	Adult	AD	(Nishimura et al. 2004; Millecamps et al. 2010)
ALS9	14q11.2	*ANG*	Adult	AD	(Greenway et al. 2006)
ALS10	1p36.22	*TARDBP*	Adult	AD	(Sreedharan et al. 2008; Kirby et al. 2010)
ALS11	6q21	*FIG4*	Adult	AD	(Chow et al. 2009)
ALS12	10p13	*OPTN*	Adult	AD, AR	(Maruyama et al. 2010)
ALS13	12q24.12	*ATXN2*	Adult	AD	(Elden et al. 2010)
ALS14	9p13.3	*VCP*	Adult	AD	(Johnson et al. 2010)

ALS15	Xp11.21	*UBQLN2*	Adult	X-LD	(Deng et al. 2011)
ALS16	9p13.3	*SIGMAR1*	Juvenile	AD, AR	(Luty et al. 2010; Al-Saif, Al-Mohanna, and Bohlega 2011)
ALS17	3p11.2	*CHMP2B*	Adult	AD	(Parkinson et al. 2006; Cox et al. 2010)
ALS18	17p13.2	*PFN1*	Adult	AD	(Wu et al. 2012)
ALS19	2q34	*ERBB4*	Adult	AD	(Takahashi et al. 2013)
ALS20	12q13.13	*hnRNPA1*	Adult	AD	(Kim et al. 2013)
ALS21	5q31.2	*MATR3*	Adult	AD	(Johnson et al. 2014)
ALS22	2q35	*TUBA4A*	Adult	AD	(Smith et al. 2014)
ALS23	10q22.3	*ANXA11*	Adult	AD	(Smith et al. 2017)
ALS24	4q33	*NEK1*	Adult	N/A	(Brenner et al. 2016; Kenna et al. 2016)
ALS25	12q13.3	*KIF5A*	Adult	AD	(Nicolas et al. 2018; Brenner et al. 2018)
FTDALS1	9p21.2	*C9ORF72*	Adult	AD	(Renton et al. 2011; DeJesus-Hernandez et al. 2011)
FTDALS2	22q11.23	*CHCHD10*	Adult	AD	(Bannwarth et al. 2014)
FTDALS3	5q35.3	*SQSTM1*	Adult	AD	(Fecto et al. 2011)
FTDALS4	12q14.2	*TBK1*	Adult	AD	(Cirulli et al. 2015)
IBMPFD2	7p15.2	*HNRNPA2B1*	Adult	AD	(Kim et al. 2013)
Unnamed	21q22.3	*C21orf2*	Adult	N/A	(van Rheenen et al. 2016)
Unnamed	16p13.3	*CCNF*	Adult	AD	(Williams et al. 2016)
Unnamed	2p13.3	*TIA1*	Adult	AD	(Mackenzie et al. 2017)

This table outlines the currently known genes whose mutations have been found to be associated with ALS. AD, autosomal dominant; AR, autosomal recessive; X-LD, X-linked; N/A, not available.

1.3.4 Mouse models of ALS

A significant amount of work has gone into the production of relevant mouse models of ALS to study the disease. These involve transgenic and knockin mutations in many of the most common ALS-associated genes. However, few have been able to reproduce the severe pathophysiology and lethality found in the human disease. Here, I will describe some of the genetic ALS mouse models that are most relevant to the work done in this thesis.

1.3.4.1 Mutant SOD1 mouse

At least 12 different human ALS-causing SOD1 mutants have been transgenically overexpressed in mice to create models of ALS (Turner and Talbot 2008). The most widely used and characterized model of ALS is the one of these that overexpresses the $SOD1^{G93A}$ mutant (Gurney et al. 1994). The reason this model is the preeminent model of study in the field is that it most closely exhibits the pathology of human ALS, including the progressive loss of over 40% of the MNs in the lumbar spinal cord, extensive denervation of neuromuscular junctions (NMJ), resulting in progressive weakness and ultimately fatality within 4-5 months of age. However, while the $SOD1^{G93A}$-Tg mouse does an excellent job of reproducing the lower MN pathology of ALS, it is important to note that it does not show any evidence of degeneration of upper MN.

While the $SOD1^{G93A}$ mutation is relatively uncommon in fALS, its use in the study of ALS is helpful in that it retains the normal enzymatic activity of SOD1, providing evidence that the pathology seen is due to the toxic gain of function of the mutation rather than the loss of function of the enzyme. What this gain of function may be is explored further in following sections. As will be evident, but is worth noting here, the molecular disease mechanisms of ALS are also very closely replicated in the $SOD1^{G93A}$-Tg mouse, including the development of protein inclusions and gliosis in affected areas (Nardo et al. 2016).

One caveat to this mouse model is the fact that the progression of the disease is sensitive to the transgene copy number. The mouse model generally expresses 15-20 copies of the transgene, and the breeding of the mouse can result in spontaneous deletion of copy number, which causes amelioration of the disease and must be accounted for in studies that involve extensive breeding (Lutz 2018; Zwiegers, Lee, and Shaw 2014). It is also important to note, that while the pathology that develops in these mice is understood to be due to the mutation of SOD1, the comparable

overexpression of wild-type SOD1 (wtSOD1) can cause axonopathy in mice, though nowhere near the level found in $SOD1^{G93A}$-Tg mouse (Joyce et al. 2011).

The progression of disease in this model is also sensitive to the background strain of the mouse in which the transgene is expressed. Namely, the $SOD1^{G93A}$ mutation is most commonly used in the C57BL/6J background or in the mixed B6/SJL background, which exhibit an average survival of 5 and 4 months, respectively (Heiman-Patterson et al. 2005).

1.3.4.2 Mutant FUS mouse

There is a sustained interest and effort in the field to develop mouse models of ALS that are not reliant on the mutation of SOD1 (Morrice, Gregory-Evans, and Shaw 2018). While the SOD1 mouse models do model ALS well and have been proven to follow the pathogenic traits of disease found in humans, a diversity of models would be useful, particularly to study pathogenic effects of ALS not usually associated with SOD1 such as RNA mishandling. To that end, mice that transgenically express ALS-causing mutations in TARDBP, FUS, and C9orf27 have been strongly pursued (Funikov et al. 2018; Sharma et al. 2016; Stephenson and Amor 2017).

Two such models of FUS mutation were fairly recently developed in one study (Sharma et al. 2016). One expresses FUS^{R521C}, a mutant protein that causes typical adult-onset ALS in patients, and one expresses FUS^{P525L}, a mutant that causes a much more aggressive, juvenile form of ALS (Conte et al. 2012; Vance et al. 2009). The authors of the study that made these mouse models showed that both show evidence of progressive ALS-like disease over the course of 3 years. Furthermore, the rate of progression of disease pathology is consistent with the severity of disease that each mutant causes in humans. That is to say, both display a progressive loss of MNs in the SC, mislocalization of FUS to the cytoplasm in MNs, and denervation of muscles, with the

FUS^{P525L}-Tg model displaying a more severe degree of all three parameters. Indeed, the FUS^{P525L}-Tg model also displays a decrease in motor function at 3 years of age.

Since the mice were initially designed to express the protein under the condition of the excision by Cre-recombinase of a transcriptional STOP signal, the authors were also able to specifically express the FUS mutants in MNs, which they demonstrated was sufficient to cause neurodegeneration. Finally, they also showed that neither the MN-specific deletion of Fus in the mouse nor the transgenic expression of wild-type FUS produced similar pathogenic effects, showing that the ALS-like disease in these mice was specific to a gain-of-function ALS-causing mutation in FUS.

1.3.4.3 Wobbler mouse

The wobbler mouse is a mouse with an autosomal recessive genetic mutation that arose spontaneously in 1956 in the Institute of Animal Genetics of Edinburgh, and exhibits MN degeneration, and associated motor symptoms, giving rise to its name (Falconer 1956). This mutation was later found to be a missense L967Q mutation in Vps54, one of four subunits of the Golgi-associated retrograde protein (GARP) complex (Schmitt-John et al. 2005). The GARP complex is one of numerous complexes involved in the tethering of incoming retrograde vesicles from the endosome to the TGN (Perez-Victoria et al. 2010). The $Vps54^{L967Q}$ mutation results in the destabilization of the GARP complex and, as such, the breakdown of endosomal transport in degenerating MNs (Palmisano et al. 2011; Karlsson et al. 2013).

It is important to note that no mutations in VPS54, or indeed any components of the GARP complex have been associated to ALS in humans (Meisler et al. 2008). However, the similarities in the disease progressions of ALS and the wobbler mouse have still made it an intriguing model

in the study of ALS. The wobbler mouse exhibits various hallmarks of ALS pathophysiology, including hyperreflexia, progressive muscle weakness, and respiratory failure resulting from the degeneration of both upper and lower MN, ending in premature fatality by 16 months (Duchen and Strich 1968; Boillee, Peschanski, and Junier 2003). Furthermore, the wobbler mouse also reproduces a number of the disease mechanisms seen in ALS, including protein aggregation, gliosis, and many of the mechanisms outlined below (Duchen and Strich 1968; Moser, Bigini, and Schmitt-John 2013; Dennis and Citron 2009).

1.3.5 Disease mechanisms of ALS

A unifying theory of the mechanistic cause of neurodegeneration in ALS has proven to be elusive. Through a combination of the study of models of ALS and the analysis of disease-associated genes, disturbances in the normal function of numerous cellular and molecular pathways have been shown to be associated to ALS. While none have been proven to be the definitive cause of neurodegeneration in the disease, it is possible that any, or indeed any combination of such disturbances may contribute to the pathogenesis of ALS. Here, I will describe some of the mechanisms which have been shown to possibly be involved in ALS.

1.3.5.1 Proteinopathy

The presence of abnormal intracellular protein aggregates in ALS implies that they are either a consequence or a cause of dysfunction in the disease. The fact that three of the most common genes whose mutations cause ALS encode proteins that are found in inclusion bodies associated with ALS—SOD1, TARDBP, and FUS—further indicates that this proteinopathy is important in the disease. Indeed, it has been shown that one of the main effects of ALS-causing

mutations in these three proteins is their propensity to misfold and aggregate (Nomura et al. 2014; Scotter, Chen, and Shaw 2015; Prasad et al. 2019). However, how the formation of these protein aggregate may result in disease pathology is a poorly understood phenomenon.

The ability of heat shock proteins (HSP) to ameliorate ALS pathology via the reduction of protein aggregates provides strong evidence that protein aggregation acts as a toxic mechanism in ALS. HSPs are chaperone proteins which have an important role in maintaining cellular proteostasis and ensuring the correct folding of proteins in the cell (San Gil et al. 2017; Neef, Jaeger, and Thiele 2011). In one study, the levels of HSPs as well as those of heat shock factor 1 (HSF1), the major transcription factor for HSPs, were shown to be decreased in neuronal tissues from ALS patients as well as from a TDP-43 transgenic mouse model of ALS (Chen et al. 2016). Furthermore, the *in vitro* activation and inhibition of HSF1 were shown to decrease and increase, respectively, the aggregation of TDP-43. The HSF1-induced decrease of protein aggregation was then shown to rescue the cytotoxic effects of TDP-43 overexpression. In another, similar study, SC tissues from $SOD1^{G93A}$-Tg displayed a decrease in chaperone activity (Bruening et al. 1999). Primary motor neurons from this same model were then shown *in vitro* to display a decrease in protein aggregation as well as a prolonged survival in response to the overexpression of HSP70. In response to the evidence that HSP-mediated solubilization of protein aggregates can rescue neuronal toxicity in the context of ALS, therapies have ben developed to target the up-regulation of HSPs in patients, one—arimoclomol—of which is currently in phase III clinical trials, following promising phase II trials (McDermott 2019; Benatar et al. 2018).

A prion-like model for the inter-cellular spread of disease has become increasingly popular in multiple neurodegenerative disorders, including ALS (Brundin, Melki, and Kopito 2010; Zhang, Nie, and Chen 2018; Frost and Diamond 2010). In prion diseases, such as Creutzfeldt–Jakob

disease (CJD), a protein normally found in the cell is misfolded in such a way that it creates a seed that causes other proteins of the same type to similarly misfold and aggregate. This results in insoluble aggregates that move from cell to cell, causing neurodegeneration (Baldwin and Correll 2019). Evidence for the prion-like hypothesis has been presented in ALS involving the *in vitro* transmission of misfolded SOD1 between cells (Grad et al. 2014; Munch and Bertolotti 2011). More recently, since TDP-43 aggregates are more common in ALS, the prion-like potential of TDP-43 has been further explored, and the seeding of TDP-43 aggregates *in vitro* has resulted in the formation of increased TDP-43 aggregates in cells (Feiler et al. 2015; Smethurst et al. 2016; Nonaka et al. 2013). Furthermore, the fact that FUS and TDP-43 contain low complexity domains similar to prion domains in yeast, and that a number of ALS-causing mutations are found in said domains has provided further evidence for this model (Harrison and Shorter 2017).

1.3.5.2 RNA transport and metabolism

The fact that both FUS and TDP-43 contain RNA-binding domains, and are heavily involved in the processing of RNA has raised interest in the possibility that the pathogenesis of ALS involves the misregulation of RNA (Buratti and Baralle 2001; Winton, Igaz, et al. 2008; Buratti and Baralle 2008; Colombrita et al. 2012; Iko et al. 2004). Indeed, while both of these proteins function and are normally found in the nucleus, ALS-associated mutations in both of them result in their sequestration in the cytoplasm, where they cannot carry out their normal function (Dormann et al. 2010; Vance et al. 2009; Van Deerlin et al. 2008; Winton, Van Deerlin, et al. 2008). Furthermore, studies in *in vitro* as well as *in vivo* models of ALS have shown that the reduced expression of both of these genes as well as the expression of their mutated forms results in both a neurodegenerative phenotype and wide-ranging changes in the RNA-expression profiles

of affected cells (Kabashi et al. 2010; Vaccaro et al. 2012; Polymenidou et al. 2011; Shiga et al. 2012; Alami et al. 2014; Lagier-Tourenne et al. 2012; Nakaya et al. 2013; Scekic-Zahirovic et al. 2016; De Santis et al. 2017). Other known ALS-associated genes known to have functions in RNA processing include ataxin-2 (ATXN2), heterogeneous nuclear ribonucleoprotein A1 (hnRNPA1), heterogeneous nuclear ribonucleoprotein A2 B1 (hnRNPA2 B1), matrin 3 (MATR3), T-cell-restricted intracellular antigen-1 (TIA1), senataxin (SETX), and angiogenin (ANG) (Ostrowski, Hall, and Mekhail 2017; Dreyfuss et al. 1993; Alarcon et al. 2015; Coelho et al. 2015; Forch et al. 2000; Yamasaki et al. 2009; Bennett and La Spada 2018).

The hexanucleotide expansion of C9orf72 has also been shown cause the RNA product of the gene to form RNA foci (Gendron et al. 2013). Such foci have been shown to bind and sequester RNA-binding proteins, including TDP-43 and FUS, thus causing alterations in RNA metabolism (Simon-Sanchez et al. 2012; Donnelly et al. 2013; Lee et al. 2013; Mori et al. 2013; Bajc Cesnik et al. 2019). Finally, while SOD1 does not contain an RNA-binding domain normally, evidence has shown that the misfolding of mutant SOD1 may cause it to abnormally bind to certain mRNAs, altering their expression profiles (Lu et al. 2007; Chen et al. 2014).

1.3.5.3 Endoplasmic reticulum stress

The excessive accumulation of proteins in the endoplasmic reticulum (ER) causes ER stress, inducing a signaling pathway known as the unfolded protein response (UPR), which maintains proteostasis by promoting proper folding and degradation of proteins (Wang and Kaufman 2014; Walter and Ron 2011). However, should the UPR fail to maintain proper proteostasis over an extended period of time, it instead initiates an apoptotic cascade leading to cell death (Schroder and Kaufman 2005; Oakes and Papa 2015).

Studies in tissues from both sALS patients and from the SOD1^{G93A}-Tg mouse model have shown an increase in MN and glial ER stress, abnormal morphology of the ER, and the detachment of ribosomes from the rough ER (rER) (Lautenschlaeger, Prell, and Grosskreutz 2012; Dal Canto and Gurney 1995; Oyanagi et al. 2008; Atkin et al. 2008; Jaronen et al. 2013). In fact, the presence of ER stress in SOD1^{G93A}-Tg mice precedes the onset of ALS symptoms, indicating an involvement in the early pathogenesis of disease (Saxena, Cabuy, and Caroni 2009; Tobisawa et al. 2003; Dal Canto and Gurney 1995). While evidence of ER stress involvement in ALS has mostly focused on the effect of mutant SOD1, it has been shown that mutations in TDP-43, FUS, and C9orf72 are also associated with an increase in ER stress (Dafinca et al. 2016; Walker et al. 2013; Wang, Zhou, et al. 2015; Farg et al. 2012; Atkin et al. 2008). Furthermore, the mutation of sigma non-opioid intracellular receptor 1 (SIGMAR1), an ER chaperone that is highly expressed in MNs and regulates the flux of calcium between the ER and the mitochondria, is known to cause a juvenile form of ALS (Al-Saif, Al-Mohanna, and Bohlega 2011; Ruscher and Wieloch 2015; Mavlyutov et al. 2010). One study has also pointed to a possible role of vesicle-associated membrane protein-associated protein B (VAPB) in the UPR (Suzuki et al. 2009).

1.3.5.4 Mitochondrial dysfunction

The proper maintenance of mitochondrial function is crucial in the function of the mammalian cell, particularly in the energetically costly neuron (Nicholls and Budd 2000; Engl and Attwell 2015). The vacuolization and fragmentation of mitochondria is one of the hallmarks of a degenerating MN in ALS, and has been consistently found in the pathology of ALS patients as well as in cell and animal models of ALS (Sasaki and Iwata 2007; Hong et al. 2012; Magrane et al. 2014; Wang, Li, et al. 2013; Vande Velde et al. 2011). The fact that the disruption of the

mitochondrial structure is a mechanism of disease in ALS is supported by the fact that mutations in coiled-coil-helix-coiled-coil-helix domain containing 10 (CHCHD10), a protein located at the contact sites between the outer and inner membrane of the mitochondria, disrupt the mitochondrial cristae structure, causing ALS (Bannwarth et al. 2014; Genin et al. 2016).

The balance and correct regulation of mitochondrial fission and fusion is paramount to mitochondrial health, as fusion allows them to dilute any defects in any individual mitochondrion, and fission allows for the sequestration and elimination of said defects through mitophagy—macroautophagy that engulfs and degrades mitochondria (Westrate et al. 2014). However, as noted above, the balance is heavily weighted towards fission in the context of ALS, and ALS-causing mutations are known to result in fragmented mitochondria via the dysregulation of the proteins that regulate fusion (Ferri et al. 2010; Wang, Li, et al. 2013). Defects in mitophagy further contribute to the disruption in mitochondrial quality control, as Parkin, a major regulator in marking mitochondria for mitophagy, has been shown to be regulated by TDP-43 and FUS. Indeed, decreased levels of Parkin have been shown in sALS patient MNs as well as upon the loss of TDP-43 or FUS in mice (Lagier-Tourenne et al. 2012). Mitochondrial dynamics in ALS are further disrupted via the impaired axonal transport of mitochondria, which is seen in multiple ALS mouse models as well as in patient samples (Sasaki and Iwata 2007; Magrane et al. 2014; Bilsland et al. 2010; Shan et al. 2010). Due to the exceptionally long axons of MNs, they are likely exceptionally sensitive to defects in mitochondrial trafficking, and an inability for mitochondria to arrive to and function at axon ends results in a lack of support for the axon terminal, and therefore, axon retraction. The mechanism for how mitochondrial transport disruption is not certain, but it is known that kinesin family member 5A (KIF5A) regulates the anterograde transport of mitochondria, and that its mutation can cause ALS (Campbell et al. 2014; Nicolas et al. 2018).

Studies have shown that besides the dysregulation of mitochondrial dynamics, dysfunction in the mitochondria occurs via multiple axes, including defects in the electron transport chain and in calcium buffering, and the production of reactive oxygen species (ROS). Mutations in SOD1, TDP-43, and FUS have been shown to localize the proteins to mitochondria, where they disrupt and decrease the efficiency of the ETC, such that the mitochondria cannot meet the energy requirements of the neuron (Ferri et al. 2006; Wang, Wang, Lu, et al. 2016; Deng et al. 2015). ROS are a by-product of the ETC which, while normally reduced by enzymes in the cell—including SOD1 among others—, can, left unchecked, cause oxidative damage to nucleotides, proteins, and lipids in the cell and, particularly, the mitochondria (Murphy et al. 2008; Kim et al. 2015). Increased levels of ROS and oxidative damage have been widely reported in patient samples as well as various models of ALS (Mitsumoto et al. 2008; Smith et al. 1998; Shaw et al. 1995; Shibata et al. 2001; Chang et al. 2008; Hong et al. 2012; Deng et al. 2015). Finally, a dysregulation in calcium homeostasis has been reported across multiple models of ALS as well as in patient tissues (Damiano et al. 2006; 1997; Morotz et al. 2012; Siklos et al. 1996; Van Den Bosch et al. 2000). This has been attributed to the loss of contact sites between mitochondria and the ER, known as mitochondria-associated ER membranes (MAM), which allow the exchange of calcium between the two organelles (Stoica et al. 2014; Bernard-Marissal et al. 2015; Manfredi and Kawamata 2016). As noted above, the ALS-associated gene SIGMAR1 is known to regulate the flux of calcium at the MAM.

1.3.5.5 Glutamate excitotoxicity

Classically, the AMPA glutamate receptor has been typified as being calcium-impermeable and inducing activation through permeability of sodium. However, AMPA receptors missing the

GluR2 subunit have been shown to be calcium-permeable, thus bringing calcium into the cell upon their activation by glutamate (Isaac, Ashby, and McBain 2007; Williams et al. 1997). These GluR2-deficient AMPA receptors have been shown to be relatively highly expressed in MNs. Excitotoxicity is then caused when the excessive activation of these receptors results in a build-up of abnormal levels of calcium in the cell, which has a number of downstream toxic effects (Corona and Tapia 2007; Kawahara et al. 2003). Glutamate excitotoxicity has been highly implicated in ALS. Indeed, riluzole, one of the only drugs used to treat ALS, is a known glutamate inhibitor (Andreadou et al. 2008; Fumagalli et al. 2008). Two mechanisms have been proposed whereby glutamate excitotoxicity may be induced in ALS.

First, an increase in the basal levels of glutamate would cause excitotoxicity through the continual re-activation of AMPA receptors. Evidence for this possibility has shown that levels of glutamate are increased in the plasma of ALS patients, and glutamate-receptor antagonism can rescue the excitotoxic effect of cerebrospinal fluid (CSF) from patients on neuronal cultures (Sen et al. 2005; Andreadou et al. 2008). One of the main proposed mechanisms of how glutamate builds up in ALS involves the failure of astrocytes to clear glutamate. Normally, astrocytes clear glutamate from the extracellular space via the glutamate transporter excitatory amino acid transporter 2 (EAAT2) (Robinson 1998). However, EAAT2 expression has been shown to be decreased in the context of ALS, both in patients and in various mutant SOD1 mouse models, resulting in defects in glutamate clearance (Lin et al. 1998; Bendotti et al. 2001; Canton et al. 1998; Warita et al. 2002). Furthermore, the overexpression of EAAT2 in $SOD1^{G93A}$-Tg mice has shown to slow disease progression (Guo et al. 2003).

The second possible mechanism of glutamate toxicity in ALS is the result of the inherent hyperexcitability of the MNs themselves. Indeed, the circuitry of MNs in both ALS patients and

SOD1^{G93A}-Tg mice has shown hyperexcitable disturbances (Vucic and Kiernan 2013; van Zundert et al. 2008). As explained above, MNs express relatively high levels of GluR2-deficient AMPA receptors, but the levels of functional GluR2 have been found to be even further decreased in ALS patient samples (Takuma et al. 1999). Furthermore, the overexpression of GluR2 in SOD1^{G93A}-Tg mice showed a delay of disease onset and increased survival (Tateno et al. 2004).

1.3.5.6 Glial toxicity

The toxic effects of glia on MNs in the context of ALS have been well documented by our lab and others. Such study has found that the co-culture of MNs on primary astrocytes from SOD1^{G93A}-Tg mice or from post-mortem sALS patients induces MN toxicity (Nagai et al. 2007; Di Giorgio et al. 2008; Re et al. 2014; Haidet-Phillips et al. 2011). A similar, though less striking toxicity has been seen on MN co-culture with microglia (Xiao et al. 2007). Various studies have shown this effect to also take place *in vivo* via the degeneration of MNs in the context of astrocytes from either sALS patients or from ALS mouse models (Tong et al. 2013; Qian et al. 2017; Papadeas et al. 2011; Clement et al. 2003; Yamanaka et al. 2008).

The precise mechanism of glial-induced MN death is unknown and is an area of active research. However, the toxicity of SOD1^{G93A}-Tg mouse astrocytes is replicated upon treatment of MNs with media conditioned on these astrocytes, suggesting that this toxicity is due to the release of a toxic factor rather than the lack of a beneficial effect (Nagai et al. 2007). Furthermore, the effects of SOD1^{G93A}-Tg astrocytes on MNs that have been shown include the downregulation of GluR2 expression, a decrease in antioxidant support, and the activation of the interferon-gamma (IFN-γ) and necroptosis pathways (Cassina et al. 2008; Re et al. 2014; Van Damme et al. 2007; Vargas et al. 2006; Aebischer et al. 2011).

1.3.5.7 Endosomal trafficking dysfunction in ALS

Alterations in endosomal trafficking have been well-established in multiple neurodegenerative disorders, including ALS. Connections with ALS include known roles for ALS-associated genes in endosomal trafficking as well as functional studies showing deficiencies in certain pathways in the context of the disease. In section 1.1, I outlined the multiple axes along which endosomal trafficking occurs in the cell. Here, I will review the evidence that has been found tying endosomal trafficking dysfunction to ALS.

1.3.5.7.1 Endocytosis

While there has historically been limited evidence for it, recently, studies have pointed to a possible role for the involvement of endocytosis in ALS pathogenesis. First, an *in vitro* study has shown that the aggregation of proteins, including that of the ALS-causing $SOD1^{A4V}$, induced an inhibition in CME mediated by the sequestration of HSC70 (Yu et al. 2014). Similarly, other studies have shown that the overexpression of either FUS or TDP-43 also results in the inhibition of CME (Liu et al. 2019; Liu, Coyne, et al. 2017). Furthermore, the cytotoxic effects of FUS and TDP-43 are ameliorated by the upregulation of endocytosis (Liu et al. 2019; Liu, Coyne, et al. 2017). Finally, a study on the function of the C9orf72 protein showed that its depletion results in the inhibition of endocytosis, implicating that its physiological function, which is currently incompletely understood, may involve the regulation of endocytosis (Farg et al. 2014).

1.3.5.7.2 Golgi-to-Endosome Transport

Similarly spare evidence has been found for the involvement of Golgi-to-endosome transport in ALS pathology. However, of particular note is the fact that Bunina bodies have been shown to contain SORCS2 in human samples (Miki et al. 2018; Mori et al. 2015). The study that initially showed this finding also showed that ALS patient samples displayed decreased immunoreactivity for sortilin and SORL1 (Mori et al. 2015). Furthermore, the study of sortilin in ALS has shown that TDP-43 regulates its splicing and expression (Colombrita et al. 2015; Prudencio et al. 2012; Tann et al. 2019). Rare variants in SORT1 have also been associated with FTD and, possibly, with fALS (Belzil et al. 2012; Philtjens et al. 2018). Finally, induced MNs (iMN) and fibroblasts from patients with C9orf72-associated ALS-FTD showed the abnormal localization and function of MPRs (Shi et al. 2018; Aoki et al. 2017). Altogether, these studies point to the possible involvement in ALS of deficiencies in the Golgi-to-endosome transport receptors.

1.3.5.7.3 Endosomal Maturation

As described above, the proper coating of the endosome with endosomal markers such as Rab5 and EEA1 is crucial to its function and proper maturation. Alterations in this coat can have devastating effects on normal protein trafficking function in the cell. Indeed, this is what is seen upon the disturbance of the function or expression of alsin, the protein encoded by the *ALS2* gene, whose mutation can cause ALS (Hadano et al. 2001; Panzeri et al. 2006; Lai et al. 2009; Hadano et al. 2006). Under normal conditions, alsin associates to EEA1 and functions as a GEF for Rab5, but ALS-associated mutations create a truncated alsin which can no longer bind EEA1 (Panzeri et al. 2006; Topp et al. 2004). The downstream effects of this have been studied in alsin-deficient

mice which exhibit reduced endosomal size due to deceased endosomal fusion, a disruption in the transport of proteins, including brain-derived neurotrophic factor and GluR2, and progressive degeneration of cerebellar and MNs (Hadano et al. 2006; Devon et al. 2006; Lai et al. 2006). Recent studies into the function of C9orf72 have shown that it is also a Rab GEF. Though it is a field of active study which particular Rabs it activates, it has been widely shown to colocalize with and activate Rab5 and Rab7 (Iyer, Subramanian, and Acharya 2018; Farg et al. 2014; Aoki et al. 2017).

Two other proteins involved in endosomal maturation have been shown to be associated to ALS: CHMP2B and spastic paraplegia-11 (SPG11) (Parkinson et al. 2006; Orlacchio et al. 2010). CHMP2B has, as noted above, an important role in endosomal maturation, as it forms part of the ESCRT-III complex, so its mutation predictably causes defects in endosomal/lysosomal transport and lysosomal storage pathology (Clayton et al. 2015; Clayton et al. 2018). Meanwhile, SPG11 has an, as of yet, poorly characterized role in endosomal maturation, but it is known that it forms part of the adaptor protein complex 5 (AP5), whose depletion results in swollen MVBs and the impaired trafficking of CI-MPR (Hirst et al. 2011).

1.3.5.7.4 Macroautophagy

The buildup of aggregated proteins as well as defective mitochondria are hallmarks of ALS, so their proper clearance is of vital importance. However, the study of the pathology of ALS and various ALS-associated genes have shown that a deficiency in said clearance via autophagy may itself be a causative mechanism in the disease.

Optineurin (OPTN) is a protein that binds LC3 and the myosin VI motor protein, aiding in the trafficking of autophagosomes to lysosomes (Tumbarello et al. 2012). Multiple ALS-causing

mutations in as well as the depletion of OPTN have been proven to reduce the ability of OPTN to bind to myosin VI, thus preventing the fusion of the autophagosome with the lysosome necessary for proper autophagy (Wild et al. 2011; Sundaramoorthy et al. 2015; Shen et al. 2015). Furthermore, a study in sALS patient SC MNs showed similarly reduced binding of OPTN with myosin VI as well as OPTN-positive inclusions (Sundaramoorthy et al. 2015). Relevantly, ALS-associated mutations in TANK-binding kinase 1 (TBK1) are known to disrupt its physiological activity of phosphorylating OPTN and p62—another autophagy-related protein (Gijselinck et al. 2015; Oakes, Davies, and Collins 2017; Cirulli et al. 2015).

ALS-causing mutations in SOD1 and FUS have also proven to disrupt the initiation of autophagy (Nassif et al. 2014; Ryu et al. 2014). Tissues from ALS-FTD patients with the C9orf72 expansion have also been shown to express markers of impaired autophagy (Al-Sarraj et al. 2011). The study of iMNs from these patients has shown swollen autophagosomes, indicating that they are non-functional (Aoki et al. 2017).

1.3.5.7.5 Recycling

Evidence of the involvement of recycling defects in ALS start with the above described wobbler mouse. While, as mentioned above, no mutations in the GARP complex have been linked to ALS, the fact that its destabilization so closely reproduces ALS pathology in mice is of great interest. It is important to note, given the subject of this thesis, that, while they work via similar pathways, no direct interaction has been established between the retromer and the GARP complex. Indeed, the GARP complex has been shown to take part in the retrograde trafficking of CI-MPR (Perez-Victoria, Mardones, and Bonifacino 2008).

The interaction of ALS-associated genes with Rab11 also provides some evidence as to the involvement of retrograde trafficking in ALS. Namely, Rab11 is one of the main Rabs on which C9orf72 has been shown to have GEF activity (Iyer, Subramanian, and Acharya 2018). In one study, TDP-43 function has been shown to be important in the regulation of Rab11-positive recycling endosomes (Schwenk et al. 2016). Specifically, the knockdown of TDP-43 in cultured neurons resulted in decreased dendritic trafficking of Rab11-positive endosomes, resulting in dendrite loss, which was phenocopied with the dominant-negative expression of Rab11.

Finally, during the course of two studies, despite not being the primary subject of study, findings have shown possible connections between ALS and the retromer. First, Western blots run on iPSc-derived MN from ALS-FTD patients with a C9orf72 expansion showed a trend towards the decreased expression of VPS26, though the finding was not statistically significant (Aoki et al. 2017). Another study was performed on a *Drosophila* model of ALS which expresses a loss of function mutation in the fly orthologue of the human ALS-associated gene VAMP-associated protein B (VAPB) (Sanhueza et al. 2015). The study involved a screen of overexpressed genes to see which rescued the defects in eye morphology seen in the model, and one of the identified rescuers of pathology was VPS35.

1.4 Specific Aims

Given the extensive evidence of the involvement of both endosomal trafficking dysfunction in ALS and retromer dysfunction in neurodegenerative disease, over the course of my work, I sought to see whether retromer dysfunction may be involved in the pathology of ALS. In this thesis, I present this work over the course of three chapters (2-4).

In Chapter 2, I present an analysis of the expression profile of retromer components in human ALS patient samples and in SOD1^{G93A}-Tg mice, both *in vivo* and *in vitro*. Generally, I show a widespread decrease in retromer levels in the context of ALS.

In Chapter 3, I then explore the possible causes for decreased expression of retromer in ALS as well as some of the downstream effects of this deficiency, including APP trafficking and MN viability.

In Chapter 4, I study the effect of the repletion of retromer levels in the SOD1^{G93A}-Tg mice via pharmacological and viral means. Strikingly, I find that rather than ameliorate disease progression, the upregulation of the retromer in these mice causes the enhanced progression of disease in these mice.

To follow up on the results in Chapter 4, in Chapter 5, I performed a corollary study in which I decreased retromer levels in the SOD1^{G93A}-Tg mice via the heterozygous deletion of an allele of Vps35. Interestingly, and in keeping with the results of Chapter 4, this resulted in the amelioration of disease phenotypes in mice.

Overall, my conclusions for this work are that, while there is indeed a decrease in retromer expression in the context of ALS, this is not necessarily a pathogenic mechanism, and may indeed be a compensatory mechanism by the cell to maintain homeostasis. Further work is warranted in unravelling (1) what the possible beneficial downstream effects of retromer dysfunction in the context of ALS are and (2) whether there is a therapeutic benefit to be found in the inhibition of retromer function for this disease.

CHAPTER 2

RETROMER QUANTIFICATION IN CELLS AND TISSUES FROM ALS PATIENTS AND MOUSE MODELS OF ALS

2.1 Introduction

The retromer is a protein complex that is involved in the trafficking of proteins from the endosome to the trans-Golgi network (TGN) or to the plasma membrane (PM), a process known as recycling. The central defining core components of the retromer are vacuolar protein sorting 35 (Vps35), Vps29, and Vps26 (Seaman 2005; Hierro et al. 2007; Haft et al. 2000). Vps26 in mammals has two paralogues, Vps26a and Vps26b, which exhibit some functional differences, though Vps26a seems to be the subunit predominantly used in the retromer (Kerr et al. 2005; Collins et al. 2008; Gallon et al. 2014). Vps29 has two isoforms that arise from alternative splicing, though the functional difference between the two isoforms is not well understood (Wu et al. 2019). The retromer complex is vital to the normal function of the cell, and indeed the complete deletion of either Vps35 or Vps26a in mice has proven to be embryonically lethal (Tang, Erion, et al. 2015).

Recent research has shown that the dysfunction of the retromer complex is likely a major factor in the pathogenesis of multiple neurodegenerative diseases. The first evidence of this connection came from the finding that the entorhinal cortexes of patients with Alzheimer's disease (AD) have a decreased expression of retromer core components. This deficiency was shown to be found both in the expression of the mRNA encoding for VPS35 and in the protein levels of VPS35 and VPS26 (Small et al. 2005). Since then, samples from affected tissues of patients with Parkinson's disease (PD), Down's Syndrome (DS), Progressive Supranuclear Palsy (PSP), and Pick's disease have shown to have deficiencies in the expression of components of the retromer

complex (Small et al. 2005; Zhao, Perera, et al. 2018; Wang, Zhao, et al. 2013; Vagnozzi et al. 2019). Further, mouse models of AD, PD, and DS have replicated these deficiencies (Chu and Pratico 2017; MacLeod et al. 2013; Wang, Zhao, et al. 2013). Evidence of retromer involvement, particularly in AD and PD has further grown, including both in functional studies of the interaction and in disease-associated genetic mutations in retromer functional subunits. Most notably, the partial loss of function mutation of VPS35 has been shown to cause PD (Zavodszky et al. 2014; McGough et al. 2014; Seaman and Freeman 2014; Vilarino-Guell et al. 2011; Follett et al. 2014; Zimprich et al. 2011).

Pathological mechanisms of neurodegenerative diseases tend to overlap with each other. Especially since most neurodegeneration is accompanied by defects in proteostasis that lead to protein aggregation, defects in endosomal trafficking are often apparent in most neurodegenerative diseases. Despite this, currently, no studies have explored the possible involvement of the retromer in the pathology of amyotrophic lateral sclerosis (ALS).

ALS is neurodegenerative disorder of the upper and lower motor neurons (MNs) characterized by muscle weakness, paralysis, and death within 3-5 years after diagnosis (Rowland and Shneider 2001). While ALS is mainly sporadic (sALS), it presents in a familial (fALS) form in ~10% of patients as a result of gene mutations (Byrne et al. 2011). Since both forms of ALS are virtually indistinguishable, it is expected that they share pathogenic mechanisms, and thus, the study of models of fALS has the potential to uncover pathogenic mechanisms for sALS. One commonly mutated gene in fALS encodes for superoxide dismutase 1 (SOD1) (Lattante et al. 2012; Pasinelli and Brown 2006), and overexpression of mutant $SOD1^{G93A}$ in transgenic (Tg) mice reproduces most hallmarks of ALS including selective degeneration of MNs, progressive muscle weakness, and premature fatality. Studies in systems using astrocytes from these mice or from

patients with either fALS or sALS have shown that astrocyte toxicity to MNs may play an important role in ALS-related neurodegeneration (Cassina et al. 2005; Di Giorgio et al. 2007; Di Giorgio et al. 2008; Nagai et al. 2007; Sreedharan and Brown 2013; Re et al. 2014).

Since the retromer has been heavily implicated in neurodegeneration, I sought to determine whether the connection between retromer deficiency and neurodegeneration extends to ALS. Accordingly, I performed a descriptive study, looking at the expression levels of Vps35, Vps26a, and Vps29 in different contexts of the disease. I predominantly did so by employing the SOD1^{G93A}-Tg mouse, and I then extended the study to looking at expression levels of the retromer core components in human post-mortem samples from ALS patients. Given the direct involvement of both MNs and astrocytes in ALS, I concentrated my study on expression levels in these cells as well as in tissue lysates. Overall, I showed that the expression of the retromer core components is decreased in both mouse models of fALS and in human samples of sALS.

2.2 Results

2.2.1 Characterization of retromer expression in SOD1^{G93A}-Tg mouse tissues

To examine the possible defect of retromer in ALS, I choose to begin my work by looking at the expression of retromer components in the spinal cord (SC) of the SOD1^{G93A}-Tg mouse. I choose to look at three time-points: post-natal day 60 (P60), before the onset of disease in this model; P90, the time at which symptoms of disease are first seen in these mice; and P120, the time at which the disease has progressed into overt pathology, 10-20 days before expected fatality in these mice.

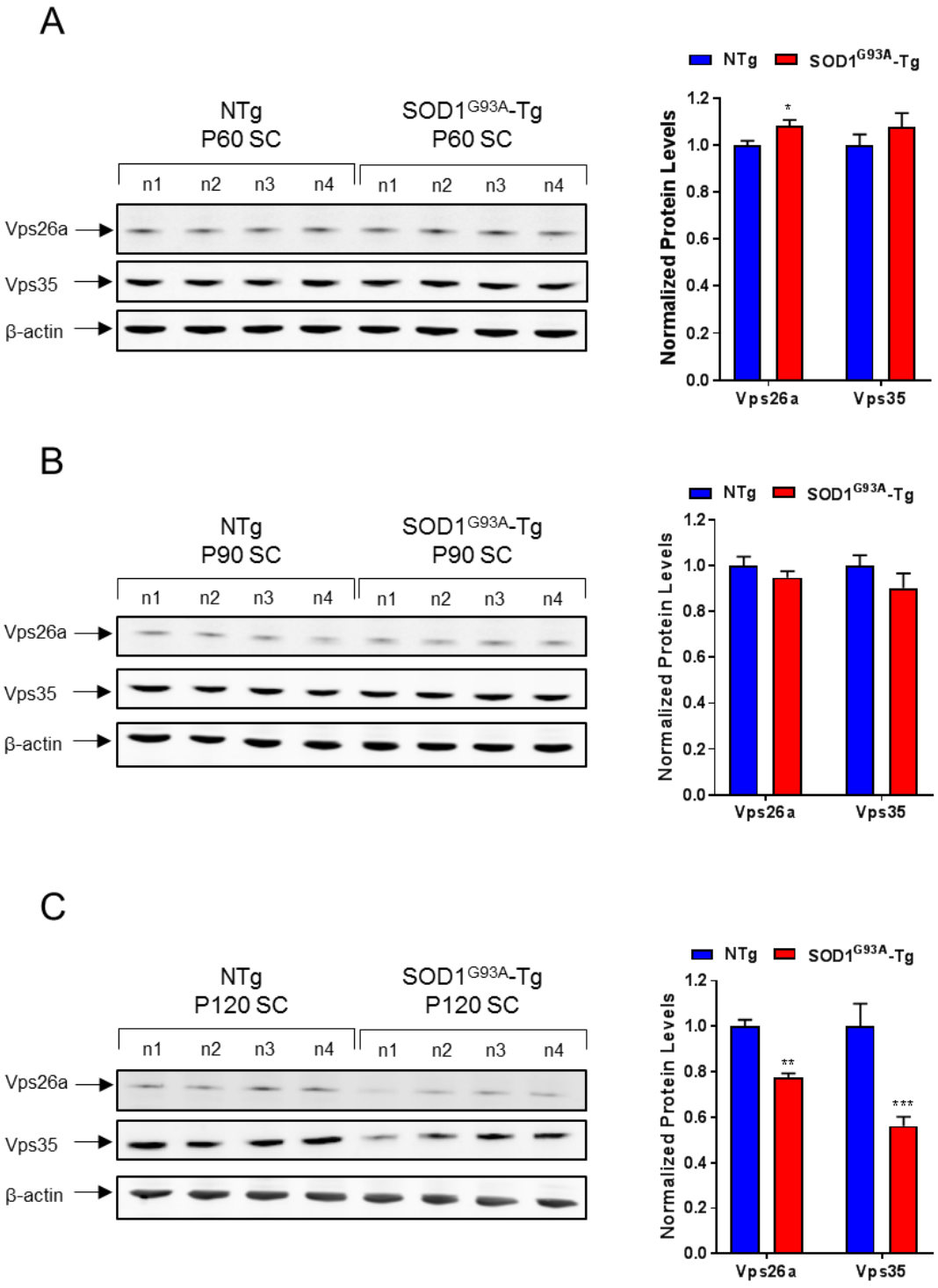

Figure 2.1 Retromer Core Components Exhibit Lower Expression in the Spinal Cord of SOD1^{G93A}-Tg Mice in an Age-Dependent Manner

Western blots were run on SC lysates from SOD1^{G93A}-Tg and NTg mice and quantified at P60 (A), P90 (B), and P120 (C). Results presented as mean ± SEM. n=4, *P<0.05, **p<0.01, ***p<0.001 in unpaired Student t-test.

I performed Western blot analysis of the lysate of SC from SOD1^{G93A}-Tg mice for Vps35 and Vps26a, two of the core components of the retromer. While I attempted to perform Western blot analysis of Vps29 as well, the antibody I used revealed poorly defined band to properly quantify this subunit. Testing alterative antibodies did not improve the signal and thus Vps29 Western blotting was not assessed in mouse tissue but, as shown later, on cell systems, where the signal was much sharper on the form of well-defined doublet corresponding to the two splice variants of the protein. Western blots in the SC at P60 showed that there was a slight statistically significant increase in Vps26a (Student t-test, p=0.026) and no statistically significant change in Vps35 (Student t-test, p=0.32) (Fig. 2.1A). At P90, there was no statistically significant change in either Vps26a (Student t-test, p=0.31) or Vps35 (Student t-test, p=0.25) (Fig 2.1B). Thus, at earlier stages of disease, I observed either no or mild changes in the expression levels of retromer core components. In contrast, at P120, I saw a large drop in the protein expression of both Vps35 (Student t-test, p=0.000025) and Vps26a (Student t-test, p=0.0052), consistent with a defect in the retromer at a more advanced stage of the disease in this mouse model of ALS (Fig. 2.1C).

In AD, the decreased expression of VPS35 protein has been correlated to the decreased expression of VPS35 mRNA (Small et al. 2005). Furthermore, the disruption of mRNA processing has been well tied to ALS (Colombrita et al. 2015; Gendron et al. 2013; Chen et al. 2014). Thus, to determine whether the reduction in retromer component levels in the SOD1^{G93A}-Tg mice SC was due to the reduction of mRNA expression, I performed quantitative RT-PCR on the lysate of these same SC. Intriguingly, rather than a decrease in expression, I saw modest, though statistically significant increases in Vps35 at P60 (Student t-test, p=0.016) and in Vps26a at P120 (Student t-test, p=0.028) and at least a small trend towards an increased expression of both Vps35 (Student t-test, P90 p=0.099, P120 p=0.37) and Vps26a (Student t-test, P60 p=0.24, P90 p=0.34) mRNA

across ages (Fig.2.2). Thus, these results indicated that decreased content of proteins for the retromer core components in SOD1^{G93A}-Tg mouse SC are not due to a loss of expression of their respective mRNAs. Accordingly, the changes in retromer proteins in the symptomatic SOD1^{G93A}-Tg mouse SC originate most likely from alterations in retromer subunits translation and/or degradation.

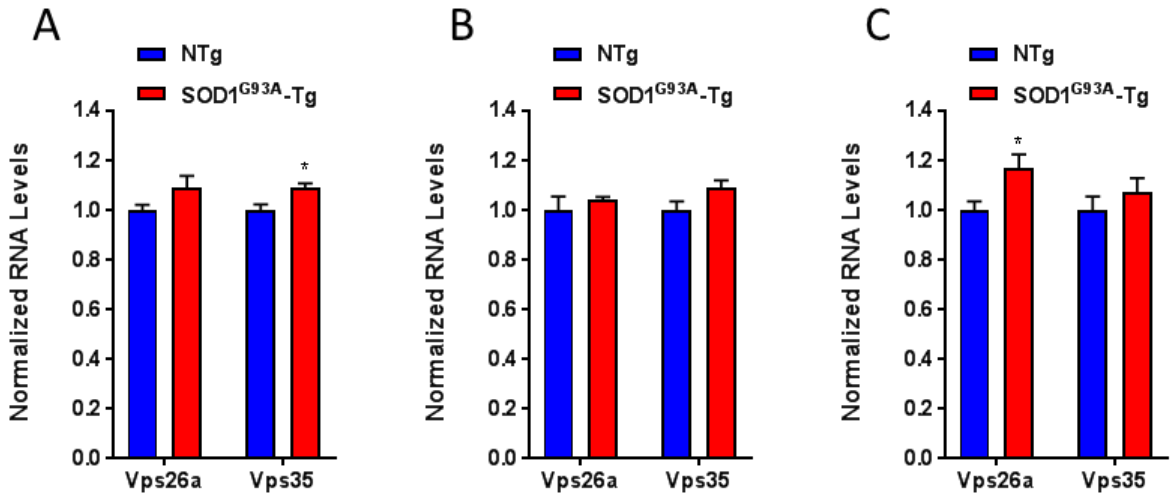

Figure 2.2 mRNA of Retromer Core Components Exhibit No Decreases in Expression in the Spinal Cord of SOD1^{G93A}-Tg Mice Over Time

qPCR analysis of SC lysates from SOD1^{G93A}-Tg and NTg mice and quantified at P60 (A), P90 (B), and P120 (C). Results presented as mean ± SEM. n=4, *P<0.05 in unpaired Student t-test.

SOD1^{G93A}-Tg mice express high levels of the SOD1^{G93A} transgene, and the G93A mutation does not affect SOD1 enzymatic activity (Gurney et al. 1994; Hayward et al. 2002). Thus, changes found in the SOD1^{G93A}-Tg mouse could conceivably be due to merely the overexpression of SOD1 protein and the increase in its physiological function. To make sure that the retromer deficiency I had found the SOD1^{G93A}-Tg mouse SC was due specifically to the ALS-associated mutation of SOD1, I employed a Tg mouse which overexpresses the wild-type form of SOD1 (wtSOD1) to similar levels as those found in the SOD1^{G93A}-Tg mouse and shows no overt ALS-like pathology.

Remarkably, at P120, contrary to the changes in identified in SC of SOD1^{G93A}-Tg mouse, Western blot analysis of SC of wtSOD1-Tg did not display any statistically significant changes in Vps35 and Vps26a (Fig. 2.3). Rather, if anything, I saw a trend towards an increased expression of both Vps26a (Student t-test, t(x)=, p=0.16) and Vps35 (Student t-test, p=0.19).

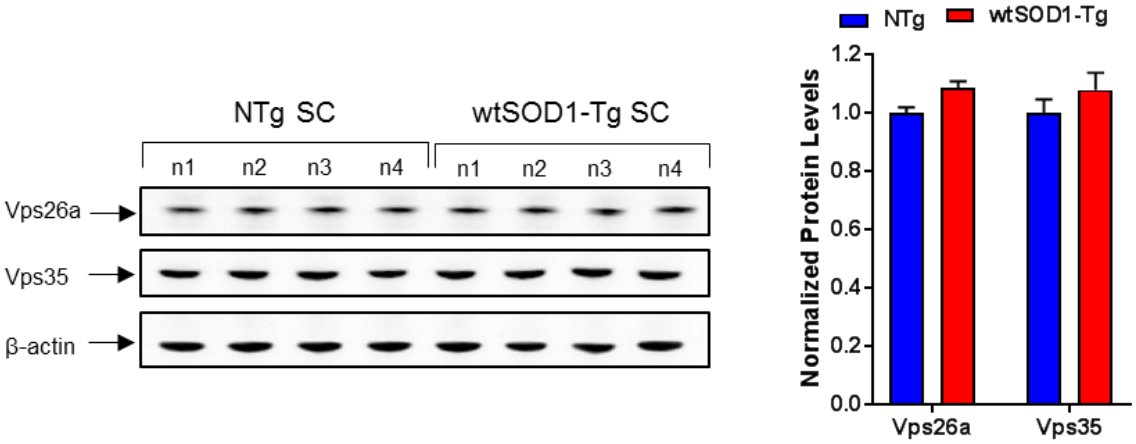

Figure 2.3 Retromer Core Components Exhibit No Changes in Expression in the Spinal Cord of wtSOD1-Tg Mice

A Western blots was run on SC lysates from wtSOD1-Tg and NTg mice and quantified at P120. Results presented as mean ± SEM. n=4, not significant in unpaired Student t-test.

I next sought to determine the tissue specificity of retromer deficiency in the SOD1^{G93A}-Tg mouse, since mutant SOD1 is ubiquitously expressed both inside and outside the CNS. To this end, I performed Western blot analysis on lysates from two other neural tissues in these mice at P120, namely the cerebral cortex and the cerebellum. I found that, akin to the SC, both the of these selected CNS regions displayed deficiencies in retromer core proteins (Fig. 2.4A, B). The cortex showed a modest, though statistically significant decrease in the levels of both Vps35 (Student t-test, p=0.00013) and Vps26a (Student t-test, p=0.0052), and the cerebellum showed a significant decrease in the levels of Vps35 (Student t-test, p=0.013) with only a trend towards decreased levels of Vps26a (Student t-test, p=0.18). Since retromer deficiency seems to be widespread in neural

tissues, I looked at expression of retromer core components in the kidney of SOD1^{G93A}-Tg mice to determine whether retromer deficiency was widespread throughout the body. However, I saw no significant change in either Vps35 (Student t-test, p=0.96) or Vps26a (Student t-test, p=0.73) in the kidney of these mice, indicating that retromer deficiency is likely restricted to neural tissues of the SOD1^{G93A}-Tg mouse (Fig. 2.4C).

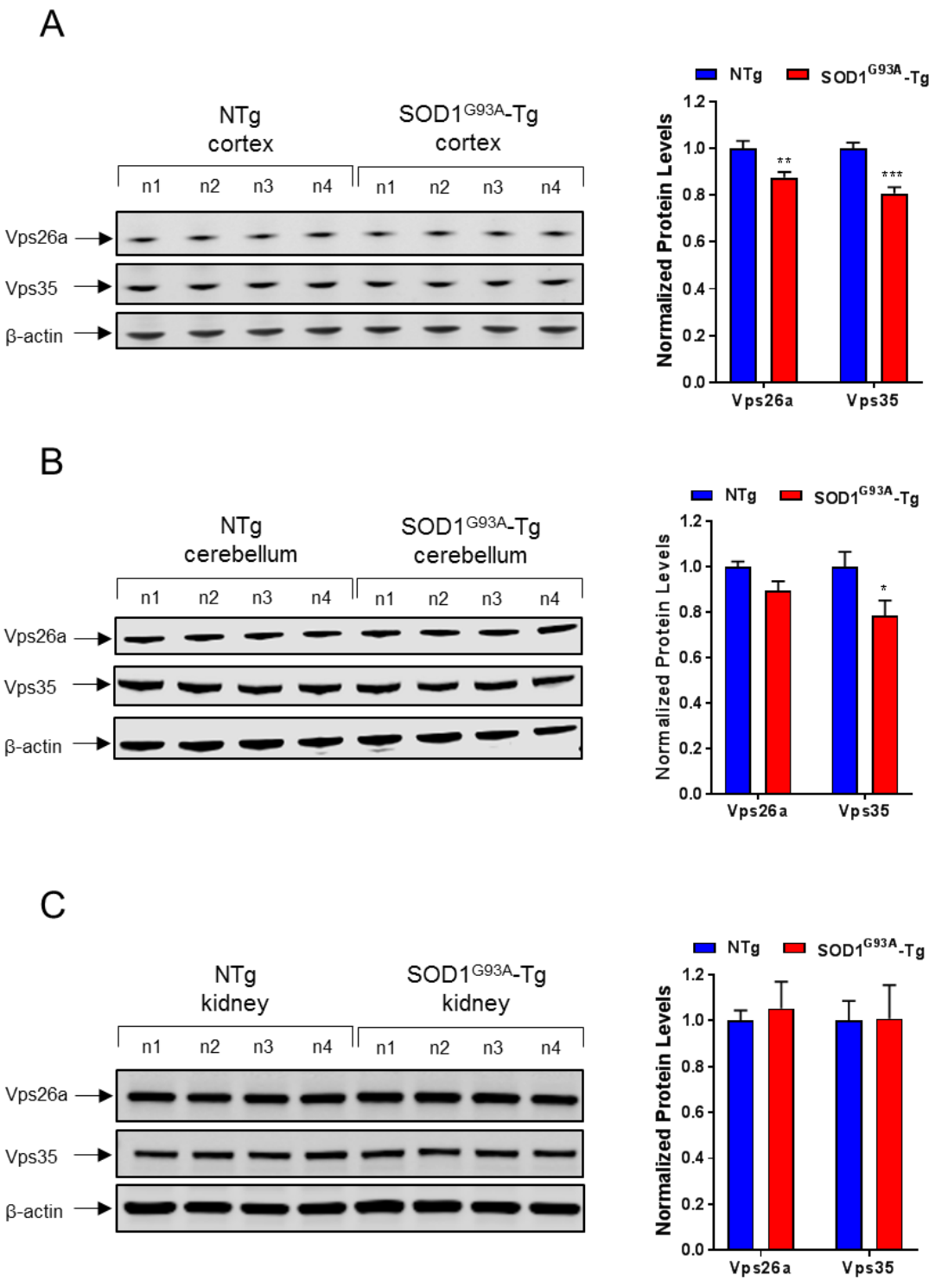

Figure 2.4 Retromer Core Components Exhibit Lower Expression in the Neural Tissues, but Not Non-Neural Tissues of SOD1^{G93A}-Tg Mice

Western blots were run on lysates from the cortex (A), cerebellum (B), and kidney (C) of SOD1^{G93A}-Tg and NTg mice and quantified. Results presented as mean ± SEM. n=4, *P<0.05, **p<0.01, ***p<0.001 in unpaired Student t-test.

2.2.2 Characterization of retromer expression in ALS-affected neural cells in the SOD1^{G93A}-Tg mouse

The bulk volume of tissue in the CNS comes, not from neurons, but from glial cells. Thus, the decrease of expression in retromer components in the whole lysate of the SC does not necessarily imply an equivalent decrease in neurons, let alone in specifically MNs. Thus, I explored various avenues of quantifying the levels of expression of retromer core components in SC MNs.

There are currently no protocols that consistently produce a pure population of MNs from adult mouse SC. However, the culture of cortical neurons from embryonic mouse brains can easily produce a neuronal population of at least 90%. I thus cultured neurons from the cortex of SOD1^{G93A}-Tg mouse embryos and age-matched non-transgenic (NTg) controls. After allowing them to grow for 7 days, I then collected them and performed Western blot analysis on these neurons, which showed no changes in expression of either Vps35 (Student t-test, p=0.22) or Vps26a (Student t-test, p=0.65) (Fig. 2.5A). However, since neurons in the SOD1^{G93A}-Tg mouse cortex have not shown any significant pathological change, it remains possible that MNs are specifically affected by changes in the retromer. Furthermore, since these neurons were taken from mouse embryos, and the retromer deficiency I have found in SOD1^{G93A}-Tg mouse neural tissues seems to be time-sensitive (i.e. seen at P120 but not at P60), it is possible that these neurons were not yet mature enough to display changes in the retromer. I also attempted to see whether a difference could be seen in MNs specifically by culturing and differentiated a MN-like NSC34 cell line stably transfected with an empty vector, wtSOD1, SOD1^{G93A}, or SOD1^{G37R}, generously provided by the lab of Dr Pamela Shaw. However, I saw no differences in these cells of any of the

retromer core components (one-way ANOVA, Vps26a p=0.063, Vps29 p=0.39, Vps35 p=0.47) (Fig. 2.5C, D), which could still be due to the aspects of these cells that are not MN-like.

In an attempt to overcome this potential issue, I decided to quantify the immunofluorescent signal generated by immunohistochemistry (IHC) on sectioned SC from $SOD1^{G93A}$-Tg and NTg mice at P120, when the retromer deficiency in the SC seems to be robust. Mean fluorescence intensity (MFI) analysis of the cell bodies of at least 20 MNs expressing the MN marker choline acetyltransferase (ChAT) from two mice of each condition showed that MNs expressed significantly lower levels of Vps35 (Student t-test, $p<10^{-10}$) (Fig. 2.5E, F). Although quantification of IHC signal must be taken with caution given the fact that quantification of this method is fraught with a host of problems, still these results provide major support to the notion that the observed defect in retromer core subunits in whole SC extracts involves MNs.

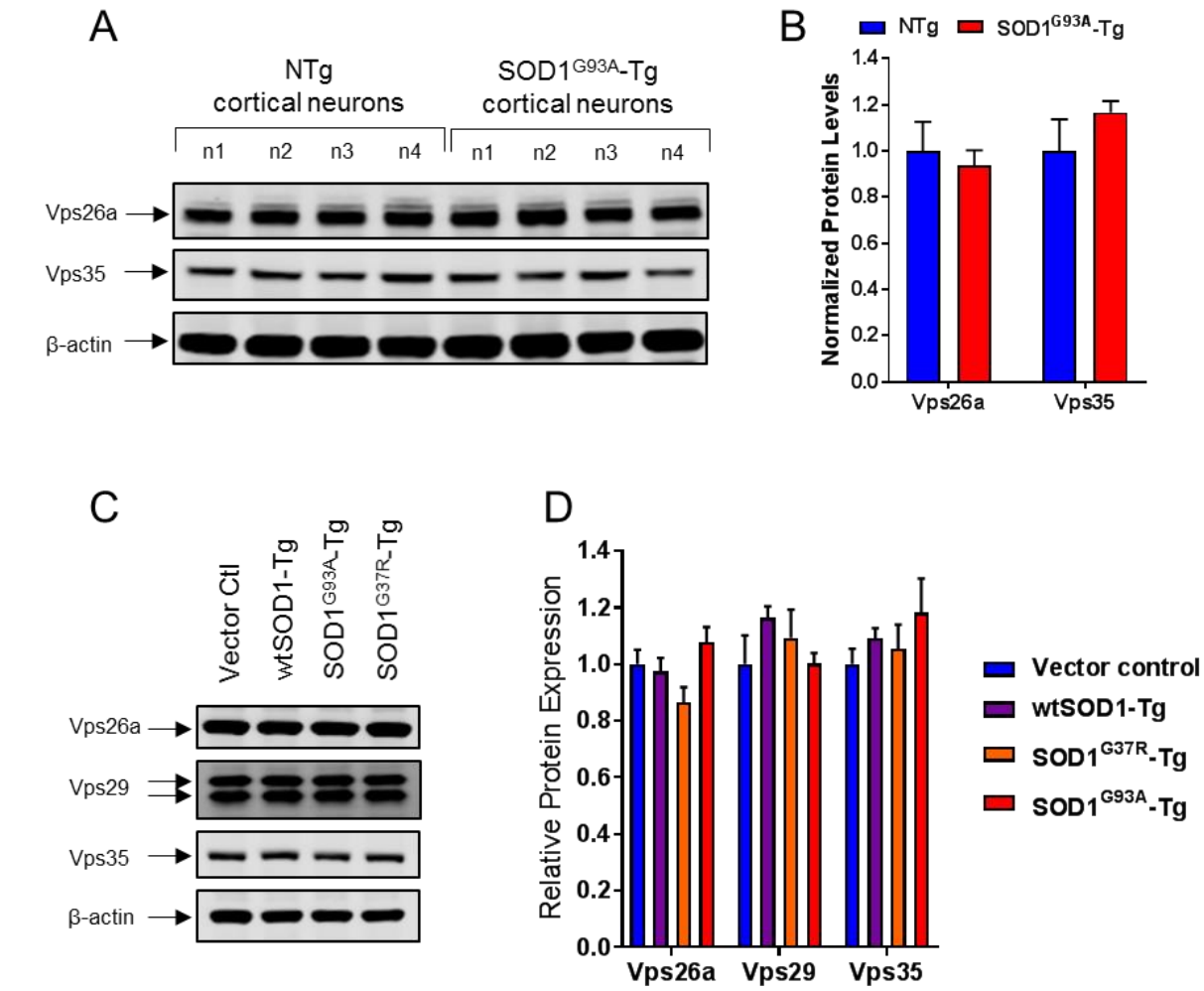
A
NTg cortical neurons
SOD1G93A-Tg cortical neurons
n1 n2 n3 n4 n1 n2 n3 n4
Vps26a
Vps35
β-actin
B
NTg
SOD1G93A-Tg
Normalized Protein Levels
1.4
1.2
1.0
0.8
0.6
0.4
0.2
0.0
Vps26a
Vps35
C
Vector Ctl
wtSOD1-Tg
SOD1G93A-Tg
SOD1G37R-Tg
Vps26a
Vps29
Vps35
β-actin
D
Relative Protein Expression
1.4
1.2
1.0
0.8
0.6
0.4
0.2
0.0
Vps26a
Vps29
Vps35
Vector control
wtSOD1-Tg
SOD1G37R-Tg
SOD1G93A-Tg

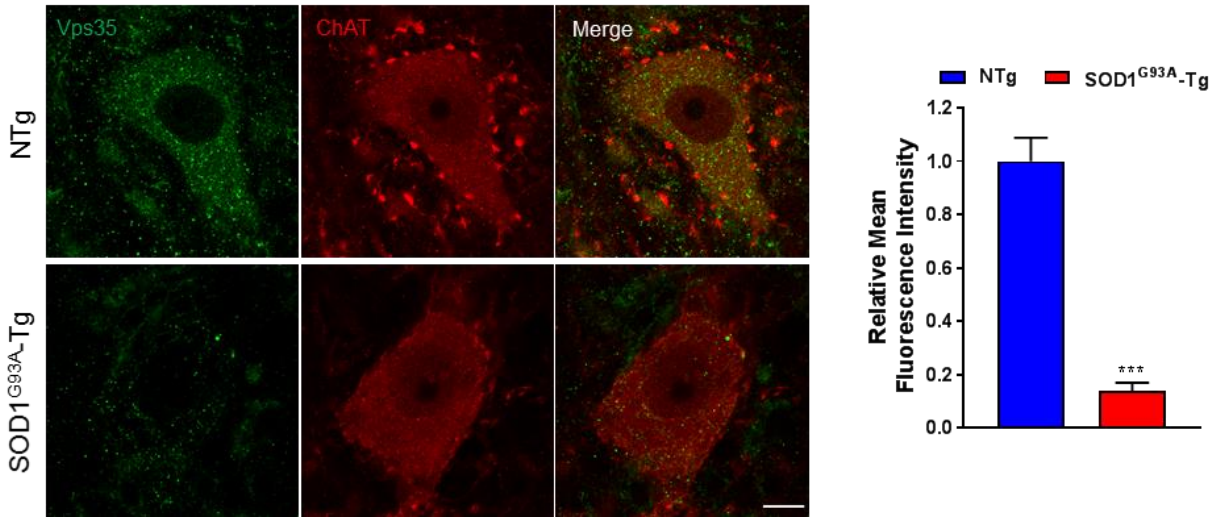
E
Vps35
ChAT
Merge
NTg
SOD1G93A-Tg
F
NTg
SOD1G93A-Tg
Relative Mean Fluorescence Intensity
1.2
1.0
0.8
0.6
0.4
0.2
0.0
***

Figure 2.5 *In Vivo* Motor Neurons, but Not Cultured Cortical Neurons or NSC-34 Cells, Expressing SOD1^{G93A} Express Lower Levels Retromer

A Western blot was run on neurons cultured from the cortex of SOD1^{G93A}-Tg and NTg mouse embryos at E13 (A) and quantified (B). Another Western blot was run on NSC-34 cells expressing an empty vector, wild-type human SOD1, or one of two mutated human SOD1 genes. A representative blot is presented here (C) with quantification of 5 independent experiments (D). Immunohistochemistry was performed for Vps35 (green) and ChAT (red) on SC sections from SOD1^{G93A}-Tg and NTg mice at P120, of which a representative stain is presented per condition (E). ChAT was used as a marker of MNs, and mean fluorescence intensity of Vps35 immunostaining was quantified (F). All results presented as mean ± SEM. (A, B) n=4, unpaired Student t-test. (C, D) n=5, one-way ANOVA. (E, F) n=20 neurons imaged from 2 animals per condition, ***p<0.001, unpaired Student t-test, scale bar indicates 10μm.

Astrocytes have been shown to have an important role in the pathogenesis of ALS, causing toxicity in MNs. As I mentioned above, glial cells, and particularly, astrocytes are the most abundant cells in the CNS. Thus, it is likely that the retromer deficiency seen in the CNS of SOD1^{G93A}-Tg mice is also seen in disease-affected astrocytes. Indeed, the fact that retromer deficiency was seen most strongly in disease affected areas and was not present in cultured cortical neurons may indicate that retromer deficiency occurs in cells involved in the pathogenesis of the disease such as MNs and astrocytes. Our lab has extensive experience in the culturing of primary astrocytes from mice, so I decided to investigate whether astrocytes from SOD1^{G93A}-Tg mice displayed a deficiency in retromer expression. I cultured astrocytes from NTg and from SOD1^{G93A}-Tg mice at P3 and then collected these cells and ran Western blot analysis for the expression of Vps35, Vps26a, and Vps29. Despite the fact that these cells were collected at P3, I found that SOD1^{G93A}-Tg astrocytes displayed a significant reduction in the expression of all three of these retromer components (Student t-test, Vps26a p=0.0059, Vps29 p=0.000013, Vps35 p=0.00015) (Fig. 2.6A, B). Similarly to the nature of retromer deficiency in SOD1^{G93A}-Tg mouse SC, the decrease in expression of retromer component proteins in SOD1^{G93A}-Tg astrocytes did not correlate with a significant change in mRNA levels of these components as measured by qRT-PCR (Student t-test, Vps26a p=0.62, Vps29 p=0.84, Vps35 p=0.58) (Fig 2.6C).

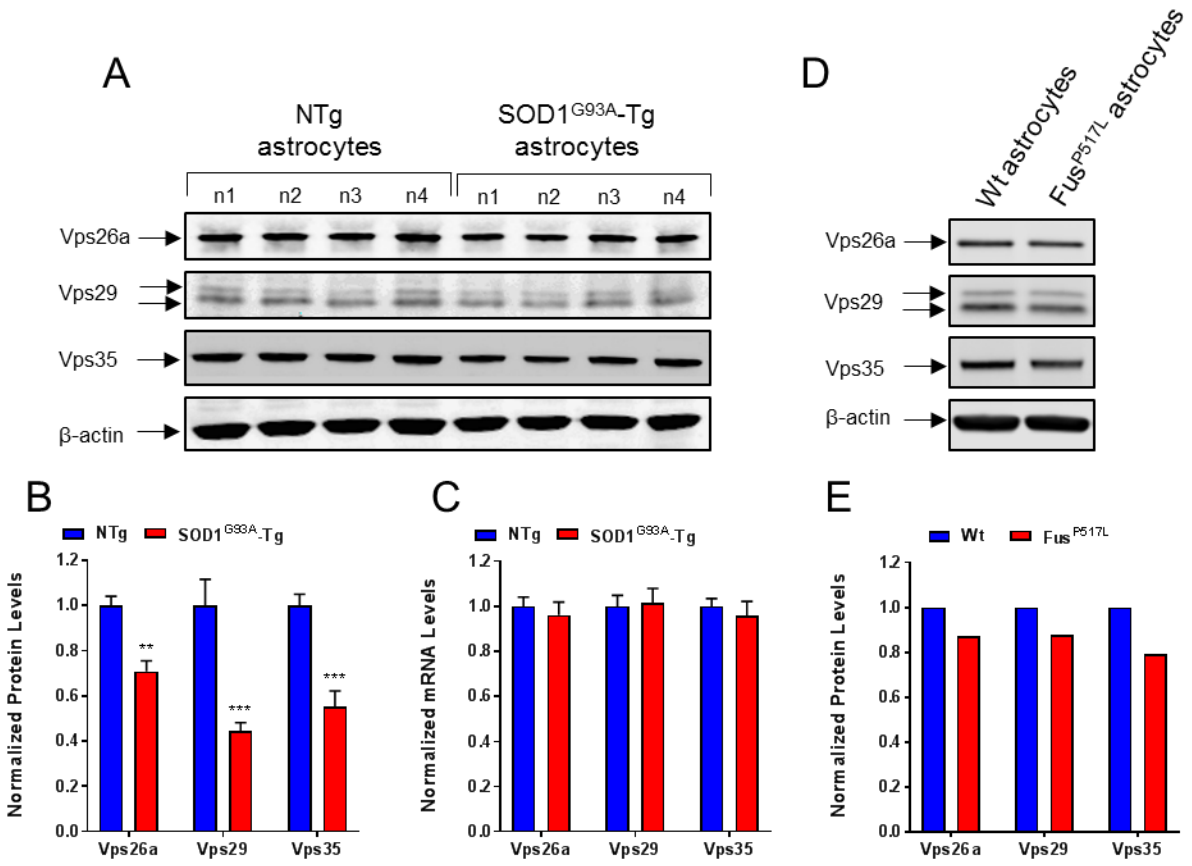

Figure 2.6 Cultured Astrocytes from ALS Mouse Models Show a Decrease in Expression of Retromer Components

A Western blot was run on astrocytes cultured from the cortex of SOD1^{G93A}-Tg and NTg mouse embryos at P3 (A) and quantified (B). qPCR analysis was also performed on these astrocytes and normalized to Gapdh expression (C). Another Western blot was run on astrocytes cultured from the cortex of Fus^{P517L} mutant mice and Wt mouse at P3 (D) and quantified (E). (A-C) Results presented as mean ± SEM. n=4, **p<0.01, ***p<0.001, unpaired Student t-test. (E, F) Results presented from a single replicate, n=1, no statistics performed.

Next, I wondered whether or not the alterations in the expression of the retromer subunits were specific to mouse expressing mutant SOD1. To address this question, I turned my attention to another mouse model of ALS produced by Dr. Neil Shneider in which mice have a P517L point mutation in both alleles of the *Fus* gene, the mouse equivalent of the human FUS^{P525L} ALS-causing mutation. His lab generously provided me with a sample of astrocytes cultured from one of these

mice and a wild-type control littermate. I ran a Western blot analysis on these samples, and saw a decrease in the expression of Vps35, Vps26a, and Vps29 in the astrocyte sample from the Fus^{P517L} mutant mice (Fig. 2.6D, E). Importantly, this analysis was performed on a single replicate of mutant and control astrocytes, so further analysis of more biological replicates is warranted. However, should this result hold true on further analysis, it would provide evidence that the decrease in retromer expression in $SOD1^{G93A}$-Tg mice is not specific to the mutation of SOD1, but rather to ALS.

Table 2.1 Clinical Information on Patients from Whom Post Mortem Samples Were Taken for Tissue Analysis

PATIENT	GROUP NAME	RACE	GENDER	AGE AT ONSET	AGE AT DEATH	DISEASE DURATION (MONTHS)	SITE OF ONSET	PHENOTYPE
1	Non-Neurological Control	White	Female	N/A	57	N/A	N/A	N/A
2	Non-Neurological Control	Black/African American	Female	N/A	63	N/A	N/A	N/A
3	Non-Neurological Control	Black/African American	Male	N/A	68	N/A	N/A	N/A
4	Non-Neurological Control	White	Male	N/A	59	N/A	N/A	N/A
5	Non-Neurological Control	Black/African American	Male	N/A	51	N/A	N/A	N/A
6	Non-Neurological Control	White	Female	N/A	74	N/A	N/A	N/A
7	Non-Neurological Control	Black/African American	Male	N/A	48	N/A	N/A	N/A
8	ALS	White	Male	66	67	19	Limb	Lower motor neuron predominant (LMND)
9	ALS	White	Male	68	72	48	Axial Limb Other: Respiratory	Lower motor neuron predominant (LMND)
10	ALS	White	Male	58	69	127	Limb	Lower motor neuron predominant (LMND)
11	ALS	White	Female	50	54	45	Limb	UMN=LMN
12	ALS	White	Male	?	53	?	?	?
13	ALS	White	Female	65	67	29	Bulbar Limb	UMN=LMN
14	ALS	White	Female	67	68	17	Limb	UMN=LMN

2.2.3 Characterization of retromer expression in ALS-affected human tissues and cells

Since I have found a deficiency in the retromer in two mouse models of ALS, a natural next step is to see whether a similar deficiency can be found in human tissues from ALS patients. To this end, I acquired post-mortem samples of cervical SC from patients with ALS and from control patients with no known neurological disease from the Target ALS Human Postmortem Tissue Core. Clinical data of the patients these samples are from can be found in Table 2.1. Remarkably and in striking contrast to what I have experienced with the mouse tissues, with the human samples, despite the fact that great care was taken to matched samples for age, form of ALS, and post-mortem delay, I found large variability from case-to-case for both VPS35 and VPS26a by Western blot analysis (Fig. 2.7A, B). Thus, despite the fact that I detected a trend towards a decrease in expression in both proteins in ALS samples, neither difference reached statistical significance (Student t-test, VPS35 $p=0.21$, VPS26A $p=0.27$) between ALS and control samples. Given the variability of the data and despite the meaningful effect size of this experiment (Cohen's $d > 0.6$), it is thus not surprising that the power to detect a significant difference using 7 replicates for each group is only 0.3. Thus, there is a 70% risk of false negative. To correct for this high type-II error, I ran a power analysis, which revealed that a sample size of over 30 samples per condition would be necessary to reach a conventional power of 0.8, a sample size that I thought much too large to be pursued. On qRT-PCR analysis, I also found no significant change in the mRNA expression of VPS35 (Student t-test, $p=0.41$), VPS29 (Student t-test, $p=0.91$), or VPS26A (Student t-test, $p=0.79$), which was also accompanied by high variability among samples (Fig. 2.7C).

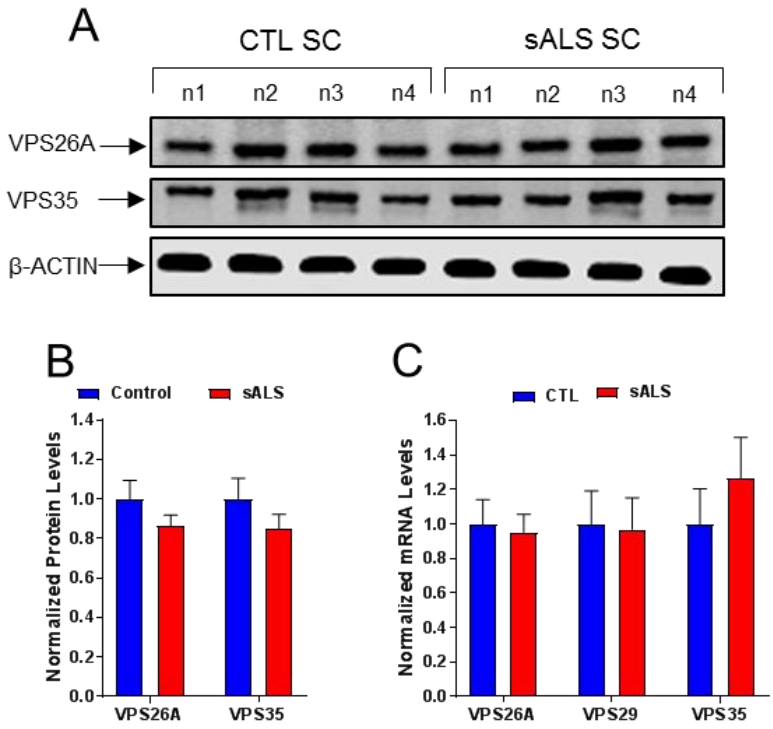

Figure 2.7 ALS Patient SC Samples Show No Change in Retromer Expression

A Western blot was run on post mortem cervical SC samples from sALS and control patients. A representative blot is presented here (A) with quantification of 7 replicates per group (B). qPCR analysis was also performed on these samples and normalized to Gapdh expression (C). All results presented as mean ± SEM. n=7, unpaired Student t-test.

I next tried to see whether there was any change in retromer component expression in human patients that could be found in a more controlled *in vitro* system looking at specific cell types that were otherwise obfuscated when looking at whole tissue. There is currently no method of acquiring primary MNs from post-mortem patient samples, so the study of human MNs has been restricted to the study of MNs differentiated from human stem cells. To that end, I acquired induced pluripotent stem cells (iPSC), which had been de-differentiated from cells from either ALS patients with a known mutation in SOD1 or from control patients with no known neurological disease. I got 3 mutant SOD1 iPSC lines and 2 control lines from the Columbia Stem Cell Core.

A third control iPSC line was generously provided by the lab of Dr. Michael Boland. Karyotyping performed on all lines by the core or by the Boland lab showed no abnormalities. Clinical data for the patients can be found on Table2.2.

Table 2.2 Clinical Information on Patients from Whom iPSCs were Generated

PATIENT	GROUP NAME	RACE	GENDER	BIOPSY AGE	SOD1 MUTATION	FAMILY HISTORY OF DISEASE
1	Non-Neurological Control	Caucasian	Male	37	N/A	No
2	Non-Neurological Control	Caucasian	Female	49	N/A	No
3	Non-Neurological Control	Caucasian	Female	44	N/A	No
4	ALS	Caucasian	Female	31	SOD1 A4V	No
5	ALS	Caucasian	Female	65	SOD1 H44R	Yes
6	ALS	Caucasian	Female	43	SOD1 A4V	Yes

Our lab has experience using a published method of fast differentiation of MNs from iPSCs, the protocol for which can be found in the Methods and Methods section of this thesis. This method produces a cell population that is roughly 70% MNs as indicated by expression of the homeobox protein MN marker HB9. This has previously been published and our lab has replicated this level of MN purity. I performed this differentiation protocol on iPSC from SOD1-ALS patients and from control patients and ran a Western blot analysis for the expression of VPS35, VPS26A, and VPS29. This showed that the iPSC-derived MN from ALS patients showed a significant decrease in the expression of VPS35 (Student t-test, $p=0.0090$). There was no significant change in the expression of VPS26A (Student t-test, $p=0.47$) or VPS29, but a marked trend was noted in decreased VPS29 expression (Student t-test, $p=0.083$). This provided evidence that a deficiency in

the retromer in the context of ALS was not specific to the mouse, but rather could be found in the context of human ALS as well.

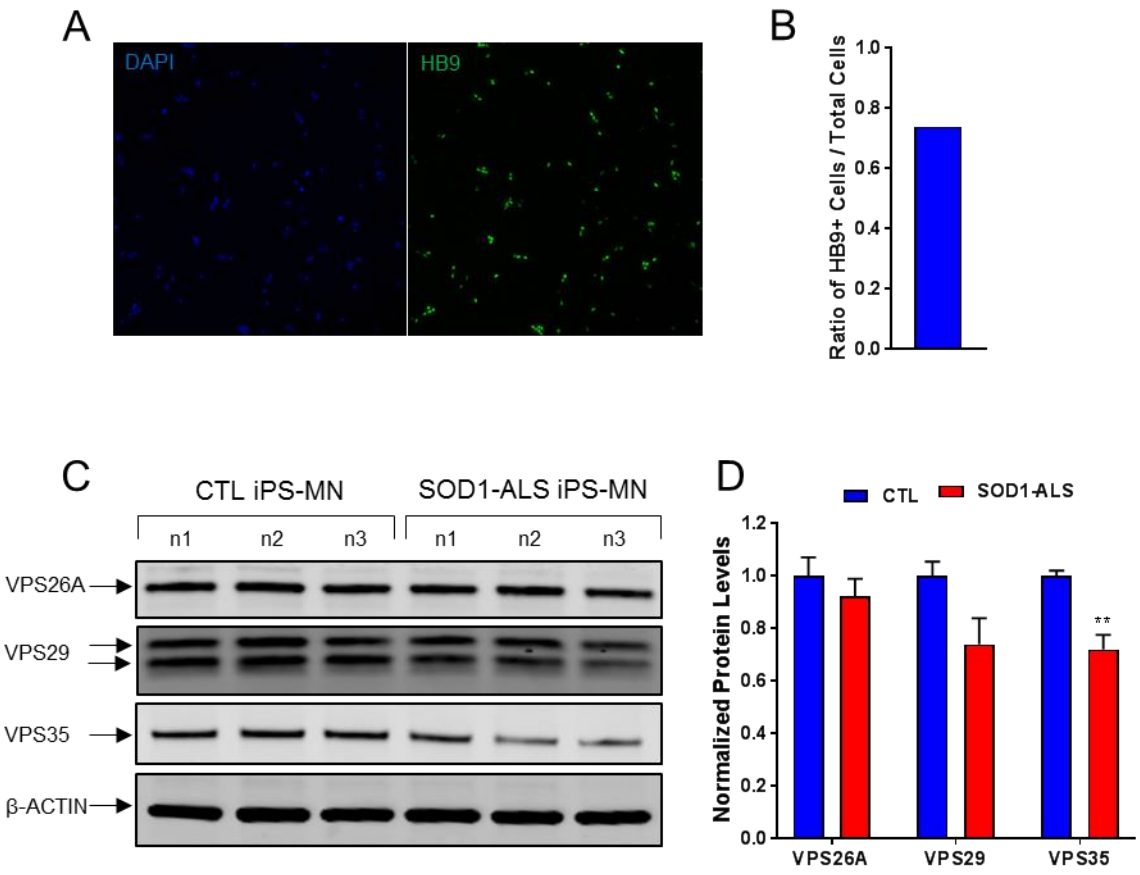

Figure 2.8 iPS-Derived MNs from SOD1-ALS Patients Express Lower Levels of VPS35

iPSCs from SOD1-ALS and control (CTL) patients were differentiated into MNs. Immunocytochemistry for MN marker HB9 (A) was quantified (B), serving as validation of successful differentiation of iPS-MN. A Western blot was then run on these iPS-MNs for retromer core proteins (C) and quantified (D). (A, B) Results are presented as ratio of HB9+ cells per total cells as indicated by nuclear DAPI counterstain, from a single replicate. n=1, no statistics performed. (C, D) Results presented as mean ± SEM. n=3, **p<0.01, unpaired Student t-test.

Since both MNs and astrocytes in the SOD1^{G93A}-Tg mouse model showed a deficiency in the retromer, I then sought to determine whether astrocytes from ALS patients showed a similar decrease in retromer expression. I am in the process of differentiating the exact same human iPSC lines used for MNs to astrocytes, but the protocol for iPSC-derived astrocytes requires a longer

time to achieve (Roybon et al. 2013). Therefore, while pursuing this road, I took advantage of our bank of primary astrocytes cultured from tissues from patients with sALS and from control patients with no known neurological disease (Re et al. 2014). I performed a Western blot analysis on lysates collected from these astrocytes and found that sALS astrocytes expressed a statistically significant decrease in VPS35 (Student t-test, p=0.024), VPS26A (Student t-test, p=0.0024), and VPS29 (Student t-test, p=0.012), compared to control astrocytes. Data for the patients from which these astrocytes were cultured can be found in Table 2.3. The decreased expression of retromer core components in these cells provides evidence that not only MNs, but also astrocytes display a deficiency in the retromer, similar to what I have found in the $SOD1^{G93A}$-Tg mouse model.

I also performed qRT-PCR analysis on these cultured human astrocytes and found a marked increase in the expression of VPS35 (Student t-test, p=0.025), VPS26A (Student t-test, p=0.0021), and VPS29 (Student t-test, p=0.00085). These results suggest that human astrocytes may be the site of a compensatory mechanism, possibly in response to the retromer dysfunction caused by the decreased expression of retromer proteins. Incidentally, in project independent to the work done for this thesis, I performed an unbiased RNAseq analysis of these astrocytes and found an enrichment for the PI3K pathway, which is crucial to not only retromer function, but also to endosomal trafficking as a whole. Genes from the pathway that were upregulated include PIK3CA, JAK2, and AKT3.

Table 2.3 Clinical Information on Patients from Whom Primary Astrocytes Were Cultured Post Mortem

PATIENT	GROUP NAME	RACE	GENDER	AGE AT ONSET	AGE AT DEATH	DISEASE DURATION (YEARS)
1	Non-Neurological Control	Caucasian	Female	N/A	58	N/A
2	Non-Neurological Control	Caucasian	Male	N/A	24	N/A
3	Non-Neurological Control	Caucasian	Female	N/A	87	N/A
4	Non-Neurological Control	Caucasian	Male	N/A	66	N/A
5	Non-Neurological Control	Caucasian	Male	N/A	81	N/A
6	ALS	Caucasian	Female	74	75	1
7	ALS	Caucasian	Male	68	73	5
8	ALS	Caucasian	Female	?	73	?
9	ALS	Caucasian	Male	58	70	12
10	ALS	Caucasian	Female	48	52	4
11	ALS	Caucasian	Male	?	61	?
12	ALS	Caucasian	Female	59	59	1 week

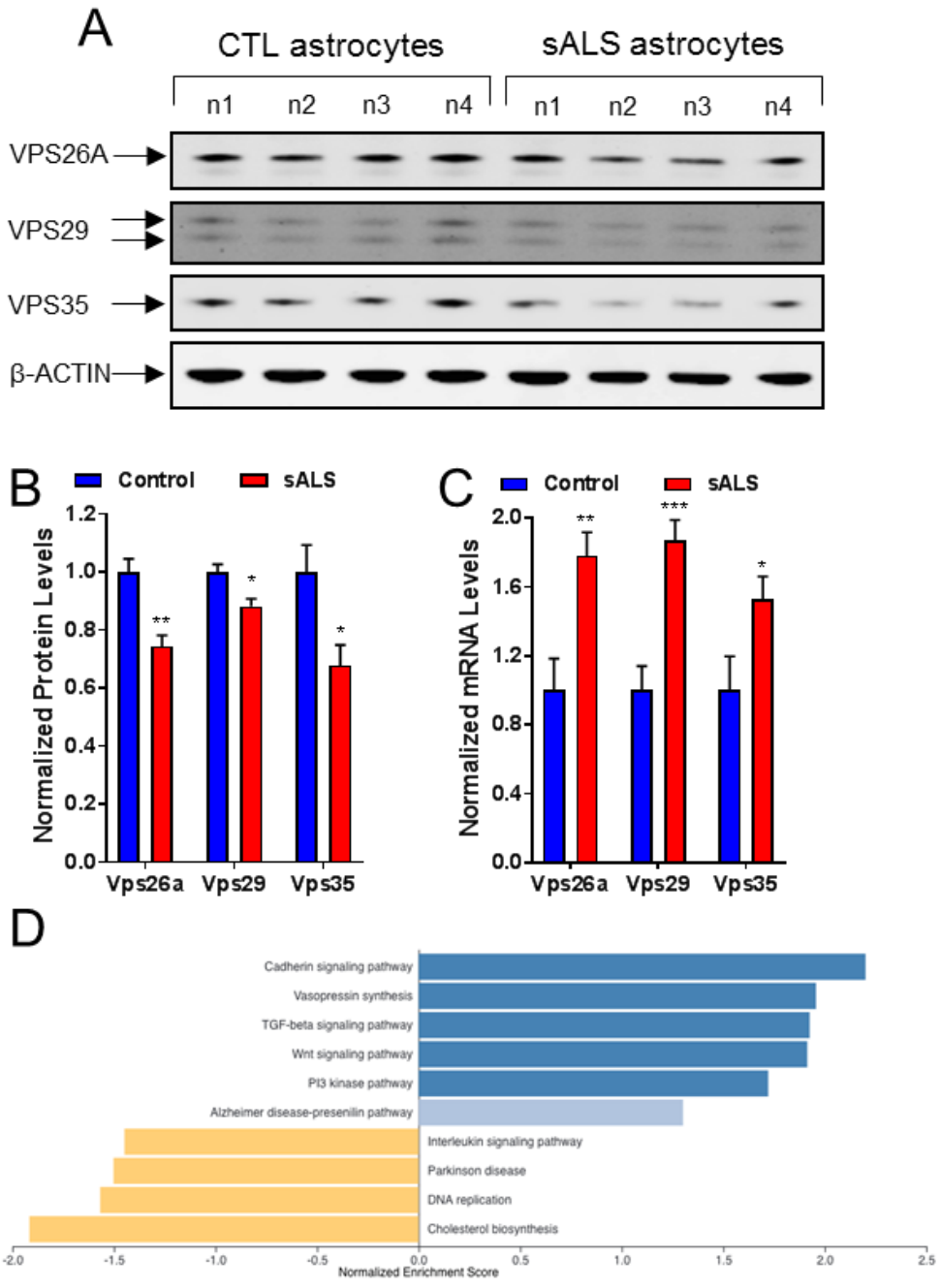

Figure 2.9 Primary Astrocytes Cultured from sALS Patients Express Lower Levels of Retromer Core Components

Primary astrocytes were cultured from post-mortem cortical tissues from sALS and control (CTL) patients. A Western blot was run on these astrocytes for retromer core components, of which a representative blot is presented here (A) with quantification of 5-7 replicates per group (B). qPCR analysis was also performed on these samples and normalized to Gapdh expression (C). RNAseq has also been performed on these samples, of which results from GSEA for Gene ontology pathway (Panther) enrichment analysis are presented here (D). (A-C) Results presented as mean ± SEM. n=5-7, *p<0.05, **p<0.01, ***p<0.001, unpaired Student t-test. (D) Results presented as top hits from normalized enrichment score. n=5-7, dark blue=FDR<0.05, PANTHER analysis.

2.3 Discussion

In this chapter, I sought to determine whether there was a possible connection between the retromer and ALS. I did so by following the model of previous studies that have linked other neurodegenerative diseases to the retromer. Since deficiencies in retromer components have been found specifically in the affected areas of various neurodegenerative diseases, I looked at the affected tissues and cells in the $SOD1^{G93A}$-Tg mouse and in ALS patients. Previously, a study performed on iPS-derived MNs from patients with an ALS-causing expansion in the C9orf72 gene showed an incidental trend towards the decreased expression of VPS26A. However, this thesis presents the first comprehensive demonstration of a decrease in the expression of retromer components in the context of ALS. This decrease was seen consistently in the context of the $SOD1^{G93A}$-Tg mouse and in the culture of human cells affected by ALS.

2.3.1 Retromer depletion in ALS MNs

As MNs are the primary cell type associated with the pathology of ALS, any alterations in the functional processes of these cells are immediately suspect. It is difficult to obtain a pure enough population of MNs to be able to study retromer deficiencies in these cells. Thus, in my work, I have employed a number of avenues to study MNs via quantitative analysis of IHC and the use of iPSC-derived MN. From these, two experiments showed a decrease in the expression of Vps35.

As mentioned in the result section, the quantification of fluorescence intensity of IHC, while appealing, must be taken with caution, as this approach is fraught with a host of possible technical problems such differences in tissue fixation, background fluorescence, signal amplification by antibodies, and poor linearity of the signal, to cite only a few. That said,

quantification of the mean fluorescence intensity (MFI) of protein IHC has often been employed to predict relative differences in protein expression between conditions. My analysis of relative MFI of Vps35 IHC in SC MNs showed a stark difference between P120 SOD1^{G93A}-Tg mice and control NTg mice. Thus, while it cannot be said that proteins expression necessarily differs between the two conditions to the extent that the MFI differs, my data indicate a strong likelihood that there is a difference to at least some extent.

These data are supported, and indeed enhanced by my finding that MNs derived from iPSCs from ALS patients with known ALS-causing SOD1 mutations show a decreased expression of VPS35 as well as trend towards decreased expression of VPS29. Not only does this provide further evidence that ALS-causing SOD1 mutations decrease retromer expression in MNs, but it also shows that the effect is not specific to the context of the mouse model and is generalizable to human cells.

As the list of known retromer cargoes is ever-growing, and currently includes hundreds of candidates, the possible downstream effects of retromer deficiency in MNs are numerous and require further study. Possibilities for such study include retromer cargoes that are known to be mistrafficked by the retromer in neurons in other neurodegenerative diseases, including the AMPA glutamate receptor, cathepsin D, APP, and CI-MPR. Indeed, of these, the AMPA glutamate receptor and APP have been variously implied in the pathology of ALS. Briefly, studies have found that the altered trafficking and composition of the AMPA glutamate receptor results in greater calcium influx into the cell, which induces excitotoxicity in MNs (Corona and Tapia 2007; Kawahara et al. 2003). APP fragments have been shown to be increased in ALS patient cerebrospinal fluid (CSF), and have been proposed as biomarkers for the disease (Steinacker et al. 2011; Stanga et al. 2018).

2.3.2 Retromer depletion in ALS astrocytes

Studies performed in our lab have shown that cultured ALS-affected astrocytes induce the degeneration of MNs. This was shown via experiments where NTg mouse MNs were co-cultured with astrocytes from the $SOD1^{G93A}$-Tg ALS mouse model, resulting in the degeneration of the MNs (Nagai et al. 2007). While the mechanism for this toxicity is not yet completely understood, further experiments showed that direct contact between astrocytes and MNs was not necessary for it to happen, as treatment of MNs with media conditioned on $SOD1^{G93A}$-Tg astrocytes resulted in a similar toxic effect, indicating that astrocytes were releasing a toxic factor rather than failing to support MNs viability (Nagai et al. 2007). Later study also showed that astrocytes cultured from post-mortem cortical tissues of patients with ALS had similar toxic effects on MNs (Re et al. 2014; Haidet-Phillips et al. 2011). Interestingly, this toxicity from patient-cultured astrocytes occurs regardless of whether the patent has the sporadic or the familial form of the disease, indicating that astrocyte-induced toxicity is not specific to any specific ALS-causing mutation, but is rather a generalizable mechanism of neurotoxicity in ALS. Studies from other labs have also supported this idea, as MN toxicity has since been shown to be induced by multiple models of ALS-affected astrocytes, including from transgenic mice with ALS-causing mutations in FUS (Kia et al. 2018; Ajmone-Cat et al. 2019; Rojas et al. 2014). Altogether, these findings have shown that decoding the mechanism of ALS is vital to our understanding of the disease.

The fact that I saw a consistent decrease in retromer expression in both $SOD1^{G93A}$-Tg mouse astrocytes and patient sALS astrocytes indicates that the retromer may be involved in the mechanism of toxicity caused by these cells on MNs. Indeed, the fact that astrocyte toxicity seems to occur due to the release of a toxic factor provides clues that improper protein processing and trafficking, and specifically, retromer dysfunction, may be involved in astrocyte-induced MN

toxicity. Indeed, retromer depletion has been shown to cause the improper processing and secretion of various protein products including Wnt and toxic fragments of APP (Sullivan et al. 2011; Belenkaya et al. 2008; Mecozzi et al. 2014; Small et al. 2005; Bhalla et al. 2012; Ansell-Schultz et al. 2018; Zhang et al. 2011). It is thus possible that retromer depletion may be involved in the formation and secretion of toxic factors from astrocytes. However, data that I will present in later chapters indicated that if, in fact, retromer depletion is involved in the toxic effects of astrocytes on MNs, it is possible that such depletion, rather than contributing to toxicity, may be a protective mechanism, inhibiting such toxicity. While the retromer has been extensively studied in multiple cell types, including neurons and microglia, there is currently no literature on the effects of retromer function on astrocyte biology. The results of my research indicate that the study of astrocytes, particularly in the context of ASL, could benefit from a deeper exploration into the retromer and the effects of its dysfunction within them.

2.3.3 Retromer depletion coincides with active ALS pathology

Deficiencies in retromer expression in this study were found across multiple tissues and cells from the SOD1^{G93A}-Tg mouse model of ALS. Similarly, multiple cultured cell types from patients with ALS showed such deficiencies. However, of interest are also the samples from the SOD1^{G93A}-Tg mouse which showed no such change in the levels of retromer expression. Included are the lysates from mouse SCs at P60 and P90. At P60, mice do not yet show overt signs of ALS pathology, which start to appear around P90. While these lysates showed no significant decrease, when looked at together, the apparent progression from P60 to P90 to P120 shows what might be an interesting trajectory. At P60, SOD1^{G93A}-Tg mice seemed to express slightly higher levels of both Vps35 and Vps26a compared to NTg mice, of which Vps26a was statistically significant.

Conversely, at P90, they then showed a slight, but not statistically significant trend towards decreased expression of both Vps35 and Vps26a. Ultimately, at P120, a robust decrease in expression was seen. This seeming progressive decrease gives way for further, higher powered studies performed at shorter intervals of disease progression, which it is possible could show a steady decrease over the lifetime of the mouse, possibly buffered by a compensatory increase in mRNA, rather than a complete lack of change ending in a precipitous decline at P120.

In any case, it is clear that pre-symptomatically, $SOD1^{G93A}$-Tg mice do not show any particularly appreciable deficiency in the retromer. Cortical neuronal cultures and kidney lysates from these mice as well as SC lysates from wtSOD1-Tg mice also showed no change in retromer expression. What all of these samples have in common is that none are known to show any overt pathology of ALS. Although the cortical neurons, kidney, and pre-symptomatic SC samples all overexpress the same $SOD1^{G93A}$ protein that the P120 SC does, and the wtSOD1-Tg mouse overexpresses the same levels of enzymatically active SOD1, it seems that the fact that these tissues are minimally or entirely unaffected by disease may either result or even be partially influenced by the lack of retromer depletion. By this model, it makes sense that ALS-affected astrocytes and MNs show a deficiency in retromer, as these cell types, as outlined above, are known to be directly involved in the pathogenesis of ALS. Further, the presence of retromer deficiency in P120 cortex and cerebellum may be linked to the fact that glia make up the bulk of the volume of neural tissues, and it has been shown that astrocytes induce MN degeneration regardless of the part of the CNS they originated from. While I saw no statistically significant change in SC samples from patients with ALS—which are obviously affected by ALS pathology—the trends I saw in these samples and the low power does not allow me to exclude a difference with certainty. Furthermore, since patient often display different levels of pathology in different

areas of the spinal cord, it is possible that retromer expression may correlate with level of pathology in the area where the spinal cord sample was taken. Thus, upon further study, we may see a relationship between levels of retromer expression and levels of ALS pathology within the same area.

2.3.4 Expression of retromer proteins and mRNAs in ALS tissues and cells

Further study, some of which will be explored in later chapters of this thesis, involves looking at the upstream causes of retromer deficiency, and how it intersects with ALS pathogenesis. Since I did not find any reduction in mRNA associated to the decrease of protein levels of retromer core components, the work presented in this chapter enabled me to discount the possibility of a change in transcription of retromer components as the contributing factor to retromer deficiency. On first glance, this is rather surprising, as most studies that have shown a decrease in the expression of retromer core proteins in the context of neurodegeneration have shown a concomitant, likely causative decrease in mRNA levels coding for them. Indeed, the finding that first connected the retromer to any neurodegenerative disease involved a decrease in the expression of VPS35 mRNA as measures by microarray on AD patient tissue. This finding then ultimately led to finding a deficiency in protein levels of VPS26 and VPS35 in these tissues. Thus, the fact that retromer core protein-coding mRNA show no change in the context of ALS, and indeed show an increase in sALS patient astrocytes and $SOD1^{G93A}$-Tg mouse SCs runs counter to much of the history of the connection between neurodegeneration and the retromer.

However, a recent study in Pick's disease and PSP showed similar results to those I have seen for ALS here, albeit in post-mortem tissue samples from patients (Vagnozzi et al. 2019). In that study, tissues from affected patients had decreased levels of retromer core proteins, but there

was no accompanying change in mRNA levels. Thus, these results appear and sound quite relevant to the work done in this thesis, as Pick's disease is a form of frontotemporal dementia (FTD), which exhibits a high comorbidity, shares some associated gene mutations, and is thought to exist on a spectrum with ALS (Renton et al. 2011; DeJesus-Hernandez et al. 2011; Bannwarth et al. 2014; Fecto et al. 2011; Cirulli et al. 2015). Thus, the results of my study are consistent with the results from a disease most closely linked to ALS, though the upstream cause of retromer core protein deficiency remains a mystery.

The well-established role of RNA misregulation in ALS, including the fact that FUS and TDP-43—two of the proteins whose mutation is most often associated to ALS—are both RNA-binding proteins, might also have indicated that retromer protein deficiencies may have been the result of decreased mRNA expression. However, the results from my experiments indicate that ALS pathology mostly does not seem to have a deleterious effect on the expression of retromer core protein-encoding mRNA. Indeed, quite the opposite, it seems, might be the case, as SC lysates from $SOD1^{G93A}$-Tg mice, and especially astrocytes from patients with sALS showed a remarkable increase in the expression of such mRNA This could be indicative of a currently poorly understood mechanism known as genetic compensation in which the cell upregulates mRNA production in response to a reduction in the downstream effects of the protein it encodes (Rossi et al. 2015; El-Brolosy and Stainier 2017). Similar such effects have been seen in C. elegans, which has two paralogues encoding for superoxide dismutase, *sod-1* and *sod-5*, and in which the deletion of the sod-1 gene causes the upregulation in mRNA levels of the *sod-5* gene (Yanase et al. 2009). Further research may elucidate the mechanism whereby retromer mRNA is upregulated in response to the depletion of the retromer, and whether this process is specific to the context of ALS pathology or not.

Interestingly, RNAseq data from another project I have been conducting have shown that genes involved in the PI3K pathway are also upregulated in sALS astrocytes. PI3K functions in the formation of phosphatidylinositol 3-phosphate (PI3P), a lipid found on the membranes of early endosomes, and is directly involved in the recruitment of the retromer complex to the endosomal membrane (Shin et al. 2005; Xu et al. 2001; Ghai et al. 2011; Ghai et al. 2015). Thus, the upregulation of genes involved in the PI3K pathway and in the retromer may follow similar processes of the cell attempting to correct a dysfunction it is sensing through altered transcription. Indeed, it is possible that the depletion of the retromer may be due to changes in the lipid composition of the endosome. Interestingly, one of the genes that was upregulated in the RNAseq screen was AKT3, whose overexpression in MNs has been shown to be neuroprotective in $SOD1^{G93A}$-Tg mice (Peviani et al. 2014). The connection between the results of these two analyses could be further explored via the study of possible alterations in lipid metabolism in sALS astrocytes and its effect on the retromer.

2.3.5 Retromer deficiency not specific to mutations in SOD1

The finding that tissues and cells from the $SOD1^{G93A}$-Tg mouse show a decrease in retromer expression provides compelling evidence for the involvement of retromer deficiency in ALS. This is further supported by the fact a similar deficiency is seen in MNs derived from iPSCs from patients with SOD1-related ALS. However, these data alone would not preclude the possibility that it is specifically the mutation of SOD1 that results in retromer deficiency. Indeed, while SOD1-related ALS is clinically indistinguishable from sporadic ALS, it has been shown that certain features are specific, or at least highly correlated to ALS caused by a mutation in SOD1, including the aggregation of SOD1, the lack of TDP-43 aggregation, and a higher likelihood of

lower MN-predominant disease, and a decreased likelihood of comorbidity with FTD. The fact that I noted retromer deficiency in the context of non-SOD1-related ALS, particularly in sALS patient astrocytes shows that the mechanism of retromer deficiency is generalizable to ALS as a whole. This was further supported by the apparent decrease in retromer expression in astrocytes from Fus^{P517L} mutant mice, though this was seen in a single replicate, and replication of the experiment is warranted.

CHAPTER 3

CAUSES AND EFFECTS OF RETROMER DEFICIENCY IN SOD1^{G93A}-TG ASTROCYTES *IN VITRO*

3.1 Introduction

In the previous chapter, I demonstrated that the context of ALS results in retromer depletion both in neural tissues from the SOD1^{G93A}-Tg mouse model of ASL and in multiple CNS cell types, both in SOD1^{G93A}-Tg mice and in ALS patients. In this chapter, I will study some of the possible upstream causes of retromer deficiency as well as some of the downstream effects.

3.1.1 Degradation of retromer proteins

Retromer protein deficiency has been found in the context of multiple neurodegenerative diseases, and when this is the case, most often, an accompanying decrease in the level of retromer mRNA is also found. This has been the case for AD, PD, and DS (Wang, Zhao, et al. 2013; Small et al. 2005; MacLeod et al. 2013). This would indicate that the reason for the decreased expression of retromer protein in these diseases is in fact the decreased expression of retromer-coding mRNAs. Whether this is due to a decrease in transcription or to the mishandling of the mRNA post-transcription is unknown. However, my results in Chapter 2 have shown that ALS pathology does not seem to cause a decrease in retromer mRNA expression. Thus, the root of the difference in retromer protein expression in ALS is likely either a difference in the translation of these mRNAs or to the differential degradation of retromer proteins.

Previous studies have shown that the stability of the retromer complex is integral to the expression levels of its components. Namely, the depletion of Vps35, Vps26a, or Vps29 has been

shown to cause a reduction in the protein levels of the remaining retromer components, indicating that if the complex cannot be formed, the components are solubilized and degraded (Mecozzi et al. 2014; Fuse et al. 2015; Bhalla et al. 2012). Furthermore, pharmacological chaperones have been made that stabilize the formation of the retromer complex at the binding site between Vps35 and Vps29 (Mecozzi et al. 2014). Treatment of cells with these chaperones has been shown to increase the levels of retromer protein and function in the cells, showing further proof that the stability of the complex is one of the main determinants of retromer protein expression (Mecozzi et al. 2014).

While the effects of retromer disruption on the degradation of other proteins is widely studies, there is precious little research on the actual methodology of the degradation of retromer proteins themselves. One study using proteasomal and lysosomal inhibitors in the context of the knockdown of retromer core proteins has shown that the proteasome is responsible for the degradation of Vps35 and Vps26a (Fuse et al. 2015). However, the mode of degradation of Vps29 is unknown. The fact that Vps35 and Vps26a degradation occurs at the proteasome makes intuitive sense, as both of these are generally found in the cytoplasm when not associated to the retromer complex. How these proteins get targeted to the proteasome has not been a major subject of study. One study showed that the PD-associated protein parkin is involved in the ubiquitination of Vps35, and while it confirmed that Vps35 was degraded by the proteasome, parkin-mediated ubiquitination was shown to not be associated to Vps35 degradation (Williams et al. 2018).

3.1.2 Retromer trafficking of APP

AD is characterized by the accumulation of toxic Aβ fragments of APP in the brain. At least in part due to this, starting with the first study to connect the retromer to AD, the trafficking of APP by the retromer and the effects of retromer dysfunction on APP processing have been the

subject of intense study (Small et al. 2005). These effects have been shown to be two-fold. First, the retromer is known to traffic SORL1, which itself binds APP (Reitz et al. 2013; Fjorback et al. 2012). Thus, the disruption of the retromer prevents the trafficking of APP away from the endosome, where it is more likely to undergo cleavage by BACE1, the first step towards the formation of Aβ (Jiang, Li, et al. 2014; Checler 1995; Bhalla et al. 2012; Muhammad et al. 2008). Second, the retromer has also been shown to traffic BACE1 away from the endosome (He et al. 2005; Wang et al. 2012). Since BACE1 works optimally at the acidity levels of the endosome, if the retromer fails to traffic it away from the endosome, it is more likely to cleave APP found there, producing Aβ.

The depletion of the retromer, due to a combination of these effects, has shown to be integral to the proper processing of APP. Studies that induce a deficiency in the retromer have shown that this results in APP being more highly concentrated in the endosome and cleaved to form and secrete higher levels of Aβ both *in vitro* and *in vivo* (Toh et al. 2018; Bhalla et al. 2012; Muhammad et al. 2008; Small et al. 2005). Conversely, treatment of cells with the above mentioned retromer pharmacological chaperones results in an attenuation of Aβ production (Mecozzi et al. 2014). Altogether, the alteration of APP trafficking and processing has been one of the most well-characterized effects of retromer deficiency.

3.2 Results

In the previous chapter, I reported on reductions in the retromer core subunits in both human sALS and mouse fALS tissues and cells. In this new chapter, I thus sought to shed some light onto the reasons why this deficiency occurs as well as on downstream effects of this deficiency. To address these questions, I decided to focus on primary astrocytes from $SOD1^{G93A}$-

Tg and NTg mice for three main reasons: (i) these astrocytes show a consistent and robust decrease in retromer protein expression; (ii) they are an easily attainable, purifiable, and expandable *in vitro* cell model; and (iii) they have a well-established role in the pathogenesis of ALS in mice.

3.2.1 Retromer expression is independent of astrocyte activation state

It has been proposed that in neurodegenerative disorders like ALS, astrocytes may adopt a neurotoxic phenotype, called A1 (Liddelow et al. 2017). This A1 phenotype is thought to result from the exposure of astrocyte to interleukin-1alpha (Il-1α), tumor necrosis factor alpha (TNFα), and complement component 1, q subcomponent (C1q) released by neighboring microglia (Liddelow et al. 2017). I thus first wondered whether the observed retromer alterations could be a feature of the A1 phenotype by which astrocytes, for example, rearrange their protein subcellular distributions to promote neurotoxic mediators. To test this idea, I cultured NTg astrocytes, and treated them with Il-1α, TNFα, and C1q for 7 days. After that treatment, I collected the astrocytes, and first confirmed that upon exposure to Il-1α/TNFα/C1q, astrocytes are enriched in at least some of the published A1 gene set (Liddelow et al. 2017). Specifically, I found a statistically significant upregulation of H2-D1 (paired Student t-test, p=0.0026) and Serping1 (paired Student t-test, p=0.015), and a trend towards upregulated H2-T23 (paired Student t-test, p=0.11) (Fig. 3.1A). I then looked at the level of expression of retromer proteins in these Il-1α/TNFα/C1q-treated astrocytes, and I found that, as assessed by Western blot, the levels of neither Vps35 (paired Student t-test, p=0.79) nor Vps26a (paired Student t-test, p=0.53) proteins differ between astrocytes treated with Il-1α/TNFα/C1q and those treated with vehicle control (Fig. 3.1B, C). Thus, the activation state of astrocytes in ALS is unlikely to be a major determinant of retromer expression.

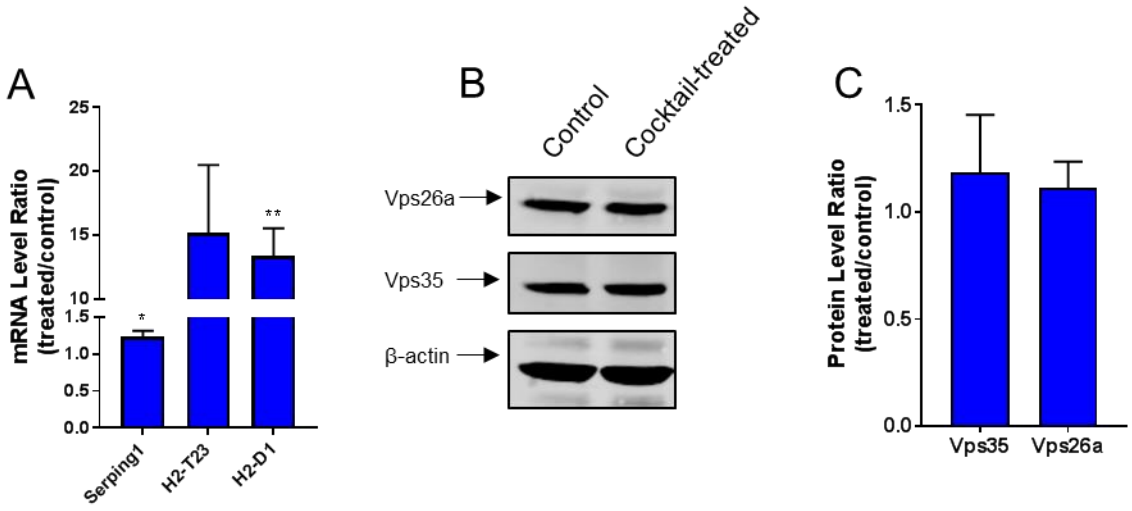

Figure 3.1 A1 Activation of Astrocytes Incites No Significant Changes in Retromer Expression

NTg astrocytes were treated with Il-1α, TNFα, and C1q for 7 days and collected at the end of treatment. qRT-PCR analysis was performed for mRNA markers of A1 activation (A). Western blot was performed on these astrocytes for retromer component levels. A representative blot is presented here (B) with quantification of 5 replicates per group (C). All results presented as fold change between astrocytes treated with A1 cocktail to those treated with vehicle, mean ± SEM. n=5, *p<0.05, **p<0.01 in paired Student t-test.

3.2.2 Retromer degradation rate is independent of astrocyte SOD1^{G93A} transgene expression

In Chapter 2, I saw that decreases in retromer protein expression in ALS tissues and cells never coincided with decreases in levels of mRNA expression. In fact, when there was a change in mRNA levels, the content of mRNAs for the retromer core components were increased instead. This mRNA/protein discrepancy argues that the observed changes in retromer protein expression are likely due to a post-transcriptional mechanism. Thus, I decided to examine whether an increase in the degradation of the retromer complex in the context of ALS may account for the reductions in retromer protein. To look at the degradation rate of retromer components in SOD1^{G93A}-Tg and NTg astrocytes, I inhibited protein translation by treating astrocytes of both genotypes with

cycloheximide for 0, 12, or 24 hours and then followed the amount of retromer core proteins by Western blot, over time.

First, I confirmed that the cycloheximide treatment successfully impaired translation. A Western blot for Cyclin D3, a cell cycle protein known to have a short half-life and often used as a control for cycloheximide treatment, showed a significant time-dependent decline in expression in both SOD1^{G93A}-Tg and the NTg astrocytes (Fig. 3.2A). These results confirm that, under our experimental conditions, cycloheximide treatment not only inhibited protein translation, but also did so comparably in both SOD1^{G93A}-Tg and the NTg astrocytes. Likewise, I found that all three core subunits declined over time in both SOD1^{G93A}-Tg and the NTg astrocytes (Fig. 3.2). However, I found no significant difference in the rates of decay for any of the three subunits between the SOD1^{G93A}-Tg and the NTg astrocytes: Vps35 (extra sum-of-squares F test, p=0.95), Vps26a (extra sum-of-squares F test, p=0.12), and Vps29 (extra sum-of-squares F test, p=0.67). This indicated that the difference in retromer expression between the two conditions was likely pre- or peri-translational. Nonetheless, I cannot exclude with certainty that the difference in retromer subunits may be due difference in degradation since the studied retromer components seem to have a fairly long half-life, as evidenced by this assay, and thus an assay longer than 24 hours might have been useful to tease out subtler changes in degradation. However, I have found that astrocytes develop marked toxicity when treated with cycloheximide for more than 24 hours, preventing me from carrying on any reliable such longer experiment.

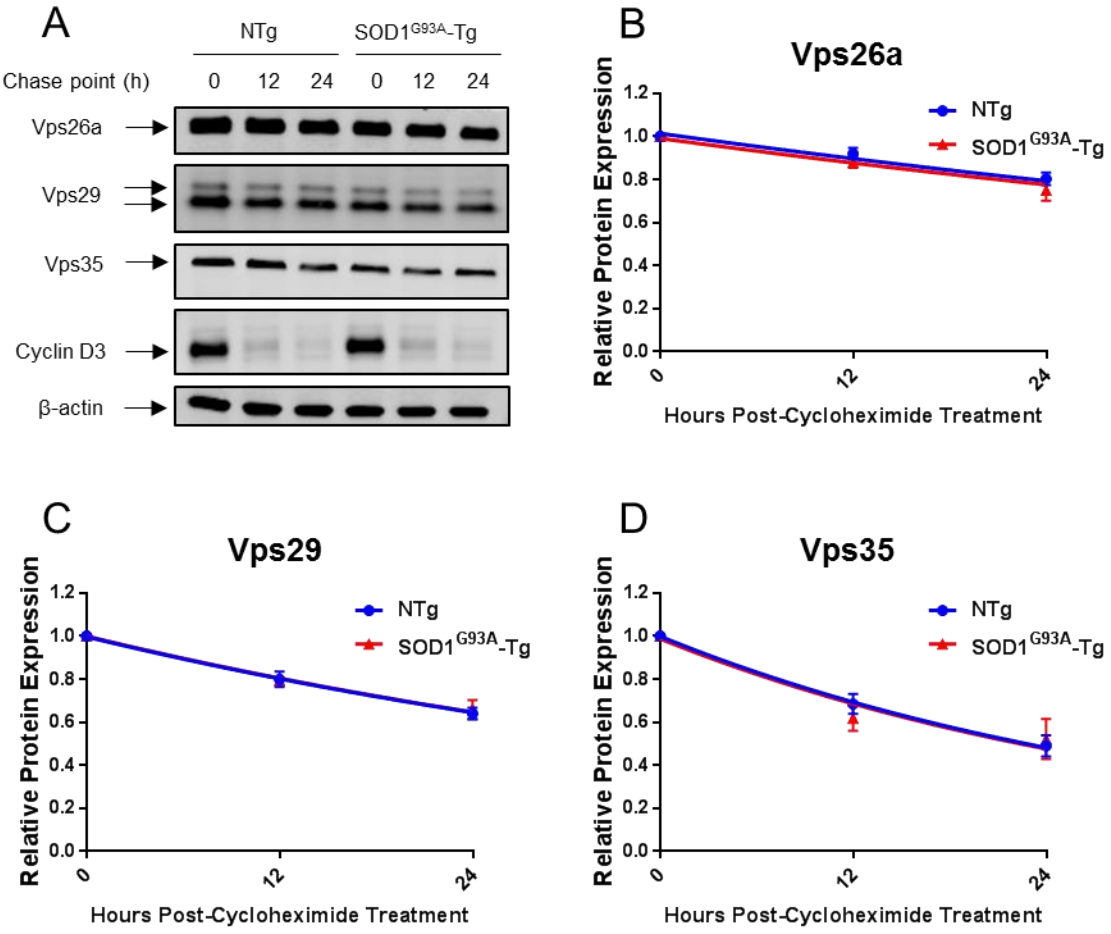

Figure 3.2 Cycloheximide Chase Assay for Retromer Proteins in NTg and SOD1^{G93A}-Tg Astrocytes

NTg and SOD1^{G93A}-Tg astrocytes were treated with cycloheximide for 0, 12, or 24 hours. A Western blot was run on collected lysates from these cells. A representative blot is presented here (A). Decay of protein expression in each group is plotted with a best-fit one phase decay curve for Vps26a (B), Vps29 (C), and Vps35 (D). All results presented as fold change from time point 0 for each genotype, mean ± SEM. n=4, no significance in extra sum-of-squares F test for degradation rate constant K.

3.2.3 APP trafficking and processing in SOD1^{G93A}-Tg astrocytes

To determine whether the observed reductions in retromer subunit expression are associated with an altered retromer function, next, I thought to examine the processing of APP in SOD1^{G93A}-Tg astrocytes. This experiment was prompted by previous demonstrations that deficiencies in retromer function cause an increase in the secretion of Aβ, a cleavage product the

retromer cargo APP (Bhalla et al. 2012; Small et al. 2005). Accordingly, I cultured both SOD1^{G93A}-Tg and NTg astrocytes for 7 days and then collected the media they were cultured in. Members of the lab of Dr Scott Small then ran an enzyme-linked immunosorbent assay (ELISA) on these samples using a kit that detects Aβ42 (Invitrogen, cat. # KMB3441). This analysis revealed significantly higher levels of Aβ42 in culture media conditioned with SOD1^{G93A}-Tg astrocytes compared to those in media conditioned with NTg astrocytes (Fig. 3.3). Thus, this result supports the idea that SOD1^{G93A}-Tg astrocytes exhibit higher rates of APP processing and secretion of Aβ42 fragments.

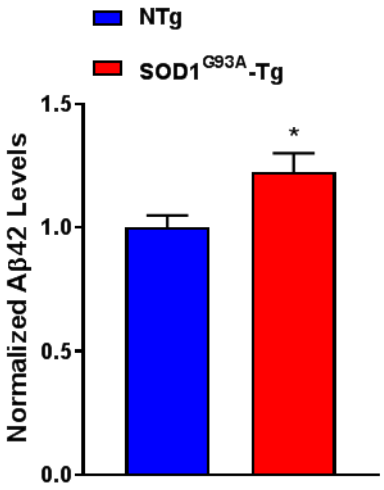

Figure 3.3 ELISA for Aβ42 in NTg and SOD1^{G93A}-Tg Astrocytes

NTg and SOD1^{G93A}-Tg astrocytes were plated, and media was conditioned on them for 7 days. The media was then collected, and an ELISA for the Aβ42 fragment was performed and normalized to total protein levels in the media. Results presented as mean ± SEM. n=4-5, *p<0.05 in unpaired Student t-test.

In light of these results, I then assessed the localization of APP within SOD1^{G93A}-Tg astrocytes as another proxy of retromer function. Accordingly, I performed immunocytochemistry (ICC) to examine the co-localization between APP and EEA1 (a marker of the early endosomal membrane) to determine whether APP is being mistrafficked and sequestered in the endosome.

Indeed, such co-localization has previously been shown to be increased in response to a deficiency in the retromer (Bhalla et al. 2012). However, I found no significant difference in the co-localization indices between SOD1^{G93A}-Tg and NTg astrocytes (Fig. 3.4D). I also found no evidence of swelling of endosomal size between SOD1^{G93A}-Tg and NTg astrocytes (Fig. 3.4C), a feature that has been reported with retromer ablation (Bhalla et al. 2012). Lastly, I performed an ICC to evaluate the co-localization between APP and Vps35 as a basic test of whether the retromer deficiency I had found in SOD1^{G93A}-Tg astrocytes caused APP to be trafficked by the retromer to a lesser extent. With this approach, I found that ICC signal for APP did co-localize with Vps35-positive vesicles to a significantly lesser extent in SOD1^{G93A}-Tg and NTg astrocytes (Fig. 3.5E). Thus, while APP mistrafficking and alterations in endosomal dynamics are not overt in SOD1^{G93A}-Tg astrocytes, the above cited results are in keeping with a subtle retromer deficiency.

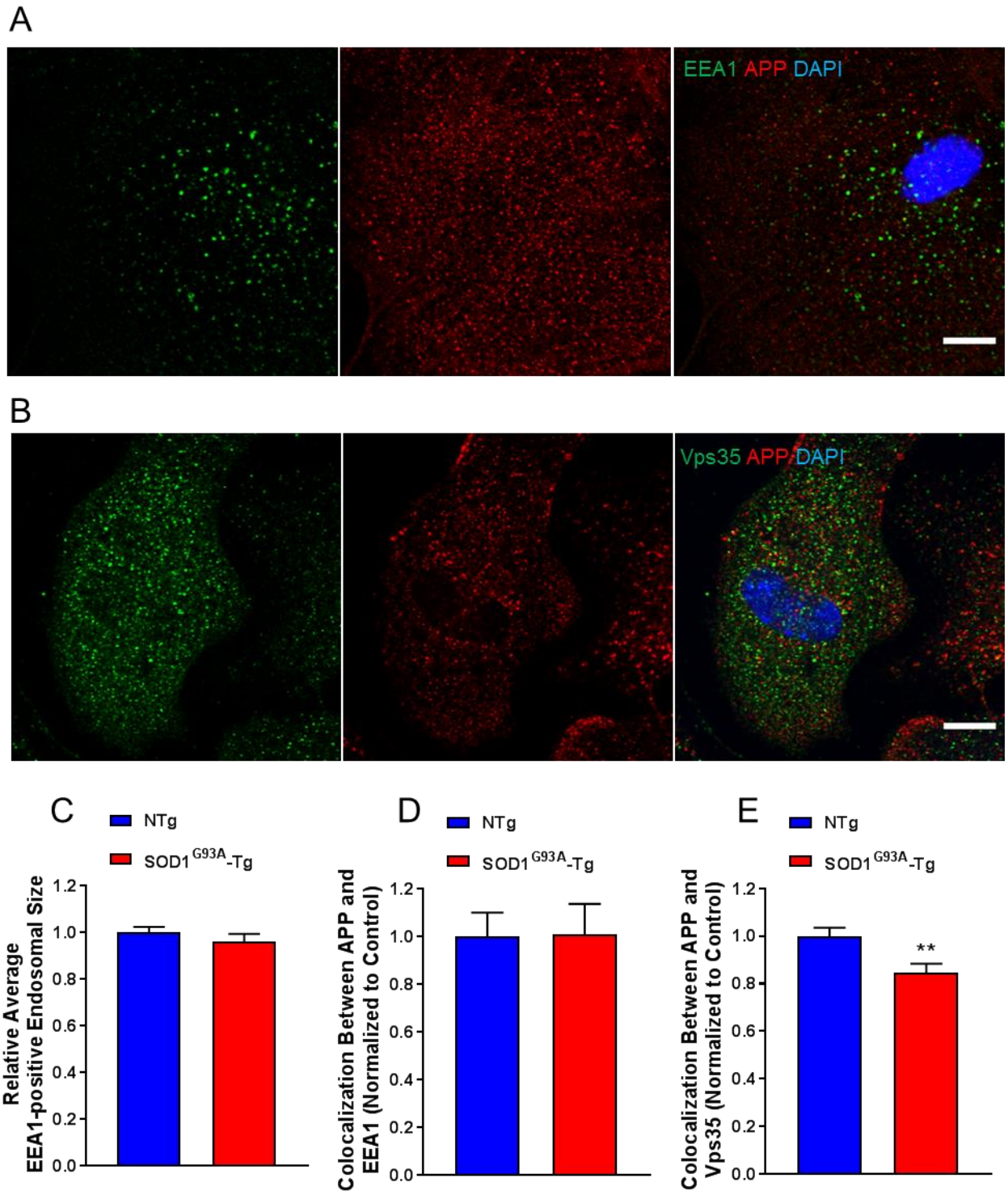

Figure 3.4 Co-localization Analysis for APP Trafficking in NTg and SOD1^{G93A}-Tg Astrocytes

ICC was performed on NTg and SOD1^{G93A}-Tg astrocytes. Representative images for EEA1 co-stain with APP (A) and for Vps35 co-stain with APP (B) on NTg astrocytes are shown. Endosomal size was quantified via image particle analysis of EEA1 stain (C). Relative levels of co-localization of APP in either EEA1 (D) or Vps35 (E) over total APP were quantified. Scale bars are 10μm. All results presented as fold difference from average of NTg, mean ± SEM. n>30 fields of imaging from at least 3 independent experiments, *p<0.05 in unpaired Student t-test.

3.2.4 Neurotoxicity due to retromer depletion in an in vitro system

In light of the above results, I then sought to determine whether retromer deficiency is sufficient to cause MN toxicity. To this end, I first made a lentivirus that expressed a plasmid graciously provided by the Small lab, which produces a short hairpin RNA (shRNA) against Vps35. I validated that treatment of astrocytes over 5 days resulted in the dramatically reduced expression of Vps35, both in mRNA (Student t-test, p=0.00019) and in protein (Student t-test, p=0.000018). I also observed that the depletion of Vps35 in astrocytes, as previously documented in other cells (Bhalla et al. 2012; Fuse et al. 2015), causes a concomitant reduction in Vps26a (Student t-test, p=0.000034) and Vps29 (Student t-test, p=0.0032) despite the fact that mRNAs coding for both Vps26a and Vps29 showed no change (Student t-test, Vps26a p=0.79, Vps29 p=0.81) (Fig. 3.5A-C). This is likely due to the destabilization of the retromer complex and ensuing increase in Vps26a and Vps29 degradation. I also noted that the silencing of Vps35 did not induce any overt astrocyte death over the course of at least one month.

Using this Vps35 shRNA virus as well as a virus expressing control shRNA, I designed an experiment to test the effect of retromer depletion on astrocyte-induced MN toxicity. I treated NTg astrocytes with either Vps35 shRNA or control shRNA. I then differentiated MNs from mouse embryonic stem (ES) cells expressing GFP under the HB9 motor neuron promoter. I plated these ES-derived MNs (ESMN) on the virus-treated astrocytes and traced the level of MN death over time. Interestingly, I found that ESMNs plated on astrocytes which had been depleted of Vps35 died at a faster rate than ESMNs plated on control shRNA-treated astrocytes (paired Student t-test, Day 2 p=0.0018, Day 3 p=0.0079, Day 4 p=0.0018, Day 5 p=0.0033, Day 6 p=0.025, Day 7 p=0.034). Thus, a deficiency retromer expression can kill MNs via a non-cell autonomous mechanism.

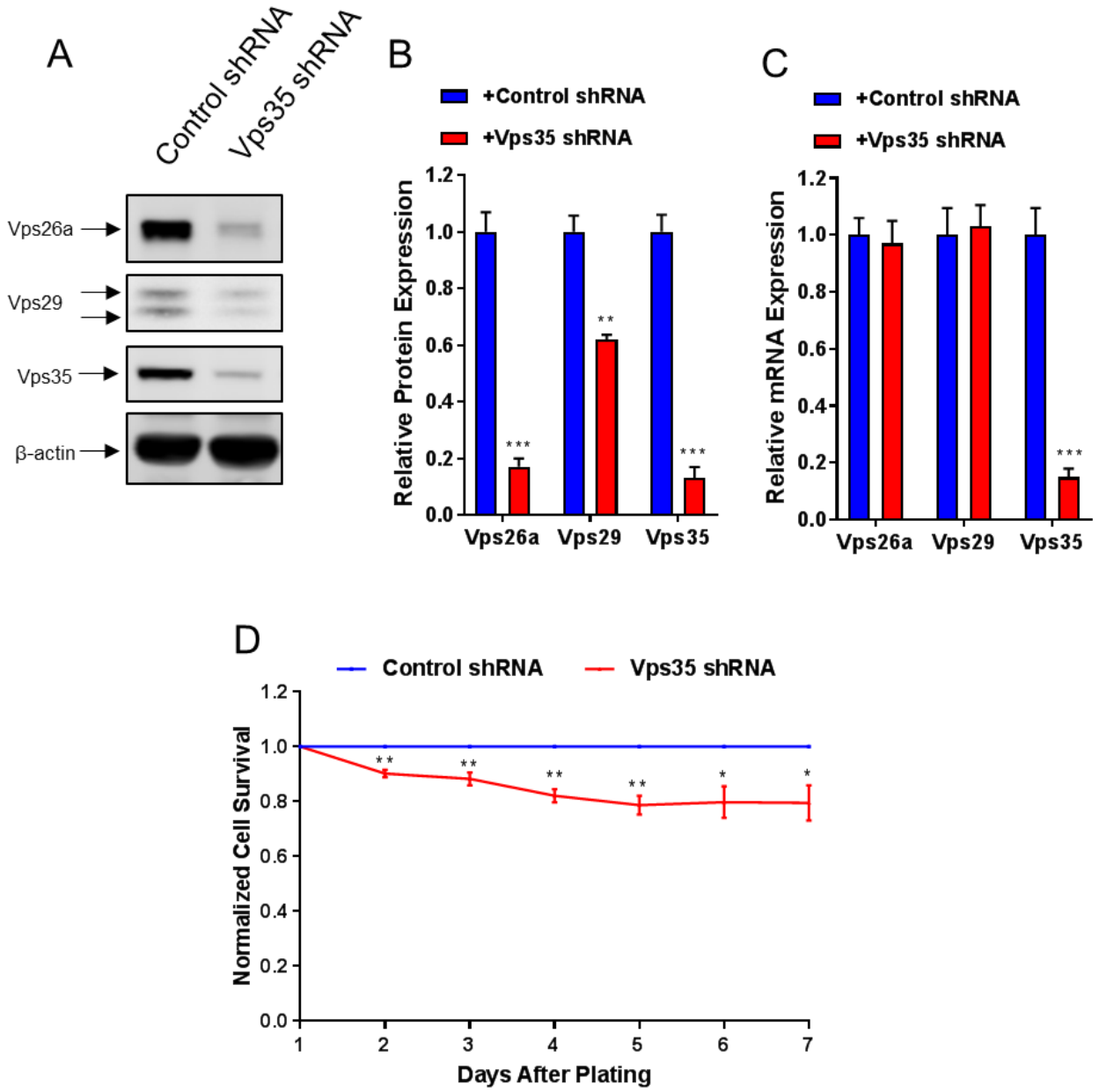

Figure 3.5 Astrocytes with a Depletion of Retromer Induce Toxicity in MNs

NTg astrocytes were treated for 5 days with either Vps35 shRNA or control shRNA. Knockdown was validated by Western blot for retromer proteins. A representative blot is presented here (A) with quantification of 4 replicates per treatment group (B). qRT-pCR of these astrocytes was also performed for retromer protein-coding mRNA (C). An experiment was run in which treated astrocytes were co-cultured with ES-derived MNs expressing GFP under the HB9 promoter, and the relative viability of the MNs over time was assessed (D). All results presented as mean ± SEM. (B, C) n=4, **p<0.01, ***p<0.001 in unpaired Student t-test. (D) n=5, *p<0.05, **p<0.01 in paired Student t-test.

Since I have also found a deficiency in the expression of Vps35 in MNs, I went on to see whether the downregulation of Vps35 via treatment with Vps35 shRNA could also induce cell-autonomous toxicity in the MNs. To do this, I again differentiated ESMNs expressing GFP under the HB9 promoter. However, as I have noted above, a decrease in the expression of at least one type of non-MN cells cultured with MNs could by itself induce toxicity. Thus, in order to study the specific cell-autonomous mechanisms of MN degeneration, a highly-enriched MN culture was essential, and the differentiation of ESMNs generally produces a population of cells that is about 20% MNs, with the rest being a mix of neural-lineage cells, including astrocytes. In order to achieve a pure population of ESMNs, after dissociation of the cultures, I brought the differentiated cells to the Columbia Stem Cell Initiative (CSCI) Flow Cytometry Core, where they put the cells through fluorescence activated cell sorting (FACS) to separate GFP- from non-GFP-expressing cells (Fig. 3.6A). Thus, we produced a highly enriched population of neurons that expressed the MN marker HB9. I then cultured these MNs and after 24 hours in culture, I treated them with either Vps35 shRNA or control shRNA. I collected mRNA from these cells 3 days post-treatment, and found, via qRT-PCR, a consistent downregulation of Vps35 mRNA (One sample t-test, $p=0.0011$) with no significant change in Vps26a mRNA (One sample t-test, $p=0.36$) (Fig. 3.6B). Imaging and tracking of cell survival in this enriched ESMN culture showed that retromer depletion produced a time-dependent increase in cell-autonomous MN loss (paired Student t-test, Day 1 $p=0.73$, Day 2 $p=0.86$, Day 3 $p=0.22$, Day 4 $p=0.0017$, Day 5 $p=0.017$, Day 6 $p=0.014$, Day 7 $p=0.012$) (Fig. 3.6C). I repeated this experiment independently thrice from three differentiations of ES cells to MNs. Of note, there was no difference in survival up to 3 days post-treatment. However, as I have noted above, retromer component proteins have a fairly long half-life. Thus, the fact that MN degeneration does not occur significantly until 4 days post-treatment likely has

to do with the amount of time it takes for retromer depletion to reach toxic threshold in the cell. Once it does, it appears that retromer depletion causes an even larger increase in cell autonomous toxicity than in cell non-autonomous toxicity from astrocytes.

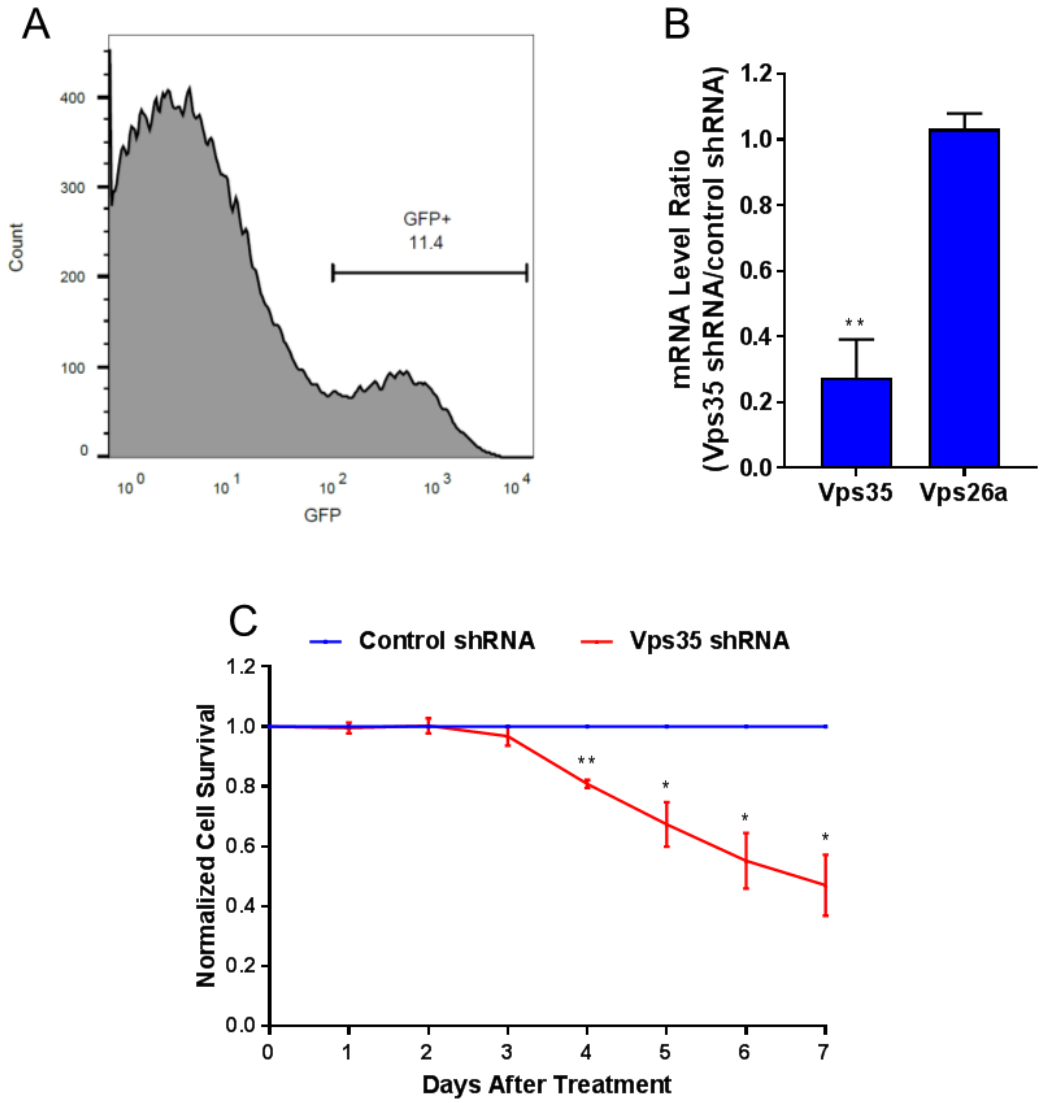

Figure 3.6 Depletion of the Retromer Induces Cell-Autonomous Toxicity in MNs

Mouse ES cells expressing GFP under the promoter of the motor neuron marker HB9 were differentiated into MNs. These cells were then sorted through FACS for GFP expression. Shown here is a histogram of a FACS gating that was used for one of the experiments (A). Purified GFP-expressing MNs were plated and treated with either Vps35 shRNA or control shRNA. The treatment was validated through qRT-PCR of the cells 3 days after treatment showing a decrease in the targeted Vps35 mRNA and not in Vps26a mRNA (B). The relative viability of these cells by treatment was monitored over time (C). (B, C) Results presented as fold change between MNs treated with Vps35 shRNA to those treated with control shRNA, mean ± SEM. n=3, *p<0.05, **p<0.01 in paired Student t-test.

3.3 Discussion

In this chapter, I followed up on the results of Chapter 2, where I had found a deficiency in the retromer in the context of ALS. I was curious what the possible upstream causes and downstream effects of retromer deficiency in ALS could be, so I used astrocytes cultured from $SOD1^{G93A}$-Tg mice, which showed a robust deficiency in the retromer as an *in vitro* model for ALS-induced retromer deficiency.

3.3.1 Retromer protein degradation

Since differences in mRNA expression seemed to not be the cause of retromer protein depletion in ALS, I posited that retromer protein degradation may be a differing factor in protein expression. Studies in mutant SOD1 have shown that misfolded SOD1 has a tendency to create abnormal protein-protein interactions that often disrupt functioning protein complexes. For example, one study has noted that mutant $SOD1^{G93A}$ and $SOD1^{G37R}$ are translocated into the nucleus of the cells in the spinal cords of Tg mice. There, they can bind to and disrupt the survival motor neuron protein (SMN) complex, which as the name suggests, is essential to the survival or MNs (Gertz, Wong, and Martin 2012). Furthermore, and of particular relevance to my research, it has been shown that the G93A, G85R, and A4V ALS-causing mutations in SOD1 cause SOD1 to bind to the dynein complex, preventing proper retrograde trafficking by this complex (Zhang et al. 2007). Since retromer expression is highly sensitive to the proper composition of the retromer complex, it is possible that retromer complex destabilization could be induced by a context of ALS, be that the expression of mutated SOD1 or otherwise.

However, I did not note a difference in the rate of decay of the retromer between NTg and $SOD1^{G93A}$-Tg astrocytes. It is important to note that what I did find via my cycloheximide chase

experiment is that the retromer core components seem to have a long half-life, both in NTg and SOD1^{G93A}-Tg astrocytes. As such is the case, it is difficult to say that the results of this experiment definitively mean that there are no changes in the rate of degradation of these proteins. Indeed, it is possible that a slight change in the rate of degradation could, over time, build up to retromer deficiency. However, with these limitations in mind, the fact that I saw no change in the rate of degradation indicates that it may be worth looking at changes in the translation of the retromer component mRNAs. As I have mentioned previously, the sequestration and mishandling of mRNAs has proven to be a part of ALS pathology. Briefly, the ALS associated proteins FUS and TDP-43 are RNA-binding proteins that regulate RNA processing, the ALS-causing expansion of C9orf72 can induce its RNA product to create RNA foci that sequester RNA handling machinery, and the mutation of SOD1 can cause it to abnormally bind to and sequester mRNA (Gendron et al. 2013; Buratti and Baralle 2001; Colombrita et al. 2012; Lu et al. 2007). Thus an experiment that assesses the level of effective translation of mRNAs in ribosomes may shed some further light on the causative factor for retromer protein deficiency. One such experiment would be polysome fractionation in which mRNA-associated ribosomes are separated in a gradient, and the distribution of a given mRNA transcript is assessed, comparing whether it is more enriched in fractions containing actively translating polysome fractions or in those containing ribosomes associated with a lower translation rate.

3.3.2 APP processing in ALS

In this chapter, I performed a series of experiments looking at APP trafficking in SOD1^{G93A}-Tg astrocytes as a possible downstream effect of retromer deficiency. It is important to note that while I show evidence that retromer deficiency and increased Aβ production co-occur in

SOD1^{G93A}-Tg astrocytes, this does not necessarily mean that one is causative of the other. While it is known that a deficiency in the retromer may lead to such an effect, the increased release of Abets fragments can be induced by a number of processes that would have to be examined to be certain that retromer deficiency is the main cause of Aβ production in the context of SOD1^{G93A}-Tg astrocytes. However, by showing a decrease in the colocalization of APP with Vps35, I provide some further evidence that indeed the retromer is trafficking APP to a lesser extent in SOD1^{G93A}-Tg astrocytes. Further studies looking at the trafficking dynamics of APP by the retromer in ALS cells, perhaps via live imaging and tracking, may provide further insight into how retromer deficiency affects cellular and molecular dynamics specifically in the context of ALS.

Of particular interest to these studies is the fact that APP has been variously implicated in ALS pathogenesis in a number of ways. First, the CSF of patients with ALS has been shown to have increased levels of Aβ, such that Aβ has been proposed as a biomarker for the disease (Steinacker et al. 2011; Stanga et al. 2018). Furthermore, a study in SOD1^{G93A}-Tg mice showed that the genetic ablation of APP in these animals resulted in clinical improvement as well as benefits to motor neuron survival, implicating APP in disease pathogenesis (Bryson et al. 2012). Finally, data which is currently in submission from our lab has shown that the misprocessing of APP, and specifically, β-secretase activity in astrocytes may be involved in the toxicity of astrocytes on MNs. Altogether, while APP is not the central topic of study of this thesis, the data from this chapter provide evidence for the possible interplay of retromer function and APP processing in ALS.

3.3.3 Neurotoxicity of retromer depletion

In this chapter, I showed that retromer depletion in either astrocytes or MNs can induce toxicity in MNs in an *in vitro* system. The implications of this are clear in the possible pathogenesis of ALS, considering that I have shown both of these cell populations to have a deficiency in the retromer in ALS and that MNs have been shown to die both of cell-autonomous and cell-non-autonomous mechanisms in ALS. However, especially in light of the work presented in later chapters of this thesis, it is important to take some caveats of these experiments into account. First, the treatment of cells with Vps35 shRNA results in a dramatic decrease in retromer expression, far greater than any deficiency I found in ALS tissues or cells. It is clear from multiple studies on the retromer, including this thesis, that the effect of retromer deficiency is highly dose-dependent. Indeed, the complete deletion of Vps35 or Vps26a has proven to cause lethality during embryonic development (Tang, Erion, et al. 2015). Meanwhile, a single allele deletion of Vps35 results in a viable mouse with a normal life span, though with a modest loss of dopaminergic neurons in the substantia nigra at advanced ages (Tang, Erion, et al. 2015).

Furthermore, Vps35 shRNA treatment induces a relatively sudden decrease in retromer expression. In contrast, the deficiency in retromer in tissues from $SOD1^{G93A}$-Tg animals would indicate that retromer deficiency in the context of ALS progresses more insidiously over time. It is possible that a decrease in the expression of the retromer may be tolerated by the cell if it is given enough time to effect compensatory mechanisms to make up for the loss of retromer function. Thus, while I have shown that retromer deficiency is sufficient to cause neurodegeneration both cell-autonomously and cell-non-autonomously, the application of these data to implications in ALS must be done with caution.

CHAPTER 4

RETROMER REPLETION IN SOD1^{G93A}-TG MICE

4.1 Introduction

As detailed in the *General Introduction* Chapter, there is increasing attention being paid to the hypothesis that retromer defects may be a shared molecular alteration in adult-onset neurodegenerative disorders. Indeed, deficiencies in the expression of retromer proteins have been found in multiple degenerative disorders, including Alzheimer's disease (AD), Parkinson's disease (PD), Down's syndrome (DS), Progressive Supranuclear Palsy (PSP), and Pick's disease (Small et al. 2005; Zhao, Perera, et al. 2018; Wang, Zhao, et al. 2013; Vagnozzi et al. 2019). These findings led me to ask whether ALS belongs to the growing list of neurodegenerative conditions linked to retromer defects. Relevant to this question, in Chapter 2 of this thesis, I showed a deficiency in the expression of retromer core components in tissue samples and cells from mouse models of ALS and patients affected with this fatal disease. These investigations indicated that the reduced expression of retromer core proteins became detectable in symptomatic SOD1^{G93A}-Tg mice in spinal cord and to lesser extents in the cerebral cortex and cerebellum, but not in non-neural tissues such as kidney. Of note, as I have shown to be the case for ALS and the SOD1^{G93A}-Tg mouse model, mouse models of AD, PD, and DS have shown similar such deficiencies (Chu and Pratico 2017; MacLeod et al. 2013; Wang, Zhao, et al. 2013). In Chapter 3, I generated a series of findings in cultured cells from SOD1^{G93A}-Tg mice supporting the conclusion that the structural defects in the retromer documented in Chapter 2 are associated with functional alterations using primarily APP processing and trafficking as functional proxy. In Chapter 3, I also showed that retromer deficiency could result in MN death, both in a cell-autonomous and in a cell-non-

autonomous manner, findings in keeping with the idea that retromer defects in ALS, as proposed in AD and PD, may contribute to neurodegeneration.

Thus, as a next step toward further characterizing the role of the retromer in ALS pathogenesis, I sought to determine the impact of therapy aimed at correcting retromer expression on the ALS-like phenotype in $SOD1^{G93A}$-Tg mice. The rationale here was that if retromer defects do indeed contribute to MN degeneration in ALS, then, mitigating them should attenuate neurodegeneration and, if so, have far-reaching implications for the treatment of ALS. Yet, before presenting my results for such an intervention in $SOD1^{G93A}$-Tg mice, it is important to provide some information about previous investigations performed to increase retromer expression as this will set the stage for the work done in this chapter.

4.1.1 Upregulation of retromer components in mouse models of neurodegeneration

One of the first of these such upregulation studies was performed in a mouse model of DS (Wang, Zhao, et al. 2013). While SNX27 is not considered one of the core components of the retromer, its primary function is to forms part of the retromer complex, and SNX27 is vital to the recruitment of the retromer to the endosome and of various retromer cargoes to the retromer (Clairfeuille et al. 2016; Ghai et al. 2014). A study performed on Ts65Dn mice, a well-characterized model of DS, showed that these mice replicated a decrease found in DS patients in the hippocampal expression of SNX27 (Wang, Zhao, et al. 2013). This prompted the authors to perform a study in which they injected the hippocampus of adult mice with an adeno-associated virus (AAV) that overexpressed SNX27. They found that DS-like defects normally found in Ts65Dn mice, including impaired long-term potentiation (LTP) and novel object recognition, were corrected in mice overexpressing SNX27.

Another similar study was also performed in a mouse model of PD, which overexpresses alpha-synuclein (SNCA), the primary protein whose aggregation is associated with PD (Dhungel et al. 2015). The authors found a deficiency in Vps35 expression in this mouse model and proceeded to inject the hippocampi of these mice at adulthood with lentiviral vectors overexpressing Vps35. In response to this gene therapy, the authors found that the levels of SNCA in the mouse's hippocampus decreased and that hippocampal neurons were spared from the degeneration usually seen in this specific mouse line (Dhungel et al. 2015).

A third upregulation study was performed in 3xTg mice, a well-characterized model of AD that harbors three mutant transgenes, one of which is APP (Li, Chiu, and Pratico 2019). While the authors did not report any baseline differences in retromer expression in these mice, they chose to study Vps35 overexpression in these animals due to the reported connection between the retromer and AD (Small et al. 2005; Vardarajan et al. 2012; Chu and Pratico 2017). Here, the authors injected mice at P1 intracerebroventricularly (ICV) with an AAV that expressed VPS35 under a neuronal promoter. They found that 3xTg mice injected with this construct displayed a rescue in disease associated pathology and phenotypes, including lower levels of Aβ production and improvement on memory testing.

Collectively, these three selected studies support the idea that in the context of retromer defect, overexpressing retromer core component such as Vps35 is achievable by viral vector and may have beneficial effects. As such, these previous studies provide major impetus to the experimental design and to one of the approaches used in this Chapter 4 to mitigate retromer defect.

4.1.2 Overexpression of Vps35 in a drosophila model of ALS

It is also particularly relevant to the work in this chapter to elaborate briefly on a study conducted on a *Drosophila* model of ALS which carries a loss of function mutation in the fly orthologue of the human ALS-associated gene VAMP-associated protein B (VAPB) (Sanhueza et al. 2015). This model displays an eye neurodegenerative phenotype, and the authors of this study conducted a screen for genes whose overexpression suppressed or enhanced this phenotype. Interestingly, one of the genes which had a suppressive effect was Vps35.

Altogether, the aforementioned studies support the conclusion that overexpression of retromer is beneficial is a variety of models of neurodegenerative disorders. However, upon performing studies designed to test the effect of overexpression of Vps35 in ALS, I found that the opposite was, in fact, the case, in that, retromer repletion in $SOD1^{G93A}$-Tg mice exacerbated rather than ameliorated the ALS-like phenotype seen in these animals.

4.2 Results

4.2.1 Pharmacological stabilization of the retromer in $SOD1^{G93A}$-Tg mice

To evaluate whether repletion of retromer levels had any effects on ALS-like pathology in $SOD1^{G93A}$-Tg mice, I first employed a retromer chaperone. Our collaborators in the lab of Dr Scott Small have developed small molecules that serve as stabilizing chaperones to the retromer core and have been shown *in vitro* to increase retromer levels in cells (Mecozzi et al. 2014). Further, retromer chaperones can inhibit the production of toxic APP fragments in neurons, as shown by decreases in the β C-terminal fragment of APP (β-CTF) in the cell as well as in secreted Aβ (Mecozzi et al. 2014). This indicates that chaperone-mediated retromer stabilization results in a functional improvement in the retromer. Further study of these chaperones by the Small Lab has

indicated that one of them, R33, when injected intraperitoneally (IP) daily into mice for 14 days at a dose of 50mg/kg of R33 in 5% DMSO (determined as the maximum tolerated dose), crosses the blood-brain barrier, as evidenced by its high brain/plasma ratio after (Fig. 4.1A). There, R33 can increase the level of retromer expression in the forebrain as well as decrease levels of the β-CTF, similar to its effect *in vitro* (Fig. 4.1B).

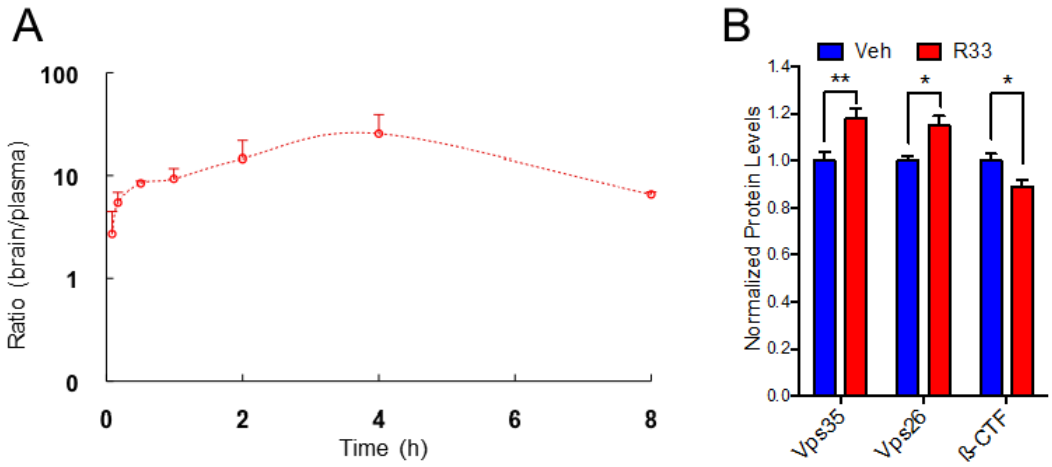

Figure 4.1 R33 Crosses the Blood-Brain Barrier and Stabilizes the Retromer Complex

Data and figure provided by the lab of Dr. Scott Small. (A) Plot of ratio of presence of drug in brain over that in plasma as measured by liquid chromatography with mass spectrometry. (B) Quantification of Western blot for retromer core components and βCTF in WT mouse forebrains in response to two weeks of daily R33 or vehicle treatment. Results presented as mean ± SEM. n=7, *p<0.05, **p<0.01 in unpaired t-test

To begin, I performed a pilot study in which I treated SOD1^{G93A}-Tg mice with a similar regimen of R33 for 7 days beginning at P100. At P107, I ran a Western blot on SC lysates of these mice which showed a marked increase in the levels of Vps35 in the mouse in response to R33 treatment (one-way ANOVA followed by Holm-Sidak's multiple comparisons test, adjusted p=0.048) (Fig. 4.2).

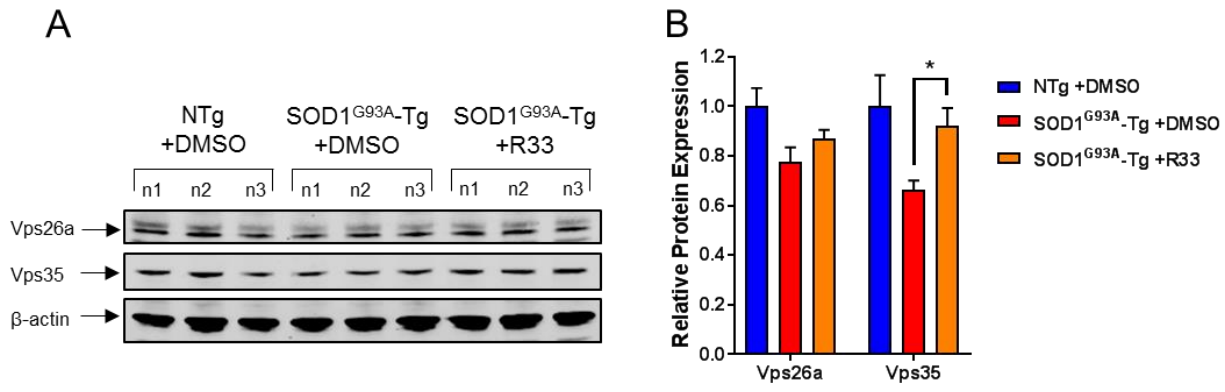

Figure 4.2 R33 Repletes Retromer Levels in the SOD1^{G93A}-Tg Mouse SC

SOD1^{G93A}-Tg mice were treated daily with R33 for 7 days, and a Western blot comparing them to SOD1^{G93A}-Tg mice treated with vehicle DMSO was run on their spinal cords (A) and quantified (B). Results presented as mean ± SEM. n=3, *p<0.05 in one-way ANOVA followed by Holm-Sidak's multiple comparisons test.

4.2.2 Effects of R33 treatment on clinical progression of disease in SOD1^{G93A}-Tg mice

Based on these results, I then went on to perform a small experiment in which I sought to determine whether chronic treatment of mice with R33 was a possible candidate that could attenuate ALS-like phenotypes in SOD1^{G93A}-Tg mice. I had two experimental arms: six SOD1^{G93A}-Tg mice were injected as described above with R33, and six additional SOD1^{G93A}-Tg mice were injected with DMSO vehicle. I performed these injections daily starting at P60 until the mice were sacrificed.

During the lifetime of these mice, I weighed them twice per week. As loss of body weight due to muscle atrophy is a feature of disease in both ALS patients and SOD1^{G93A}-Tg mice, the time at which mice lose 10% of their peak body weight is often used as a marker of clinical onset (Liu et al. 2005; Dermentzaki et al. 2019). Using this parameter, I found no significant difference in clinical onset between SOD1^{G93A}-Tg mice treated with R33 compared to those treated with vehicle (Log-rank Mantel-Cox test, p=0.70) (Fig. 4.3A).

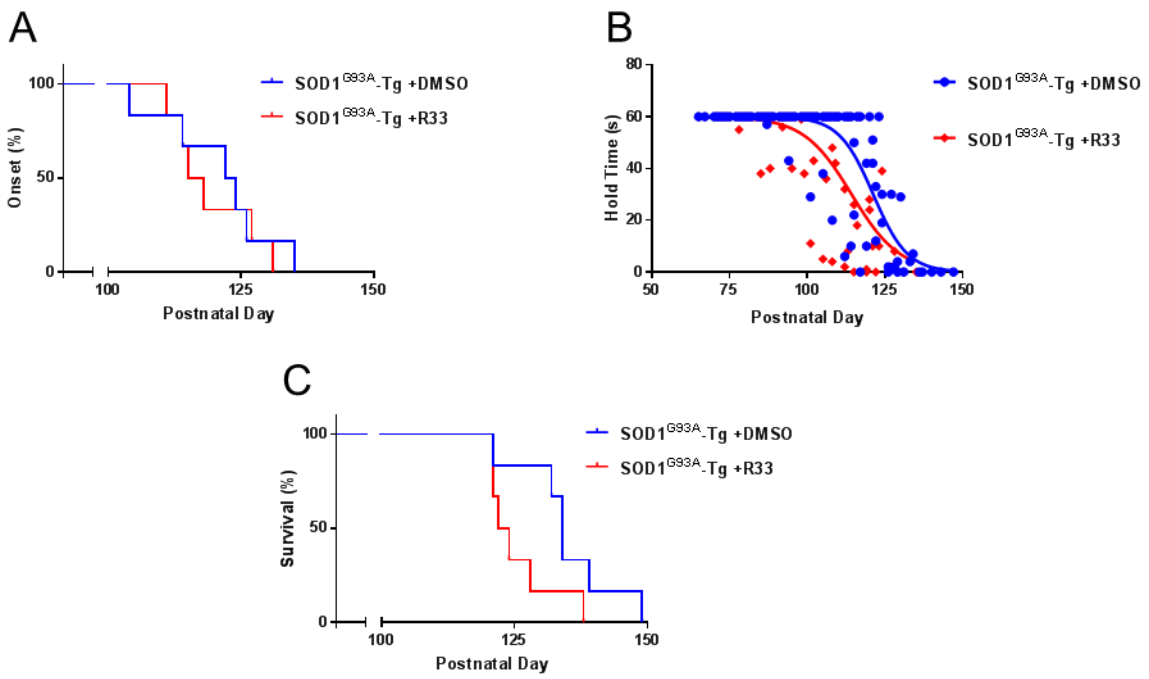

Figure 4.3 Clinical Analysis of R33-Treated SOD1^{G93A}-Tg Mice

SOD1^{G93A}-Tg mice were treated daily with either R33 or DMSO vehicle from P60 to end-stage. Mice were clinically assessed for age of onset as determined by age at which a mouse lost 10% of its peak body weight (A), decay of motor function as determined by weekly inverted grid tests starting at P60 (B), and overall survival as determined by age at which end-stage was reached (C). (A, C) n=6, not significant in Log-rank Mantel-Cox test. (B) Results presented as values of individual trials with best-fit curves for each treatment group. n=6, $p<0.001$ in extra sum-of-squares F test for LogIC50, not significant in extra sum-of-squares F test for HillSlope.

I also monitored the mice for motor behavior once per week using the inverted grid test, a test of mouse grip strength. In this test, a mouse is placed on a grid which is then inverted and suspended in the air over soft padding. The mouse hangs onto the grid with all four limbs, and the amount of time it takes for the mouse to fall, as best of three trials, is recorded. For this test, a latency to fall of 60 seconds is used as the maximum. The values of these tests are then compiled, and charted to determine the progression of motor deficits. Values for mice from each treatment group are fit to a sigmoid curve and compared to each other via the extra sum-of-squares F test for two parameters: the rate of decay is measured by the HillSlope, and the point at which a deficiency

of one half is reached is measured by the LogIC50. These tests, run on R33-treated mice, showed that they exhibited no significant change in the rate of decay of their motor performance (extra sum-of-squares F test, p=0.16) but did show a significantly earlier motor impairment (extra sum-of-squares F test, p=0.00020) (Fig. 4.3B).

Lastly, I examined the effect of R33 administration on the survival of SOD1^{G93A}-Tg mice. At the end of the progression of their disease, SOD1^{G93A}-Tg mice exhibit extreme muscle wasting and weakness, which can ultimately result in failure to breathe and swallow. As such, mice are humanely sacrificed before they die of these causes, when they start exhibiting an inability to right themselves from being laid in the supine position in less than 30 seconds, a clinical stage equated to end-stage and used to define survival. While there was no statistically significant change in the survival of R33-treated mice compared to their DMSO counterparts (Log-rank Mantel-Cox test, p=0.070), there was a trend towards decreased survival in the R33-treated group (Fig. 4.3C), an observation that is worth noting in light of the results presented below for the viral vector approach.

In light of the ambiguous results obtained for R33, which can be interpreted as this pharmacological agent having either no protective effect or even perhaps exacerbating the ALS-like phenotype in SOD1^{G93A}-Tg mice, I decided to limit my study of R33 in this mouse model of ALS to the presented behavioral studies. However, to pursue my investigation of the question as to whether correcting retromer protein expression could have beneficial effects in SOD1^{G93A}-Tg mice, I next thought to utilize an approach of gene therapy as opposed to pharmacology to avoid possible toxic and off-target confounds.

4.2.3 Viral overexpression of VPS35 in SOD1^{G93A}-Tg mice

Previous studies conducted in mice have shown that overexpression of VPS35 via viral delivery with an adeno-associated virus (AAV) is sufficient to increase the expression of retromer components as a whole, resulting in increased retromer functionality (Li, Chiu, and Pratico 2019). Furthermore, the targeting of VPS35 is the most specific way to target the retromer, as of the core components, VPS29 has been shown to be involved in at least one other protein complex, and VPS26 has two mammalian isoforms, either of which can take part in the retromer (McNally et al. 2017; Kerr et al. 2005). Thus, I obtained two AAV9 vectors (Virovek, Hayward, CA): one expressing green fluorescent protein (GFP), and one expressing VPS35, both under the strong and ubiquitous promoter cytomegalovirus (CMV). Using these two viruses, I performed a study similar to the one I had performed using R33 using the lab validated *in vivo* viral vector injection protocol that calls for a single intracerebroventricular (ICV) injection (5 μl at a viral titer of $1x10^{+14}$) at P1: 24 SOD1^{G93A}-Tg mice received the VPS35-AAV9 and 23 SOD1^{G93A}-Tg mice received the GFP-AAV9.

First, I confirmed that, in my hands, such an injection resulted in an increase in retromer expression. By Western blot, I established that injection with the AAV9-VPS35 in SOD1^{G93A}-Tg mice did result in increased expression in the SC of, not only total Vps35 levels (Student t-test, p=0.0016), but also of Vps26a levels (Student t-test, p=0.0018), compared to the expression in AAV9-GFP-injected mice (Fig. 4.4A, B). Furthermore, I performed IHC on sections from mice injected with the AAV9-GFP. This confirmed that AAV9-GFP particles robustly expressed their viral load in MNs, as defined by the expression of the MN marker choline acetyltransferase (ChAT), as well as in astrocytes, as defined by the expression of the astrocyte marker glial fibrillary acidic protein (GFAP) (Fig. 4.4C, D). As done in the lab for other studies, I found that with this

protocol, about 60% of MNs were successfully infected and about 70% of astrocytes. Of note, this dual cell-type transduction is advantageous for this work since I have reported in Chapter 2 that the retromer defect involves at least MNs and astrocytes and in Chapter 3 that low retromer expression is deleterious to MN both in a cell autonomous and non-cell autonomous manner. Also important to note is the fact that the AAV9-GFP and AAV9-VPS35 viruses were ordered from and produced in tandem by Virovek, which presupposes that the AAV9-VPS35 produces a similar expression profile of its viral load as the AAV9-GFP.

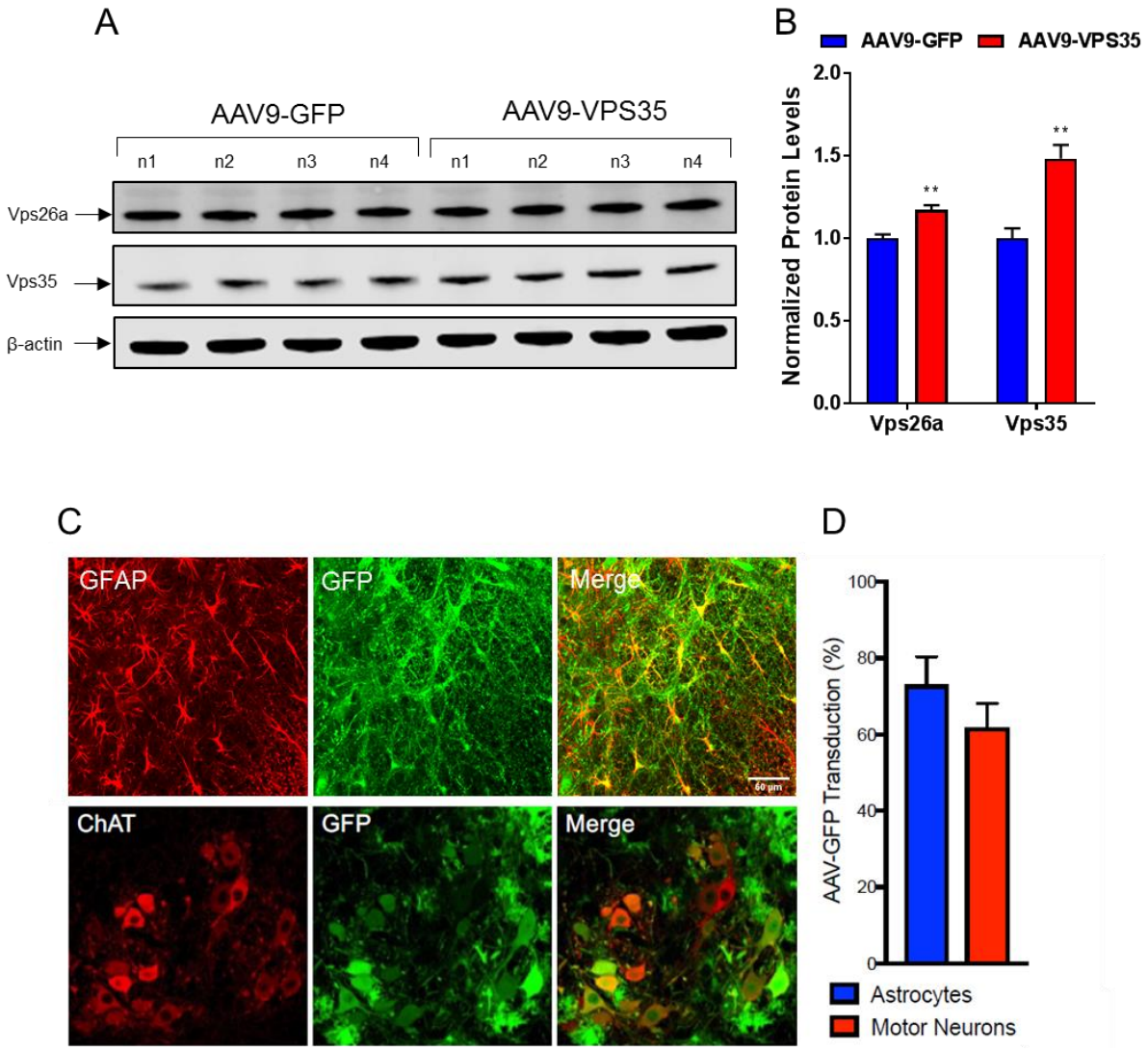

Figure 4.4 Validation of Retromer Overexpression in SOD1^{G93A}-Tg Mice Injected with AAV9-VPS35

SOD1^{G93A}-Tg mice were injected ICV at P1 with either AAV9-GFP or AAV9-VPS35. Western blot analysis of SC lysates from these mice was performed at P90 (A) and quantified (B). IHC was performed on P90 SC from mice injected with AAV9-GFP, staining for the MN marker ChAT, and the astrocyte marker GFAP (C). Using these markers, the percentages of astrocytes and MNs expressing GFP was quantified (D). All results presented as mean ± SEM. (A, B) n=4, **p<0.01 in unpaired t-test. (C, D) n=3, no statistics performed.

4.2.4 Effects of AAV9-VPS35 treatment on clinical progression of disease in SOD1^{G93A}-Tg mice

I then performed similar battery of tests on these SOD1^{G93A}-Tg mice than I did on the SOD1^{G93A}-Tg mice I had tested for R33. First, I weighed these mice twice per week and saw no statistically significant change in the clinical onset between mice injected with AAV9-VPS35 compared to controls injected with AAV9-GFP (Fig. 4.5A). However, in keeping with the apparent earlier onset I had found for R33 treatment, I likewise noted a trend towards an earlier onset in SOD1^{G93A}-Tg mice injected with AAV9-VPS35 as compared to those injected with AAV9-GPF (Log-rank Mantel-Cox test, p=0.063).

I performed the inverted grid test on these mice weekly as well. One variation in how the test was performed is notable here in that rather than limiting the maximum hang time for these mice to 60 seconds, I sought to increase the sensitivity of this test to detect motor deficits by increasing the limit to 120 seconds. On this test, I found that as measured by the HillSlope and LogIC50 of the two groups' fit, mice which had been injected with AAV9-VPS35 showed an increase in the rate of decay of motor performance (extra sum-of-squares F test, p=0.0031) as well as, as had been seen in the R33 mice, a slightly, but statistically significantly earlier motor deficiency (extra sum-of-squares F test, p=0.00048) (Fig. 4.5B). Strikingly, survival analysis of these mice also showed a 10.5 days earlier mortality for mice injected with AAV9-VPS35 compared to those injected with AAV9-GFP (Fig. 4.5C). In aggregate, the clinical data cited above, support the idea that the overexpression of VPS35 by using viral vector gene therapy and,

to a lesser extent, by using pharmacological small molecules, rather than attenuating the expression of the ALS-phenotype in SOD1^{G93A}-Tg mice appears to exacerbate it.

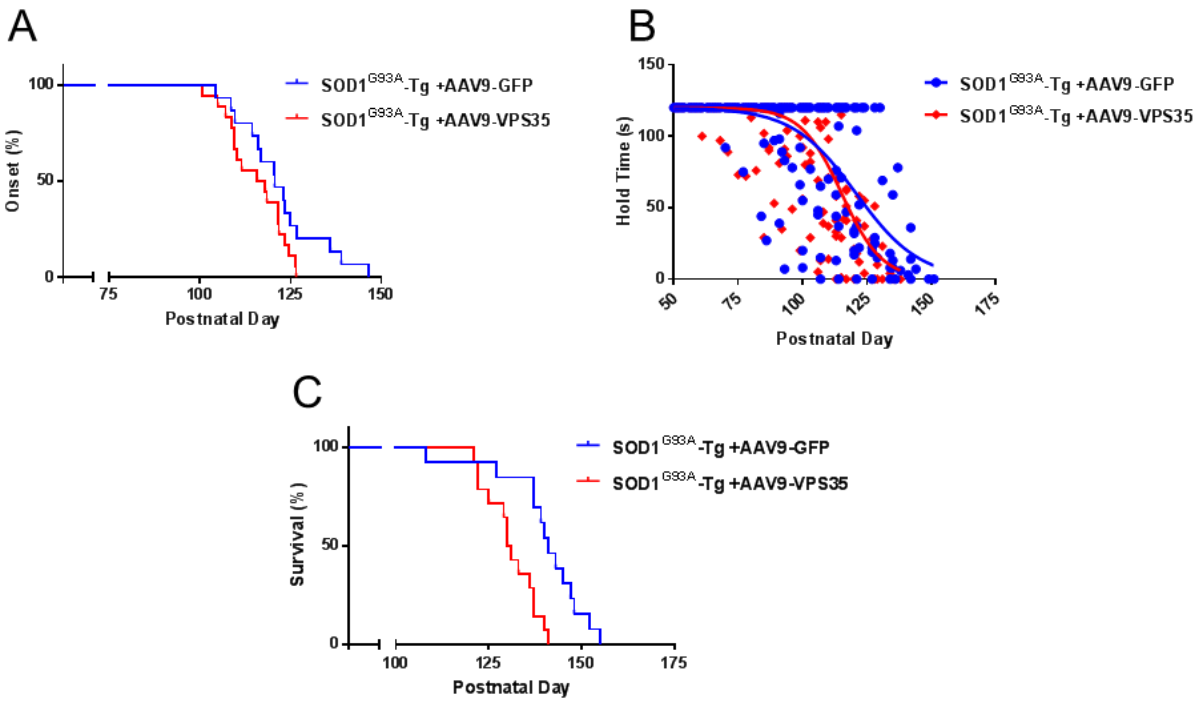

Figure 4.5 Clinical Analysis of AAV9-Injected SOD1^{G93A}-Tg Mice

SOD1^{G93A}-Tg mice were injected ICV at P1 with either AAV9-VPS35 or AAV9-GFP control. Mice were clinically assessed for age of onset as determined by age at which a mouse lost 10% of its peak body weight (A), decay of motor function as determined by weekly inverted grid tests starting at P50 (B), and overall survival as determined by age at which end-stage was reached (C). (A) n=13-14, not significant in Log-rank Mantel-Cox test. (B) Results presented as values of individual trials with best-fit curves for each treatment group. n=13-14, $p<0.001$ in extra sum-of-squares F test for LogIC50, $p<0.01$ in extra sum-of-squares F test for HillSlope. (C) n=13-14, $p<0.01$ in Log-rank Mantel-Cox test.

4.2.5 Effects of AAV9-VPS35 treatment on histopathology of SOD1^{G93A}-Tg mice

To further elaborate on the effects of VPS35 overexpression in SOD1^{G93A}-Tg mice, I examined these mice for their histopathology. I began by counting the numbers of MNs in the SCs of these mice by performing IHC for ChAT on vibratome-cut 70 μm-thick sections from the L4 and L5 segments of the lumbar cords of these mice at both P90 (early symptomatic) and P120

(severely symptomatic). For this work, MNs were designated as ChAT-positive neurons in the ventral horn of these SC sections, and are reported as MN numbers per section. I found that at P90, AAV9-VPS35-injected SOD1^{G93A}-Tg mice had a modest, but statistically significantly smaller number of SC MNs compared to AAV9-GFP-injected SOD1^{G93A}-Tg mice (Fig. 4.6A, B). At P120, this difference was much more pronounced in that AAV9-VPS35-injected SOD1^{G93A}-Tg mice showed ~33% fewer SC MNs compared to AAV9-GFP-injected SOD1^{G93A}-Tg mice (Fig. 4.6A, C). Thus, increasing VPS35 in the CNS, and specifically in the SC, appears to be associated with both a clinical and a neuropathological exacerbation of the ALS-like phenotype in SOD1^{G93A}-Tg mice.

To continue the examination of neuropathological sequelae to VPS35 overexpression in SOD1^{G93A}-Tg mice, I assessed the level of innervation in the *tibialis anterior* muscle of experimental mice at P120. I collected and performed IHC on 20-μm-thick sections of the muscle, labeling the presynaptic terminal of neuromuscular junctions (NMJ) with synaptophysin, and the post-synaptic terminal with fluorescence-conjugated alpha-bungarotoxin (BTX). Level of NMJ innervation was determined as the amount of BTX-positive NMJs that co-localized with synaptophysin out of total BTX-positive NMJs. A minimum of 100 NMJs were assessed per replicate. There was no significant difference in the proportion of innervated NMJs between AAV9-VPS35-injected SOD1^{G93A}-Tg and AAV9-GFP-injected SOD1^{G93A}-Tg mice (Student t-test, $p=0.36$) (Fig. 4.7). However, a trend towards decreased innervation was noted in AAV9-VPS35-injected SOD1^{G93A}-Tg mice despite large variability among samples.

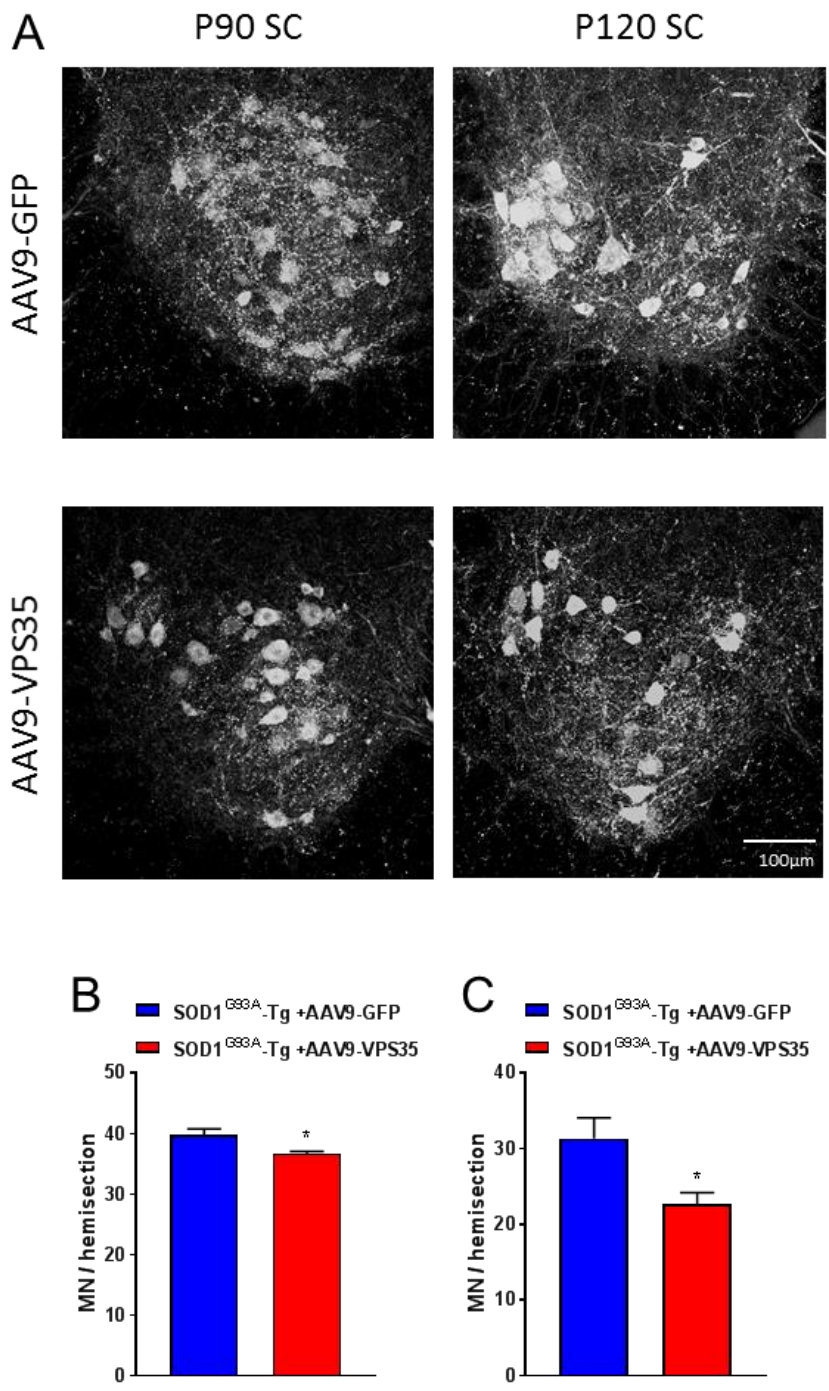

Figure 4.6 Quantification of MN Degeneration in AAV9-Injected SOD1^{G93A}-Tg Mice

AAV9-injected SOD1^{G93A}-Tg mice were sacrificed and IHC for ChAT was performed on sections of the L4-L5 lumbar SC, and the ventral horn was imaged. Maximum projections of representative images are shown (A). MNs were then quantified as a function of ChAT-positive neurons in the ventral horn per hemisection at P90 (B) and at P120 (C). All results presented as mean ± SEM. n=3, *$p<0.05$ in unpaired t-test.

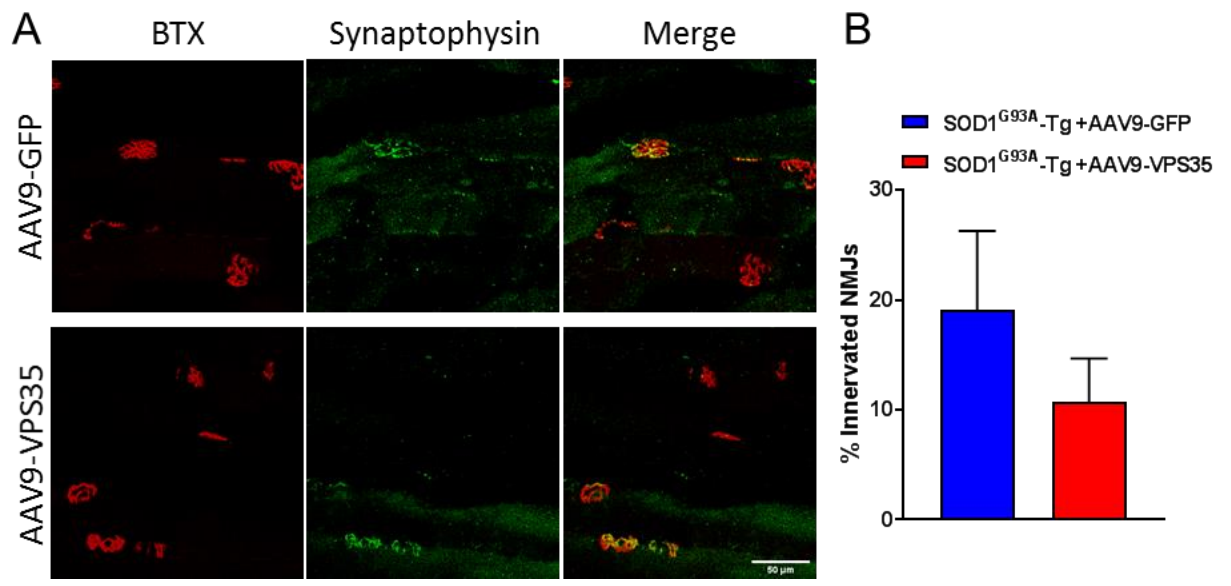

Figure 4.7 Quantification of NMJ Innervation in AAV9-Injected SOD1^{G93A}-Tg Mice

AAV9-injected SOD1^{G93A}-Tg mice were sacrificed and IHC for synaptophysin and α-bungarotoxin (BTX) was performed on sections of the tibialis anterior at P120. Maximum projections of representative images are shown (A). At least 100 BTX-positive NMJs were then quantified per replicate, and percentage of NMJs staining for synaptophysin was recorded (B). Results presented as mean ± SEM. n=3, not significant in unpaired t-test.

4.3 Discussion

In Chapters 2 and 3, I found and elaborated on a deficiency in the retromer I found in cells from ALS patients and cells and tissues from ALS mouse models. Since retromer deficiency and its sequelae have only ever been associated with deleterious effects on the biology of cell and animal systems, in this chapter, I tested the hypothesis that retromer repletion could confer a therapeutic benefit to the SOD1^{G93A}-Tg mouse model of ALS. To do so, I employed two different methods of retromer repletion: one pharmacological, and one viral. Remarkably, rather than seeing any attenuation of disease phenotype in SOD1^{G93A}-Tg mice, I saw either trends toward or statistically significant exacerbations of both clinical and neuropathological parameters in study groups whose retromer levels had been increased.

4.3.1 Implications for retromer deficiency in ALS

The counterintuitive results of this study reframe the retromer deficiencies found in Chapter 1. In mouse models of most neurodegenerative diseases that have been linked to deficiencies in the retromer, an exogenous increase in retromer expression leads to an amelioration of disease pathology (Wang, Zhao, et al. 2013; Dhungel et al. 2015; Li, Chiu, and Pratico 2019). I have here shown that the case with ALS and the $SOD1^{G93A}$-Tg mouse is the opposite. It is possible that rather than being a contributor to or a negative effect of disease, retromer deficiency in the context of ALS is a compensatory mechanism that confers an, as yet, unknown therapeutic benefit to ALS pathology, a question that is explored further in Chapter 5. It is important to note that the mice used in this chapter, that is $SOD1^{G93A}$-Tg mice on a B6/SJL mixed background, have been previously shown to have a median life span of between 120 to 130 days, which is closer to what I observed in the mice injected with VPS35-AAV9 (median 130) than in those injected with GFP-AAV9 (median 141) (Gurney et al. 1996; Sher et al. 2014). GFP overexpression is a commonly used control for viral treatment in these mice, and has never shown to induce an alteration in ALS pathology (Leyton-Jaimes, Kahn, and Israelson 2019; Nanou et al. 2013; Thomsen et al. 2014; Lasiene et al. 2016). Furthermore, all studies performed in this chapter were done in littermates in a randomized manner making it more likely that any changes in control baselines were due to the shared genetics of all experimental animals. However, the differences in this study with historical data do indicate that the use of untreated controls in future studies would be beneficial to enhance the certainty that GFP transduction is not impacting disease phenotype.

4.3.2 R33 chaperone toxicity

The results showing that R33 treatment accelerated disease in SOD1^{G93A}-Tg mice are consistent with my findings in mice treated with VPS35-AAV9. However, I cannot discount other possibilities as to why R33 seemed to exacerbate the clinical features of disease phenotype in these mice. It is possible that R33 has toxic side effects which have not been apparent in other studies, either due to the fact that I treated these mice for over two months—more time than mice have ever been treated with R33 before—or to the context of another concurrent disease pathology, in which ALS exacerbates the toxicity of R33. Upon the initial recording of these results, it was also considered that rescue of retromer levels in SOD1^{G93A}-Tg mice could itself be toxic to these mice. However, this was deemed unlikely due to the fact that retromer expression has been performed in the context of multiple mouse models of neurodegenerative diseases and has never shown such toxicity or exacerbation of pathology. Thus, the possibility that R33 could, independent of its effect on retromer expression, induce toxicity in mice led me to continue to pursue the possibility that retromer repletion could rescue ALS pathology in SOD1^{G93A}-Tg mice. Upon reflection on these results, after having seen that viral overexpression induces similar advancement of disease, parsimony would suggest that the unanticipated effect of R33 may, in fact, likely be linked to its stabilization of the retromer. However, it cannot be discounted with certainty that R33 did not also affect the outcomes of the presented studies via an unintended off-target effect in SOD1^{G93A}-Tg mice.

4.3.3 Relationship between clinical and pathological disease progression in VPS35-AAV9-treated SOD1^{G93A}-Tg mice

In this study, I found that the repletion of retromer levels in SOD1^{G93A}-Tg mice resulted in a more advanced disease progression. Both mice treated with R33 and mice virally overexpressing VPS35 showed a worse clinical pathology compared to controls. Further study of VPS35-AAV9-treated SOD1^{G93A}-Tg mice showed that this clinical decline was accompanied by an increase in MN death in the SC when compared to GFP-AAV9-treated SOD1^{G93A}-Tg mice, indicating that the cause of worsened progression in these mice is linked to increased ALS-like tissue pathology. By contrast, I found no significant difference in the level of innervation of the *tibialis anterior* between these two groups. Usually, the level of innervation of the NMJ correlates with changes in clinical pathology in SOD1^{G93A}-Tg mice—i.e. mice with worse clinical pathology tend to be found to have lower NMJ innervation. However, the apparent discrepancy here may be attributed to a number of possible reasons.

First, while I noted no significant difference in innervation of the *tibialis anterior* between the two treatment groups, I did notice a large variability in the level on NMJ innervation. Assuming the variability and mean difference in NMJ innervation I found in these groups, power analysis shows that in order to find a significant difference between these two groups with a conventional power of 0.8, a study would have to include 19 mice per group. Thus, assessment of *tibialis anterior* innervation in additional mice may be required to reach a conclusion that is not fraught with a high type II error.

At least part of the reason for this high variability may be the fact that these mice were injected with an AAV9 which infects about 60% of MNs, so variability may arise merely due to

the chances of which specific neurons have been infected and whether they happen to be the ones that innervate the *tibialis anterior*.

An alternative explanation may involve the fact that I looked at NMJ innervation in these mice at P120, which is a fairly advanced time of disease and in limb muscle notoriously susceptible to the diseases process. Thus, it is possible that at an earlier time point, differential innervation of the *tibialis anterior* in these mice may be found.

Lastly, the *tibialis anterior* has been shown to be one of the muscles most susceptible to the diseases process in SOD1^{G93A}-Tg mice (Kaplan et al. 2014; Dibaj, Schomburg, and Steffens 2015). Thus, it is possible that if at P120, I would have also investigated other muscles in these mice which are more resistant to the disease process (e.g. *Soleus*), I might have detected differences in NMJ denervation consistent with the observed differences seen in motor behavior and survival.

4.3.4 Implications for other diseases

As I reviewed above, repletion of the retromer has been shown to produce a clinical benefit in multiple mouse models of neurological diseases (Wang, Zhao, et al. 2013; Dhungel et al. 2015; Li, Chiu, and Pratico 2019). As such, a growing interest has developed in the possibility for disease-modifying therapies that increase retromer function, whether by viral or pharmacological means, particularly in the fields of PD and AD (Small and Petsko 2015; Eleuteri and Albanese 2019; Zhang, Huang, et al. 2018; Reitz 2018). Previously, the possibility that retromer stabilization could have unintended toxic effects has been mentioned, and the fact that, thus far, no animal model has been shown to have any apparent toxic effects from excess retromer, has generally assuaged those concerns (Small and Petsko 2015; Reitz 2018; Zhang, Huang, et al. 2018). The work of this chapter provides the first evidence that retromer stabilization may, in fact, have

deleterious consequences that require further evaluation before retromer stabilizing treatment is brought to the clinic. This, of course, comes with the caveat that this study was performed in a mouse model of ALS that experiences severe disease pathology. It is possible that retromer stabilization may only be toxic in the context of ALS and that the treatment of patients with retromer-stabilizing therapy may still prove a viable therapeutic target in other neurological diseases.

Should this be the case, caution would still be warranted with such therapy. Frontotemporal dementia (FTD) has been shown to co-occur in about 10% of ALS patients, which along with the two diseases sharing genetic determinants, has resulted in a growing understanding of FTD and ALS being a spectrum of disease rather than two independent diseases (Lomen-Hoerth 2004; Ferrari et al. 2011; Guerreiro, Bras, and Hardy 2015). Due to the fact that FTD results in a host of diverse psychiatric, cognitive, and neurological symptoms, patients with FTD experience a high rate of misdiagnosis, most often with AD (Beber and Chaves 2013; Musa et al. 2019). Thus, particularly should FTD prove to also be negatively affected by retromer stabilization, great care would have to be taken in diagnosis before retromer stabilization was pursued as a treatment in patients with FTD.

CHAPTER 5

PARTIAL DELETION OF VPS35 IN SOD1^{G93A}-TG MICE

5.1 Introduction

In the previous chapter, I showed that repletion of the retromer in SOD1^{G93A}-Tg mice, which have a baseline decrease in retromer expression, resulted in them experiencing both clinical and pathological worsening of disease. These findings led me to question whether the depletion in the retromer in these mice was a protective rather than a deleterious molecular event. In light of these unexpected outcomes and provocative hypothesis, I thus wondered whether some further reduction in retromer expression could have therapeutic effects in ALS.

The exogenous depletion of the retromer in mice has been extensively studied, both in otherwise genetically unaltered mice and in Tg mouse models of neurologic diseases (Vagnozzi et al. 2019; Wen et al. 2011). As briefly mentioned in Chapter 4, changes in VPS35 are the most specific way to target the retromer, as VPS29 also takes part in the retriever complex and the presence of two isoforms of VPS26 makes retromer alteration via their targeting more difficult (McNally et al. 2017; Kerr et al. 2005). Thus, the lab of Dr Wen-Cheng Xiong has generated, and, over the course of several publications, characterized a mouse with a single allele deletion of Vps35 (Wen et al. 2011; Liu et al. 2014; Ye et al. 2019; Tang, Liu, et al. 2015; Liu, Tang, et al. 2017; Tang, Erion, et al. 2015). Briefly, these studies have shown that mice heterozygous for Vps35 exhibit a subtle degeneration of dopaminergic neurons in the substantia nigra after 12 months, likely due to impairments in mitochondrial dynamics; impairments in dendritic spine maturation in the hippocampus, likely due to impairments in AMPA receptor trafficking; and degenerative effects in the retina and cornea.

Furthermore, in one study, the lab crossed Vps35 heterozygous mice with the Tg2576 mouse model of AD, which has since been shown to have an inherent deficiency in Vps35 expression (Wen et al. 2011; Chu and Pratico 2017). This study showed that the single allele knockout of Vps35 in these mice exacerbated AD-like pathology in these mice, including cognitive deficits, increased production of Aβ, and impaired synaptic transmission.

Finally, another study recently performed by the lab of Dr Domenico Praticò showed that the P301S mouse model of tauopathy displayed a deficiency in the retromer, and found that injection of AAV expressing a Vps35 shRNA in these mice to exacerbate their retromer deficiency also exacerbated both their cognitive and their motor deficits (Vagnozzi et al. 2019).

Altogether, there is no precedent for the exogenous deficiency of retromer in mouse models of neurodegeneration being beneficial or even neutral to their pathology. Despite this, given my findings in the $SOD1^{G93A}$-Tg mice that I have presented in Chapters 2-4, I sought to determine whether this model, and perhaps ALS as a whole may be an exception.

5.2 Results

5.2.1 Heterozygous deletion of Vps35

In light of the fact that in Chapter 4, I found that overexpressing Vps35 led to an exacerbation of the ALS-like phenotype in $SOD1^{G93A}$-Tg mice, I then wondered what the effect of deleting Vps35 might be in this mouse model of ALS. To address this question, I employed a Cre-lox-based conditional mouse Vps35 knockout line generated by the lab of Dr Scott Small, which they graciously shared with me for this work. This mouse was built with LoxP sites flanking exons 3-5 of Vps35. Cre-recombinase can therefore induce a deletion of these exons of Vps35, resulting in the failure of producing Vps35 protein. For their work in Alzheimer's disease (AD), they have

crossed these mutant mice with mice expressing Cre under the forebrain neuronal CamKIIα promoter. They found that the generated mice are viable and have a knockout of Vps35 in forebrain neurons as seen in IHC (Fig. 5.1A). Their Western blot of whole forebrain lysate also shows a decrease in Vps35 protein levels—albeit modest, probably due to a dilution effect of other cell types—as well as a secondary decrease in other retromer components (Fig. 5.1B, C). This decrease in levels of Vps26 and Vps29 secondary to the deletion of Vps35 replicates the previously seen effects of Vps35 knockdown in cultured neurons (Bhalla, Vetanovetz et al. 2012).

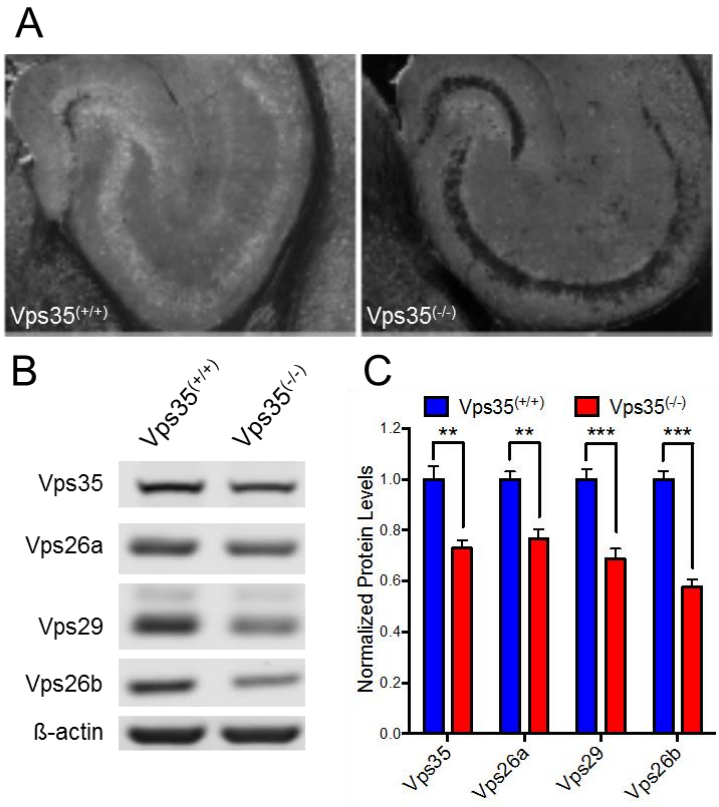

Figure 5.1 Successful Conditional Knockout of Vps35 in Neurons

Data and figure provided by the Small Lab. Mice with a heterozygous conditional knockout Vps35 gene were bred to express Cre under the forebrain neuronal CamKIIα promoter. IHC for Vps35 shows a lack of Vps35 expression in neurons of the hippocampus (A). A Western blot for Vps35 was run on hippocampal samples from these mice and controls. A representative blot is presented here (B) with quantification of 7 replicates per group (C). Results presented as mean ± SEM. n=7, **p<0.01, ***p<0.001 in unpaired Student t-test

In Chapter 2, I found a retromer deficiency in both MNs and astrocytes of the SOD1^{G93A}-Tg mouse, indicating that the effects of retromer dynamics in this mouse may not be limited to a single cell type. Thus, I chose to study the effect of a complete heterozygous deletion of Vps35 on the disease progression of SOD1^{G93A}-Tg mice, rather than knocking out Vps35 in any single cell type. To create a Vps35 heterozygote mouse from the floxed Vps35 line, I first crossed it with a mouse expressing Cre under the CMV promoter. This CMV-Cre gene induces recombination across cell types in the mouse, including, importantly, the gametes. This cross, thus, resulted in a mouse that was effectively a Vps35 heterozygote. I then crossed this resulting mouse with an NTg mouse to separate out the Vps35 null allele from the CMV-Cre transgene, resulting in a true Vps35 heterozygote with no other genetic alterations. Finally, the cross between the Vps35 heterozygous and the SOD1^{G93A}-Tg mice resulted in the mice I ultimately used for my experiments in this Chapter. A visual schematic of the breeding paradigm for these mice is provided in Figure 5.2.

It is important to note here that all experiments done in the SOD1^{G93A}-Tg mouse in Chapters 2-4 have been performed on mice with the mixed B6/SJL background. However, the fact that the founder conditional Vps35 knockout mice produced by the lab of Dr Scott Small were produced in the B6 background necessitated for these experiments to be undertaken in SOD1^{G93A}-Tg mice with the B6 background. These mice have been shown to have a similar, though slowed disease progression as compared to those with the B6/SJL background (Heiman-Patterson et al. 2005).

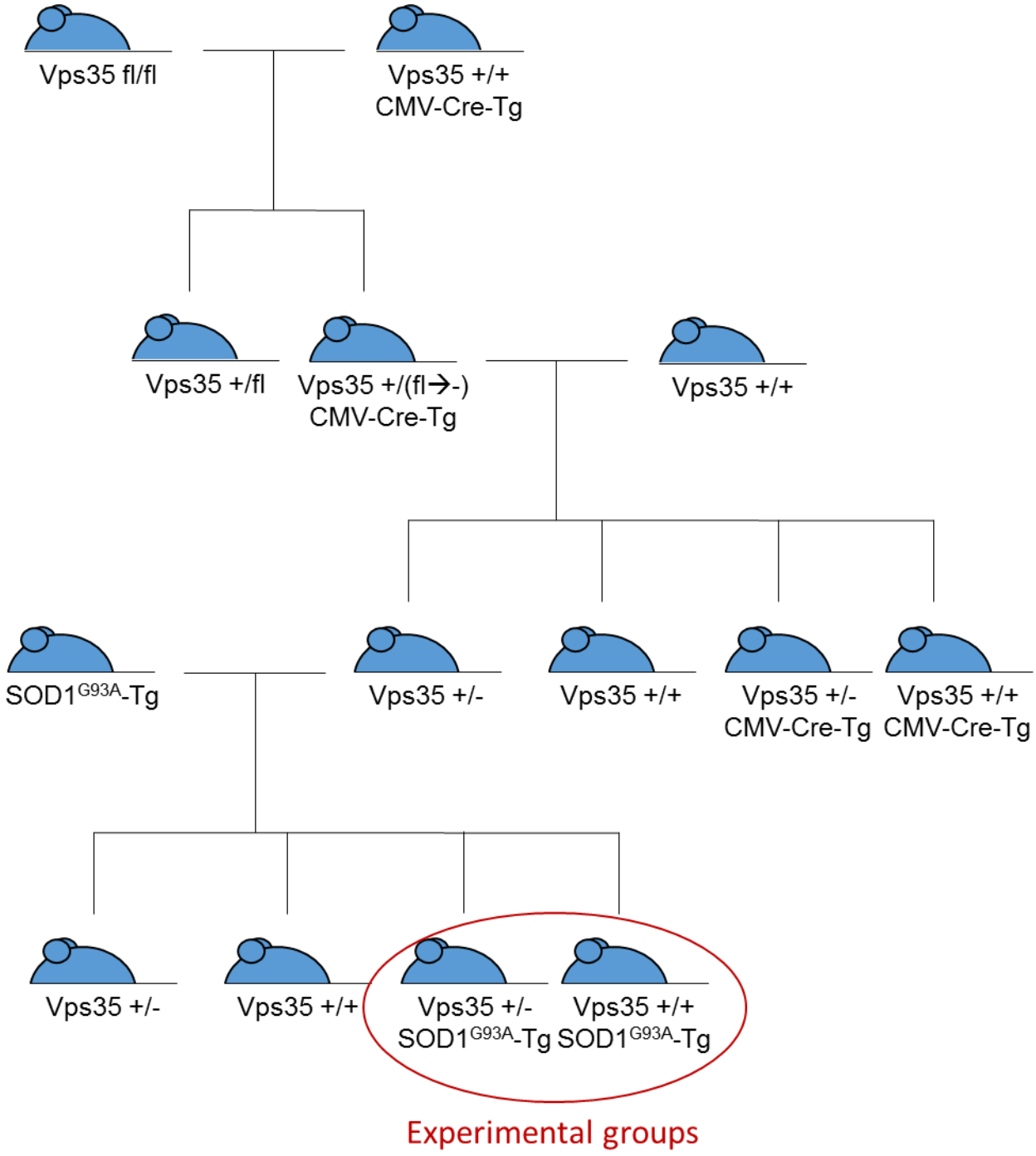

Figure 5.2 Breeding Scheme for Vps35 Heterozygous SOD1^{G93A}-Tg Mice

Mice homozygous for the conditional knockout floxed (fl) allele of Vps35 were bred with mice expressing Cre under the CMV promoter (CMV-Cre-Tg). Of the resulting mice, in those that expressed CMV-Cre transgene, Cre induced recombination of the floxed Vps35 allele, resulting in a tissue-wide heterozygous knockout. These were then crossed with a NTg mouse, resulting in, among other genotypes, a Vps35 heterozygous mouse with no transgene. This mouse was then bred with a SOD1^{G93A}-Tg mouse, and those that expressed the SOD1^{G93A} transgene were used in the experiments described in this Chapter.

Before, reporting the results for the cross between Vps35 conditional mutant and SOD1^{G93A}-Tg mice, it is worth mentioning the effects that a widespread deletion of 1 or 2 alleles for Vps35 using a CMV-Cre mouse line might have on the lower motor neuron pathway. I was consistently unable to obtained viable Vps35$^{-/-}$ pups by genotyping more than 6 litters, consistent with the previous reports showing that abrogating Vps35 in mice is lethal (Wen et al. 2011). In contrast, I found that Vps35$^{+/-}$ pups were viable and were indistinguishable from their Vps35$^{+/+}$ littermates in terms of their morphometry and development. More importantly, up to 1.5 years, Vps35$^{+/-}$ mice did not show any evidence of clinical ALS-like phenotype.

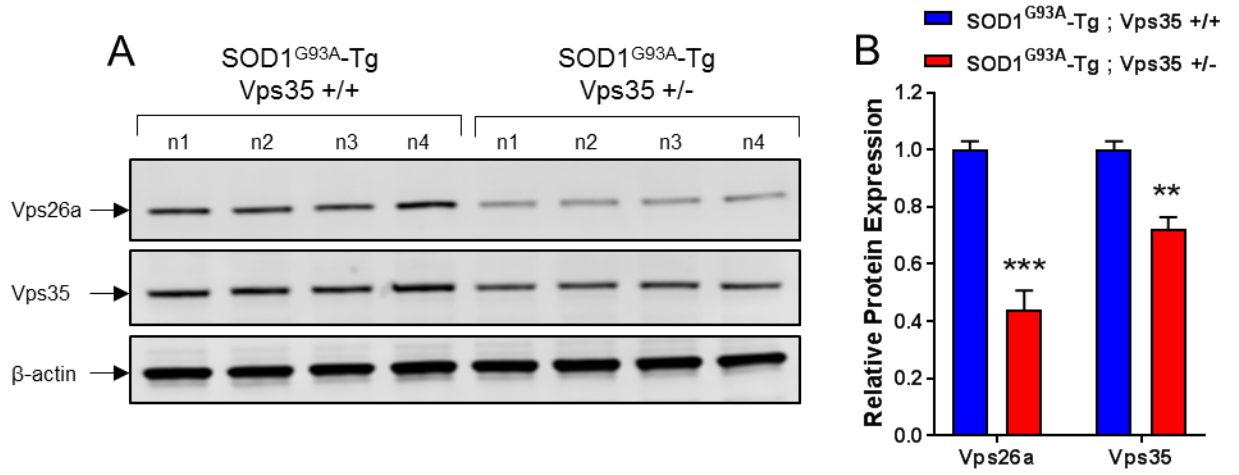

Figure 5.3 Hemizygous Vps35 deletion decreases retromer protein levels

A western blot was run comparing retromer protein expression levels between Vps35 heterozygous and Vps35 homozygous wild-type SOD1^{G93A}-Tg mice at P120 (A) and quantified (B). Results presented as mean ± SEM. n=4, **p<0.01, ***p<0.001 in unpaired Student t-test

Previous studies have shown that the single allele deletion of Vps35 in mice produced a robust decrease in the CNS in levels of expression of not only Vps35, but also of Vps26a (Tang, Erion, et al. 2015). I confirmed that this was still the case if the heterozygote mouse also expressed the SOD1^{G93A} transgene via a Western blot of SCs from Vps35 wild-type SOD1^{G93A}-Tg and Vps35

heterozygote SOD1^{G93A}-Tg mice at P120. Indeed, the Vps35 heterozygote mice displayed a robust decrease in both Vps35 (Student t-test, p=0.0016) and Vps26a (Student t-test, p=0.00028) expression in the SC (Fig. 5.3). Of note, protein expression was not compared between Vps35$^{+/-}$;SOD1^{G93A}-Tg and Vps35$^{+/+}$;NTg mice. However, it can be deduced that the changes found in the present experiment compound with those found in Chapter 2 between SOD1^{G93A}-Tg and NTg mice to produce an even greater retromer expression decrease.

5.2.2 Effects of single allele deletion of Vps35 on clinical progression of disease in SOD1^{G93A}-Tg mice

On these mice, I then ran a similar series of clinical tests to those that I had performed in Chapter 4 on mice injected with AAV9 virus. First, I weighed these mice twice per week, and recorded the time of onset as defined in Chapter 4. Here, I saw a statistically significant delay of onset in the Vps35$^{+/-}$;SOD1^{G93A}-Tg mice compared to Vps35$^{+/+}$;SOD1^{G93A}-Tg mice (Log-rank Mantel-Cox test, p=0.00043) (Fig. 5.4A). I also performed the inverted grid test on these mice as I had in the AAV9-injected mice, and found that Vps35$^{+/-}$;SOD1^{G93A}-Tg mice compared to Vps35$^{+/+}$;SOD1^{G93A}-Tg mice displayed both a delay in motor impairment and a slower rate of motor performance decay, as measured by changes in the HillSlope (extra sum-of-squares F test, p=0.032) and the LogIC50 (extra sum-of-squares F test, p=0.000000019), respectively, in the best fit curves (Fig. 5.4B). Finally, Vps35$^{+/-}$;SOD1^{G93A}-Tg mice compared to Vps35$^{+/+}$;SOD1^{G93A}-Tg mice reached end-stage significantly 17 days later (Log-rank Mantel-Cox test, p=0.0014), supporting the notion that they survived longer (Fig. 5.4C). Overall, these data are consistent with and expand on the findings of Chapter 4, showing that a decrease in the expression of the retromer

complex causes the mirror effect of Vps35 overexpression in that it attenuates the clinical expression of the ALS-like phenotype in SOD1^{G93A}-Tg mice.

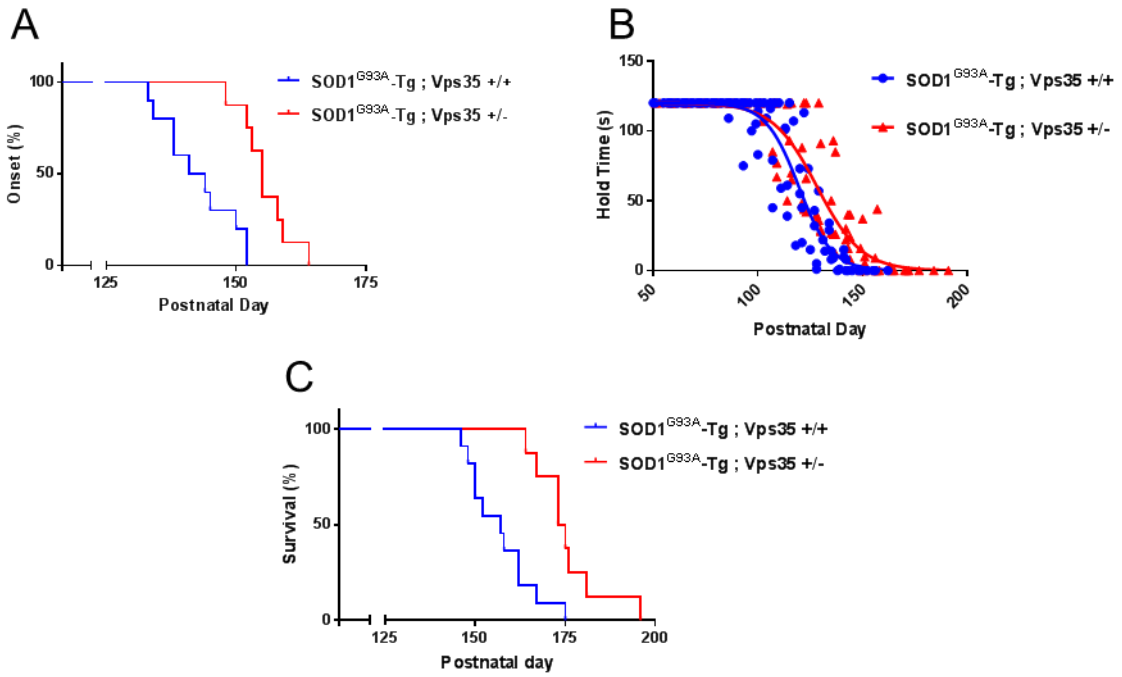

Figure 5.4 Clinical Analysis of Vps35 Heterozygous and Wild-Type Vps35 Homozygous SOD1^{G93A}-Tg Mice

SOD1^{G93A}-Tg mice with either homozygous wild-type Vps35 or with a heterozygous deletion in Vps35 were clinically assessed for age of onset as determined by age at which a mouse lost 10% of its peak body weight (A), decay of motor function as determined by weekly inverted grid tests starting at P50 (B), and overall survival as determined by age at which end-stage was reached (C). (A) n=8, $p<0.001$ in Log-rank Mantel-Cox test. (B) Results presented as values of individual trials with best-fit curves for each treatment group. n=8, $p<0.001$ in extra sum-of-squares F test for LogIC50, $p<0.05$ in extra sum-of-squares F test for HillSlope. (C) n=8, $p<0.01$ in Log-rank Mantel-Cox test.

5.2.3 Effects of single allele deletion of Vps35 on histopathology of SOD1^{G93A}-Tg mice

I also performed the same set of neuropathological studies in these knockout mice as those performed on AAV9-injected mice in Chapter 4. MN quantification in these mice showed that Vps35$^{+/-}$;SOD1^{G93A}-Tg mice had ~30% more SC MNs at P120 compared to age-matched Vps35$^{+/+}$;SOD1^{G93A}-Tg mice (Fig. 5.5A, B); although this difference did not reach significance

likely because of the high variability of the MN counts in Vps35$^{+/-}$;SOD1^{G93A}-Tg mice (Student t-test, p=0.065). Remarkably, in contrast with the findings for clinical parameters and MN counts, quantification of NMJ innervation of the *tibialis anterior* showed a statistically significant greater denervation of this specific limb muscle in Vps35$^{+/-}$;SOD1^{G93A}-Tg compared to Vps35$^{+/+}$;SOD1^{G93A}-Tg mice (Student t-test, p=0.0096).

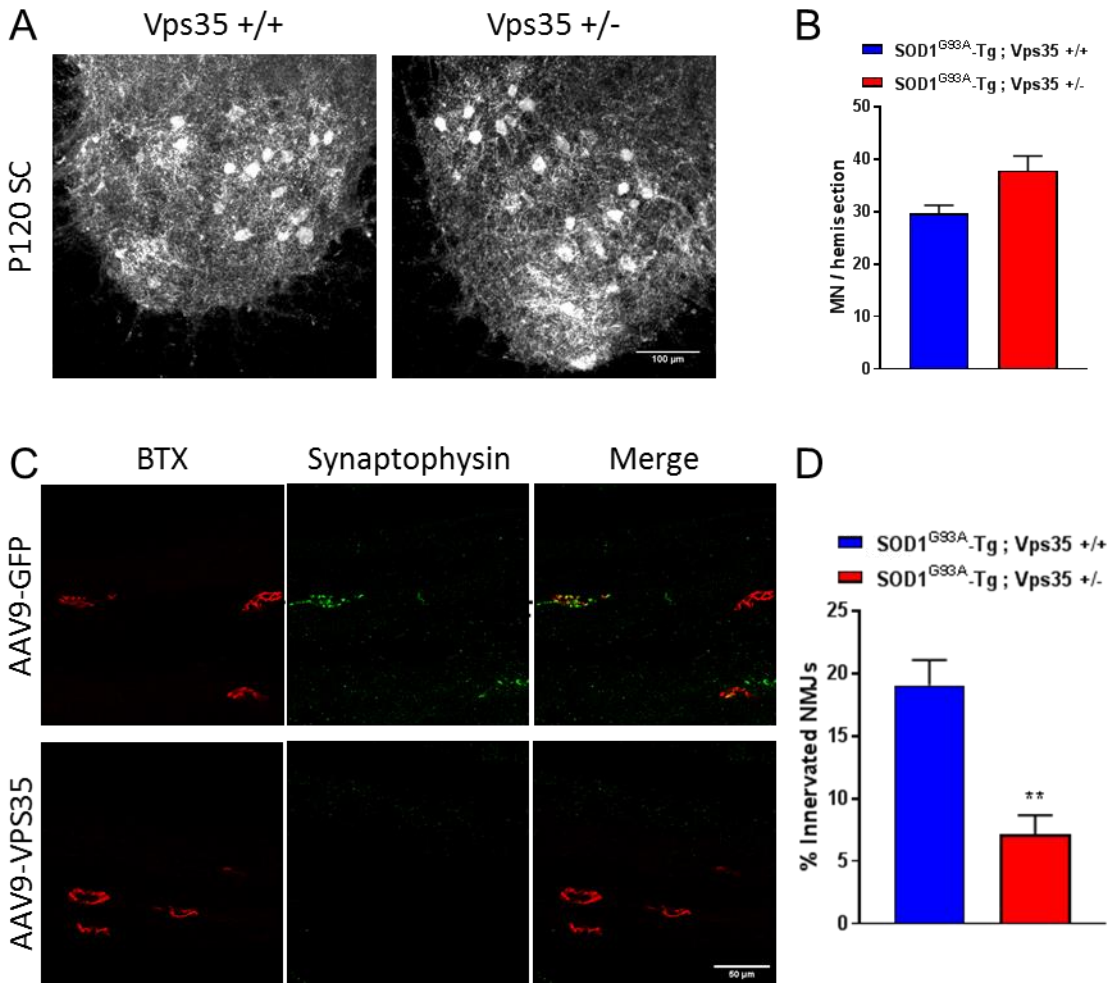

Figure 5.5 Pathology Analysis of Vps35 Heterozygous and Wild-Type Vps35 Homozygous SOD1^{G93A}-Tg Mice at P120

SOD1^{G93A}-Tg mice with either homozygous wild-type Vps35 or with a heterozygous deletion in Vps35 were sacrificed, and IHC for ChAT was performed on sections of the L4-L5 lumbar SC, and the ventral horn was imaged. Maximum projections of representative images are shown (A). MNs were then quantified as a function of ChAT-positive neurons in the ventral horn per hemisection at P120 (B). IHC for synaptophysin and α-bungarotoxin (BTX) was also performed on sections of the tibialis anterior of these mice at P120. Maximum projections of representative images are shown (C). At least 100 BTX-positive NMJs were then quantified per replicate, and percentage of NMJs staining for synaptophysin was recorded (D). All results presented as mean ± SEM. n=3, **p<0.01 in unpaired t-test.

5.2.4 Effects of single allele deletion of Vps35 in astrocytes on MN viability in vitro

Despite the results for NMJ denervation in Vps35$^{+/-}$;SOD1^{G93A}-Tg mice, it seems that a superimposed partial deficit in these mice is associated with better clinical outcomes and MN counts compared to Vps35$^{+/+}$;SOD1^{G93A}-Tg mice. Furthermore, there seems to be no overt motor pathology in plain Vps35$^{+/-}$ mice. Yet, in Chapter 3, I have shown that Vps35 shRNA-mediated retromer silencing in astrocytes and MNs caused neurotoxicity *in vitro*. One notable difference between these experiments, besides the context of being *in vivo* versus *in vitro*, is that Vps35 shRNA produces a severe and acute depletion of retromer expression in the order of about 90% whereas Vps35$^{+/-}$ mutant allele produces a chronic depletion of only about 50%. It is thus, possible that the apparently discrepant results reported between Chapter 3 and Chapters 4 & 5 stem from temporal and magnitude differences.

To test this possibility, I repeated the MN/astrocyte co-culture experiments from Chapter 3. However, instead of using treatment with shRNA, I used astrocytes from NTg mice either homozygous or heterozygous for Vps35. I cultured these astrocytes and then plated ES-derived HB9-GFP expressing MNs on top and assessed for differences in viability. Strikingly, I found that these astrocytes did not induce the same toxicity as astrocytes treated with Vps35 shRNA (Student t-test, Day 2 p=0.71, Day 3 p=0.48, Day 4 p=0.33, Day 5 p=0.46, Day 6 p=0.56, Day 7 p=0.69) (Fig. 5.6). Thus, this last experiment suggests that neurotoxicity caused by Vps35 deficit is

governed by a toxic threshold above which the cell can withstand and compensate for the defect while below it produces a degenerative effect.

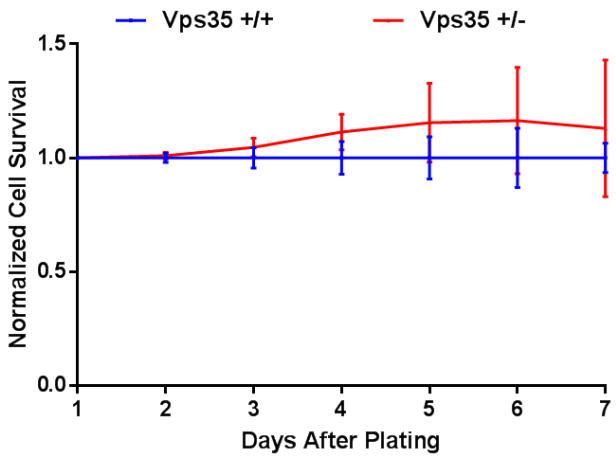

Figure 5.6 Astrocytes with a Modest Depletion of Retromer Do Not Reproduce Toxicity in MNs

Astrocytes from either Vps35 homozygous or heterozygous mice were co-cultured with ES-derived MNs expressing GFP under the HB9 promoter, and the relative viability of the MNs over time was assessed. Results presented as mean ± SEM. n=4, not significant in unpaired Student t-test.

5.3 Discussion

In previous chapters, I demonstrated that a retromer deficiency found in the context of ALS, when repleted in the SOD1^{G93A}-Tg mouse, exacerbated ALS-like disease found in these mice. In this chapter, I followed up on this finding, hypothesizing that the inverse might also be true: i.e. the further depletion of retromer expression in these mice could confer a therapeutic benefit to their ALS-like disease. On at least some parameters, I found that this was, indeed, the case. Indeed, by studying differences in the progression of disease in Vps35$^{+/+}$;SOD1^{G93A}-Tg mice and Vps35$^{+/-}$;SOD1^{G93A}-Tg mice, I found that inducing a retromer reduction was associated with a clinical benefit, including prolonged survival, as well as an attenuated loss of SC MNs. It has been shown that small changes in the background of SOD1^{G93A}-Tg mice can lead to similar effects

on these mice. However, there is little doubt that changes in disease are due to changes in retromer expression due to the fact that in this study, the Vps35$^{+/+}$;SOD1^{G93A}-Tg mice and Vps35$^{+/-}$;SOD1^{G93A}-Tg mice compared were littermates (Heiman-Patterson et al. 2005). Furthermore, changes found in previous studies in the Vps35$^{+/-}$ mice without the SOD1^{G93A} transgene are unlikely to be involved in the findings in this study due to the fact that such changes have only been found at ages as late as 12 months, much later than the lifespan of the SOD1^{G93A}-Tg mice (Wen et al. 2011; Liu et al. 2014; Ye et al. 2019; Tang, Liu, et al. 2015; Liu, Tang, et al. 2017; Tang, Erion, et al. 2015).

In this study, I found that a single allele deletion of Vps35 resulted in a significant rescue to the clinical pathology of the SOD1^{G93A}-Tg mouse. This was accompanied by an increase in the survival of MNs in the SCs of mice with a reduction of Vps35, which is the converse of my findings in Chapter 4 in which I overexpressed Vps35. Together, these data suggest that MN survival in the SOD1^{G93A}-Tg mouse may be modulated by the levels of Vps35 and related retromer core proteins. This view is in stark contrast with a wide array of studies in other models of neurodegenerative disease which have shown that degeneration of dopaminergic neurons in the substantia nigra as well as AD-, PD-, and tauopathy- related protein processing defects tend to be found upon the depletion of the retromer (Wen et al. 2011; Tang, Erion, et al. 2015; Vagnozzi et al. 2019). Thus, this study marks a possible degenerative and/or protective pathway that seems to be specific to MNs in the context of ALS.

If my genetic modulations of Vps35 expression in SOD1^{G93A}-Tg mice provided coherent clinical and SC MN counts, both Vps35 overexpression and partial deletion were associated with severe *tibialis anterior* denervation. While greater muscle denervation in of SOD1^{G93A}-Tg mice is to be expected in response to interventions which cause, for example, shorter survival and greater

SC MN loss, it is challenging to explain how greater muscle denervation in of SOD1^{G93A}-Tg mice could be seen in response to interventions which cause longer survival and smaller SC MN loss in these mice. As mentioned in Chapter 4, to shed light onto this striking discrepancy between MN counts and NMJ denervation, additional time points and muscles may have to be studied. Furthermore, it is assumed that MN counts and NMJ innervation in Vps35$^{+/-}$;SOD1^{G93A}-Tg mice and Vps35$^{+/+}$;SOD1^{G93A}-Tg mice are the same at pre-symptomatic stage when no neuropathological signs are yet detectable (e.g. P30-45), but this supposition will also have to be established. Lastly, since Vps35 deletion is present since birth, could it be that some compensatory mechanisms develop whereby more sprouting and ensuing larger motor units take place allowing for better motor performance in the face of NMJ denervation? That said, whatever is the actual explanation for the discrepancy between SC MN counts and NMJ denervation in Vps35$^{+/-}$;SOD1^{G93A}-Tg mice vs Vps35$^{+/+}$;SOD1^{G93A}-Tg mice, the excess in NMJ denervation associated with the partial deletion of Vps35 is most consistent with studies in other neuronal populations and diseases. Indeed, it is possible that, as has been observed in the hippocampus of Vps35 heterozygous mice without SOD1 overexpression, synaptic deficiencies may be widespread and include MNs upon the depletion of Vps35 (Tian et al. 2015).

Finally, I had found that the *in vivo* results of this chapter were at odds with the *in vitro* results of Chapter 3, which had shown that exogenously induced retromer deficiency in astrocytes or in MNs resulted in MN loss. My experiment showing that Vps35$^{+/-}$ astrocytes—which exhibit a milder retromer deficiency than that produced by shRNA silencing—did not induce *in vitro* MN toxicity implies that a certain amount of retromer deficiency is tolerated by the neural system. A drop beyond that threshold then results in the toxic effects of retromer deficiency becoming overwhelming.

Overall, in conjunction with previous chapters, the work done in this study provides evidence that the proper regulation of the retromer is paramount to the progression of disease in $SOD1^{G93A}$-Tg mice. While the complete or near-complete removal of retromer has significant toxic effects both *in vitro* and *in vivo*, a partial depletion may be tolerable to cells such as MNs while limiting the possibly detrimental trafficking of a specific retromer cargos. This view will be revisited in greater detail in the next chapter.

CHAPTER 6

GENERAL DISCUSSION

Deficiencies in the retromer have been connected to a host of neurologic and neurodegenerative disorders, including Alzheimer's disease (AD), Parkinson's disease (PD), Down's syndrome (DS), Progressive Supranuclear Palsy (PSP), and Pick's disease (Small et al. 2005; Zhao, Perera, et al. 2018; Wang, Zhao, et al. 2013; Vagnozzi et al. 2019). This thesis represents the first comprehensive study to add ALS to this growing list of retromer-associated diseases. As such, this work has the potential to uncover previously unknown pathways of disease and therapeutic targets in ALS. In Chapters 2 and 3, I have shown that, similarly to what has been found in the aforementioned diseases, ALS shares a deficiency in the retromer with functional sequelae. Intriguingly, however, the results from Chapters 4 and 5 have demonstrated that the connection between retromer deficiency and ALS is unique from what has been found in any other disease thus far. In the $SOD1^{G93A}$-Tg ALS mouse model, exogenous upregulation and downregulation of the retromer resulted in deterioration and amelioration of disease, respectively, the opposite of what has been found in studies of other neurological diseases (Vagnozzi et al. 2019; Wen et al. 2011; Wang, Zhao, et al. 2013; Dhungel et al. 2015; Li, Chiu, and Pratico 2019).

The in-depth discussion of the studies performed for chapters of this thesis can mostly be found in the Discussion sections of their respective chapter. Thus, here, I will focus on the overall implications of this work and future directions that could lead to a deeper understanding of the interplay between ALS and the retromer.

Future studies expanding on this research are already currently underway, and necessarily include the exploration of cell specificity in retromer deficiency-associated therapy. The methods

I used in Chapters 4 and 5 to exogenously increase and decrease retromer expression in SOD1^{G93A}-Tg mice, by design, affected a multiplicity of cell types. As, in Chapter 2, I had found that at least both astrocytes and MNs were affected by a deficiency in retromer expression in ALS, the general alteration of retromer expression across cell types was warranted as a measure of the pathological relevance of retromer expression in ALS. Now that I have found that a ubiquitous decrease in retromer expression is beneficial in SOD1^{G93A}-Tg mice, further work can distinguish which cells mediate this benefit. In this context, the first two cell types to consider are, of course, MNs and astrocytes, as data reported in this thesis support a retromer defect in at least these two main cell types. To address this important question of cell-specificity, in parallel to the work I have presented in this thesis, I have bred the conditional knockout Vps35 mice, which Dr Small provided for my work in Chapter 5, with mice expressing Cre-recombinase under the ChAT promoter for MN specificity. I have then bred the resulting mice with SOD1^{G93A}-Tg mice, which has resulted in Vps35$^{f/+}$;ChAT-Cre-Tg;SOD1^{G93A}-Tg mice, which replicate the conditions of the Vps35$^{+/-}$;SOD1^{G93A}-Tg mice that I used in Chapter 5, but with a single allele deletion of Vps35 in only MNs. These mice are now aging, and I anticipate that the study of these animals in the same way I studied Vps35$^{+/-}$;SOD1^{G93A}-Tg mice in Chapter 5, will reveal which aspects of disease pathology that were modified by Vps35 depletion were due specifically to a depletion in MNs. A similar paradigm done with a transgene expressing Cre-recombinase under MN-specific promotor can be done with an astrocyte-specific promoter to also shed light into the actual contribution of astrocytes in mediating the effect of Vps35 depletion on ALS-like phenotype. The growing recognition that ALS neurodegeneration results from the combination of both cell autonomous and non-cell autonomous effects makes these additional *in vivo* studies particularly insightful (Halpern, Brennand, and Gregory 2019; Chen et al. 2018; Hawrot, Imhof, and Wainger 2020; Phatnani et al.

2013). Moreover, with respect to non-cell autonomy, the focus in this work and in this discussion has been on astrocytes, but through cell-specific deletion of mutant SOD1, it was shown that other non-MN cells are also important in the expression of the ALS-like phenotype in these mice including microglia/macrophages and Schwann cells (Beers et al. 2006; Lobsiger et al. 2009; Yamanaka et al. 2008). Interestingly, while mutant SOD1 deletion in MNs, astrocytes, and microglia/macrophages attenuated the ALS-like phenotype in mutant SOD1 Tg-mice, an identical deletion in Schwann cells, for uncertain reasons, exacerbated the phenotype (Lobsiger et al. 2009; Beers et al. 2006; Yamanaka et al. 2008). The fact that the same intervention—mutant SOD1 deletion—can cause opposite effects on ALS-like phenotypes depending on which cell type is the site of the deletion raises the importance of paying great attention to cell-context when one interprets the impact of a mild reduction in retromer expression in $SOD1^{G93A}$-Tg mice. Thus, some of the unexpected results I reported in this thesis may possibly be due not only to the mild magnitude of retromer defect, but also to the kind of cells that are most affected by this deficit.

It is further notable that the retromer deficiencies described in Chapter 2 occur at a late stage of disease. In contrast, the retromer expression modifications studied in Chapters 4 and 5 were done either virally at P1 or with a germline mutation, respectively. It is possible that such early changes in retromer expression may modify ALS-like disease in $SOD1^{G93A}$-Tg mice differently than the late-stage changes found in unaltered mice. For example, an early change in retromer expression may induce a compensatory mechanism that alters other related pathways such as the COMMander pathway or the SNX dimer, altering cells' reliance on the retromer pathway. Experiments altering retromer expression at later stages of disease—via the use of, for example, tamoxifen-inducible Cre-recombinase and later viral manipulation—could address this question. The experiments done in Chapter 4 with mice treated with R33 from P60 on provide

some evidence that later alteration mimics the effects of early alteration. However, further studies may more fully answer this question.

Further study on the causes of endogenous retromer deficiencies may also shine a light on how they in a benefit to ALS pathology. In my studies, I found that retromer protein deficiencies in SOD1^{G93A}-Tg astrocytes did not correlate with a change in either mRNA expression or rate of protein degradation. As I mentioned previously, it is possible that changes in degradation are so subtle that they are undetectable over the course of 24hr. However, the alternative is that retromer protein mRNAs are not getting properly translated. Finding which of these may be the case could provide multiple diverse insights, including finding upstream mediators of ALS pathogenesis that could be exploited for treatment and attaining a better understanding of retromer biology as a whole.

In Chapter 2, I found that SOD1^{G93A}-Tg mice may not be the only mouse model of ALS to display a decrease in retromer expression. The lab of Dr Neil Shneider has developed a new model of ALS with a homozygous P517L point mutation in mouse Fus, from which they have cultured and graciously provided me a sample of astrocytes. I found that these astrocytes displayed a decrease in retromer expression, which while found in a single replicate, is consistent with my findings in SOD1^{G93A}-Tg. Furthermore, I also found that astrocytes from sALS patients with no known ALS-causing mutations also showed a decrease in retromer expression. Together, these results imply that retromer deficiency is not specific to mutations in SOD1. Thus, the repetition of the studies performed in this thesis in non-SOD1 models of ALS may confirm and provide further information on the nature of retromer deficiency in ALS. Along these lines, since the C9orf72 hexanucleotide repeat expansion is the most common genetic cause of ALS, it would be enlightening to assess retromer function in either cells or tissues from patients or mice carrying

such mutations (Alsultan et al. 2016). Indeed, I have previously mentioned that one study has already looked at the expression of VPS26A in iPSC-derived MNs from ALS-FTD patients with the C9orf72 expansion (Aoki et al. 2017). While they did not find a statistically significant difference, they did show a trend towards a decrease in the ALS-FTD cells, which, especially considering the results of the work of this thesis, merits further investigation.

Since I have found that retromer deficiency is a commonality between cells from human ALS patients and from ALS mouse models, it is thus reasonable to hypothesize that this deficiency works in similar ways between the two. That is, in $SOD1^{G93A}$-Tg mice, I found that retromer deficiency may be a biological compensatory mechanism that protects mice from what would otherwise be a more severe disease progression. It may very well then be the case that the same is true for retromer deficiency in ALS patients. Once the nature of retromer depletion-induced neuroprotection has been better elucidated in mouse models of ALS and in cells from those models, studies in human cells—particularly those that experience the phenomenon of ALS-induced retromer depletion such as iPSC-derived MN and primary astrocytes—could confirm whether retromer depletion mechanisms are shared between patients and mouse models. A finding that retromer depletion results in neuroprotection in a model of human ALS could have far-reaching implications for the treatment of ALS. In this context, some insights into the nature of the molecular basis for the observed beneficial effect of a mild retromer deficit in ALS may be gained by using a similar bioinformatics approach as has been previously used in this lab to elucidate pathogenic pathways, but this time on iPSC from ALS patients and controls.

A natural question that comes to mind when alterations in the retromer modify disease is what downstream effect of retromer function is responsible for the disease modification. In the course of my study of the retromer in ALS, I have variously looked at numerous cargoes of the

retromer using SOD1^{G93A}-Tg astrocytes as an *in vitro* model. However, most defects classically associated to retromer deficiency have proven elusive and are either unchanged in SOD1^{G93A}-Tg astrocytes or experience such subtle changes that I was not able to detect them. However, I was able to see alterations in SOD1^{G93A}-Tg astrocytes in the trafficking of APP by the retromer and in the release of Aβ fragments. Such alterations are often found as downstream effects of retromer deficiency. However, the fact that retromer deficiency in SOD1^{G93A}-Tg mice seems to be beneficial makes the release of Aβ fragments an unlikely mechanism of disease modification, as one would expect an increase in Aβ to be toxic rather than neuroprotective (Harkany et al. 2000). Having said this, APP processing can generate and shed fragments other than Aβ (O'Brien and Wong 2011). Thus, while Aβ may be convenient to quantify given the availability of reagents, it may merely reflect APP processing without being the actual pathogenic fragment. Alternatively, it is also possible that APP processing alteration is, here, a simple marker of retromer defect and that non-APP cargo(s) is/are instrumental in driving the effect on the ALS phenotype reported in this thesis. Should this be the case, identifying the retromer cargo(s) whose altered transport result in what I called "a therapeutic benefit" in SOD1^{G93A}-Tg mice, which is an area of ongoing research in the lab, would be a research direction of major potential significance.

Of relevance to the above discussion is the relationship between retromer function and AMPA glutamate receptor trafficking. Indeed, alterations in the localization of the AMPA glutamate receptor in response to retromer deficiency in neurodegenerative disease have been well documented (Tian et al. 2015; Munsie et al. 2015; Temkin et al. 2017). Conversely, the overexpression of retromer components has been shown to increase levels of AMPA receptors at the synapse (Wang, Zhao, et al. 2013). These findings are quite pertinent to ALS, as glutamate excitotoxicity has long been proposed as a, if not the, key mechanism causing MN death (Foran

and Trotti 2009). Over the years, the minimal beneficial effects of riluzole in ALS—the first of only two drugs approved to treat this disease—have been used to support the glutamate hypothesis of ALS, given the fact that this "dirty drug", among a host of actions, is advertised as a glutamate antagonist (Andreadou et al. 2008; Fumagalli et al. 2008). A proposed mechanism for how glutamate leads to toxicity in MNs involves the fact that MNs express a relatively high level of AMPA receptor deficient in the GluR2 subunit (Corona and Tapia 2007; Kawahara et al. 2003). A lack of this subunit makes the AMPA receptor permeable to calcium, which can then build up to toxic levels that cannot be adequately regulated by the cell (Isaac, Ashby, and McBain 2007; Williams et al. 1997). MNs from patients with ALS have been shown to be particularly deficient in GluR2, and indeed the overexpression of GluR2 has been shown to induce a clinically therapeutic effect in $SOD1^{G93A}$-Tg mice (Takuma et al. 1999; Tateno et al. 2004). While it is unlikely that retromer deficiency would increase levels of GluR2 in the cell, as mentioned above, deficiencies in the retromer have been shown to result in a lower amount of total AMPA receptor at the synapse (Tian et al. 2015; Munsie et al. 2015; Temkin et al. 2017). Essentially, since MNs are preferentially producing calcium-permeable AMPA receptor, a decrease in total AMPA receptor at the cell surface via a lack of retromer transport may decrease glutamate excitotoxicity and ensuing MN degeneration.

The retromer has also been linked to the proper regulation of autophagy. At least one study has shown a direct interaction between the retromer and ATG9, a protein that marks membranes used in the formation of the phagophore (Devereaux 2014). A PD-linked mutation in VPS35 has also been shown to lead to the mislocalization of ATG9, resulting in the disruption of autophagy (Zavodszky et al. 2014; Karanasios et al. 2016; Orsi et al. 2012). The disruption of autophagy has generally been thought to be of detriment to ALS, as is evidenced by the fact that multiple ALS-

associated genes regulate autophagy (Wild et al. 2011; Sundaramoorthy et al. 2015; Shen et al. 2015; Oakes, Davies, and Collins 2017). However, a study performed in $SOD1^{G93A}$-Tg mice inhibiting autophagy has shown evidence that the effects of autophagy disruption may be time-dependent (Rudnick et al. 2017). Namely, it was found that the inhibition of autophagy in $SOD1^{G93A}$-Tg mice via a conditional knockout of Atg7 in MNs results in the increased denervation of the tibialis anterior at an early age, but also in the extension of survival. Thus, studying autophagy deficiencies and changes in the transport of Atg9 caused by retromer deficiency in $SOD1^{G93A}$-Tg mice may elucidate how, at what age, and at what level, disrupted autophagy may confer a clinical benefit to $Vps35^{+/-}$;$SOD1^{G93A}$-Tg mice.

The retromer is also known to be involved in the trafficking of Wntless, which itself mediates the secretion of Wnt proteins such that the disruption of the retromer results in a decrease in the production of Wnt molecules (Belenkaya et al. 2008). Meanwhile, SCs from $SOD1^{G93A}$-Tg mice have been shown to experience an increase in Wnt expression and in the Wnt signaling cascade, which have been replicated in human tissues (Gonzalez-Fernandez et al. 2016; Chen et al. 2012; Gonzalez-Fernandez et al. 2019). These studies have implied that increased Wnt signaling may have a role in the pathogenesis of ALS. What that role may be has not been elucidated, and Wnt signaling has a large and diverse set of functions across cell types and, particularly, in neurons (He, Liao, and Pan 2018). However, studies in mitochondria have shown that Wnt signaling can result in an activation of mitochondrial biogenesis, which leads to an increase in the production of reactive oxygen species (ROS) (Yoon et al. 2010). The increased production of ROS as well as oxidative damage caused by ROS has been widely reported in samples from patients and mouse models of ALS, showing a possible link between Wnt signaling and ALS pathogenesis (Mitsumoto et al. 2008; Smith et al. 1998; Shaw et al. 1995; Shibata et al.

2001; Chang et al. 2008; Hong et al. 2012; Deng et al. 2015). The study of alterations in Wnt signaling and in ROS production in response to retromer deficiency in SOD1^{G93A}-Tg mice may provide some insight into how retromer depletion affects disease progression in these mice.

A study in the interactome of the retromer has shown that interferon gamma (IFNγ) receptor 2 (IFNGR2) is lost from the cell surface upon VPS35 depletion (Steinberg et al. 2013). Interestingly, it has been shown that IFNγ may be involved in cell death in motor neurons, as it is found to be elevated in SCs of ALS patients and SOD1^{G93A}-Tg mice (Aebischer et al. 2011; Aebischer et al. 2012). Furthermore, the antibody neutralization of IFNγ in the cerebrospinal fluid (CSF) has been shown to produce a clinical benefit in the motor behavior of SOD1^{G93A}-Tg mice (Otsmane et al. 2014). Thus, it is possible that a decrease in IFNGR2 at the cell surface due to retromer depletion could replicate an effective neutralization of IFNγ signaling.

Overall, due to the fact that the retromer regulates the trafficking of an ever-growing list of hundreds of proteins, it is possible that the missorting of any one or any combination of these proteins may contribute to retromer depletion-induced neuroprotection in SOD1^{G93A}-Tg mice. Thus, perhaps the best future study of the effects of retromer depletion would involve an unbiased proteomic screen. In one study, stable isotope labeling with amino acids in culture (SILAC) followed by mass spectrometry identified differences in surface expression of proteins in response to the knockdown of SNX27 or VPS35 (Steinberg et al. 2013). Similarly, the performance of SILAC followed by mass spectrometry on cells—most easily, astrocytes—from NTg and SOD1^{G93A}-Tg mice with or without a heterozygous deletion of Vps35 could identify possible disease-modifying cargoes via the overlap of alterations among these groups.

The work I have presented for this thesis provides strong support for the idea that the retromer is involved in the pathogenesis of ALS. While in most diseases, this would imply that retromer dysfunction is pathogenic, in ALS, I have shown that retromer dysfunction is therapeutic. Furthermore, the progression of ALS is highly sensitive to the level of retromer expression, which requires precise regulation, such that an excess of either depletion or repletion of the retromer is deleterious in ALS.

CHAPTER 7

EXPERIMENTAL PROCEDURES

7.1 Mice

For this project, *Mus musculus* mice were used. All mice were housed and bred in the Central Animal Care Facility located in the William Black Building in the pathogen-free barrier area of the Animal Care Facility (Room #BB-1918). For *in vivo* experiments, three weeks after delivery, pups will be weaned and separated. Columbia University's approved Animal Welfare Assurance is #A3007-01. All procedures are approved by the Institutional Animal Care and Use Committee (IACUC).

7.1.1 Lines of mice

- WT: All breeding or experiments requiring wild-type mice used C57bl/6 or B6/SJL mice from the Jackson Laboratory.
- $SOD1^{G93A}$-Tg: Mice in the C57bl/6 or B6/SJL background expressing SOD1 that harbors the G93A familial ALS mutation have been described as generated by Jackson Laboratory (Gurney et al. 1994). These transgenic mice were also used to provide experimental primary astrocytes and animals for the *in vivo* experiments. Genotyping was done from 5mm tail tip cuttings from P2-5 by PCR following the protocol published by the Jackson Laboratory.
- $Vps35^{Fl/Fl}$: These mutant mice were used to provide our source of animals for *in vivo* experiments of Chapter 5. The Vps35Fl/Fl mice were generated by the Small lab by injecting ES cells into the inner cell mass of C57BL/6J blastocysts. A floxed allele of the Vps35 gene contains loxP sites flanking exon 3-5. The injected blastocysts were then implanted into the uterus of

pseudopregnant foster mothers for further development. The LacZ-Neo cassette flanked by Flp recombinase recognition site (Frt) was removed by crossing mice carrying the Vps35-neo-lacZ-flox allele to FLPe transgenic mice (ROSA26-FLPe), which express an Flp recombinase, to generate Vps35-loxP mice. Homozygous mice are viable, fertile, normal in size and do not display any gross physical or behavioral abnormalities. Genotyping was done from 5mm tail tip cuttings from P2-5 by standard PCR using the following primers: Vps35Loxp gtF (TGTTTTGGTAACTTCTGTGACCTT) Vps35Loxp gtR (AGCCTTTTCAGTGGACTCAGAT).

- CMV-Cre-Tg: The generation of mice expressing Cre recombinase under the CMV promoter in the C57bl/6 background by Jackson Laboratory has been described (Schwenk, Baron, and Rajewsky 1995). These transgenic mice were used to provide our source of animals for the *in vivo* experiments in Chapter 5. Genotyping was done from 5mm tail tip cuttings from P2-5 by PCR following the protocol published by the Jackson Laboratory.

7.2 Western blotting

All Western blot analyses done for this thesis work were performed on mouse tissues, human post-mortem samples, and different cultured cell types. For mouse tissues, mice were euthanized with via intraperitoneal (ip) overdose injection of ketamine and xylazine, and perfused with cold PBS for 4 minutes at a rate of 10mL/min. Select tissues were then dissected and immediately frozen at -80°C. Human samples were collected post-mortem by pathologists with patient consent and frozen. Cultured cells were detached, centrifuged, and immediately frozen at -80°C as pellets.

Once collected, protein from tissues and cells were extracted with RIPA buffer [150mM NaCl, 25mM Tris pH 8.0, 1% Triton X-100, 0.5% sodium deoxycholate, 1mM EDTS, 0.1% SDS,

protease inhibitor cocktail (cOmplete Mini™, Sigma), and phosphatase inhibitor (PhosSTOP™, Sigma)]. For tissues, samples were flash frozen in liquid nitrogen and crushed with a mortar and pestle. Resulting samples were then homogenized through a small bore 27-gauge needle in 10μL of RIPA per 1mg of sample. For cells, 500μL of RIPA was used per an estimated 1 million cells, and homogenization took place through a small bore 27-gauge needle. Thereafter, all mouse and human tissues and cells were processed for Western blot in a similar fashion. Homogenates were centrifuged at 10,000g for 10 minutes, and the supernatant was collected. Protein concentration of samples was quantified using the Bradford Quick Start™ assay (Bio-Rad). Samples were diluted to 2μg of protein per 1μL in ultrapure water and 2:5 dilution of stock sample buffer (Tris-HCl ph 6.8, 10% SDS, 25% glycerol, 5% β-mercaptoethanol, and 0.05% Bromophenol blue). Samples were then boiled at 95°C for 10 minutes and either stored at -80°C or allowed to cool and loaded.

30μg of protein sample was loaded into wells of a 5-12% Bis-Tris gel (NuPAGE®, ThermoFisher) submerged in MOPS buffer (NuPAGE®, ThermoFisher). Gels were run at a maximum of 45mA or 150V. After running, proteins were transferred onto 0.22-μm pore–size nitrocellulose membrane using transfer buffer (14.4g/L glycine, 3g/L Tris base, 20% methanol, and 0.05% SDS) at a maximum of 150mA or 35V for 1.5 hr.

Membranes were blocked in commercially available blocking buffer (Blocking buffer for fluorescent Western blotting, Rockland) for 1hr, and indicated antibodies were diluted as indicated in Table 7.1, and incubated on the membrane overnight at 4°C. Membranes were then washed three times for 5min in 0.1% PBS-Tween 20. Indicated secondary antibodies (Li-Cor® IR-680 or IR-800 dye conjugated) were diluted 1:10,000 in blocking buffer, and incubated on the membrane for 1hr at room temperature. Membranes were then washed three more 5min in 0.1% PBS-Tween

20, prior being imaged, and protein bands were quantified on a Li-Cor® Odyssey Imaging system (Lincoln, NE).

Table 7.1 Antibodies Used

Target	Host	Used in WB/ICC/IHC (Dilution)	Company	Catalogue #
APP C-terminal	rabbit	ICC (1:1000)	Calbiochem	171610
β-Actin	mouse	WB (1:40,000)	Sigma	A5441
ChAT	goat	IHC (1:250)	Sigma	AB144P
Cyclin D3	mouse	WB (1:1000)	Cell Signaling	2936S
EEA1	goat	ICC (1:500)	Santa Cruz Biotechnology	sc-6415
GFAP	rabbit	IHC (1:500)	DAKO	z0334
HB9	rabbit	ICC (1:1000)	abcam	ab26128
Vps26a	rabbit	WB (1:2000)	abcam	ab23892
Vps29	goat	WB (1:1000)	Sigma	SAB2501105
Vps35	mouse	WB (1:1000), ICC (1:1000), IHC (1:500)	abcam	ab57632

7.3 Quantitative reverse transcriptase PCR (qRT-PCR)

All qRT-PCR done for this thesis work were performed on mouse tissues, human post-mortem samples, and different cultured cell types. Both mouse and human tissues and cultured cells were prepared as described in 7.1 and then stored at -80°C until used.

Once collected, RNA from tissues and cells were extracted with TRI Reagent (TRI Reagent®, cat. # T9424, Sigma) following the manufacturer's protocol. Samples were

homogenized using a small bore 27-gauge needle. After initial RNA extraction, DNAse treatment was performed for 25 minutes at 37°C using rDNAseI (Ambion). After DNAse treatment, an additional phenol-chloroform extraction of the RNA was performed and the pellet was resuspended in DEPC-treated water (ThermoFisher) and quantified by Nanodrop (Thermo Scientific). 1ug of RNA was used per sample to make cDNA with the RevertAid First Strand cDNA Synthesis Kit (ThermoFisher) following manufacturer's protocol and primed with both random hexamers and oligo(dT) primers.

Table 7.2 Primers Used for qPCR

Target	Forward Primer (5' to 3')	Reverse Primer (5' to 3')
Mouse Vps35	CCAGGCTGTGAAGGTTCAGTCATT	CCAAGCATATTGGAGGCATGCTTC
Mouse Vps29	TGCACCAAGGAGAGCTACGACTAT	ATCTTGAACTGGCCCACAGTCACA
Mouse Vps26a	ATGGCGAGTCTGTCTCAGGAAAGGTA	TCCTTGATGCTCTAGCCTCTTTCCAG
Mouse H2-D1	TCCGAGATTGTAAAGCGTGAAGA	ACAGGGCAGTGCAGGGATAG
Mouse H2-T23	GGACCGCGAATGACATAGC	GCACCTCAGGGTGACTTCAT
Mouse Serping1	ACAGCCCCCTCTGAATTCTT	GGATGCTCTCCAAGTTGCTC
Mouse Gapdh	AATGTGTCCGTCGTGGATCTGA	GATGCCTGCTTCACCACCTTCT
Human VPS35	GCTTACCAGCTGGCTTTTCGAT	GCACTGATAGTCTGGTGGGCAAAT
Human VPS29	TCAAGACTCTGGCTGGTGATGTTC	CTGTCCAACAGTCACAACTTTCTGTTC
Human VPS26A	CGGAGAATCCGTTTCAGGAAAGGT	TCCTTGGTGTTCTAGCCTCTTTCCAG
Human GAPDH	CTCAACGACCACTTTGTCAAGCTC	TCTTACTCCTTGGAGGCCATGT

qRT-PCR was performed with the QuantStudio® 3 Real-Time PCR System (Applied Biosystems®) using SYBR™ Green dye (ThermoFisher). Primers used can be found in Table 7.2.

7.4 Primary cortical neuron culture

All cortical neuron cultured used for this thesis work derived from embryos collected from a pregnant female at E13 and placed in sterile cold HBSS (Gibco) where the cortex was dissected and the tail was collected for genotyping. Cortices were placed in a dilution of 45% glucose (Sigma) 1:100 in PBS where they were cut into small pieces with scissors. Trypsin-EDTA (Gibco) was added to a final concentration of 0.025% and the tube was placed at 37°C for 10min and inverted periodically. Cortex fragments were then transferred to a solution containing L15 medium (Gibco), 0.4% BSA (Invitrogen), and 0.01mg/mL DNAse (Worthington Biochemical). In this medium, cortex was mechanically dissociated via trituration and undissociated fragments were allowed to settle. Supernatant was then collected, and centrifuged at 300g for 5min. Resultant cells were resuspended in media identical to the motor neuron (MN) media described above, counted, and plated on laminin-coated plastic dishes.

7.5 Culture and differentiation of induced pluripotent stem cells (iPSC)

All iPSC used for this thesis work were produced, karyotyped, and generously provided by the Columbia Stem Cell Core or by the lab of Dr Michael Boland. iPSCs were maintained in culture with Essential 8 Basal Medium (Gibco) with 10μM Y-27632 ROCK inhibitor (Tocris), and 100 U/mL penicillin and 100 μg/mL streptomycin (Invitrogen). Differentiation via formation of embryoid bodies was performed as previously described (Maury et al. 2015) with some

modification. At Day 0, cells were washed and dissociated with Accutase (Life Technologies) and replated on non-adherent plastic plates in N2B27 medium [1:1 ADMEM/F12 (Life Technologies) and Neurobasal medium (Life Technologies) with 100 U/mL penicillin and 100 µg/mL streptomycin (Invitrogen), 2mM glutamine (Life Technologies), 0.1mM β-Mercaptoethanol (Life Technologies), B27 Supplement minus Vitamin A (Life Technologies), and N2 supplement (Life Technologies)] with 20µM SB431542 (Stemgent), 0.1µM LDN193189 (Stemgent), and 3µM CHIR99021 (Selleck). After 2 days, 100nM retinoic acid (Sigma) was added. On Day 4, CHIR99021 was removed, and 500nM SAG (EMD Calbiochem) was added. On Day 7, SB431542 and LDN193189 were removed. On Day 9, 10µM DAPT (Tocris) was added. On Day 11, 10ng/mL BDNF and GDNF (R&D systems) were added. Finally, on Day 14, the resulting embryoid bodies were collected for experiments.

7.6 Primary astrocyte culture

All cultured primary astrocytes used for this thesis work derived from mouse pups at postnatal day 3 obtained from the cross between NTg and $SOD1^{G93A}$-Tg mice. DNA from pups was extracted for genotyping by PCR, and cortex was dissected and meninges were removed. Cortex was dissociated mechanically via 20 passages through an 18-gauge needle in astrocyte medium [1:1 Dubelco Modified Eagle's medium (DMEM): F10 medium (Invitrogen), 10% fetal bovine serum (Invitrogen), 100 U/mL penicillin and 100 µg/mL streptomycin (Invitrogen), and 2mM glutamine (Invitrogen)]. Cells were then plated on 75 cm^2 flasks in astrocyte media tor 2 weeks in a humidified incubator at 37°C under 5% CO_2. Media was changed twice per week. The resulting culture includes a population of 95% GFAP+ astrocytes and 5% of CD11b+ microglia. Microglia were eliminated via agitation on a rotary shaker at 200rpm for 6hr and washed off with

PBS. Astrocytes could then be either collected for Western blot or qRT-PCR, or plated on either plastic plates or glass coverslips coated with rat collagen (Corning). Human astrocytes cultures were collected as previously described (De Groot et al. 1997; Re et al. 2014) and maintained in astrocyte media.

7.6.1 Immunocytochemistry

Cells used for immunocytochemistry were plated on glass coverslips and allowed to attach and grow for 2 days. Cells were then washed with PBS and fixed with 4% PFA for 20min at 4°C. PFA was then washed off with PBS 3 times for 5min. Then, cells were first incubated in a blocking solution (0.1% PBS-Triton X, 5% normal donkey serum) for 1hr and then with primary antibodies (diluted at concentrations specified in Table 7.1 in blocking solution) overnight at 4°C. Cells were then washed 3 times for 5min in 0.1% PBS-Triton X prior being incubated with the indicated secondary antibodies conjugated to Alexafluor-488, -594, and -647 (Invitrogen; diluted 1:400 in blocking solution along with 1:1000 DAPI counterstain (Sigma)) for 1hr at room temperature. Cells were then washed again 3 times for 5min in 0.1% PBS-Triton X prior being covered with a thin glass coverslip on Fluoromount-G medium (Invitrogen). Images were taken on a Leica SP8 LIGHTNING confocal microscope equipped with a 63x objective and analyzed with the Fiji distribution of ImageJ software (NIH).

7.6.2 Cultured astrocyte drug treatments

Astrocytes cultured for drug treatments were plated on rat collagen-coated plastic, allowed to grow in astrocyte media for 2 days, and media was replaced with media with indicated drugs diluted in it. Treatments include either cycloheximide (10μg/mL, Cayman Chemical) or a cocktail

of 3 ng/ml Il-1α (Sigma), 30 ng/ml TNFα (Cell Signaling Technology), and 400 ng/ml C1q (MyBioSource).

7.6.3 Astrocyte conditioned medium ELISA

For Aβ42 ELISA, astrocytes were plated for two days, washed, and then cultured in serum-free media for 7 days. After 7 days, the media conditioned on the astrocytes was collected and spun down at 1000g for 10min to pellet cell debris, and the supernatant was used as recommended by the manufacturer (Amyloid beta 42 Mouse ELISA Kit, Invitrogen, Catalog # KMB3441). Aβ42 concentration was normalized to total protein as measured by BCA protein assay.

7.6.4 Cultured astrocyte and MN lentiviral infection

Lentiviral vector preparation was done on HEK 293T cells (ATCC) using the CalPhos Mammalian Transfection Kit (Clontech) as recommended by the manufacturer, using a plasmid DNA mix of 5:2:3:10 of pLP1 (Invitrogen), pLP2 (Invitrogen), pLP-VSV.G (Invitrogen), and shRNA plasmid (kindly provided by Dr Scott Small). Supernatant with viral vectors collected was centrifuged at 500g for 5min to separate detached cells and debris, and the supernatant was filtered through a 0.22μm filter unit (ThermoScientific). Viral vectors were concentrated via ultracentrifugation at 50,000g for 120min from which the supernatant was disposed, and the pelleted lentiviral vectors were resuspended in PBS. The lentivial titer was measured via the use of the Lenti-X qRT-PCR Titration Kit (Clontech) as recommended by the manufacturer, and astrocytes or MNs were treated as previously described at a multiplicity of infection (MOI) of 15, which the lab has previously shown to be optimal for infecting these two mouse cell types with minimal toxicity (Re et al. 2014).

7.7 Embryonic stem cell-derived motor neuron culture

All embryonic stem cells (ES) used for this thesis work were derived from Tg *Hlxb9-GFP1Tmj* mice expressing eGFP under the mouse HB9 promoter were differentiated as previously described with some modification (Wichterle et al. 2002). ES were grown in embryonic stem cell media [DMEM (Millipore Embryomax DMEM), 15% ES-FBS (EmbryoMax), 100 U/mL penicillin and 100 µg/mL streptomycin (Invitrogen), 2mM Glutamine (Gibco), 1% Non-essential Amino Acids (Chemicon), 1% 100x Nucleosides (Chemicon), 1% β-Mercaptoethanol (Millipore), 1% Na-Pyruvate (100mM, Sigma), 1:1000 LIF (Chemicon ESGRO)] for 2 days on gelatinized T25 flasks. Cells were then trypsinized and grown in suspension in αDFNK medium [1:1 Advanced DMEM/F12 (Gibco) and Neurobasal A (Gibco) with 10% Knock out Serum Replacement (Invitrogen), 100 U/mL penicillin and 100 µg/mL streptomycin (Invitrogen), 2mM Glutamine (Gibco), and 1% β-Mercaptoethanol (Millipore)]. 2 Days late, cells were grown in αDFNK medium with 1µM retinoic acid (Sigma) and 0.25µM SAG (Calbiochem) for 3 days. Then, cells were transferred to αDFNK medium without retinoic acid or SAG for 1 day, after which, cells were dissociated using Trypsin-EDTA (Gibco).

Resulting cells were either plated on astrocytes or concentrated in MN media [Neurobasal Medium (Gibco), 2% Horse Serum (Gibco), 2% B27 Supplement (Gibco), 100 U/mL penicillin and 100 µg/mL streptomycin (Invitrogen), 0.25% β-Mercaptoethanol (Millipore), and 0.5mM glutamine (Gibco), supplemented with 10 ng/mL glia-derived neurotrophic factor (GDNF), 10 ng/mL brain-derived neurotrophic factor (BDNF), and 10 ng/mL ciliary neurotrophic factor (CNTF), all trophic factors from R&D systems] to about 5 million cells/mL to be processed by FACS for GFP-positive purification.

7.7.1 FACS for GFP-positive motor neurons

Cells resulting from ES differentiation to MNs were suspended in MN media at a concentration of 5 million cells/mL and filtered through a 35µm nylon mesh (Corning). Cell sorting was performed by the Columbia Stem Cell Initiative (CSCI) Flow Cytometry Core using a Becton Dickinson FACS Aria cytometer (BD Biosciences). Cells were gated for expression of GFP and collected. GFP-positive motor neurons were then centrifuged at 300g for 5min, resuspended in motor neuron media, and plated on laminin-coated plastic wells.

7.7.2 Quantification of GFP-positive motor neurons

Images for the quantification of ES-derived MNs were taken using a TROPHOS fluorescence fast plate imaging system as previously reported (Ikiz et al. 2015). Images were analyzed for MN counts by the MetaMorph® Microscopy Automation and Image Analysis Software (Molecular Devices).

7.8 Immunohistochemistry of spinal cord

All spinal cord immunohistochemistry done for this thesis work were performed on mouse spinal cord following the previously reported protocol (REF). Briefly, mice were sacrificed and perfused with cold PBS for 4min at a rate of 10mL/min, followed by perfusion with cold 4% PFA for 8min at the same rate. Spinal cords were then carefully dissected and post-fixed in 4% PFA overnight at 4°C. The L4-L5 segments were dissected out with a razor blade, PFA was replaced with 30% sucrose in PBS, and the spinal cord was allowed to sink in the solution for at least 48hr. Spinal cord was set in OCT (Tissue-Tek®) in molds, frozen, and cryosectioned in 20µm sections mounted on glass slides.

Sections were first incubated in blocking solution (0.1% PBS-Triton X, 10% normal donkey serum) for 1hr and then in indicated primary antibodies (diluted in blocking solution to the concentration specified in Table 7.1) overnight at 4°C. Sections were then washed 3 times for 5min in 0.1% PBS-Triton X prior to being incubated with secondary antibodies conjugated to Alexafluor-488, -594, and -647 (Invitrogen; diluted 1:400 in blocking solution along with 1:1000 DAPI counterstain (Sigma)) for 1hr at room temperature. Sections were then washed again 3 times for 5min in 0.1% PBS-Triton X and covered with a thin glass coverslip. Images of at least 20 neurons, each from a different hemisection, were taken on a Leica SP8 LIGHTNING confocal microscope equipped with a 63x objective and analyzed with the Fiji distribution of ImageJ software (NIH).

7.9 AAV9-mediated overexpression

AAV9 viruses were produced by Virovek (Hayward, CA). For AAV9-mediated protein overexpression, mice were genotyped at P0, and $SOD1^{G93A}$-Tg were injected intracerebroventricularly following the protocol routinely used in the Motor Neuron Center (REF) with $5x10^{14}$ viral particles. Injection took place using a 27-gauge needle with a 10µL syringe at a location approximately one third of the distance from the intersection between the sagittal and transverse sutures, and the eye, perpendicular to the skull about 2mm deep.

7.10 Inverted grid test

This motor performance test is routinely used in the lab and originate from the publication of Olivan et al. (Olivan et al. 2015) with minor modifications. In brief, for this test, mice were placed on a grid and allowed to grip it with all four limbs. The grid was then inverted and elevated

over soft padding, resulting in the mouse hanging inverted from the grid. Score was recorded as maximum hold time out of three trials up to either 60sec or 120sec. Animals were tested once per week within 3 hr before their night cycle began.

7.11 Spinal cord motor neuron quantification

For this quantitative morphological study, mice were sacrificed and perfused with cold PBS for 4min at a rate of 10mL/min, followed by perfusion with cold 4% PFA for 8min at the same rate. Spinal cords were then carefully dissected and post-fixed in 4% PFA overnight at 4°C. PFA was replaced with PBS, and the L4-L5 segment of the spinal cord, as defined by its ventral roots was cut out under a microscope with a razor blade. L4-L5 segments were set vertically in a mold in 4% agarose. A vibratome was then used to cut 70μm-thick sections, of which every other section was collected for immunostaining (an average of 20 sections).

Sections were first incubated in blocking solution (0.5% PBS-Triton X, 5% normal donkey serum) for 1hr prior being incubated with a primary goat anti-ChAT antibody (Sigma, Catalog # AB144P; diluted 1:250 in blocking solution) for 3 days at 4°C. Sections were then washed 6 times for 15min in 0.5% PBS-Triton X prior being incubated with a secondary anti-goat antibody conjugated to Alexafluor-594 (Invitrogen; diluted 1:400 in blocking solution) for 3hr at room temperature. Sections were then washed again 6 times for 15min in 0.5% PBS-Triton X, mounted on glass slides and covered with a thin glass coverslip. Stacks of images were taken on a Leica SP8 LIGHTNING confocal microscope equipped with a 20x objective and quantified. A MN was defined as a ChAT-positive cell in the ventral horn of the spinal cord.

7.12 Neuromuscular junction innervation quantification

For this other quantitative morphological study, mice were sacrificed and perfused with cold PBS for 4min at a rate of 10mL/min, followed by perfusion with cold 4% PFA for 8min at the same rate. The tibialis anterior muscle was then carefully dissected and incubated in PBS overnight at 4°C. PBS was replaced with 30% sucrose in PBS, and the tibialis anterior was allowed to sink in the solution for at least 48hr. Muscle was set in OCT (Tissue-Tek®) in molds, frozen, and cryosectioned in 20µm sections mounted on glass slides.

Sections were first incubated in blocking solution (0.1% PBS-Triton X, 10% normal donkey serum) for 1hr and then incubated with a primary guinea pig anti-synaptophysin-1 antibody (Synaptic Systems, Catalog # 101 004; diluted 1:500 in blocking solution) overnight at 4°C. Sections were then washed 3 times for 5min in 0.1% PBS-Triton X, prior to being incubated with a secondary anti-guinea pig antibody conjugated to Alexafluor-488 or -647 (Invitrogen; diluted 1:400 in blocking solution along with fluorescent-conjugated alpha-bungarotoxin (BTX; 1/200 α-bungarotoxin conjugated to Alexafluor-555, Invitrogen)) for 1hr at room temperature. Sections were then washed again 3 times for 5min in 0.1% PBS-Triton X and covered with a thin glass coverslip. Images were taken on a Leica SP8 LIGHTNING confocal microscope equipped with a 20x objective and quantified. At least 100 neuromuscular junctions as defined by the presence of BTX staining were imaged and assessed for innervation as defined by the presence of synaptophysin staining.

7.13 Statistical analyses

All data sets presented in this thesis are depicted as mean ± SEM, unless stated otherwise. Results correspond to at least three independent experiments and each experiment is the average

of 2-3 technical replicates or 3-6 coverslips or 6 96-wells per time point and per condition. For cultured cell quantification, values express the relative total number of neurons counted in 6 fields at 10x objective. Differences between means were analyzed by a two-tailed Student's t-test. Differences among means were analyzed by one-way ANOVA with the different genotypes or treatments as the independent factors. When ANOVA showed significant differences, pair-wise comparisons between means were tested by Newman-Keuls post-hoc testing. Kinetics data were fitted by a non-linear iterative least squares method. Given the nature of the data, i.e. temporal decay of motor function or a temporal decay in protein levels, a variable slope dose response equation or a one-phase exponential decay equation were selected, respectively; more complex models failed to improve the fitting of the data and were thus not considered for the analyses. Then, the different curves were compared by the method of Extra Sum-of-Squares F test. This method is a form of ANOVA which tests whether one curve can fit all data sets. To compare survival between mouse genotypes and treatments, the nonparametric Kaplan-Meier statistics was used as before (Dermentzaki et al. 2019). Prior to any analysis, each dataset was tested for normal distribution and equality of variance and, should either criterion be violated, the appropriate non-parametric test was used. In all analyses, the null hypothesis was rejected at the 0.05 level. All analyses where done with the software GraphPad Prism version 5 (San Diego, CA).

CHAPTER 8

REFERENCES

Aebischer, J., P. Cassina, B. Otsmane, A. Moumen, D. Seilhean, V. Meininger, L. Barbeito, B. Pettmann, and C. Raoul. 2011. 'IFNgamma triggers a LIGHT-dependent selective death of motoneurons contributing to the non-cell-autonomous effects of mutant SOD1', *Cell Death Differ*, 18: 754-68.

Aebischer, J., A. Moumen, V. Sazdovitch, D. Seilhean, V. Meininger, and C. Raoul. 2012. 'Elevated levels of IFNgamma and LIGHT in the spinal cord of patients with sporadic amyotrophic lateral sclerosis', *Eur J Neurol*, 19: 752-9, e45-6.

Agromayor, M., N. Soler, A. Caballe, T. Kueck, S. M. Freund, M. D. Allen, M. Bycroft, O. Perisic, Y. Ye, B. McDonald, H. Scheel, K. Hofmann, S. J. Neil, J. Martin-Serrano, and R. L. Williams. 2012. 'The UBAP1 subunit of ESCRT-I interacts with ubiquitin via a SOUBA domain', *Structure*, 20: 414-28.

Ajmone-Cat, M. A., A. Onori, C. Toselli, E. Stronati, M. Morlando, I. Bozzoni, E. Monni, Z. Kokaia, G. Lupo, L. Minghetti, S. Biagioni, and E. Cacci. 2019. 'Increased FUS levels in astrocytes leads to astrocyte and microglia activation and neuronal death', *Sci Rep*, 9: 4572.

Al-Chalabi, A., O. Hardiman, M. C. Kiernan, A. Chio, B. Rix-Brooks, and L. H. van den Berg. 2016. 'Amyotrophic lateral sclerosis: moving towards a new classification system', *Lancet Neurol*, 15: 1182-94.

Al-Saif, A., F. Al-Mohanna, and S. Bohlega. 2011. 'A mutation in sigma-1 receptor causes juvenile amyotrophic lateral sclerosis', *Ann Neurol*, 70: 913-9.

Al-Sarraj, S., A. King, C. Troakes, B. Smith, S. Maekawa, I. Bodi, B. Rogelj, A. Al-Chalabi, T. Hortobagyi, and C. E. Shaw. 2011. 'p62 positive, TDP-43 negative, neuronal cytoplasmic and intranuclear inclusions in the cerebellum and hippocampus define the pathology of C9orf72-linked FTLD and MND/ALS', *Acta Neuropathol*, 122: 691-702.

Alam, S. L., C. Langelier, F. G. Whitby, S. Koirala, H. Robinson, C. P. Hill, and W. I. Sundquist. 2006. 'Structural basis for ubiquitin recognition by the human ESCRT-II EAP45 GLUE domain', *Nat Struct Mol Biol*, 13: 1029-30.

Alami, N. H., R. B. Smith, M. A. Carrasco, L. A. Williams, C. S. Winborn, S. S. W. Han, E. Kiskinis, B. Winborn, B. D. Freibaum, A. Kanagaraj, A. J. Clare, N. M. Badders, B. Bilican, E. Chaum, S. Chandran, C. E. Shaw, K. C. Eggan, T. Maniatis, and J. P. Taylor. 2014. 'Axonal transport of TDP-43 mRNA granules is impaired by ALS-causing mutations', *Neuron*, 81: 536-43.

Alarcon, C. R., H. Goodarzi, H. Lee, X. Liu, S. Tavazoie, and S. F. Tavazoie. 2015. 'HNRNPA2B1 Is a Mediator of m(6)A-Dependent Nuclear RNA Processing Events', *Cell*, 162: 1299-308.

Alsultan, A. A., R. Waller, P. R. Heath, and J. Kirby. 2016. 'The genetics of amyotrophic lateral sclerosis: current insights', *Degener Neurol Neuromuscul Dis*, 6: 49-64.

Amador-Ortiz, C., W. L. Lin, Z. Ahmed, D. Personett, P. Davies, R. Duara, N. R. Graff-Radford, M. L. Hutton, and D. W. Dickson. 2007. 'TDP-43 immunoreactivity in hippocampal sclerosis and Alzheimer's disease', *Ann Neurol*, 61: 435-45.

Amerik, A. Y., J. Nowak, S. Swaminathan, and M. Hochstrasser. 2000. 'The Doa4 deubiquitinating enzyme is functionally linked to the vacuolar protein-sorting and endocytic pathways', *Mol Biol Cell*, 11: 3365-80.

Andersen, O. M., J. Reiche, V. Schmidt, M. Gotthardt, R. Spoelgen, J. Behlke, C. A. von Arnim, T. Breiderhoff, P. Jansen, X. Wu, K. R. Bales, R. Cappai, C. L. Masters, J. Gliemann, E. J. Mufson, B. T. Hyman, S. M. Paul, A. Nykjaer, and T. E. Willnow. 2005. 'Neuronal sorting protein-related receptor sorLA/LR11 regulates processing of the amyloid precursor protein', *Proc Natl Acad Sci U S A*, 102: 13461-6.

Andersen, P. M. 2006. 'Amyotrophic lateral sclerosis associated with mutations in the CuZn superoxide dismutase gene', *Curr Neurol Neurosci Rep*, 6: 37-46.

Andreadou, E., E. Kapaki, P. Kokotis, G. P. Paraskevas, N. Katsaros, G. Libitaki, V. Zis, C. Sfagos, and D. Vassilopoulos. 2008. 'Plasma glutamate and glycine levels in patients with amyotrophic lateral sclerosis: the effect of riluzole treatment', *Clin Neurol Neurosurg*, 110: 222-6.

Ansell-Schultz, A., J. F. Reyes, M. Samuelsson, and M. Hallbeck. 2018. 'Reduced retromer function results in the accumulation of amyloid-beta oligomers', *Mol Cell Neurosci*, 93: 18-26.

Antonescu, C. N., F. Aguet, G. Danuser, and S. L. Schmid. 2011. 'Phosphatidylinositol-(4,5)-bisphosphate regulates clathrin-coated pit initiation, stabilization, and size', *Mol Biol Cell*, 22: 2588-600.

Aoki, Y., R. Manzano, Y. Lee, R. Dafinca, M. Aoki, A. G. L. Douglas, M. A. Varela, C. Sathyaprakash, J. Scaber, P. Barbagallo, P. Vader, I. Mager, K. Ezzat, M. R. Turner, N. Ito, S. Gasco, N. Ohbayashi, S. El Andaloussi, S. Takeda, M. Fukuda, K. Talbot, and M. J. A. Wood. 2017. 'C9orf72 and RAB7L1 regulate vesicle trafficking in amyotrophic lateral sclerosis and frontotemporal dementia', *Brain*, 140: 887-97.

Arai, T., M. Hasegawa, H. Akiyama, K. Ikeda, T. Nonaka, H. Mori, D. Mann, K. Tsuchiya, M. Yoshida, Y. Hashizume, and T. Oda. 2006. 'TDP-43 is a component of ubiquitin-positive tau-negative inclusions in frontotemporal lobar degeneration and amyotrophic lateral sclerosis', *Biochem Biophys Res Commun*, 351: 602-11.

Arai, T., T. Nonaka, M. Hasegawa, H. Akiyama, M. Yoshida, Y. Hashizume, K. Tsuchiya, T. Oda, and K. Ikeda. 2003. 'Neuronal and glial inclusions in frontotemporal dementia with or without motor neuron disease are immunopositive for p62', *Neurosci Lett*, 342: 41-4.

Atkin, J. D., M. A. Farg, A. K. Walker, C. McLean, D. Tomas, and M. K. Horne. 2008. 'Endoplasmic reticulum stress and induction of the unfolded protein response in human sporadic amyotrophic lateral sclerosis', *Neurobiol Dis*, 30: 400-7.

Axe, E. L., S. A. Walker, M. Manifava, P. Chandra, H. L. Roderick, A. Habermann, G. Griffiths, and N. T. Ktistakis. 2008. 'Autophagosome formation from membrane compartments enriched in phosphatidylinositol 3-phosphate and dynamically connected to the endoplasmic reticulum', *J Cell Biol*, 182: 685-701.

Bache, K. G., A. Brech, A. Mehlum, and H. Stenmark. 2003. 'Hrs regulates multivesicular body formation via ESCRT recruitment to endosomes', *J Cell Biol*, 162: 435-42.

Baetz, N. W., and J. R. Goldenring. 2013. 'Rab11-family interacting proteins define spatially and temporally distinct regions within the dynamic Rab11a-dependent recycling system', *Mol Biol Cell*, 24: 643-58.

Bajc Cesnik, A., S. Darovic, S. Prpar Mihevc, M. Stalekar, M. Malnar, H. Motaln, Y. B. Lee, J. Mazej, J. Pohleven, M. Grosch, M. Modic, M. Fonovic, B. Turk, M. Drukker, C. E. Shaw,

and B. Rogelj. 2019. 'Nuclear RNA foci from C9ORF72 expansion mutation form paraspeckle-like bodies', *J Cell Sci*, 132.

Balderhaar, H. J., J. Lachmann, E. Yavavli, C. Brocker, A. Lurick, and C. Ungermann. 2013. 'The CORVET complex promotes tethering and fusion of Rab5/Vps21-positive membranes', *Proc Natl Acad Sci U S A*, 110: 3823-8.

Baldwin, K. J., and C. M. Correll. 2019. 'Prion Disease', *Semin Neurol*, 39: 428-39.

Ballard, C., S. Gauthier, A. Corbett, C. Brayne, D. Aarsland, and E. Jones. 2011. 'Alzheimer's disease', *Lancet*, 377: 1019-31.

Bandres-Ciga, S., N. E. Mencacci, R. Duran, F. J. Barrero, F. Escamilla-Sevilla, S. Morgan, J. Hehir, F. Vives, J. Hardy, and A. M. Pittman. 2016. 'Analysis of the genetic variability in Parkinson's disease from Southern Spain', *Neurobiol Aging*, 37: 210.e1-10.e5.

Bannwarth, S., S. Ait-El-Mkadem, A. Chaussenot, E. C. Genin, S. Lacas-Gervais, K. Fragaki, L. Berg-Alonso, Y. Kageyama, V. Serre, D. G. Moore, A. Verschueren, C. Rouzier, I. Le Ber, G. Auge, C. Cochaud, F. Lespinasse, K. N'Guyen, A. de Septenville, A. Brice, P. Yu-Wai-Man, H. Sesaki, J. Pouget, and V. Paquis-Flucklinger. 2014. 'A mitochondrial origin for frontotemporal dementia and amyotrophic lateral sclerosis through CHCHD10 involvement', *Brain*, 137: 2329-45.

Barbeito, L. H., M. Pehar, P. Cassina, M. R. Vargas, H. Peluffo, L. Viera, A. G. Estevez, and J. S. Beckman. 2004. 'A role for astrocytes in motor neuron loss in amyotrophic lateral sclerosis', *Brain Res Brain Res Rev*, 47: 263-74.

Barone, P., A. Antonini, C. Colosimo, R. Marconi, L. Morgante, T. P. Avarello, E. Bottacchi, A. Cannas, G. Ceravolo, R. Ceravolo, G. Cicarelli, R. M. Gaglio, R. M. Giglia, F. Iemolo, M. Manfredi, G. Meco, A. Nicoletti, M. Pederzoli, A. Petrone, A. Pisani, F. E. Pontieri, R. Quatrale, S. Ramat, R. Scala, G. Volpe, S. Zappulla, A. R. Bentivoglio, F. Stocchi, G. Trianni, and P. D. Dotto. 2009. 'The PRIAMO study: A multicenter assessment of nonmotor symptoms and their impact on quality of life in Parkinson's disease', *Mov Disord*, 24: 1641-9.

Barouch, W., K. Prasad, L. E. Greene, and E. Eisenberg. 1994. 'ATPase activity associated with the uncoating of clathrin baskets by Hsp70', *J Biol Chem*, 269: 28563-8.

Bartuzi, P., D. D. Billadeau, R. Favier, S. Rong, D. Dekker, A. Fedoseienko, H. Fieten, M. Wijers, J. H. Levels, N. Huijkman, N. Kloosterhuis, H. van der Molen, G. Brufau, A. K. Groen, A. M. Elliott, J. A. Kuivenhoven, B. Plecko, G. Grangl, J. McGaughran, J. D. Horton, E. Burstein, M. H. Hofker, and B. van de Sluis. 2016. 'CCC- and WASH-mediated endosomal sorting of LDLR is required for normal clearance of circulating LDL', *Nat Commun*, 7: 10961.

Beber, B. C., and M. L. F. Chaves. 2013. 'Evaluation of patients with behavioral and cognitive complaints: misdiagnosis in frontotemporal dementia and Alzheimer's disease', *Dement Neuropsychol*, 7: 60-65.

Beers, D. R., J. S. Henkel, Q. Xiao, W. Zhao, J. Wang, A. A. Yen, L. Siklos, S. R. McKercher, and S. H. Appel. 2006. 'Wild-type microglia extend survival in PU.1 knockout mice with familial amyotrophic lateral sclerosis', *Proc Natl Acad Sci U S A*, 103: 16021-6.

Belenkaya, T. Y., Y. Wu, X. Tang, B. Zhou, L. Cheng, Y. V. Sharma, D. Yan, E. M. Selva, and X. Lin. 2008. 'The retromer complex influences Wnt secretion by recycling wntless from endosomes to the trans-Golgi network', *Dev Cell*, 14: 120-31.

Belzil, V. V., C. Andre-Guimont, M. R. Atallah, H. Daoud, N. Dupre, J. P. Bouchard, W. Camu, P. A. Dion, and G. A. Rouleau. 2012. 'Analysis of the SORT1 gene in familial amyotrophic lateral sclerosis', *Neurobiol Aging*, 33: 1845.e7-9.

Benatar, M., J. Wuu, P. M. Andersen, N. Atassi, W. David, M. Cudkowicz, and D. Schoenfeld. 2018. 'Randomized, double-blind, placebo-controlled trial of arimoclomol in rapidly progressive SOD1 ALS', *Neurology*, 90: e565-e74.

Bendotti, C., M. Tortarolo, S. K. Suchak, N. Calvaresi, L. Carvelli, A. Bastone, M. Rizzi, M. Rattray, and T. Mennini. 2001. 'Transgenic SOD1 G93A mice develop reduced GLT-1 in spinal cord without alterations in cerebrospinal fluid glutamate levels', *J Neurochem*, 79: 737-46.

Bennett, C. L., and A. R. La Spada. 2018. 'Senataxin, A Novel Helicase at the Interface of RNA Transcriptome Regulation and Neurobiology: From Normal Function to Pathological Roles in Motor Neuron Disease and Cerebellar Degeneration', *Adv Neurobiol*, 20: 265-81.

Berman, D. E., D. Ringe, G. A. Petsko, and S. A. Small. 2015. 'The use of pharmacological retromer chaperones in Alzheimer's disease and other endosomal-related disorders', *Neurotherapeutics*, 12: 12-8.

Bernard-Marissal, N., J. J. Medard, H. Azzedine, and R. Chrast. 2015. 'Dysfunction in endoplasmic reticulum-mitochondria crosstalk underlies SIGMAR1 loss of function mediated motor neuron degeneration', *Brain*, 138: 875-90.

Bhalla, A., C. P. Vetanovetz, E. Morel, Z. Chamoun, G. Di Paolo, and S. A. Small. 2012. 'The location and trafficking routes of the neuronal retromer and its role in amyloid precursor protein transport', *Neurobiol Dis*, 47: 126-34.

Bilsland, L. G., E. Sahai, G. Kelly, M. Golding, L. Greensmith, and G. Schiavo. 2010. 'Deficits in axonal transport precede ALS symptoms in vivo', *Proc Natl Acad Sci U S A*, 107: 20523-8.

Blackstone, C., C. J. O'Kane, and E. Reid. 2011. 'Hereditary spastic paraplegias: membrane traffic and the motor pathway', *Nat Rev Neurosci*, 12: 31-42.

Boillee, S., M. Peschanski, and M. P. Junier. 2003. 'The wobbler mouse: a neurodegeneration jigsaw puzzle', *Mol Neurobiol*, 28: 65-106.

Bolos, M., M. Llorens-Martin, J. R. Perea, J. Jurado-Arjona, A. Rabano, F. Hernandez, and J. Avila. 2017. 'Absence of CX3CR1 impairs the internalization of Tau by microglia', *Mol Neurodegener*, 12: 59.

Borg Distefano, M., L. Hofstad Haugen, Y. Wang, H. Perdreau-Dahl, I. Kjos, D. Jia, J. P. Morth, J. Neefjes, O. Bakke, and C. Progida. 2018. 'TBC1D5 controls the GTPase cycle of Rab7b', *J Cell Sci*, 131.

Bosco, D. A., G. Morfini, N. M. Karabacak, Y. Song, F. Gros-Louis, P. Pasinelli, H. Goolsby, B. A. Fontaine, N. Lemay, D. McKenna-Yasek, M. P. Frosch, J. N. Agar, J. P. Julien, S. T. Brady, and R. H. Brown, Jr. 2010. 'Wild-type and mutant SOD1 share an aberrant conformation and a common pathogenic pathway in ALS', *Nat Neurosci*, 13: 1396-403.

Brach, T., C. Godlee, I. Moeller-Hansen, D. Boeke, and M. Kaksonen. 2014. 'The initiation of clathrin-mediated endocytosis is mechanistically highly flexible', *Curr Biol*, 24: 548-54.

Bradley, W. G., P. Good, C. G. Rasool, and L. S. Adelman. 1983. 'Morphometric and biochemical studies of peripheral nerves in amyotrophic lateral sclerosis', *Ann Neurol*, 14: 267-77.

Braell, W. A., D. M. Schlossman, S. L. Schmid, and J. E. Rothman. 1984. 'Dissociation of clathrin coats coupled to the hydrolysis of ATP: role of an uncoating ATPase', *J Cell Biol*, 99: 734-41.

Braschi, E., V. Goyon, R. Zunino, A. Mohanty, L. Xu, and H. M. McBride. 2010. 'Vps35 mediates vesicle transport between the mitochondria and peroxisomes', *Curr Biol*, 20: 1310-5.

Brenner, D., K. Muller, T. Wieland, P. Weydt, S. Bohm, D. Lule, A. Hubers, C. Neuwirth, M. Weber, G. Borck, M. Wahlqvist, K. M. Danzer, A. E. Volk, T. Meitinger, T. M. Strom, M. Otto, J. Kassubek, A. C. Ludolph, P. M. Andersen, and J. H. Weishaupt. 2016. 'NEK1 mutations in familial amyotrophic lateral sclerosis', *Brain*, 139: e28.

Brenner, D., R. Yilmaz, K. Muller, T. Grehl, S. Petri, T. Meyer, J. Grosskreutz, P. Weydt, W. Ruf, C. Neuwirth, M. Weber, S. Pinto, K. G. Claeys, B. Schrank, B. Jordan, A. Knehr, K. Gunther, A. Hubers, D. Zeller, C. Kubisch, S. Jablonka, M. Sendtner, T. Klopstock, M. de Carvalho, A. Sperfeld, G. Borck, A. E. Volk, J. Dorst, J. Weis, M. Otto, J. Schuster, K. Del Tredici, H. Braak, K. M. Danzer, A. Freischmidt, T. Meitinger, T. M. Strom, A. C. Ludolph, P. M. Andersen, and J. H. Weishaupt. 2018. 'Hot-spot KIF5A mutations cause familial ALS', *Brain*, 141: 688-97.

Brooks, B. R. 1994. 'El Escorial World Federation of Neurology criteria for the diagnosis of amyotrophic lateral sclerosis. Subcommittee on Motor Neuron Diseases/Amyotrophic Lateral Sclerosis of the World Federation of Neurology Research Group on Neuromuscular Diseases and the El Escorial "Clinical limits of amyotrophic lateral sclerosis" workshop contributors', *J Neurol Sci*, 124 Suppl: 96-107.

Brown, F. R., 3rd, M. K. Greer, E. H. Aylward, and H. H. Hunt. 1990. 'Intellectual and adaptive functioning in individuals with Down syndrome in relation to age and environmental placement', *Pediatrics*, 85: 450-2.

Bruening, W., J. Roy, B. Giasson, D. A. Figlewicz, W. E. Mushynski, and H. D. Durham. 1999. 'Up-regulation of protein chaperones preserves viability of cells expressing toxic Cu/Zn-superoxide dismutase mutants associated with amyotrophic lateral sclerosis', *J Neurochem*, 72: 693-9.

Brundin, P., R. Melki, and R. Kopito. 2010. 'Prion-like transmission of protein aggregates in neurodegenerative diseases', *Nat Rev Mol Cell Biol*, 11: 301-7.

Bryson, J. B., C. Hobbs, M. J. Parsons, K. D. Bosch, A. Pandraud, F. S. Walsh, P. Doherty, and L. Greensmith. 2012. 'Amyloid precursor protein (APP) contributes to pathology in the SOD1(G93A) mouse model of amyotrophic lateral sclerosis', *Hum Mol Genet*, 21: 3871-82.

Bugarcic, A., Y. Zhe, M. C. Kerr, J. Griffin, B. M. Collins, and R. D. Teasdale. 2011. 'Vps26A and Vps26B subunits define distinct retromer complexes', *Traffic*, 12: 1759-73.

Bull, M. J. 2011. 'Health supervision for children with Down syndrome', *Pediatrics*, 128: 393-406.

Buratti, E., and F. E. Baralle. 2001. 'Characterization and functional implications of the RNA binding properties of nuclear factor TDP-43, a novel splicing regulator of CFTR exon 9', *J Biol Chem*, 276: 36337-43.

Buratti, E., and F. E. Baralle. 2008. 'Multiple roles of TDP-43 in gene expression, splicing regulation, and human disease', *Front Biosci*, 13: 867-78.

Burd, C., and P. J. Cullen. 2014. 'Retromer: a master conductor of endosome sorting', *Cold Spring Harb Perspect Biol*, 6.

Burd, C. G., and S. D. Emr. 1998. 'Phosphatidylinositol(3)-phosphate signaling mediated by specific binding to RING FYVE domains', *Mol Cell*, 2: 157-62.

Burda, P., S. M. Padilla, S. Sarkar, and S. D. Emr. 2002. 'Retromer function in endosome-to-Golgi retrograde transport is regulated by the yeast Vps34 PtdIns 3-kinase', *J Cell Sci*, 115: 3889-900.

Burkhardt, J. K., C. J. Echeverri, T. Nilsson, and R. B. Vallee. 1997. 'Overexpression of the dynamitin (p50) subunit of the dynactin complex disrupts dynein-dependent maintenance of membrane organelle distribution', *J Cell Biol*, 139: 469-84.

Burre, J., M. Sharma, and T. C. Sudhof. 2018. 'Cell Biology and Pathophysiology of alpha-Synuclein', *Cold Spring Harb Perspect Med*, 8.

Butz, E. S., U. Chandrachud, S. E. Mole, and S. L. Cotman. 2019. 'Moving towards a new era of genomics in the neuronal ceroid lipofuscinoses', *Biochim Biophys Acta Mol Basis Dis*: 165571.

Byrne, S., C. Walsh, C. Lynch, P. Bede, M. Elamin, K. Kenna, R. McLaughlin, and O. Hardiman. 2011. 'Rate of familial amyotrophic lateral sclerosis: a systematic review and meta-analysis', *J Neurol Neurosurg Psychiatry*, 82: 623-7.

Cabrera, M., M. Nordmann, A. Perz, D. Schmedt, A. Gerondopoulos, F. Barr, J. Piehler, S. Engelbrecht-Vandre, and C. Ungermann. 2014. 'The Mon1-Ccz1 GEF activates the Rab7 GTPase Ypt7 via a longin-fold-Rab interface and association with PI3P-positive membranes', *J Cell Sci*, 127: 1043-51.

Cai, B., S. S. Giridharan, J. Zhang, S. Saxena, K. Bahl, J. A. Schmidt, P. L. Sorgen, W. Guo, N. Naslavsky, and S. Caplan. 2013. 'Differential roles of C-terminal Eps15 homology domain proteins as vesiculators and tubulators of recycling endosomes', *J Biol Chem*, 288: 30172-80.

Cai, X. D., T. E. Golde, and S. G. Younkin. 1993. 'Release of excess amyloid beta protein from a mutant amyloid beta protein precursor', *Science*, 259: 514-6.

Campbell, P. D., K. Shen, M. R. Sapio, T. D. Glenn, W. S. Talbot, and F. L. Marlow. 2014. 'Unique function of Kinesin Kif5A in localization of mitochondria in axons', *J Neurosci*, 34: 14717-32.

Canton, T., J. Pratt, J. M. Stutzmann, A. Imperato, and A. Boireau. 1998. 'Glutamate uptake is decreased tardively in the spinal cord of FALS mice', *Neuroreport*, 9: 775-8.

Canuel, M., S. Lefrancois, J. Zeng, and C. R. Morales. 2008. 'AP-1 and retromer play opposite roles in the trafficking of sortilin between the Golgi apparatus and the lysosomes', *Biochem Biophys Res Commun*, 366: 724-30.

Cao, C., J. M. Backer, J. Laporte, E. J. Bedrick, and A. Wandinger-Ness. 2008. 'Sequential actions of myotubularin lipid phosphatases regulate endosomal PI(3)P and growth factor receptor trafficking', *Mol Biol Cell*, 19: 3334-46.

Cao, T. T., H. W. Deacon, D. Reczek, A. Bretscher, and M. von Zastrow. 1999. 'A kinase-regulated PDZ-domain interaction controls endocytic sorting of the beta2-adrenergic receptor', *Nature*, 401: 286-90.

Caplan, S., N. Naslavsky, L. M. Hartnell, R. Lodge, R. S. Polishchuk, J. G. Donaldson, and J. S. Bonifacino. 2002. 'A tubular EHD1-containing compartment involved in the recycling of major histocompatibility complex class I molecules to the plasma membrane', *EMBO J*, 21: 2557-67.

Carlton, J., M. Bujny, B. J. Peter, V. M. Oorschot, A. Rutherford, H. Mellor, J. Klumperman, H. T. McMahon, and P. J. Cullen. 2004. 'Sorting nexin-1 mediates tubular endosome-to-TGN transport through coincidence sensing of high- curvature membranes and 3-phosphoinositides', *Curr Biol*, 14: 1791-800.

Carlton, J. G., M. V. Bujny, B. J. Peter, V. M. Oorschot, A. Rutherford, R. S. Arkell, J. Klumperman, H. T. McMahon, and P. J. Cullen. 2005. 'Sorting nexin-2 is associated with

tubular elements of the early endosome, but is not essential for retromer-mediated endosome-to-TGN transport', *J Cell Sci*, 118: 4527-39.

Carri, M. T., A. Ferri, A. Battistoni, L. Famhy, R. Gabbianelli, F. Poccia, and G. Rotilio. 1997. 'Expression of a Cu,Zn superoxide dismutase typical of familial amyotrophic lateral sclerosis induces mitochondrial alteration and increase of cytosolic Ca2+ concentration in transfected neuroblastoma SH-SY5Y cells', *FEBS Lett*, 414: 365-8.

Carroll, S. Y., H. E. Stimpson, J. Weinberg, C. P. Toret, Y. Sun, and D. G. Drubin. 2012. 'Analysis of yeast endocytic site formation and maturation through a regulatory transition point', *Mol Biol Cell*, 23: 657-68.

Cassina, P., A. Cassina, M. Pehar, R. Castellanos, M. Gandelman, A. de Leon, K. M. Robinson, R. P. Mason, J. S. Beckman, L. Barbeito, and R. Radi. 2008. 'Mitochondrial dysfunction in SOD1G93A-bearing astrocytes promotes motor neuron degeneration: prevention by mitochondrial-targeted antioxidants', *J Neurosci*, 28: 4115-22.

Cassina, P., M. Pehar, M. R. Vargas, R. Castellanos, A. G. Barbeito, A. G. Estevez, J. A. Thompson, J. S. Beckman, and L. Barbeito. 2005. 'Astrocyte activation by fibroblast growth factor-1 and motor neuron apoptosis: implications for amyotrophic lateral sclerosis', *J Neurochem*, 93: 38-46.

Cebollero, E., A. van der Vaart, M. Zhao, E. Rieter, D. J. Klionsky, J. B. Helms, and F. Reggiori. 2012. 'Phosphatidylinositol-3-phosphate clearance plays a key role in autophagosome completion', *Curr Biol*, 22: 1545-53.

Chandra, M., and B. M. Collins. 2018. 'The Phox Homology (PX) Domain', *Adv Exp Med Biol*.

Chang, J. L., C. Lomen-Hoerth, J. Murphy, R. G. Henry, J. H. Kramer, B. L. Miller, and M. L. Gorno-Tempini. 2005. 'A voxel-based morphometry study of patterns of brain atrophy in ALS and ALS/FTLD', *Neurology*, 65: 75-80.

Chang, Y., Q. Kong, X. Shan, G. Tian, H. Ilieva, D. W. Cleveland, J. D. Rothstein, D. R. Borchelt, P. C. Wong, and C. L. Lin. 2008. 'Messenger RNA oxidation occurs early in disease pathogenesis and promotes motor neuron degeneration in ALS', *PLoS One*, 3: e2849.

Checler, F. 1995. 'Processing of the beta-amyloid precursor protein and its regulation in Alzheimer's disease', *J Neurochem*, 65: 1431-44.

Chen, H. J., J. C. Mitchell, S. Novoselov, J. Miller, A. L. Nishimura, E. L. Scotter, C. A. Vance, M. E. Cheetham, and C. E. Shaw. 2016. 'The heat shock response plays an important role in TDP-43 clearance: evidence for dysfunction in amyotrophic lateral sclerosis', *Brain*, 139: 1417-32.

Chen, H., M. W. Kankel, S. C. Su, S. W. S. Han, and D. Ofengeim. 2018. 'Exploring the genetics and non-cell autonomous mechanisms underlying ALS/FTLD', *Cell Death Differ*, 25: 648-62.

Chen, H., K. Qian, Z. Du, J. Cao, A. Petersen, H. Liu, L. W. th Blackbourn, C. L. Huang, A. Errigo, Y. Yin, J. Lu, M. Ayala, and S. C. Zhang. 2014. 'Modeling ALS with iPSCs reveals that mutant SOD1 misregulates neurofilament balance in motor neurons', *Cell Stem Cell*, 14: 796-809.

Chen, Y., K. Chen, W. Song, X. Chen, B. Cao, R. Huang, B. Zhao, X. Guo, J. Burgunder, J. Li, and H. F. Shang. 2013. 'VPS35 Asp620Asn and EIF4G1 Arg1205His mutations are rare in Parkinson disease from southwest China', *Neurobiol Aging*, 34: 1709.e7-8.

Chen, Y., Y. Guan, Z. Zhang, H. Liu, S. Wang, L. Yu, X. Wu, and X. Wang. 2012. 'Wnt signaling pathway is involved in the pathogenesis of amyotrophic lateral sclerosis in adult transgenic mice', *Neurol Res*, 34: 390-9.

Chen, Y. Z., C. L. Bennett, H. M. Huynh, I. P. Blair, I. Puls, J. Irobi, I. Dierick, A. Abel, M. L. Kennerson, B. A. Rabin, G. A. Nicholson, M. Auer-Grumbach, K. Wagner, P. De Jonghe, J. W. Griffin, K. H. Fischbeck, V. Timmerman, D. R. Cornblath, and P. F. Chance. 2004. 'DNA/RNA helicase gene mutations in a form of juvenile amyotrophic lateral sclerosis (ALS4)', *Am J Hum Genet*, 74: 1128-35.

Cheng, X., X. Ma, X. Ding, L. Li, X. Jiang, Z. Shen, S. Chen, W. Liu, W. Gong, and Q. Sun. 2017. 'Pacer Mediates the Function of Class III PI3K and HOPS Complexes in Autophagosome Maturation by Engaging Stx17', *Mol Cell*, 65: 1029-43.e5.

Chio, A., G. Logroscino, B. J. Traynor, J. Collins, J. C. Simeone, L. A. Goldstein, and L. A. White. 2013. 'Global epidemiology of amyotrophic lateral sclerosis: a systematic review of the published literature', *Neuroepidemiology*, 41: 118-30.

Chou, K. L., R. A. Koeppe, and N. I. Bohnen. 2011. 'Rhinorrhea: a common nondopaminergic feature of Parkinson's disease', *Mov Disord*, 26: 320-3.

Chow, C. Y., J. E. Landers, S. K. Bergren, P. C. Sapp, A. E. Grant, J. M. Jones, L. Everett, G. M. Lenk, D. M. McKenna-Yasek, L. S. Weisman, D. Figlewicz, R. H. Brown, and M. H. Meisler. 2009. 'Deleterious variants of FIG4, a phosphoinositide phosphatase, in patients with ALS', *Am J Hum Genet*, 84: 85-8.

Choy, R. W., M. Park, P. Temkin, B. E. Herring, A. Marley, R. A. Nicoll, and M. von Zastrow. 2014. 'Retromer mediates a discrete route of local membrane delivery to dendrites', *Neuron*, 82: 55-62.

Christoforou, A., K. A. McGhee, S. W. Morris, P. A. Thomson, S. Anderson, A. McLean, H. S. Torrance, S. Le Hellard, B. S. Pickard, D. StClair, W. J. Muir, D. H. Blackwood, D. J. Porteous, and K. L. Evans. 2011. 'Convergence of linkage, association and GWAS findings for a candidate region for bipolar disorder and schizophrenia on chromosome 4p', *Mol Psychiatry*, 16: 240-2.

Chu, J., and D. Pratico. 2017. 'The retromer complex system in a transgenic mouse model of AD: influence of age', *Neurobiol Aging*, 52: 32-38.

Cirulli, E. T., B. N. Lasseigne, S. Petrovski, P. C. Sapp, P. A. Dion, C. S. Leblond, J. Couthouis, Y. F. Lu, Q. Wang, B. J. Krueger, Z. Ren, J. Keebler, Y. Han, S. E. Levy, B. E. Boone, J. R. Wimbish, L. L. Waite, A. L. Jones, J. P. Carulli, A. G. Day-Williams, J. F. Staropoli, W. W. Xin, A. Chesi, A. R. Raphael, D. McKenna-Yasek, J. Cady, J. M. Vianney de Jong, K. P. Kenna, B. N. Smith, S. Topp, J. Miller, A. Gkazi, A. Al-Chalabi, L. H. van den Berg, J. Veldink, V. Silani, N. Ticozzi, C. E. Shaw, R. H. Baloh, S. Appel, E. Simpson, C. Lagier-Tourenne, S. M. Pulst, S. Gibson, J. Q. Trojanowski, L. Elman, L. McCluskey, M. Grossman, N. A. Shneider, W. K. Chung, J. M. Ravits, J. D. Glass, K. B. Sims, V. M. Van Deerlin, T. Maniatis, S. D. Hayes, A. Ordureau, S. Swarup, J. Landers, F. Baas, A. S. Allen, R. S. Bedlack, J. W. Harper, A. D. Gitler, G. A. Rouleau, R. Brown, M. B. Harms, G. M. Cooper, T. Harris, R. M. Myers, and D. B. Goldstein. 2015. 'Exome sequencing in amyotrophic lateral sclerosis identifies risk genes and pathways', *Science*, 347: 1436-41.

Citron, M., T. Oltersdorf, C. Haass, L. McConlogue, A. Y. Hung, P. Seubert, C. Vigo-Pelfrey, I. Lieberburg, and D. J. Selkoe. 1992. 'Mutation of the beta-amyloid precursor protein in familial Alzheimer's disease increases beta-protein production', *Nature*, 360: 672-4.

Clairfeuille, T., C. Mas, A. S. Chan, Z. Yang, M. Tello-Lafoz, M. Chandra, J. Widagdo, M. C. Kerr, B. Paul, I. Merida, R. D. Teasdale, N. J. Pavlos, V. Anggono, and B. M. Collins. 2016. 'A molecular code for endosomal recycling of phosphorylated cargos by the SNX27-retromer complex', *Nat Struct Mol Biol*, 23: 921-32.

Clayton, E. L., C. Milioto, B. Muralidharan, F. E. Norona, J. R. Edgar, A. Soriano, P. Jafar-Nejad, F. Rigo, J. Collinge, and A. M. Isaacs. 2018. 'Frontotemporal dementia causative CHMP2B impairs neuronal endolysosomal traffic-rescue by TMEM106B knockdown', *Brain*, 141: 3428-42.

Clayton, E. L., S. Mizielinska, J. R. Edgar, T. T. Nielsen, S. Marshall, F. E. Norona, M. Robbins, H. Damirji, I. E. Holm, P. Johannsen, J. E. Nielsen, E. A. Asante, J. Collinge, and A. M. Isaacs. 2015. 'Frontotemporal dementia caused by CHMP2B mutation is characterised by neuronal lysosomal storage pathology', *Acta Neuropathol*, 130: 511-23.

Clement, A. M., M. D. Nguyen, E. A. Roberts, M. L. Garcia, S. Boillee, M. Rule, A. P. McMahon, W. Doucette, D. Siwek, R. J. Ferrante, R. H. Brown, Jr., J. P. Julien, L. S. Goldstein, and D. W. Cleveland. 2003. 'Wild-type nonneuronal cells extend survival of SOD1 mutant motor neurons in ALS mice', *Science*, 302: 113-7.

Cocucci, E., F. Aguet, S. Boulant, and T. Kirchhausen. 2012. 'The first five seconds in the life of a clathrin-coated pit', *Cell*, 150: 495-507.

Coelho, M. B., J. Attig, N. Bellora, J. Konig, M. Hallegger, M. Kayikci, E. Eyras, J. Ule, and C. W. Smith. 2015. 'Nuclear matrix protein Matrin3 regulates alternative splicing and forms overlapping regulatory networks with PTB', *EMBO J*, 34: 653-68.

Collins, B. M., S. J. Norwood, M. C. Kerr, D. Mahony, M. N. Seaman, R. D. Teasdale, and D. J. Owen. 2008. 'Structure of Vps26B and mapping of its interaction with the retromer protein complex', *Traffic*, 9: 366-79.

Colombrita, C., E. Onesto, E. Buratti, P. de la Grange, V. Gumina, F. E. Baralle, V. Silani, and A. Ratti. 2015. 'From transcriptomic to protein level changes in TDP-43 and FUS loss-of-function cell models', *Biochim Biophys Acta*, 1849: 1398-410.

Colombrita, C., E. Onesto, F. Megiorni, A. Pizzuti, F. E. Baralle, E. Buratti, V. Silani, and A. Ratti. 2012. 'TDP-43 and FUS RNA-binding proteins bind distinct sets of cytoplasmic messenger RNAs and differently regulate their post-transcriptional fate in motoneuron-like cells', *J Biol Chem*, 287: 15635-47.

Conte, A., S. Lattante, M. Zollino, G. Marangi, M. Luigetti, A. Del Grande, S. Servidei, F. Trombetta, and M. Sabatelli. 2012. 'P525L FUS mutation is consistently associated with a severe form of juvenile amyotrophic lateral sclerosis', *Neuromuscul Disord*, 22: 73-5.

Corona, J. C., and R. Tapia. 2007. 'Ca2+-permeable AMPA receptors and intracellular Ca2+ determine motoneuron vulnerability in rat spinal cord in vivo', *Neuropharmacology*, 52: 1219-28.

Costa, J., M. Swash, and M. de Carvalho. 2012. 'Awaji criteria for the diagnosis of amyotrophic lateral sclerosis:a systematic review', *Arch Neurol*, 69: 1410-6.

Coutinho, M. F., M. J. Prata, and S. Alves. 2012. 'A shortcut to the lysosome: the mannose-6-phosphate-independent pathway', *Mol Genet Metab*, 107: 257-66.

Cox, L. E., L. Ferraiuolo, E. F. Goodall, P. R. Heath, A. Higginbottom, H. Mortiboys, H. C. Hollinger, J. A. Hartley, A. Brockington, C. E. Burness, K. E. Morrison, S. B. Wharton, A. J. Grierson, P. G. Ince, J. Kirby, and P. J. Shaw. 2010. 'Mutations in CHMP2B in lower motor neuron predominant amyotrophic lateral sclerosis (ALS)', *PLoS One*, 5: e9872.

Cremona, O., G. Di Paolo, M. R. Wenk, A. Luthi, W. T. Kim, K. Takei, L. Daniell, Y. Nemoto, S. B. Shears, R. A. Flavell, D. A. McCormick, and P. De Camilli. 1999. 'Essential role of phosphoinositide metabolism in synaptic vesicle recycling', *Cell*, 99: 179-88.

Cui, Y., J. M. Carosi, Z. Yang, N. Ariotti, M. C. Kerr, R. G. Parton, T. J. Sargeant, and R. D. Teasdale. 2019. 'Retromer has a selective function in cargo sorting via endosome transport carriers', *J Cell Biol*, 218: 615-31.

Cullen, P. J., and F. Steinberg. 2018. 'To degrade or not to degrade: mechanisms and significance of endocytic recycling', *Nat Rev Mol Cell Biol*, 19: 679-96.

Cullen, V., M. Lindfors, J. Ng, A. Paetau, E. Swinton, P. Kolodziej, H. Boston, P. Saftig, J. Woulfe, M. B. Feany, L. Myllykangas, M. G. Schlossmacher, and J. Tyynela. 2009. 'Cathepsin D expression level affects alpha-synuclein processing, aggregation, and toxicity in vivo', *Mol Brain*, 2: 5.

Dafinca, R., J. Scaber, N. Ababneh, T. Lalic, G. Weir, H. Christian, J. Vowles, A. G. Douglas, A. Fletcher-Jones, C. Browne, M. Nakanishi, M. R. Turner, R. Wade-Martins, S. A. Cowley, and K. Talbot. 2016. 'C9orf72 Hexanucleotide Expansions Are Associated with Altered Endoplasmic Reticulum Calcium Homeostasis and Stress Granule Formation in Induced Pluripotent Stem Cell-Derived Neurons from Patients with Amyotrophic Lateral Sclerosis and Frontotemporal Dementia', *STEM CELLS*, 34: 2063-78.

Dal Canto, M. C., and M. E. Gurney. 1995. 'Neuropathological changes in two lines of mice carrying a transgene for mutant human Cu,Zn SOD, and in mice overexpressing wild type human SOD: a model of familial amyotrophic lateral sclerosis (FALS)', *Brain Res*, 676: 25-40.

Damiano, M., A. A. Starkov, S. Petri, K. Kipiani, M. Kiaei, M. Mattiazzi, M. Flint Beal, and G. Manfredi. 2006. 'Neural mitochondrial Ca2+ capacity impairment precedes the onset of motor symptoms in G93A Cu/Zn-superoxide dismutase mutant mice', *J Neurochem*, 96: 1349-61.

de Carvalho, M., R. Dengler, A. Eisen, J. D. England, R. Kaji, J. Kimura, K. Mills, H. Mitsumoto, H. Nodera, J. Shefner, and M. Swash. 2008. 'Electrodiagnostic criteria for diagnosis of ALS', *Clin Neurophysiol*, 119: 497-503.

De Groot, C. J., C. H. Langeveld, C. A. Jongenelen, L. Montagne, P. Van Der Valk, and C. D. Dijkstra. 1997. 'Establishment of human adult astrocyte cultures derived from postmortem multiple sclerosis and control brain and spinal cord regions: immunophenotypical and functional characterization', *J Neurosci Res*, 49: 342-54.

De Luca, M., L. Cogli, C. Progida, V. Nisi, R. Pascolutti, S. Sigismund, P. P. Di Fiore, and C. Bucci. 2014. 'RILP regulates vacuolar ATPase through interaction with the V1G1 subunit', *J Cell Sci*, 127: 2697-708.

de Renzis, S., B. Sonnichsen, and M. Zerial. 2002. 'Divalent Rab effectors regulate the sub-compartmental organization and sorting of early endosomes', *Nat Cell Biol*, 4: 124-33.

De Santis, R., L. Santini, A. Colantoni, G. Peruzzi, V. de Turris, V. Alfano, I. Bozzoni, and A. Rosa. 2017. 'FUS Mutant Human Motoneurons Display Altered Transcriptome and microRNA Pathways with Implications for ALS Pathogenesis', *Stem Cell Reports*, 9: 1450-62.

de Souza, P. V. S., W. B. V. de Rezende Pinto, G. N. de Rezende Batistella, T. Bortholin, and A. S. B. Oliveira. 2017. 'Hereditary Spastic Paraplegia: Clinical and Genetic Hallmarks', *Cerebellum*, 16: 525-51.

De Strooper, B. 2010. 'Proteases and proteolysis in Alzheimer disease: a multifactorial view on the disease process', *Physiol Rev*, 90: 465-94.

DeJesus-Hernandez, M., I. R. Mackenzie, B. F. Boeve, A. L. Boxer, M. Baker, N. J. Rutherford, A. M. Nicholson, N. A. Finch, H. Flynn, J. Adamson, N. Kouri, A. Wojtas, P. Sengdy, G.

Y. Hsiung, A. Karydas, W. W. Seeley, K. A. Josephs, G. Coppola, D. H. Geschwind, Z. K. Wszolek, H. Feldman, D. S. Knopman, R. C. Petersen, B. L. Miller, D. W. Dickson, K. B. Boylan, N. R. Graff-Radford, and R. Rademakers. 2011. 'Expanded GGGGCC hexanucleotide repeat in noncoding region of C9ORF72 causes chromosome 9p-linked FTD and ALS', *Neuron*, 72: 245-56.

Deng, H. X., W. Chen, S. T. Hong, K. M. Boycott, G. H. Gorrie, N. Siddique, Y. Yang, F. Fecto, Y. Shi, H. Zhai, H. Jiang, M. Hirano, E. Rampersaud, G. H. Jansen, S. Donkervoort, E. H. Bigio, B. R. Brooks, K. Ajroud, R. L. Sufit, J. L. Haines, E. Mugnaini, M. A. Pericak-Vance, and T. Siddique. 2011. 'Mutations in UBQLN2 cause dominant X-linked juvenile and adult-onset ALS and ALS/dementia', *Nature*, 477: 211-5.

Deng, H. X., H. Zhai, E. H. Bigio, J. Yan, F. Fecto, K. Ajroud, M. Mishra, S. Ajroud-Driss, S. Heller, R. Sufit, N. Siddique, E. Mugnaini, and T. Siddique. 2010. 'FUS-immunoreactive inclusions are a common feature in sporadic and non-SOD1 familial amyotrophic lateral sclerosis', *Ann Neurol*, 67: 739-48.

Deng, J., M. Yang, Y. Chen, X. Chen, J. Liu, S. Sun, H. Cheng, Y. Li, E. H. Bigio, M. Mesulam, Q. Xu, S. Du, K. Fushimi, L. Zhu, and J. Y. Wu. 2015. 'FUS Interacts with HSP60 to Promote Mitochondrial Damage', *PLoS Genet*, 11: e1005357.

Dennis, J. S., and B. A. Citron. 2009. 'Wobbler mice modeling motor neuron disease display elevated transactive response DNA binding protein', *Neuroscience*, 158: 745-50.

Derivery, E., E. Helfer, V. Henriot, and A. Gautreau. 2012. 'Actin polymerization controls the organization of WASH domains at the surface of endosomes', *PLoS One*, 7: e39774.

Derivery, E., C. Sousa, J. J. Gautier, B. Lombard, D. Loew, and A. Gautreau. 2009. 'The Arp2/3 activator WASH controls the fission of endosomes through a large multiprotein complex', *Dev Cell*, 17: 712-23.

Dermentzaki, G., K. A. Politi, L. Lu, V. Mishra, E. J. Perez-Torres, A. A. Sosunov, G. M. McKhann, 2nd, F. Lotti, N. A. Shneider, and S. Przedborski. 2019. 'Deletion of Ripk3 Prevents Motor Neuron Death In Vitro but not In Vivo', *eNeuro*, 6.

Devereaux, K. 2014. 'The role of phosphatidylinositol 3-kinases in autophagy regulation', Columbia University.

Devon, R. S., P. C. Orban, K. Gerrow, M. A. Barbieri, C. Schwab, L. P. Cao, J. R. Helm, N. Bissada, R. Cruz-Aguado, T. L. Davidson, J. Witmer, M. Metzler, C. K. Lam, W. Tetzlaff, E. M. Simpson, J. M. McCaffery, A. E. El-Husseini, B. R. Leavitt, and M. R. Hayden. 2006. 'Als2-deficient mice exhibit disturbances in endosome trafficking associated with motor behavioral abnormalities', *Proc Natl Acad Sci U S A*, 103: 9595-600.

Dhungel, N., S. Eleuteri, L. B. Li, N. J. Kramer, J. W. Chartron, B. Spencer, K. Kosberg, J. A. Fields, K. Stafa, A. Adame, H. Lashuel, J. Frydman, K. Shen, E. Masliah, and A. D. Gitler. 2015. 'Parkinson's disease genes VPS35 and EIF4G1 interact genetically and converge on alpha-synuclein', *Neuron*, 85: 76-87.

Di Giorgio, F. P., G. L. Boulting, S. Bobrowicz, and K. C. Eggan. 2008. 'Human embryonic stem cell-derived motor neurons are sensitive to the toxic effect of glial cells carrying an ALS-causing mutation', *Cell Stem Cell*, 3: 637-48.

Di Giorgio, F. P., M. A. Carrasco, M. C. Siao, T. Maniatis, and K. Eggan. 2007. 'Non-cell autonomous effect of glia on motor neurons in an embryonic stem cell-based ALS model', *Nat Neurosci*, 10: 608-14.

Di Paolo, G., and P. De Camilli. 2006. 'Phosphoinositides in cell regulation and membrane dynamics', *Nature*, 443: 651-7.

Dibaj, P., E. D. Schomburg, and H. Steffens. 2015. 'Contractile characteristics of gastrocnemius-soleus muscle in the SOD1G93A ALS mouse model', *Neurol Res*, 37: 693-702.

Dodson, S. E., O. M. Andersen, V. Karmali, J. J. Fritz, D. Cheng, J. Peng, A. I. Levey, T. E. Willnow, and J. J. Lah. 2008. 'Loss of LR11/SORLA enhances early pathology in a mouse model of amyloidosis: evidence for a proximal role in Alzheimer's disease', *J Neurosci*, 28: 12877-86.

Donnelly, C. J., P. W. Zhang, J. T. Pham, A. R. Haeusler, N. A. Mistry, S. Vidensky, E. L. Daley, E. M. Poth, B. Hoover, D. M. Fines, N. Maragakis, P. J. Tienari, L. Petrucelli, B. J. Traynor, J. Wang, F. Rigo, C. F. Bennett, S. Blackshaw, R. Sattler, and J. D. Rothstein. 2013. 'RNA toxicity from the ALS/FTD C9ORF72 expansion is mitigated by antisense intervention', *Neuron*, 80: 415-28.

Doray, B., P. Ghosh, J. Griffith, H. J. Geuze, and S. Kornfeld. 2002. 'Cooperation of GGAs and AP-1 in packaging MPRs at the trans-Golgi network', *Science*, 297: 1700-3.

Dormann, D., R. Rodde, D. Edbauer, E. Bentmann, I. Fischer, A. Hruscha, M. E. Than, I. R. Mackenzie, A. Capell, B. Schmid, M. Neumann, and C. Haass. 2010. 'ALS-associated fused in sarcoma (FUS) mutations disrupt Transportin-mediated nuclear import', *EMBO J*, 29: 2841-57.

Dreyfuss, G., M. J. Matunis, S. Pinol-Roma, and C. G. Burd. 1993. 'hnRNP proteins and the biogenesis of mRNA', *Annu Rev Biochem*, 62: 289-321.

Duchen, L. W., and S. J. Strich. 1968. 'An hereditary motor neurone disease with progressive denervation of muscle in the mouse: the mutant 'wobbler'', *J Neurol Neurosurg Psychiatry*, 31: 535-42.

Dybwik, K., T. Tollali, E. W. Nielsen, and B. S. Brinchmann. 2010. 'Why does the provision of home mechanical ventilation vary so widely?', *Chron Respir Dis*, 7: 67-73.

Ebner, P., I. Poetsch, L. Deszcz, T. Hoffmann, J. Zuber, and F. Ikeda. 2018. 'The IAP family member BRUCE regulates autophagosome-lysosome fusion', *Nat Commun*, 9: 599.

Ehrlich, M., W. Boll, A. Van Oijen, R. Hariharan, K. Chandran, M. L. Nibert, and T. Kirchhausen. 2004. 'Endocytosis by random initiation and stabilization of clathrin-coated pits', *Cell*, 118: 591-605.

Ekblom, J., S. S. Jossan, L. Oreland, E. Walum, and S. M. Aquilonius. 1994. 'Reactive gliosis and monoamine oxidase B', *J Neural Transm Suppl*, 41: 253-8.

El-Brolosy, M. A., and D. Y. R. Stainier. 2017. 'Genetic compensation: A phenomenon in search of mechanisms', *PLoS Genet*, 13: e1006780.

Elden, A. C., H. J. Kim, M. P. Hart, A. S. Chen-Plotkin, B. S. Johnson, X. Fang, M. Armakola, F. Geser, R. Greene, M. M. Lu, A. Padmanabhan, D. Clay-Falcone, L. McCluskey, L. Elman, D. Juhr, P. J. Gruber, U. Rub, G. Auburger, J. Q. Trojanowski, V. M. Lee, V. M. Van Deerlin, N. M. Bonini, and A. D. Gitler. 2010. 'Ataxin-2 intermediate-length polyglutamine expansions are associated with increased risk for ALS', *Nature*, 466: 1069-75.

Eleuteri, S., and A. Albanese. 2019. 'VPS35-Based Approach: A Potential Innovative Treatment in Parkinson's Disease', *Front Neurol*, 10: 1272.

Engl, E., and D. Attwell. 2015. 'Non-signalling energy use in the brain', *J Physiol*, 593: 3417-29.

Erdmann, K. S., Y. Mao, H. J. McCrea, R. Zoncu, S. Lee, S. Paradise, J. Modregger, D. Biemesderfer, D. Toomre, and P. De Camilli. 2007. 'A role of the Lowe syndrome protein OCRL in early steps of the endocytic pathway', *Dev Cell*, 13: 377-90.

Falconer, DS. 1956. 'Wobbler (wr)', *Mouse News Lett*, 15: 23.

Farg, M. A., K. Y. Soo, A. K. Walker, H. Pham, J. Orian, M. K. Horne, S. T. Warraich, K. L. Williams, I. P. Blair, and J. D. Atkin. 2012. 'Mutant FUS induces endoplasmic reticulum stress in amyotrophic lateral sclerosis and interacts with protein disulfide-isomerase', *Neurobiol Aging*, 33: 2855-68.

Farg, M. A., V. Sundaramoorthy, J. M. Sultana, S. Yang, R. A. Atkinson, V. Levina, M. A. Halloran, P. A. Gleeson, I. P. Blair, K. Y. Soo, A. E. King, and J. D. Atkin. 2014. 'C9ORF72, implicated in amytrophic lateral sclerosis and frontotemporal dementia, regulates endosomal trafficking', *Hum Mol Genet*, 23: 3579-95.

Fecto, F., J. Yan, S. P. Vemula, E. Liu, Y. Yang, W. Chen, J. G. Zheng, Y. Shi, N. Siddique, H. Arrat, S. Donkervoort, S. Ajroud-Driss, R. L. Sufit, S. L. Heller, H. X. Deng, and T. Siddique. 2011. 'SQSTM1 mutations in familial and sporadic amyotrophic lateral sclerosis', *Arch Neurol*, 68: 1440-6.

Feiler, M. S., B. Strobel, A. Freischmidt, A. M. Helferich, J. Kappel, B. M. Brewer, D. Li, D. R. Thal, P. Walther, A. C. Ludolph, K. M. Danzer, and J. H. Weishaupt. 2015. 'TDP-43 is intercellularly transmitted across axon terminals', *J Cell Biol*, 211: 897-911.

Ferrari, R., D. Kapogiannis, E. D. Huey, and P. Momeni. 2011. 'FTD and ALS: a tale of two diseases', *Curr Alzheimer Res*, 8: 273-94.

Ferri, A., M. Cozzolino, C. Crosio, M. Nencini, A. Casciati, E. B. Gralla, G. Rotilio, J. S. Valentine, and M. T. Carri. 2006. 'Familial ALS-superoxide dismutases associate with mitochondria and shift their redox potentials', *Proc Natl Acad Sci U S A*, 103: 13860-5.

Ferri, A., P. Fiorenzo, M. Nencini, M. Cozzolino, M. G. Pesaresi, C. Valle, S. Sepe, S. Moreno, and M. T. Carri. 2010. 'Glutaredoxin 2 prevents aggregation of mutant SOD1 in mitochondria and abolishes its toxicity', *Hum Mol Genet*, 19: 4529-42.

Fjorback, A. W., M. Seaman, C. Gustafsen, A. Mehmedbasic, S. Gokool, C. Wu, D. Militz, V. Schmidt, P. Madsen, J. R. Nyengaard, T. E. Willnow, E. I. Christensen, W. B. Mobley, A. Nykjaer, and O. M. Andersen. 2012. 'Retromer binds the FANSHY sorting motif in SorLA to regulate amyloid precursor protein sorting and processing', *J Neurosci*, 32: 1467-80.

Follett, J., S. J. Norwood, N. A. Hamilton, M. Mohan, O. Kovtun, S. Tay, Y. Zhe, S. A. Wood, G. D. Mellick, P. A. Silburn, B. M. Collins, A. Bugarcic, and R. D. Teasdale. 2014. 'The Vps35 D620N mutation linked to Parkinson's disease disrupts the cargo sorting function of retromer', *Traffic*, 15: 230-44.

Foran, E., and D. Trotti. 2009. 'Glutamate transporters and the excitotoxic path to motor neuron degeneration in amyotrophic lateral sclerosis', *Antioxid Redox Signal*, 11: 1587-602.

Forch, P., O. Puig, N. Kedersha, C. Martinez, S. Granneman, B. Seraphin, P. Anderson, and J. Valcarcel. 2000. 'The apoptosis-promoting factor TIA-1 is a regulator of alternative pre-mRNA splicing', *Mol Cell*, 6: 1089-98.

Forrest, S. L., J. J. Kril, and G. M. Halliday. 2019. 'Cellular and regional vulnerability in frontotemporal tauopathies', *Acta Neuropathol*, 138: 705-27.

Forsaa, E. B., J. P. Larsen, T. Wentzel-Larsen, and G. Alves. 2010. 'What predicts mortality in Parkinson disease?: a prospective population-based long-term study', *Neurology*, 75: 1270-6.

Forsberg, K., P. A. Jonsson, P. M. Andersen, D. Bergemalm, K. S. Graffmo, M. Hultdin, J. Jacobsson, R. Rosquist, S. L. Marklund, and T. Brannstrom. 2010. 'Novel antibodies reveal inclusions containing non-native SOD1 in sporadic ALS patients', *PLoS One*, 5: e11552.

Freeman, C., M. N. Seaman, and E. Reid. 2013. 'The hereditary spastic paraplegia protein strumpellin: characterisation in neurons and of the effect of disease mutations on WASH complex assembly and function', *Biochim Biophys Acta*, 1832: 160-73.

Frost, B., and M. I. Diamond. 2010. 'Prion-like mechanisms in neurodegenerative diseases', *Nat Rev Neurosci*, 11: 155-9.

Fumagalli, E., M. Funicello, T. Rauen, M. Gobbi, and T. Mennini. 2008. 'Riluzole enhances the activity of glutamate transporters GLAST, GLT1 and EAAC1', *Eur J Pharmacol*, 578: 171-6.

Funikov, S. Y., A. P. Rezvykh, P. V. Mazin, A. V. Morozov, A. V. Maltsev, M. M. Chicheva, E. A. Vikhareva, M. B. Evgen'ev, and A. A. Ustyugov. 2018. 'FUS(1-359) transgenic mice as a model of ALS: pathophysiological and molecular aspects of the proteinopathy', *Neurogenetics*, 19: 189-204.

Fuse, A., N. Furuya, S. Kakuta, A. Inose, M. Sato, M. Koike, S. Saiki, and N. Hattori. 2015. 'VPS29-VPS35 intermediate of retromer is stable and may be involved in the retromer complex assembly process', *FEBS Lett*, 589: 1430-6.

Gallon, M., T. Clairfeuille, F. Steinberg, C. Mas, R. Ghai, R. B. Sessions, R. D. Teasdale, B. M. Collins, and P. J. Cullen. 2014. 'A unique PDZ domain and arrestin-like fold interaction reveals mechanistic details of endocytic recycling by SNX27-retromer', *Proc Natl Acad Sci U S A*, 111: E3604-13.

Garrus, J. E., U. K. von Schwedler, O. W. Pornillos, S. G. Morham, K. H. Zavitz, H. E. Wang, D. A. Wettstein, K. M. Stray, M. Cote, R. L. Rich, D. G. Myszka, and W. I. Sundquist. 2001. 'Tsg101 and the vacuolar protein sorting pathway are essential for HIV-1 budding', *Cell*, 107: 55-65.

Gary, J. D., A. E. Wurmser, C. J. Bonangelino, L. S. Weisman, and S. D. Emr. 1998. 'Fab1p is essential for PtdIns(3)P 5-kinase activity and the maintenance of vacuolar size and membrane homeostasis', *J Cell Biol*, 143: 65-79.

Gaullier, J. M., A. Simonsen, A. D'Arrigo, B. Bremnes, H. Stenmark, and R. Aasland. 1998. 'FYVE fingers bind PtdIns(3)P', *Nature*, 394: 432-3.

Ge, L., D. Melville, M. Zhang, and R. Schekman. 2013. 'The ER-Golgi intermediate compartment is a key membrane source for the LC3 lipidation step of autophagosome biogenesis', *Elife*, 2: e00947.

Gendron, T. F., K. F. Bieniek, Y. J. Zhang, K. Jansen-West, P. E. Ash, T. Caulfield, L. Daughrity, J. H. Dunmore, M. Castanedes-Casey, J. Chew, D. M. Cosio, M. van Blitterswijk, W. C. Lee, R. Rademakers, K. B. Boylan, D. W. Dickson, and L. Petrucelli. 2013. 'Antisense transcripts of the expanded C9ORF72 hexanucleotide repeat form nuclear RNA foci and undergo repeat-associated non-ATG translation in c9FTD/ALS', *Acta Neuropathol*, 126: 829-44.

Gendron, T. F., and L. Petrucelli. 2009. 'The role of tau in neurodegeneration', *Mol Neurodegener*, 4: 13.

Genin, E. C., M. Plutino, S. Bannwarth, E. Villa, E. Cisneros-Barroso, M. Roy, B. Ortega-Vila, K. Fragaki, F. Lespinasse, E. Pinero-Martos, G. Auge, D. Moore, F. Burte, S. Lacas-Gervais, Y. Kageyama, K. Itoh, P. Yu-Wai-Man, H. Sesaki, J. E. Ricci, C. Vives-Bauza, and V. Paquis-Flucklinger. 2016. 'CHCHD10 mutations promote loss of mitochondrial cristae junctions with impaired mitochondrial genome maintenance and inhibition of apoptosis', *EMBO Mol Med*, 8: 58-72.

Gertz, B., M. Wong, and L. J. Martin. 2012. 'Nuclear localization of human SOD1 and mutant SOD1-specific disruption of survival motor neuron protein complex in transgenic amyotrophic lateral sclerosis mice', *J Neuropathol Exp Neurol*, 71: 162-77.

Geser, F., V. M. Lee, and J. Q. Trojanowski. 2010. 'Amyotrophic lateral sclerosis and frontotemporal lobar degeneration: a spectrum of TDP-43 proteinopathies', *Neuropathology*, 30: 103-12.

Ghai, R., A. Bugarcic, H. Liu, S. J. Norwood, S. Skeldal, E. J. Coulson, S. S. Li, R. D. Teasdale, and B. M. Collins. 2013. 'Structural basis for endosomal trafficking of diverse transmembrane cargos by PX-FERM proteins', *Proc Natl Acad Sci U S A*, 110: E643-52.

Ghai, R., M. Mobli, S. J. Norwood, A. Bugarcic, R. D. Teasdale, G. F. King, and B. M. Collins. 2011. 'Phox homology band 4.1/ezrin/radixin/moesin-like proteins function as molecular scaffolds that interact with cargo receptors and Ras GTPases', *Proc Natl Acad Sci U S A*, 108: 7763-8.

Ghai, R., M. Tello-Lafoz, S. J. Norwood, Z. Yang, T. Clairfeuille, R. D. Teasdale, I. Merida, and B. M. Collins. 2014. 'Phosphoinositide binding by the SNX27 FERM domain regulates its localization at the immune synapse of activated T-cells', *Journal of Cell Science*, 128: 553-65.

Ghai, R., M. Tello-Lafoz, S. J. Norwood, Z. Yang, T. Clairfeuille, R. D. Teasdale, I. Merida, and B. M. Collins. 2015. 'Phosphoinositide binding by the SNX27 FERM domain regulates its localization at the immune synapse of activated T-cells', *J Cell Sci*, 128: 553-65.

Ghazi-Tabatabai, S., S. Saksena, J. M. Short, A. V. Pobbati, D. B. Veprintsev, R. A. Crowther, S. D. Emr, E. H. Egelman, and R. L. Williams. 2008. 'Structure and disassembly of filaments formed by the ESCRT-III subunit Vps24', *Structure*, 16: 1345-56.

Ghosh, R. N., W. G. Mallet, T. T. Soe, T. E. McGraw, and F. R. Maxfield. 1998. 'An endocytosed TGN38 chimeric protein is delivered to the TGN after trafficking through the endocytic recycling compartment in CHO cells', *J Cell Biol*, 142: 923-36.

Gijselinck, I., S. Van Mossevelde, J. van der Zee, A. Sieben, S. Philtjens, B. Heeman, S. Engelborghs, M. Vandenbulcke, G. De Baets, V. Baumer, I. Cuijt, M. Van den Broeck, K. Peeters, M. Mattheijssens, F. Rousseau, R. Vandenberghe, P. De Jonghe, P. Cras, P. P. De Deyn, J. J. Martin, M. Cruts, and C. Van Broeckhoven. 2015. 'Loss of TBK1 is a frequent cause of frontotemporal dementia in a Belgian cohort', *Neurology*, 85: 2116-25.

Gomez, T. S., and D. D. Billadeau. 2009. 'A FAM21-containing WASH complex regulates retromer-dependent sorting', *Dev Cell*, 17: 699-711.

Gomez, T. S., J. A. Gorman, A. A. de Narvajas, A. O. Koenig, and D. D. Billadeau. 2012. 'Trafficking defects in WASH-knockout fibroblasts originate from collapsed endosomal and lysosomal networks', *Mol Biol Cell*, 23: 3215-28.

Gonatas, N. K., J. O. Gonatas, and A. Stieber. 1998. 'The involvement of the Golgi apparatus in the pathogenesis of amyotrophic lateral sclerosis, Alzheimer's disease, and ricin intoxication', *Histochem Cell Biol*, 109: 591-600.

Gonatas, N. K., A. Stieber, and J. O. Gonatas. 2006. 'Fragmentation of the Golgi apparatus in neurodegenerative diseases and cell death', *J Neurol Sci*, 246: 21-30.

Gonzalez-Fernandez, C., P. Gonzalez, P. Andres-Benito, I. Ferrer, and F. J. Rodriguez. 2019. 'Wnt Signaling Alterations in the Human Spinal Cord of Amyotrophic Lateral Sclerosis Cases: Spotlight on Fz2 and Wnt5a', *Mol Neurobiol*, 56: 6777-91.

Gonzalez-Fernandez, C., R. Mancuso, J. Del Valle, X. Navarro, and F. J. Rodriguez. 2016. 'Wnt Signaling Alteration in the Spinal Cord of Amyotrophic Lateral Sclerosis Transgenic Mice: Special Focus on Frizzled-5 Cellular Expression Pattern', *PLoS One*, 11: e0155867.

Goody, R. S., M. P. Muller, and Y. W. Wu. 2017. 'Mechanisms of action of Rab proteins, key regulators of intracellular vesicular transport', *Biol Chem*, 398: 565-75.

Gordon, P. H., B. Cheng, I. B. Katz, M. Pinto, A. P. Hays, H. Mitsumoto, and L. P. Rowland. 2006. 'The natural history of primary lateral sclerosis', *Neurology*, 66: 647-53.

Grad, L. I., E. Pokrishevsky, J. M. Silverman, and N. R. Cashman. 2014. 'Exosome-dependent and independent mechanisms are involved in prion-like transmission of propagated Cu/Zn superoxide dismutase misfolding', *Prion*, 8: 331-5.

Graef, M., J. R. Friedman, C. Graham, M. Babu, and J. Nunnari. 2013. 'ER exit sites are physical and functional core autophagosome biogenesis components', *Mol Biol Cell*, 24: 2918-31.

Greenway, M. J., P. M. Andersen, C. Russ, S. Ennis, S. Cashman, C. Donaghy, V. Patterson, R. Swingler, D. Kieran, J. Prehn, K. E. Morrison, A. Green, K. R. Acharya, R. H. Brown, Jr., and O. Hardiman. 2006. 'ANG mutations segregate with familial and 'sporadic' amyotrophic lateral sclerosis', *Nat Genet*, 38: 411-3.

Guerreiro, R., J. Bras, and J. Hardy. 2015. 'SnapShot: Genetics of ALS and FTD', *Cell*, 160: 798-98.e1.

Guerreiro, R., A. Wojtas, J. Bras, M. Carrasquillo, E. Rogaeva, E. Majounie, C. Cruchaga, C. Sassi, J. S. Kauwe, S. Younkin, L. Hazrati, J. Collinge, J. Pocock, T. Lashley, J. Williams, J. C. Lambert, P. Amouyel, A. Goate, R. Rademakers, K. Morgan, J. Powell, P. St George-Hyslop, A. Singleton, and J. Hardy. 2013. 'TREM2 variants in Alzheimer's disease', *N Engl J Med*, 368: 117-27.

Guo, H., L. Lai, M. E. Butchbach, M. P. Stockinger, X. Shan, G. A. Bishop, and C. L. Lin. 2003. 'Increased expression of the glial glutamate transporter EAAT2 modulates excitotoxicity and delays the onset but not the outcome of ALS in mice', *Hum Mol Genet*, 12: 2519-32.

Gurney, M. E., F. B. Cutting, P. Zhai, A. Doble, C. P. Taylor, P. K. Andrus, and E. D. Hall. 1996. 'Benefit of vitamin E, riluzole, and gabapentin in a transgenic model of familial amyotrophic lateral sclerosis', *Ann Neurol*, 39: 147-57.

Gurney, M. E., H. Pu, A. Y. Chiu, M. C. Dal Canto, C. Y. Polchow, D. D. Alexander, J. Caliendo, A. Hentati, Y. W. Kwon, H. X. Deng, and et al. 1994. 'Motor neuron degeneration in mice that express a human Cu,Zn superoxide dismutase mutation', *Science*, 264: 1772-5.

Gustavsson, E. K., I. Guella, J. Trinh, C. Szu-Tu, A. Rajput, A. H. Rajput, J. C. Steele, M. McKeown, B. S. Jeon, J. O. Aasly, and M. J. Farrer. 2015. 'Genetic variability of the retromer cargo recognition complex in parkinsonism', *Mov Disord*, 30: 580-4.

Haas, A. K., E. Fuchs, R. Kopajtich, and F. A. Barr. 2005. 'A GTPase-activating protein controls Rab5 function in endocytic trafficking', *Nat Cell Biol*, 7: 887-93.

Hadano, S., S. C. Benn, S. Kakuta, A. Otomo, K. Sudo, R. Kunita, K. Suzuki-Utsunomiya, H. Mizumura, J. M. Shefner, G. A. Cox, Y. Iwakura, R. H. Brown, Jr., and J. E. Ikeda. 2006. 'Mice deficient in the Rab5 guanine nucleotide exchange factor ALS2/alsin exhibit age-dependent neurological deficits and altered endosome trafficking', *Hum Mol Genet*, 15: 233-50.

Hadano, S., C. K. Hand, H. Osuga, Y. Yanagisawa, A. Otomo, R. S. Devon, N. Miyamoto, J. Showguchi-Miyata, Y. Okada, R. Singaraja, D. A. Figlewicz, T. Kwiatkowski, B. A. Hosler, T. Sagie, J. Skaug, J. Nasir, R. H. Brown, Jr., S. W. Scherer, G. A. Rouleau, M. R.

Hayden, and J. E. Ikeda. 2001. 'A gene encoding a putative GTPase regulator is mutated in familial amyotrophic lateral sclerosis 2', *Nat Genet*, 29: 166-73.

Haft, C. R., M. de la Luz Sierra, R. Bafford, M. A. Lesniak, V. A. Barr, and S. I. Taylor. 2000. 'Human orthologs of yeast vacuolar protein sorting proteins Vps26, 29, and 35: assembly into multimeric complexes', *Mol Biol Cell*, 11: 4105-16.

Haidet-Phillips, A. M., M. E. Hester, C. J. Miranda, K. Meyer, L. Braun, A. Frakes, S. Song, S. Likhite, M. J. Murtha, K. D. Foust, M. Rao, A. Eagle, A. Kammesheidt, A. Christensen, J. R. Mendell, A. H. Burghes, and B. K. Kaspar. 2011. 'Astrocytes from familial and sporadic ALS patients are toxic to motor neurons', *Nat Biotechnol*, 29: 824-8.

Hailey, D. W., A. S. Rambold, P. Satpute-Krishnan, K. Mitra, R. Sougrat, P. K. Kim, and J. Lippincott-Schwartz. 2010. 'Mitochondria supply membranes for autophagosome biogenesis during starvation', *Cell*, 141: 656-67.

Halpern, M., K. J. Brennand, and J. Gregory. 2019. 'Examining the relationship between astrocyte dysfunction and neurodegeneration in ALS using hiPSCs', *Neurobiol Dis*, 132: 104562.

Hand, C. K., J. Khoris, F. Salachas, F. Gros-Louis, A. A. Lopes, V. Mayeux-Portas, C. G. Brewer, R. H. Brown, Jr., V. Meininger, W. Camu, and G. A. Rouleau. 2002. 'A novel locus for familial amyotrophic lateral sclerosis, on chromosome 18q', *Am J Hum Genet*, 70: 251-6.

Harbour, M. E., S. Y. Breusegem, and M. N. Seaman. 2012. 'Recruitment of the endosomal WASH complex is mediated by the extended 'tail' of Fam21 binding to the retromer protein Vps35', *Biochem J*, 442: 209-20.

Harding, A. E. 1983. 'Classification of the hereditary ataxias and paraplegias', *Lancet*, 1: 1151-5.

Harkany, T., I. Abraham, C. Konya, C. Nyakas, M. Zarandi, B. Penke, and P. G. Luiten. 2000. 'Mechanisms of beta-amyloid neurotoxicity: perspectives of pharmacotherapy', *Rev Neurosci*, 11: 329-82.

Harrison, A. F., and J. Shorter. 2017. 'RNA-binding proteins with prion-like domains in health and disease', *Biochem J*, 474: 1417-38.

Harrison, M. S., C. S. Hung, T. T. Liu, R. Christiano, T. C. Walther, and C. G. Burd. 2014. 'A mechanism for retromer endosomal coat complex assembly with cargo', *Proc Natl Acad Sci U S A*, 111: 267-72.

Harterink, M., F. Port, M. J. Lorenowicz, I. J. McGough, M. Silhankova, M. C. Betist, J. R. T. van Weering, Rghp van Heesbeen, T. C. Middelkoop, K. Basler, P. J. Cullen, and H. C. Korswagen. 2011. 'A SNX3-dependent retromer pathway mediates retrograde transport of the Wnt sorting receptor Wntless and is required for Wnt secretion', *Nat Cell Biol*, 13: 914-23.

Hasegawa, M., T. Arai, H. Akiyama, T. Nonaka, H. Mori, T. Hashimoto, M. Yamazaki, and K. Oyanagi. 2007. 'TDP-43 is deposited in the Guam parkinsonism-dementia complex brains', *Brain*, 130: 1386-94.

Hawrot, J., S. Imhof, and B. J. Wainger. 2020. 'Modeling cell-autonomous motor neuron phenotypes in ALS using iPSCs', *Neurobiol Dis*, 134: 104680.

Hayward, L. J., J. A. Rodriguez, J. W. Kim, A. Tiwari, J. J. Goto, D. E. Cabelli, J. S. Valentine, and R. H. Brown, Jr. 2002. 'Decreased metallation and activity in subsets of mutant superoxide dismutases associated with familial amyotrophic lateral sclerosis', *J Biol Chem*, 277: 15923-31.

He, C. W., C. P. Liao, and C. L. Pan. 2018. 'Wnt signalling in the development of axon, dendrites and synapses', *Open Biol*, 8.

He, X., F. Li, W. P. Chang, and J. Tang. 2005. 'GGA proteins mediate the recycling pathway of memapsin 2 (BACE)', *J Biol Chem*, 280: 11696-703.

Heiman-Patterson, T. D., J. S. Deitch, E. P. Blankenhorn, K. L. Erwin, M. J. Perreault, B. K. Alexander, N. Byers, I. Toman, and G. M. Alexander. 2005. 'Background and gender effects on survival in the TgN(SOD1-G93A)1Gur mouse model of ALS', *J Neurol Sci*, 236: 1-7.

Henne, W. M., E. Boucrot, M. Meinecke, E. Evergren, Y. Vallis, R. Mittal, and H. T. McMahon. 2010. 'FCHo proteins are nucleators of clathrin-mediated endocytosis', *Science*, 328: 1281-4.

Henry, A. G., J. N. Hislop, J. Grove, K. Thorn, M. Marsh, and M. von Zastrow. 2012. 'Regulation of endocytic clathrin dynamics by cargo ubiquitination', *Dev Cell*, 23: 519-32.

Hernandez, D. G., X. Reed, and A. B. Singleton. 2016. 'Genetics in Parkinson disease: Mendelian versus non-Mendelian inheritance', *J Neurochem*, 139 Suppl 1: 59-74.

Hesketh, G. G., I. Perez-Dorado, L. P. Jackson, L. Wartosch, I. B. Schafer, S. R. Gray, A. J. McCoy, O. B. Zeldin, E. F. Garman, M. E. Harbour, P. R. Evans, M. N. J. Seaman, J. P. Luzio, and D. J. Owen. 2014. 'VARP is recruited on to endosomes by direct interaction with retromer, where together they function in export to the cell surface', *Dev Cell*, 29: 591-606.

Heuser, J. 1980. 'Three-dimensional visualization of coated vesicle formation in fibroblasts', *J Cell Biol*, 84: 560-83.

Hierro, A., A. L. Rojas, R. Rojas, N. Murthy, G. Effantin, A. V. Kajava, A. C. Steven, J. S. Bonifacino, and J. H. Hurley. 2007. 'Functional architecture of the retromer cargo-recognition complex', *Nature*, 449: 1063-7.

Higashi, S., E. Iseki, R. Yamamoto, M. Minegishi, H. Hino, K. Fujisawa, T. Togo, O. Katsuse, H. Uchikado, Y. Furukawa, K. Kosaka, and H. Arai. 2007. 'Concurrence of TDP-43, tau and alpha-synuclein pathology in brains of Alzheimer's disease and dementia with Lewy bodies', *Brain Res*, 1184: 284-94.

Hirano, S., N. Suzuki, T. Slagsvold, M. Kawasaki, D. Trambaiolo, R. Kato, H. Stenmark, and S. Wakatsuki. 2006. 'Structural basis of ubiquitin recognition by mammalian Eap45 GLUE domain', *Nat Struct Mol Biol*, 13: 1031-2.

Hirst, J., L. D. Barlow, G. C. Francisco, D. A. Sahlender, M. N. Seaman, J. B. Dacks, and M. S. Robinson. 2011. 'The fifth adaptor protein complex', *PLoS Biol*, 9: e1001170.

Hodges, J. R. 2001. 'Frontotemporal dementia (Pick's disease): clinical features and assessment', *Neurology*, 56: S6-10.

Hofmann, K., and L. Falquet. 2001. 'A ubiquitin-interacting motif conserved in components of the proteasomal and lysosomal protein degradation systems', *Trends Biochem Sci*, 26: 347-50.

Hong, K., Y. Li, W. Duan, Y. Guo, H. Jiang, W. Li, and C. Li. 2012. 'Full-length TDP-43 and its C-terminal fragments activate mitophagy in NSC34 cell line', *Neurosci Lett*, 530: 144-9.

Hong, Z., Y. Yang, C. Zhang, Y. Niu, K. Li, X. Zhao, and J. J. Liu. 2009. 'The retromer component SNX6 interacts with dynactin p150(Glued) and mediates endosome-to-TGN transport', *Cell Res*, 19: 1334-49.

Horazdovsky, B. F., B. A. Davies, M. N. Seaman, S. A. McLaughlin, S. Yoon, and S. D. Emr. 1997. 'A sorting nexin-1 homologue, Vps5p, forms a complex with Vps17p and is required for recycling the vacuolar protein-sorting receptor', *Mol Biol Cell*, 8: 1529-41.

Horiuchi, H., R. Lippe, H. M. McBride, M. Rubino, P. Woodman, H. Stenmark, V. Rybin, M. Wilm, K. Ashman, M. Mann, and M. Zerial. 1997. 'A novel Rab5 GDP/GTP exchange

factor complexed to Rabaptin-5 links nucleotide exchange to effector recruitment and function', *Cell*, 90: 1149-59.

Hosokawa, N., T. Hara, T. Kaizuka, C. Kishi, A. Takamura, Y. Miura, S. Iemura, T. Natsume, K. Takehana, N. Yamada, J. L. Guan, N. Oshiro, and N. Mizushima. 2009. 'Nutrient-dependent mTORC1 association with the ULK1-Atg13-FIP200 complex required for autophagy', *Mol Biol Cell*, 20: 1981-91.

Huang, T. Y., Y. Zhao, X. Li, X. Wang, I. C. Tseng, R. Thompson, S. Tu, T. E. Willnow, Y. W. Zhang, and H. Xu. 2016. 'SNX27 and SORLA Interact to Reduce Amyloidogenic Subcellular Distribution and Processing of Amyloid Precursor Protein', *J Neurosci*, 36: 7996-8011.

Hussl, A., K. Seppi, and W. Poewe. 2013. 'Nonmotor symptoms in Parkinson's disease', *Expert Rev Neurother*, 13: 581-3.

Ikiz, B., M. J. Alvarez, D. B. Re, V. Le Verche, K. Politi, F. Lotti, S. Phani, R. Pradhan, C. Yu, G. F. Croft, A. Jacquier, C. E. Henderson, A. Califano, and S. Przedborski. 2015. 'The Regulatory Machinery of Neurodegeneration in In Vitro Models of Amyotrophic Lateral Sclerosis', *Cell Rep*, 12: 335-45.

Iko, Y., T. S. Kodama, N. Kasai, T. Oyama, E. H. Morita, T. Muto, M. Okumura, R. Fujii, T. Takumi, S. Tate, and K. Morikawa. 2004. 'Domain architectures and characterization of an RNA-binding protein, TLS', *J Biol Chem*, 279: 44834-40.

Ince, P. G., J. Evans, M. Knopp, G. Forster, H. H. Hamdalla, S. B. Wharton, and P. J. Shaw. 2003. 'Corticospinal tract degeneration in the progressive muscular atrophy variant of ALS', *Neurology*, 60: 1252-8.

Ince, P. G., J. R. Highley, J. Kirby, S. B. Wharton, H. Takahashi, M. J. Strong, and P. J. Shaw. 2011. 'Molecular pathology and genetic advances in amyotrophic lateral sclerosis: an emerging molecular pathway and the significance of glial pathology', *Acta Neuropathol*, 122: 657-71.

Isaac, J. T., M. C. Ashby, and C. J. McBain. 2007. 'The role of the GluR2 subunit in AMPA receptor function and synaptic plasticity', *Neuron*, 54: 859-71.

Itakura, E., and N. Mizushima. 2010. 'Characterization of autophagosome formation site by a hierarchical analysis of mammalian Atg proteins', *Autophagy*, 6: 764-76.

Ito, H., R. Wate, J. Zhang, S. Ohnishi, S. Kaneko, H. Ito, S. Nakano, and H. Kusaka. 2008. 'Treatment with edaravone, initiated at symptom onset, slows motor decline and decreases SOD1 deposition in ALS mice', *Exp Neurol*, 213: 448-55.

Itoh, T., N. Fujita, E. Kanno, A. Yamamoto, T. Yoshimori, and M. Fukuda. 2008. 'Golgi-resident small GTPase Rab33B interacts with Atg16L and modulates autophagosome formation', *Mol Biol Cell*, 19: 2916-25.

Iyer, S., V. Subramanian, and K. R. Acharya. 2018. 'C9orf72, a protein associated with amyotrophic lateral sclerosis (ALS) is a guanine nucleotide exchange factor', *PeerJ*, 6: e5815.

Jackson, L. P., B. T. Kelly, A. J. McCoy, T. Gaffry, L. C. James, B. M. Collins, S. Honing, P. R. Evans, and D. J. Owen. 2010. 'A large-scale conformational change couples membrane recruitment to cargo binding in the AP2 clathrin adaptor complex', *Cell*, 141: 1220-9.

Jahn, R., and R. H. Scheller. 2006. 'SNAREs--engines for membrane fusion', *Nat Rev Mol Cell Biol*, 7: 631-43.

Jalanko, A., and T. Braulke. 2009. 'Neuronal ceroid lipofuscinoses', *Biochim Biophys Acta*, 1793: 697-709.

Jaronen, M., P. Vehvilainen, T. Malm, V. Keksa-Goldsteine, E. Pollari, P. Valonen, J. Koistinaho, and G. Goldsteins. 2013. 'Protein disulfide isomerase in ALS mouse glia links protein misfolding with NADPH oxidase-catalyzed superoxide production', *Hum Mol Genet*, 22: 646-55.

Jia, D., T. S. Gomez, D. D. Billadeau, and M. K. Rosen. 2012. 'Multiple repeat elements within the FAM21 tail link the WASH actin regulatory complex to the retromer', *Mol Biol Cell*, 23: 2352-61.

Jia, D., T. S. Gomez, Z. Metlagel, J. Umetani, Z. Otwinowski, M. K. Rosen, and D. D. Billadeau. 2010. 'WASH and WAVE actin regulators of the Wiskott-Aldrich syndrome protein (WASP) family are controlled by analogous structurally related complexes', *Proc Natl Acad Sci U S A*, 107: 10442-7.

Jia, D., J. S. Zhang, F. Li, J. Wang, Z. Deng, M. A. White, D. G. Osborne, C. Phillips-Krawczak, T. S. Gomez, H. Li, A. Singla, E. Burstein, D. D. Billadeau, and M. K. Rosen. 2016. 'Structural and mechanistic insights into regulation of the retromer coat by TBC1d5', *Nat Commun*, 7: 13305.

Jiang, P., T. Nishimura, Y. Sakamaki, E. Itakura, T. Hatta, T. Natsume, and N. Mizushima. 2014. 'The HOPS complex mediates autophagosome-lysosome fusion through interaction with syntaxin 17', *Mol Biol Cell*, 25: 1327-37.

Jiang, S., Y. Li, X. Zhang, G. Bu, H. Xu, and Y. W. Zhang. 2014. 'Trafficking regulation of proteins in Alzheimer's disease', *Mol Neurodegener*, 9: 6.

Jimenez-Orgaz, A., A. Kvainickas, H. Nagele, J. Denner, S. Eimer, J. Dengjel, and F. Steinberg. 2018. 'Control of RAB7 activity and localization through the retromer-TBC1D5 complex enables RAB7-dependent mitophagy', *EMBO J*, 37: 235-54.

Joensuu, M., R. Martinez-Marmol, P. Padmanabhan, N. R. Glass, N. Durisic, M. Pelekanos, M. Mollazade, G. Balistreri, R. Amor, J. J. Cooper-White, G. J. Goodhill, and F. A. Meunier. 2017. 'Visualizing endocytic recycling and trafficking in live neurons by subdiffractional tracking of internalized molecules', *Nat Protoc*, 12: 2590-622.

Johnson, J. O., J. Mandrioli, M. Benatar, Y. Abramzon, V. M. Van Deerlin, J. Q. Trojanowski, J. R. Gibbs, M. Brunetti, S. Gronka, J. Wuu, J. Ding, L. McCluskey, M. Martinez-Lage, D. Falcone, D. G. Hernandez, S. Arepalli, S. Chong, J. C. Schymick, J. Rothstein, F. Landi, Y. D. Wang, A. Calvo, G. Mora, M. Sabatelli, M. R. Monsurro, S. Battistini, F. Salvi, R. Spataro, P. Sola, G. Borghero, G. Galassi, S. W. Scholz, J. P. Taylor, G. Restagno, A. Chio, and B. J. Traynor. 2010. 'Exome sequencing reveals VCP mutations as a cause of familial ALS', *Neuron*, 68: 857-64.

Johnson, J. O., E. P. Pioro, A. Boehringer, R. Chia, H. Feit, A. E. Renton, H. A. Pliner, Y. Abramzon, G. Marangi, B. J. Winborn, J. R. Gibbs, M. A. Nalls, S. Morgan, M. Shoai, J. Hardy, A. Pittman, R. W. Orrell, A. Malaspina, K. C. Sidle, P. Fratta, M. B. Harms, R. H. Baloh, A. Pestronk, C. C. Weihl, E. Rogaeva, L. Zinman, V. E. Drory, G. Borghero, G. Mora, A. Calvo, J. D. Rothstein, C. Drepper, M. Sendtner, A. B. Singleton, J. P. Taylor, M. R. Cookson, G. Restagno, M. Sabatelli, R. Bowser, A. Chio, and B. J. Traynor. 2014. 'Mutations in the Matrin 3 gene cause familial amyotrophic lateral sclerosis', *Nat Neurosci*, 17: 664-66.

Joyce, P. I., P. Fratta, E. M. Fisher, and A. Acevedo-Arozena. 2011. 'SOD1 and TDP-43 animal models of amyotrophic lateral sclerosis: recent advances in understanding disease toward the development of clinical treatments', *Mamm Genome*, 22: 420-48.

Kabashi, E., L. Lin, M. L. Tradewell, P. A. Dion, V. Bercier, P. Bourgouin, D. Rochefort, S. Bel Hadj, H. D. Durham, C. Vande Velde, G. A. Rouleau, and P. Drapeau. 2010. 'Gain and loss of function of ALS-related mutations of TARDBP (TDP-43) cause motor deficits in vivo', *Hum Mol Genet*, 19: 671-83.

Kabeya, Y., N. Mizushima, T. Ueno, A. Yamamoto, T. Kirisako, T. Noda, E. Kominami, Y. Ohsumi, and T. Yoshimori. 2000. 'LC3, a mammalian homologue of yeast Apg8p, is localized in autophagosome membranes after processing', *EMBO J*, 19: 5720-8.

Kadlecova, Z., S. J. Spielman, D. Loerke, A. Mohanakrishnan, D. K. Reed, and S. L. Schmid. 2017. 'Regulation of clathrin-mediated endocytosis by hierarchical allosteric activation of AP2', *J Cell Biol*, 216: 167-79.

Kaksonen, M., and A. Roux. 2018. 'Mechanisms of clathrin-mediated endocytosis', *Nat Rev Mol Cell Biol*, 19: 313-26.

Kaplan, A., K. J. Spiller, C. Towne, K. C. Kanning, G. T. Choe, A. Geber, T. Akay, P. Aebischer, and C. E. Henderson. 2014. 'Neuronal matrix metalloproteinase-9 is a determinant of selective neurodegeneration', *Neuron*, 81: 333-48.

Karam, C., S. N. Scelsa, and D. J. Macgowan. 2010. 'The clinical course of progressive bulbar palsy', *Amyotroph Lateral Scler*, 11: 364-8.

Karanasios, E., S. A. Walker, H. Okkenhaug, M. Manifava, E. Hummel, H. Zimmermann, Q. Ahmed, M. C. Domart, L. Collinson, and N. T. Ktistakis. 2016. 'Autophagy initiation by ULK complex assembly on ER tubulovesicular regions marked by ATG9 vesicles', *Nat Commun*, 7: 12420.

Karlsson, P., A. Droce, J. M. Moser, S. Cuhlmann, C. O. Padilla, P. Heimann, J. W. Bartsch, A. Fuchtbauer, E. M. Fuchtbauer, and T. Schmitt-John. 2013. 'Loss of vps54 function leads to vesicle traffic impairment, protein mis-sorting and embryonic lethality', *Int J Mol Sci*, 14: 10908-25.

Kassubek, J., A. Unrath, H. J. Huppertz, D. Lule, T. Ethofer, A. D. Sperfeld, and A. C. Ludolph. 2005. 'Global brain atrophy and corticospinal tract alterations in ALS, as investigated by voxel-based morphometry of 3-D MRI', *Amyotroph Lateral Scler Other Motor Neuron Disord*, 6: 213-20.

Kato, S., S. Horiuchi, J. Liu, D. W. Cleveland, N. Shibata, K. Nakashima, R. Nagai, A. Hirano, M. Takikawa, M. Kato, I. Nakano, and E. Ohama. 2000. 'Advanced glycation endproduct-modified superoxide dismutase-1 (SOD1)-positive inclusions are common to familial amyotrophic lateral sclerosis patients with SOD1 gene mutations and transgenic mice expressing human SOD1 with a G85R mutation', *Acta Neuropathol*, 100: 490-505.

Katoh, K., H. Shibata, H. Suzuki, A. Nara, K. Ishidoh, E. Kominami, T. Yoshimori, and M. Maki. 2003. 'The ALG-2-interacting protein Alix associates with CHMP4b, a human homologue of yeast Snf7 that is involved in multivesicular body sorting', *J Biol Chem*, 278: 39104-13.

Katzmann, D. J., C. J. Stefan, M. Babst, and S. D. Emr. 2003. 'Vps27 recruits ESCRT machinery to endosomes during MVB sorting', *J Cell Biol*, 162: 413-23.

Kauss, V., M. Dambrova, and D. L. Medina. 2019. 'Pharmacological approaches to tackle NCLs', *Biochim Biophys Acta Mol Basis Dis*: 165553.

Kawahara, Y., S. Kwak, H. Sun, K. Ito, H. Hashida, H. Aizawa, S. Y. Jeong, and I. Kanazawa. 2003. 'Human spinal motoneurons express low relative abundance of GluR2 mRNA: an implication for excitotoxicity in ALS', *J Neurochem*, 85: 680-9.

Kelly, B. T., S. C. Graham, N. Liska, P. N. Dannhauser, S. Honing, E. J. Ungewickell, and D. J. Owen. 2014. 'Clathrin adaptors. AP2 controls clathrin polymerization with a membrane-activated switch', *Science*, 345: 459-63.

Kenna, K. P., P. T. van Doormaal, A. M. Dekker, N. Ticozzi, B. J. Kenna, F. P. Diekstra, W. van Rheenen, K. R. van Eijk, A. R. Jones, P. Keagle, A. Shatunov, W. Sproviero, B. N. Smith, M. A. van Es, S. D. Topp, A. Kenna, J. W. Miller, C. Fallini, C. Tiloca, R. L. McLaughlin, C. Vance, C. Troakes, C. Colombrita, G. Mora, A. Calvo, F. Verde, S. Al-Sarraj, A. King, D. Calini, J. de Belleroche, F. Baas, A. J. van der Kooi, M. de Visser, A. L. Ten Asbroek, P. C. Sapp, D. McKenna-Yasek, M. Polak, S. Asress, J. L. Munoz-Blanco, T. M. Strom, T. Meitinger, K. E. Morrison, G. Lauria, K. L. Williams, P. N. Leigh, G. A. Nicholson, I. P. Blair, C. S. Leblond, P. A. Dion, G. A. Rouleau, H. Pall, P. J. Shaw, M. R. Turner, K. Talbot, F. Taroni, K. B. Boylan, M. Van Blitterswijk, R. Rademakers, J. Esteban-Perez, A. Garcia-Redondo, P. Van Damme, W. Robberecht, A. Chio, C. Gellera, C. Drepper, M. Sendtner, A. Ratti, J. D. Glass, J. S. Mora, N. A. Basak, O. Hardiman, A. C. Ludolph, P. M. Andersen, J. H. Weishaupt, R. H. Brown, Jr., A. Al-Chalabi, V. Silani, C. E. Shaw, L. H. van den Berg, J. H. Veldink, and J. E. Landers. 2016. 'NEK1 variants confer susceptibility to amyotrophic lateral sclerosis', *Nat Genet*, 48: 1037-42.

Kerr, M. C., J. S. Bennetts, F. Simpson, E. C. Thomas, C. Flegg, P. A. Gleeson, C. Wicking, and R. D. Teasdale. 2005. 'A novel mammalian retromer component, Vps26B', *Traffic*, 6: 991-1001.

Khurana, V., I. Elson-Schwab, T. A. Fulga, K. A. Sharp, C. A. Loewen, E. Mulkearns, J. Tyynela, C. R. Scherzer, and M. B. Feany. 2010. 'Lysosomal dysfunction promotes cleavage and neurotoxicity of tau in vivo', *PLoS Genet*, 6: e1001026.

Kia, A., K. McAvoy, K. Krishnamurthy, D. Trotti, and P. Pasinelli. 2018. 'Astrocytes expressing ALS-linked mutant FUS induce motor neuron death through release of tumor necrosis factor-alpha', *Glia*, 66: 1016-33.

Kim, D. H., D. D. Sarbassov, S. M. Ali, J. E. King, R. R. Latek, H. Erdjument-Bromage, P. Tempst, and D. M. Sabatini. 2002. 'mTOR interacts with raptor to form a nutrient-sensitive complex that signals to the cell growth machinery', *Cell*, 110: 163-75.

Kim, E., Y. Lee, H. J. Lee, J. S. Kim, B. S. Song, J. W. Huh, S. R. Lee, S. U. Kim, S. H. Kim, Y. Hong, I. Shim, and K. T. Chang. 2010. 'Implication of mouse Vps26b-Vps29-Vps35 retromer complex in sortilin trafficking', *Biochem Biophys Res Commun*, 403: 167-71.

Kim, G. H., J. E. Kim, S. J. Rhie, and S. Yoon. 2015. 'The Role of Oxidative Stress in Neurodegenerative Diseases', *Exp Neurobiol*, 24: 325-40.

Kim, H. J., N. C. Kim, Y. D. Wang, E. A. Scarborough, J. Moore, Z. Diaz, K. S. MacLea, B. Freibaum, S. Li, A. Molliex, A. P. Kanagaraj, R. Carter, K. B. Boylan, A. M. Wojtas, R. Rademakers, J. L. Pinkus, S. A. Greenberg, J. Q. Trojanowski, B. J. Traynor, B. N. Smith, S. Topp, A. S. Gkazi, J. Miller, C. E. Shaw, M. Kottlors, J. Kirschner, A. Pestronk, Y. R. Li, A. F. Ford, A. D. Gitler, M. Benatar, O. D. King, V. E. Kimonis, E. D. Ross, C. C. Weihl, J. Shorter, and J. P. Taylor. 2013. 'Mutations in prion-like domains in hnRNPA2B1 and hnRNPA1 cause multisystem proteinopathy and ALS', *Nature*, 495: 467-73.

Kim, W. K., X. Liu, J. Sandner, M. Pasmantier, J. Andrews, L. P. Rowland, and H. Mitsumoto. 2009. 'Study of 962 patients indicates progressive muscular atrophy is a form of ALS', *Neurology*, 73: 1686-92.

Kimura, N., E. Samura, K. Suzuki, S. Okabayashi, N. Shimozawa, and Y. Yasutomi. 2016. 'Dynein Dysfunction Reproduces Age-Dependent Retromer Deficiency: Concomitant Disruption

of Retrograde Trafficking Is Required for Alteration in beta-Amyloid Precursor Protein Metabolism', *Am J Pathol*, 186: 1952-66.

Kirby, J., E. F. Goodall, W. Smith, J. R. Highley, R. Masanzu, J. A. Hartley, R. Hibberd, H. C. Hollinger, S. B. Wharton, K. E. Morrison, P. G. Ince, C. J. McDermott, and P. J. Shaw. 2010. 'Broad clinical phenotypes associated with TAR-DNA binding protein (TARDBP) mutations in amyotrophic lateral sclerosis', *Neurogenetics*, 11: 217-25.

Kirchhausen, T., and S. C. Harrison. 1981. 'Protein organization in clathrin trimers', *Cell*, 23: 755-61.

Kleinberger, G., Y. Yamanishi, M. Suarez-Calvet, E. Czirr, E. Lohmann, E. Cuyvers, H. Struyfs, N. Pettkus, A. Wenninger-Weinzierl, F. Mazaheri, S. Tahirovic, A. Lleo, D. Alcolea, J. Fortea, M. Willem, S. Lammich, J. L. Molinuevo, R. Sanchez-Valle, A. Antonell, A. Ramirez, M. T. Heneka, K. Sleegers, J. van der Zee, J. J. Martin, S. Engelborghs, A. Demirtas-Tatlidede, H. Zetterberg, C. Van Broeckhoven, H. Gurvit, T. Wyss-Coray, J. Hardy, M. Colonna, and C. Haass. 2014. 'TREM2 mutations implicated in neurodegeneration impair cell surface transport and phagocytosis', *Sci Transl Med*, 6: 243ra86.

Knodler, A., S. Feng, J. Zhang, X. Zhang, A. Das, J. Peranen, and W. Guo. 2010. 'Coordination of Rab8 and Rab11 in primary ciliogenesis', *Proc Natl Acad Sci U S A*, 107: 6346-51.

Kollmann, K., S. Pohl, K. Marschner, M. Encarnacao, I. Sakwa, S. Tiede, B. J. Poorthuis, T. Lubke, S. Muller-Loennies, S. Storch, and T. Braulke. 2010. 'Mannose phosphorylation in health and disease', *Eur J Cell Biol*, 89: 117-23.

Komano, H., M. Seeger, S. Gandy, G. T. Wang, G. A. Krafft, and R. S. Fuller. 1998. 'Involvement of cell surface glycosyl-phosphatidylinositol-linked aspartyl proteases in alpha-secretase-type cleavage and ectodomain solubilization of human Alzheimer beta-amyloid precursor protein in yeast', *J Biol Chem*, 273: 31648-51.

Kostelansky, M. S., C. Schluter, Y. Y. Tam, S. Lee, R. Ghirlando, B. Beach, E. Conibear, and J. H. Hurley. 2007. 'Molecular architecture and functional model of the complete yeast ESCRT-I heterotetramer', *Cell*, 129: 485-98.

Kummel, D., and C. Ungermann. 2014. 'Principles of membrane tethering and fusion in endosome and lysosome biogenesis', *Curr Opin Cell Biol*, 29: 61-6.

Kvainickas, A., A. Jimenez-Orgaz, H. Nagele, Z. Hu, J. Dengjel, and F. Steinberg. 2017. 'Cargo-selective SNX-BAR proteins mediate retromer trimer independent retrograde transport', *J Cell Biol*, 216: 3677-93.

Kwiatkowski, T. J., Jr., D. A. Bosco, A. L. Leclerc, E. Tamrazian, C. R. Vanderburg, C. Russ, A. Davis, J. Gilchrist, E. J. Kasarskis, T. Munsat, P. Valdmanis, G. A. Rouleau, B. A. Hosler, P. Cortelli, P. J. de Jong, Y. Yoshinaga, J. L. Haines, M. A. Pericak-Vance, J. Yan, N. Ticozzi, T. Siddique, D. McKenna-Yasek, P. C. Sapp, H. R. Horvitz, J. E. Landers, and R. H. Brown, Jr. 2009. 'Mutations in the FUS/TLS gene on chromosome 16 cause familial amyotrophic lateral sclerosis', *Science*, 323: 1205-8.

Lachmann, J., E. Glaubke, P. S. Moore, and C. Ungermann. 2014. 'The Vps39-like TRAP1 is an effector of Rab5 and likely the missing Vps3 subunit of human CORVET', *Cell Logist*, 4: e970840.

Lagier-Tourenne, C., M. Polymenidou, K. R. Hutt, A. Q. Vu, M. Baughn, S. C. Huelga, K. M. Clutario, S. C. Ling, T. Y. Liang, C. Mazur, E. Wancewicz, A. S. Kim, A. Watt, S. Freier, G. G. Hicks, J. P. Donohue, L. Shiue, C. F. Bennett, J. Ravits, D. W. Cleveland, and G. W.

Yeo. 2012. 'Divergent roles of ALS-linked proteins FUS/TLS and TDP-43 intersect in processing long pre-mRNAs', *Nat Neurosci*, 15: 1488-97.

Lai, C., C. Xie, S. G. McCormack, H. C. Chiang, M. K. Michalak, X. Lin, J. Chandran, H. Shim, M. Shimoji, M. R. Cookson, R. L. Huganir, J. D. Rothstein, D. L. Price, P. C. Wong, L. J. Martin, J. J. Zhu, and H. Cai. 2006. 'Amyotrophic lateral sclerosis 2-deficiency leads to neuronal degeneration in amyotrophic lateral sclerosis through altered AMPA receptor trafficking', *J Neurosci*, 26: 11798-806.

Lai, C., C. Xie, H. Shim, J. Chandran, B. W. Howell, and H. Cai. 2009. 'Regulation of endosomal motility and degradation by amyotrophic lateral sclerosis 2/alsin', *Mol Brain*, 2: 23.

Lai, F., and R. S. Williams. 1989. 'A prospective study of Alzheimer disease in Down syndrome', *Arch Neurol*, 46: 849-53.

Lamb, C. A., T. Yoshimori, and S. A. Tooze. 2013. 'The autophagosome: origins unknown, biogenesis complex', *Nat Rev Mol Cell Biol*, 14: 759-74.

Lasiene, J., O. Komine, N. Fujimori-Tonou, B. Powers, F. Endo, S. Watanabe, J. Shijie, J. Ravits, P. Horner, H. Misawa, and K. Yamanaka. 2016. 'Neuregulin 1 confers neuroprotection in SOD1-linked amyotrophic lateral sclerosis mice via restoration of C-boutons of spinal motor neurons', *Acta Neuropathol Commun*, 4: 15.

Lata, S., G. Schoehn, A. Jain, R. Pires, J. Piehler, H. G. Gottlinger, and W. Weissenhorn. 2008. 'Helical structures of ESCRT-III are disassembled by VPS4', *Science*, 321: 1354-7.

Lattante, S., A. Conte, M. Zollino, M. Luigetti, A. Del Grande, G. Marangi, A. Romano, A. Marcaccio, E. Meleo, G. Bisogni, P. M. Rossini, and M. Sabatelli. 2012. 'Contribution of major amyotrophic lateral sclerosis genes to the etiology of sporadic disease', *Neurology*, 79: 66-72.

Lautenschlaeger, J., T. Prell, and J. Grosskreutz. 2012. 'Endoplasmic reticulum stress and the ER mitochondrial calcium cycle in amyotrophic lateral sclerosis', *Amyotroph Lateral Scler*, 13: 166-77.

Lawe, D. C., A. Chawla, E. Merithew, J. Dumas, W. Carrington, K. Fogarty, L. Lifshitz, R. Tuft, D. Lambright, and S. Corvera. 2002. 'Sequential roles for phosphatidylinositol 3-phosphate and Rab5 in tethering and fusion of early endosomes via their interaction with EEA1', *J Biol Chem*, 277: 8611-7.

Lawrence, G., C. C. Brown, B. A. Flood, S. Karunakaran, M. Cabrera, M. Nordmann, C. Ungermann, and R. A. Fratti. 2014. 'Dynamic association of the PI3P-interacting Mon1-Ccz1 GEF with vacuoles is controlled through its phosphorylation by the type 1 casein kinase Yck3', *Mol Biol Cell*, 25: 1608-19.

Lee, J. J., G. Radice, C. P. Perkins, and F. Costantini. 1992. 'Identification and characterization of a novel, evolutionarily conserved gene disrupted by the murine H beta 58 embryonic lethal transgene insertion', *Development*, 115: 277-88.

Lee, J., C. Retamal, L. Cuitino, A. Caruano-Yzermans, J. E. Shin, P. van Kerkhof, M. P. Marzolo, and G. Bu. 2008. 'Adaptor protein sorting nexin 17 regulates amyloid precursor protein trafficking and processing in the early endosomes', *J Biol Chem*, 283: 11501-8.

Lee, S., Y. C. Tsai, R. Mattera, W. J. Smith, M. S. Kostelansky, A. M. Weissman, J. S. Bonifacino, and J. H. Hurley. 2006. 'Structural basis for ubiquitin recognition and autoubiquitination by Rabex-5', *Nat Struct Mol Biol*, 13: 264-71.

Lee, Y. B., H. J. Chen, J. N. Peres, J. Gomez-Deza, J. Attig, M. Stalekar, C. Troakes, A. L. Nishimura, E. L. Scotter, C. Vance, Y. Adachi, V. Sardone, J. W. Miller, B. N. Smith, J. M. Gallo, J. Ule, F. Hirth, B. Rogelj, C. Houart, and C. E. Shaw. 2013. 'Hexanucleotide

repeats in ALS/FTD form length-dependent RNA foci, sequester RNA binding proteins, and are neurotoxic', *Cell Rep*, 5: 1178-86.

Lesage, S., and A. Brice. 2009. 'Parkinson's disease: from monogenic forms to genetic susceptibility factors', *Hum Mol Genet*, 18: R48-59.

Lesage, S., C. Condroyer, S. Klebe, A. Honore, F. Tison, C. Brefel-Courbon, A. Durr, and A. Brice. 2012. 'Identification of VPS35 mutations replicated in French families with Parkinson disease', *Neurology*, 78: 1449-50.

Leyton-Jaimes, M. F., J. Kahn, and A. Israelson. 2019. 'AAV2/9-mediated overexpression of MIF inhibits SOD1 misfolding, delays disease onset, and extends survival in mouse models of ALS', *Proc Natl Acad Sci U S A*, 116: 14755-60.

Li, H., Y. Koo, X. Mao, L. Sifuentes-Dominguez, L. L. Morris, D. Jia, N. Miyata, R. A. Faulkner, J. M. van Deursen, M. Vooijs, D. D. Billadeau, B. van de Sluis, O. Cleaver, and E. Burstein. 2015. 'Endosomal sorting of Notch receptors through COMMD9-dependent pathways modulates Notch signaling', *J Cell Biol*, 211: 605-17.

Li, J. G., J. Chiu, and D. Pratico. 2019. 'Full recovery of the Alzheimer's disease phenotype by gain of function of vacuolar protein sorting 35', *Mol Psychiatry*.

Liang, C., J. S. Lee, K. S. Inn, M. U. Gack, Q. Li, E. A. Roberts, I. Vergne, V. Deretic, P. Feng, C. Akazawa, and J. U. Jung. 2008. 'Beclin1-binding UVRAG targets the class C Vps complex to coordinate autophagosome maturation and endocytic trafficking', *Nat Cell Biol*, 10: 776-87.

Liddelow, S. A., K. A. Guttenplan, L. E. Clarke, F. C. Bennett, C. J. Bohlen, L. Schirmer, M. L. Bennett, A. E. Munch, W. S. Chung, T. C. Peterson, D. K. Wilton, A. Frouin, B. A. Napier, N. Panicker, M. Kumar, M. S. Buckwalter, D. H. Rowitch, V. L. Dawson, T. M. Dawson, B. Stevens, and B. A. Barres. 2017. 'Neurotoxic reactive astrocytes are induced by activated microglia', *Nature*, 541: 481-87.

Lim, S. Y., S. H. Fox, and A. E. Lang. 2009. 'Overview of the extranigral aspects of Parkinson disease', *Arch Neurol*, 66: 167-72.

Lin, C. L., L. A. Bristol, L. Jin, M. Dykes-Hoberg, T. Crawford, L. Clawson, and J. D. Rothstein. 1998. 'Aberrant RNA processing in a neurodegenerative disease: the cause for absent EAAT2, a glutamate transporter, in amyotrophic lateral sclerosis', *Neuron*, 20: 589-602.

Linhart, R., S. A. Wong, J. Cao, M. Tran, A. Huynh, C. Ardrey, J. M. Park, C. Hsu, S. Taha, R. Peterson, S. Shea, J. Kurian, and K. Venderova. 2014. 'Vacuolar protein sorting 35 (Vps35) rescues locomotor deficits and shortened lifespan in Drosophila expressing a Parkinson's disease mutant of Leucine-Rich Repeat Kinase 2 (LRRK2)', *Mol Neurodegener*, 9: 23.

Liu, G., A. Byrd, A. N. Warner, F. Pei, E. Basha, A. Buchanan, and J. R. Buchan. 2019. 'Cdc48/VCP and endocytosis regulate TDP-43 and FUS toxicity and turnover', *Mol Cell Biol*.

Liu, G., A. N. Coyne, F. Pei, S. Vaughan, M. Chaung, D. C. Zarnescu, and J. R. Buchan. 2017. 'Endocytosis regulates TDP-43 toxicity and turnover', *Nat Commun*, 8: 2092.

Liu, J., L. A. Shinobu, C. M. Ward, D. Young, and D. W. Cleveland. 2005. 'Elevation of the Hsp70 chaperone does not effect toxicity in mouse models of familial amyotrophic lateral sclerosis', *J Neurochem*, 93: 875-82.

Liu, K., Y. Jian, X. Sun, C. Yang, Z. Gao, Z. Zhang, X. Liu, Y. Li, J. Xu, Y. Jing, S. Mitani, S. He, and C. Yang. 2016. 'Negative regulation of phosphatidylinositol 3-phosphate levels in early-to-late endosome conversion', *J Cell Biol*, 212: 181-98.

Liu, W., F. L. Tang, J. Erion, H. Xiao, J. Ye, and W. C. Xiong. 2014. 'Vps35 haploinsufficiency results in degenerative-like deficit in mouse retinal ganglion neurons and impairment of optic nerve injury-induced gliosis', *Mol Brain*, 7: 10.

Liu, W., F. L. Tang, S. Lin, K. Zhao, L. Mei, J. Ye, and W. C. Xiong. 2017. 'Vps35-deficiency impairs SLC4A11 trafficking and promotes corneal dystrophy', *PLoS One*, 12: e0184906.

Lobsiger, C. S., S. Boillee, M. McAlonis-Downes, A. M. Khan, M. L. Feltri, K. Yamanaka, and D. W. Cleveland. 2009. 'Schwann cells expressing dismutase active mutant SOD1 unexpectedly slow disease progression in ALS mice', *Proc Natl Acad Sci U S A*, 106: 4465-70.

Loerke, D., M. Mettlen, D. Yarar, K. Jaqaman, H. Jaqaman, G. Danuser, and S. L. Schmid. 2009. 'Cargo and dynamin regulate clathrin-coated pit maturation', *PLoS Biol*, 7: e57.

Lomen-Hoerth, C. 2004. 'Characterization of amyotrophic lateral sclerosis and frontotemporal dementia', *Dement Geriatr Cogn Disord*, 17: 337-41.

Lu, L., L. Zheng, L. Viera, E. Suswam, Y. Li, X. Li, A. G. Estevez, and P. H. King. 2007. 'Mutant Cu/Zn-superoxide dismutase associated with amyotrophic lateral sclerosis destabilizes vascular endothelial growth factor mRNA and downregulates its expression', *J Neurosci*, 27: 7929-38.

Lu, Q., L. W. Hope, M. Brasch, C. Reinhard, and S. N. Cohen. 2003. 'TSG101 interaction with HRS mediates endosomal trafficking and receptor down-regulation', *Proc Natl Acad Sci U S A*, 100: 7626-31.

Lucas, M., D. C. Gershlick, A. Vidaurrazaga, A. L. Rojas, J. S. Bonifacino, and A. Hierro. 2016. 'Structural Mechanism for Cargo Recognition by the Retromer Complex', *Cell*, 167: 1623-35.e14.

Lucin, K. M., C. E. O'Brien, G. Bieri, E. Czirr, K. I. Mosher, R. J. Abbey, D. F. Mastroeni, J. Rogers, B. Spencer, E. Masliah, and T. Wyss-Coray. 2013. 'Microglial beclin 1 regulates retromer trafficking and phagocytosis and is impaired in Alzheimer's disease', *Neuron*, 79: 873-86.

Luo, W., W. Liu, X. Hu, M. Hanna, A. Caravaca, and S. M. Paul. 2015. 'Microglial internalization and degradation of pathological tau is enhanced by an anti-tau monoclonal antibody', *Sci Rep*, 5: 11161.

Luty, A. A., J. B. Kwok, C. Dobson-Stone, C. T. Loy, K. G. Coupland, H. Karlstrom, T. Sobow, J. Tchorzewska, A. Maruszak, M. Barcikowska, P. K. Panegyres, C. Zekanowski, W. S. Brooks, K. L. Williams, I. P. Blair, K. A. Mather, P. S. Sachdev, G. M. Halliday, and P. R. Schofield. 2010. 'Sigma nonopioid intracellular receptor 1 mutations cause frontotemporal lobar degeneration-motor neuron disease', *Ann Neurol*, 68: 639-49.

Lutz, C. 2018. 'Mouse models of ALS: Past, present and future', *Brain Res*, 1693: 1-10.

Ma, L., P. K. Umasankar, A. G. Wrobel, A. Lymar, A. J. McCoy, S. S. Holkar, A. Jha, T. Pradhan-Sundd, S. C. Watkins, D. J. Owen, and L. M. Traub. 2016. 'Transient Fcho1/2Eps15/RAP-2 Nanoclusters Prime the AP-2 Clathrin Adaptor for Cargo Binding', *Dev Cell*, 37: 428-43.

Mackenzie, I. R., A. M. Nicholson, M. Sarkar, J. Messing, M. D. Purice, C. Pottier, K. Annu, M. Baker, R. B. Perkerson, A. Kurti, B. J. Matchett, T. Mittag, J. Temirov, G. R. Hsiung, C. Krieger, M. E. Murray, M. Kato, J. D. Fryer, L. Petrucelli, L. Zinman, S. Weintraub, M. Mesulam, J. Keith, S. A. Zivkovic, V. Hirsch-Reinshagen, R. P. Roos, S. Zuchner, N. R. Graff-Radford, R. C. Petersen, R. J. Caselli, Z. K. Wszolek, E. Finger, C. Lippa, D. Lacomis, H. Stewart, D. W. Dickson, H. J. Kim, E. Rogaeva, E. Bigio, K. B. Boylan, J. P. Taylor, and R. Rademakers. 2017. 'TIA1 Mutations in Amyotrophic Lateral Sclerosis and

Frontotemporal Dementia Promote Phase Separation and Alter Stress Granule Dynamics', *Neuron*, 95: 808-16.e9.

MacLeod, D. A., H. Rhinn, T. Kuwahara, A. Zolin, G. Di Paolo, B. D. McCabe, K. S. Marder, L. S. Honig, L. N. Clark, S. A. Small, and A. Abeliovich. 2013. 'RAB7L1 interacts with LRRK2 to modify intraneuronal protein sorting and Parkinson's disease risk', *Neuron*, 77: 425-39.

Magrane, J., C. Cortez, W. B. Gan, and G. Manfredi. 2014. 'Abnormal mitochondrial transport and morphology are common pathological denominators in SOD1 and TDP43 ALS mouse models', *Hum Mol Genet*, 23: 1413-24.

Majerova, P., M. Zilkova, Z. Kazmerova, A. Kovac, K. Paholikova, B. Kovacech, N. Zilka, and M. Novak. 2014. 'Microglia display modest phagocytic capacity for extracellular tau oligomers', *J Neuroinflammation*, 11: 161.

Mallam, A. L., and E. M. Marcotte. 2017. 'Systems-wide Studies Uncover Commander, a Multiprotein Complex Essential to Human Development', *Cell Syst*, 4: 483-94.

Mamo, A., F. Jules, K. Dumaresq-Doiron, S. Costantino, and S. Lefrancois. 2012. 'The role of ceroid lipofuscinosis neuronal protein 5 (CLN5) in endosomal sorting', *Mol Cell Biol*, 32: 1855-66.

Manfredi, G., and H. Kawamata. 2016. 'Mitochondria and endoplasmic reticulum crosstalk in amyotrophic lateral sclerosis', *Neurobiol Dis*, 90: 35-42.

Marcusson, E. G., B. F. Horazdovsky, J. L. Cereghino, E. Gharakhanian, and S. D. Emr. 1994. 'The sorting receptor for yeast vacuolar carboxypeptidase Y is encoded by the VPS10 gene', *Cell*, 77: 579-86.

Mari, M., M. V. Bujny, D. Zeuschner, W. J. Geerts, J. Griffith, C. M. Petersen, P. J. Cullen, J. Klumperman, and H. J. Geuze. 2008. 'SNX1 defines an early endosomal recycling exit for sortilin and mannose 6-phosphate receptors', *Traffic*, 9: 380-93.

Marsh, E. W., P. L. Leopold, N. L. Jones, and F. R. Maxfield. 1995. 'Oligomerized transferrin receptors are selectively retained by a lumenal sorting signal in a long-lived endocytic recycling compartment', *J Cell Biol*, 129: 1509-22.

Maruyama, H., H. Morino, H. Ito, Y. Izumi, H. Kato, Y. Watanabe, Y. Kinoshita, M. Kamada, H. Nodera, H. Suzuki, O. Komure, S. Matsuura, K. Kobatake, N. Morimoto, K. Abe, N. Suzuki, M. Aoki, A. Kawata, T. Hirai, T. Kato, K. Ogasawara, A. Hirano, T. Takumi, H. Kusaka, K. Hagiwara, R. Kaji, and H. Kawakami. 2010. 'Mutations of optineurin in amyotrophic lateral sclerosis', *Nature*, 465: 223-6.

Massol, R. H., W. Boll, A. M. Griffin, and T. Kirchhausen. 2006. 'A burst of auxilin recruitment determines the onset of clathrin-coated vesicle uncoating', *Proc Natl Acad Sci U S A*, 103: 10265-70.

Mattera, R., Y. C. Tsai, A. M. Weissman, and J. S. Bonifacino. 2006. 'The Rab5 guanine nucleotide exchange factor Rabex-5 binds ubiquitin (Ub) and functions as a Ub ligase through an atypical Ub-interacting motif and a zinc finger domain', *J Biol Chem*, 281: 6874-83.

Maury, Y., J. Come, R. A. Piskorowski, N. Salah-Mohellibi, V. Chevaleyre, M. Peschanski, C. Martinat, and S. Nedelec. 2015. 'Combinatorial analysis of developmental cues efficiently converts human pluripotent stem cells into multiple neuronal subtypes', *Nat Biotechnol*, 33: 89-96.

Mavlyutov, T. A., M. L. Epstein, K. A. Andersen, L. Ziskind-Conhaim, and A. E. Ruoho. 2010. 'The sigma-1 receptor is enriched in postsynaptic sites of C-terminals in mouse motoneurons. An anatomical and behavioral study', *Neuroscience*, 167: 247-55.

Mayers, J. R., I. Fyfe, A. L. Schuh, E. R. Chapman, J. M. Edwardson, and A. Audhya. 2011. 'ESCRT-0 assembles as a heterotetrameric complex on membranes and binds multiple ubiquitinylated cargoes simultaneously', *J Biol Chem*, 286: 9636-45.

McCullough, J., R. D. Fisher, F. G. Whitby, W. I. Sundquist, and C. P. Hill. 2008. 'ALIX-CHMP4 interactions in the human ESCRT pathway', *Proc Natl Acad Sci U S A*, 105: 7687-91.

McCullough, J., P. E. Row, O. Lorenzo, M. Doherty, R. Beynon, M. J. Clague, and S. Urbe. 2006. 'Activation of the endosome-associated ubiquitin isopeptidase AMSH by STAM, a component of the multivesicular body-sorting machinery', *Curr Biol*, 16: 160-5.

McDermott, C. J. 2019. 'Clinical trials in amyotrophic lateral sclerosis', *Curr Opin Neurol*, 32: 758-63.

McEwan, D. G., D. Popovic, A. Gubas, S. Terawaki, H. Suzuki, D. Stadel, F. P. Coxon, D. Miranda de Stegmann, S. Bhogaraju, K. Maddi, A. Kirchof, E. Gatti, M. H. Helfrich, S. Wakatsuki, C. Behrends, P. Pierre, and I. Dikic. 2015. 'PLEKHM1 regulates autophagosome-lysosome fusion through HOPS complex and LC3/GABARAP proteins', *Mol Cell*, 57: 39-54.

McGeer, P. L., and E. G. McGeer. 2002. 'Inflammatory processes in amyotrophic lateral sclerosis', *Muscle Nerve*, 26: 459-70.

McGough, I. J., R. E. A. de Groot, A. P. Jellett, M. C. Betist, K. C. Varandas, C. M. Danson, K. J. Heesom, H. C. Korswagen, and P. J. Cullen. 2018. 'SNX3-retromer requires an evolutionary conserved MON2:DOPEY2:ATP9A complex to mediate Wntless sorting and Wnt secretion', *Nat Commun*, 9: 3737.

McGough, I. J., F. Steinberg, D. Jia, P. A. Barbuti, K. J. McMillan, K. J. Heesom, A. L. Whone, M. A. Caldwell, D. D. Billadeau, M. K. Rosen, and P. J. Cullen. 2014. 'Retromer binding to FAM21 and the WASH complex is perturbed by the Parkinson disease-linked VPS35(D620N) mutation', *Curr Biol*, 24: 1670-76.

McKee, A. C., B. E. Gavett, R. A. Stern, C. J. Nowinski, R. C. Cantu, N. W. Kowall, D. P. Perl, E. T. Hedley-Whyte, B. Price, C. Sullivan, P. Morin, H. S. Lee, C. A. Kubilus, D. H. Daneshvar, M. Wulff, and A. E. Budson. 2010. 'TDP-43 proteinopathy and motor neuron disease in chronic traumatic encephalopathy', *J Neuropathol Exp Neurol*, 69: 918-29.

McNally, K. E., R. Faulkner, F. Steinberg, M. Gallon, R. Ghai, D. Pim, P. Langton, N. Pearson, C. M. Danson, H. Nagele, L. L. Morris, A. Singla, B. L. Overlee, K. J. Heesom, R. Sessions, L. Banks, B. M. Collins, I. Berger, D. D. Billadeau, E. Burstein, and P. J. Cullen. 2017. 'Retriever is a multiprotein complex for retromer-independent endosomal cargo recycling', *Nat Cell Biol*, 19: 1214-25.

McPherson, P. S., E. P. Garcia, V. I. Slepnev, C. David, X. Zhang, D. Grabs, W. S. Sossin, R. Bauerfeind, Y. Nemoto, and P. De Camilli. 1996. 'A presynaptic inositol-5-phosphatase', *Nature*, 379: 353-7.

Mecozzi, V. J., D. E. Berman, S. Simoes, C. Vetanovetz, M. R. Awal, V. M. Patel, R. T. Schneider, G. A. Petsko, D. Ringe, and S. A. Small. 2014. 'Pharmacological chaperones stabilize retromer to limit APP processing', *Nat Chem Biol*, 10: 443-9.

Mehta, P., W. Kaye, L. Bryan, T. Larson, T. Copeland, J. Wu, O. Muravov, and K. Horton. 2016. 'Prevalence of Amyotrophic Lateral Sclerosis - United States, 2012-2013', *MMWR Surveill Summ*, 65: 1-12.

Meisler, M. H., C. Russ, K. T. Montgomery, M. Greenway, S. Ennis, O. Hardiman, D. A. Figlewicz, N. R. Quenneville, E. Conibear, and R. H. Brown, Jr. 2008. 'Evaluation of the Golgi trafficking protein VPS54 (wobbler) as a candidate for ALS', *Amyotroph Lateral Scler*, 9: 141-8.

Meraviglia, V., A. F. Ulivi, M. Boccazzi, F. Valenza, A. Fratangeli, M. Passafaro, D. Lecca, F. Stagni, A. Giacomini, R. Bartesaghi, M. P. Abbracchio, S. Ceruti, and P. Rosa. 2016. 'SNX27, a protein involved in down syndrome, regulates GPR17 trafficking and oligodendrocyte differentiation', *Glia*, 64: 1437-60.

Metcalf, D. J., A. A. Calvi, MNj Seaman, H. M. Mitchison, and D. F. Cutler. 2008. 'Loss of the Batten disease gene CLN3 prevents exit from the TGN of the mannose 6-phosphate receptor', *Traffic*, 9: 1905-14.

Mettlen, M., D. Loerke, D. Yarar, G. Danuser, and S. L. Schmid. 2010. 'Cargo- and adaptor-specific mechanisms regulate clathrin-mediated endocytosis', *J Cell Biol*, 188: 919-33.

Mettlen, M., M. Stoeber, D. Loerke, C. N. Antonescu, G. Danuser, and S. L. Schmid. 2009. 'Endocytic accessory proteins are functionally distinguished by their differential effects on the maturation of clathrin-coated pits', *Mol Biol Cell*, 20: 3251-60.

Michel, C. H., S. Kumar, D. Pinotsi, A. Tunnacliffe, P. St George-Hyslop, E. Mandelkow, E. M. Mandelkow, C. F. Kaminski, and G. S. Kaminski Schierle. 2014. 'Extracellular monomeric tau protein is sufficient to initiate the spread of tau protein pathology', *J Biol Chem*, 289: 956-67.

Miki, Y., F. Mori, Y. Seino, K. Tanji, T. Yoshizawa, H. Kijima, M. Shoji, and K. Wakabayashi. 2018. 'Colocalization of Bunina bodies and TDP-43 inclusions in a case of sporadic amyotrophic lateral sclerosis with Lewy body-like hyaline inclusions', *Neuropathology*, 38: 521-28.

Millecamps, S., F. Salachas, C. Cazeneuve, P. Gordon, B. Bricka, A. Camuzat, L. Guillot-Noel, O. Russaouen, G. Bruneteau, P. F. Pradat, N. Le Forestier, N. Vandenberghe, V. Danel-Brunaud, N. Guy, C. Thauvin-Robinet, L. Lacomblez, P. Couratier, D. Hannequin, D. Seilhean, I. Le Ber, P. Corcia, W. Camu, A. Brice, G. Rouleau, E. LeGuern, and V. Meininger. 2010. 'SOD1, ANG, VAPB, TARDBP, and FUS mutations in familial amyotrophic lateral sclerosis: genotype-phenotype correlations', *J Med Genet*, 47: 554-60.

Miller, R. G., J. D. Mitchell, M. Lyon, and D. H. Moore. 2007. 'Riluzole for amyotrophic lateral sclerosis (ALS)/motor neuron disease (MND)', *Cochrane Database Syst Rev*: CD001447.

Mir, R., F. Tonelli, P. Lis, T. Macartney, N. K. Polinski, T. N. Martinez, M. Y. Chou, A. J. M. Howden, T. Konig, C. Hotzy, I. Milenkovic, T. Brucke, A. Zimprich, E. Sammler, and D. R. Alessi. 2018. 'The Parkinson's disease VPS35[D620N] mutation enhances LRRK2-mediated Rab protein phosphorylation in mouse and human', *Biochem J*, 475: 1861-83.

Mitsumoto, H., R. M. Santella, X. Liu, M. Bogdanov, J. Zipprich, H. C. Wu, J. Mahata, M. Kilty, K. Bednarz, D. Bell, P. H. Gordon, M. Hornig, M. Mehrazin, A. Naini, M. Flint Beal, and P. Factor-Litvak. 2008. 'Oxidative stress biomarkers in sporadic ALS', *Amyotroph Lateral Scler*, 9: 177-83.

Miura, E., T. Hasegawa, M. Konno, M. Suzuki, N. Sugeno, N. Fujikake, S. Geisler, M. Tabuchi, R. Oshima, A. Kikuchi, T. Baba, K. Wada, Y. Nagai, A. Takeda, and M. Aoki. 2014. 'VPS35 dysfunction impairs lysosomal degradation of alpha-synuclein and exacerbates neurotoxicity in a Drosophila model of Parkinson's disease', *Neurobiol Dis*, 71: 1-13.

Mizuno, E., K. Kawahata, M. Kato, N. Kitamura, and M. Komada. 2003. 'STAM proteins bind ubiquitinated proteins on the early endosome via the VHS domain and ubiquitin-interacting motif', *Mol Biol Cell*, 14: 3675-89.

Mizuno, E., K. Kobayashi, A. Yamamoto, N. Kitamura, and M. Komada. 2006. 'A deubiquitinating enzyme UBPY regulates the level of protein ubiquitination on endosomes', *Traffic*, 7: 1017-31.

Mizuno, Y., Y. Fujita, M. Takatama, and K. Okamoto. 2011. 'Peripherin partially localizes in Bunina bodies in amyotrophic lateral sclerosis', *J Neurol Sci*, 302: 14-8.

Mizushima, N., A. Kuma, Y. Kobayashi, A. Yamamoto, M. Matsubae, T. Takao, T. Natsume, Y. Ohsumi, and T. Yoshimori. 2003. 'Mouse Apg16L, a novel WD-repeat protein, targets to the autophagic isolation membrane with the Apg12-Apg5 conjugate', *J Cell Sci*, 116: 1679-88.

Mizushima, N., H. Sugita, T. Yoshimori, and Y. Ohsumi. 1998. 'A new protein conjugation system in human. The counterpart of the yeast Apg12p conjugation system essential for autophagy', *J Biol Chem*, 273: 33889-92.

Mizutani, T., S. Sakamaki, N. Tsuchiya, S. Kamei, H. Kohzu, R. Horiuchi, M. Ida, R. Shiozawa, and T. Takasu. 1992. 'Amyotrophic lateral sclerosis with ophthalmoplegia and multisystem degeneration in patients on long-term use of respirators', *Acta Neuropathol*, 84: 372-7.

Mori, F., Y. Miki, K. Tanji, A. Kakita, H. Takahashi, J. Utsumi, H. Sasaki, and K. Wakabayashi. 2015. 'Sortilin-related receptor CNS expressed 2 (SorCS2) is localized to Bunina bodies in amyotrophic lateral sclerosis', *Neurosci Lett*, 608: 6-11.

Mori, K., S. Lammich, I. R. Mackenzie, I. Forne, S. Zilow, H. Kretzschmar, D. Edbauer, J. Janssens, G. Kleinberger, M. Cruts, J. Herms, M. Neumann, C. Van Broeckhoven, T. Arzberger, and C. Haass. 2013. 'hnRNP A3 binds to GGGGCC repeats and is a constituent of p62-positive/TDP43-negative inclusions in the hippocampus of patients with C9orf72 mutations', *Acta Neuropathol*, 125: 413-23.

Morotz, G. M., K. J. De Vos, A. Vagnoni, S. Ackerley, C. E. Shaw, and C. C. Miller. 2012. 'Amyotrophic lateral sclerosis-associated mutant VAPBP56S perturbs calcium homeostasis to disrupt axonal transport of mitochondria', *Hum Mol Genet*, 21: 1979-88.

Morrice, J. R., C. Y. Gregory-Evans, and C. A. Shaw. 2018. 'Animal models of amyotrophic lateral sclerosis: A comparison of model validity', *Neural Regen Res*, 13: 2050-54.

Moser, J. M., P. Bigini, and T. Schmitt-John. 2013. 'The wobbler mouse, an ALS animal model', *Mol Genet Genomics*, 288: 207-29.

Muhammad, A., I. Flores, H. Zhang, R. Yu, A. Staniszewski, E. Planel, M. Herman, L. Ho, R. Kreber, L. S. Honig, B. Ganetzky, K. Duff, O. Arancio, and S. A. Small. 2008. 'Retromer deficiency observed in Alzheimer's disease causes hippocampal dysfunction, neurodegeneration, and Abeta accumulation', *Proc Natl Acad Sci U S A*, 105: 7327-32.

Munch, C., and A. Bertolotti. 2011. 'Self-propagation and transmission of misfolded mutant SOD1: prion or prion-like phenomenon?', *Cell Cycle*, 10: 1711.

Munsie, L. N., A. J. Milnerwood, P. Seibler, D. A. Beccano-Kelly, I. Tatarnikov, J. Khinda, M. Volta, C. Kadgien, L. P. Cao, L. Tapia, C. Klein, and M. J. Farrer. 2015. 'Retromer-dependent neurotransmitter receptor trafficking to synapses is altered by the Parkinson's disease VPS35 mutation p.D620N', *Hum Mol Genet*, 24: 1691-703.

Murayama, S., K. Inoue, H. Kawakami, T. W. Bouldin, and K. Suzuki. 1991. 'A unique pattern of astrocytosis in the primary motor area in amyotrophic lateral sclerosis', *Acta Neuropathol*, 82: 456-61.

Murphy, J. M., R. G. Henry, S. Langmore, J. H. Kramer, B. L. Miller, and C. Lomen-Hoerth. 2007. 'Continuum of frontal lobe impairment in amyotrophic lateral sclerosis', *Arch Neurol*, 64: 530-4.

Murphy, M., S. Quinn, J. Young, P. Parkin, and B. Taylor. 2008. 'Increasing incidence of ALS in Canterbury, New Zealand: a 22-year study', *Neurology*, 71: 1889-95.

Musa, G., A. Slachevsky, C. Munoz-Neira, C. Mendez, R. Villagra, C. Gonzalez-Billault, A. Ibanez, M. Hornberger, and P. Lillo. 2019. 'Alzheimer's Disease or Behavioral Variant Frontotemporal Dementia? Review of Key Points Toward an Accurate Clinical and Neuropsychological Diagnosis', *J Alzheimers Dis*.

Nagai, M., D. B. Re, T. Nagata, A. Chalazonitis, T. M. Jessell, H. Wichterle, and S. Przedborski. 2007. 'Astrocytes expressing ALS-linked mutated SOD1 release factors selectively toxic to motor neurons', *Nat Neurosci*, 10: 615-22.

Nakashima-Yasuda, H., K. Uryu, J. Robinson, S. X. Xie, H. Hurtig, J. E. Duda, S. E. Arnold, A. Siderowf, M. Grossman, J. B. Leverenz, R. Woltjer, O. L. Lopez, R. Hamilton, D. W. Tsuang, D. Galasko, E. Masliah, J. Kaye, C. M. Clark, T. J. Montine, V. M. Lee, and J. Q. Trojanowski. 2007. 'Co-morbidity of TDP-43 proteinopathy in Lewy body related diseases', *Acta Neuropathol*, 114: 221-9.

Nakatogawa, H., K. Suzuki, Y. Kamada, and Y. Ohsumi. 2009. 'Dynamics and diversity in autophagy mechanisms: lessons from yeast', *Nat Rev Mol Cell Biol*, 10: 458-67.

Nakaya, T., P. Alexiou, M. Maragkakis, A. Chang, and Z. Mourelatos. 2013. 'FUS regulates genes coding for RNA-binding proteins in neurons by binding to their highly conserved introns', *RNA*, 19: 498-509.

Nandez, R., D. M. Balkin, M. Messa, L. Liang, S. Paradise, H. Czapla, M. Y. Hein, J. S. Duncan, M. Mann, and P. De Camilli. 2014. 'A role of OCRL in clathrin-coated pit dynamics and uncoating revealed by studies of Lowe syndrome cells', *Elife*, 3: e02975.

Nanou, A., A. Higginbottom, C. F. Valori, M. Wyles, K. Ning, P. Shaw, and M. Azzouz. 2013. 'Viral delivery of antioxidant genes as a therapeutic strategy in experimental models of amyotrophic lateral sclerosis', *Mol Ther*, 21: 1486-96.

Narayanan, N. S., R. L. Rodnitzky, and E. Y. Uc. 2013. 'Prefrontal dopamine signaling and cognitive symptoms of Parkinson's disease', *Rev Neurosci*, 24: 267-78.

Nardo, G., M. C. Trolese, M. Tortarolo, A. Vallarola, M. Freschi, L. Pasetto, V. Bonetto, and C. Bendotti. 2016. 'New Insights on the Mechanisms of Disease Course Variability in ALS from Mutant SOD1 Mouse Models', *Brain Pathol*, 26: 237-47.

Nassif, M., V. Valenzuela, D. Rojas-Rivera, R. Vidal, S. Matus, K. Castillo, Y. Fuentealba, G. Kroemer, B. Levine, and C. Hetz. 2014. 'Pathogenic role of BECN1/Beclin 1 in the development of amyotrophic lateral sclerosis', *Autophagy*, 10: 1256-71.

Neef, D. W., A. M. Jaeger, and D. J. Thiele. 2011. 'Heat shock transcription factor 1 as a therapeutic target in neurodegenerative diseases', *Nat Rev Drug Discov*, 10: 930-44.

Nguyen, H. P., C. Van Broeckhoven, and J. van der Zee. 2018. 'ALS Genes in the Genomic Era and their Implications for FTD', *Trends Genet*, 34: 404-23.

Nicholls, D. G., and S. L. Budd. 2000. 'Mitochondria and neuronal survival', *Physiol Rev*, 80: 315-60.

Nickerson, D. P., M. R. Russell, and G. Odorizzi. 2007. 'A concentric circle model of multivesicular body cargo sorting', *EMBO Rep*, 8: 644-50.

Nicolas, A., K. P. Kenna, A. E. Renton, N. Ticozzi, F. Faghri, R. Chia, J. A. Dominov, B. J. Kenna, M. A. Nalls, P. Keagle, A. M. Rivera, W. van Rheenen, N. A. Murphy, Jjfa van Vugt, J. T. Geiger, R. A. Van der Spek, H. A. Pliner, Shankaracharya, B. N. Smith, G. Marangi, S. D. Topp, Y. Abramzon, A. S. Gkazi, J. D. Eicher, A. Kenna, G. Mora, A. Calvo, L. Mazzini, N. Riva, J. Mandrioli, C. Caponnetto, S. Battistini, P. Volanti, V. La Bella, F. L. Conforti, G. Borghero, S. Messina, I. L. Simone, F. Trojsi, F. Salvi, F. O. Logullo, S. D'Alfonso, L. Corrado, M. Capasso, L. Ferrucci, C. A. M. Moreno, S. Kamalakaran, D. B. Goldstein, A.

D. Gitler, T. Harris, R. M. Myers, H. Phatnani, R. L. Musunuri, U. S. Evani, A. Abhyankar, M. C. Zody, J. Kaye, S. Finkbeiner, S. K. Wyman, A. LeNail, L. Lima, E. Fraenkel, C. N. Svendsen, L. M. Thompson, J. E. Van Eyk, J. D. Berry, T. M. Miller, S. J. Kolb, M. Cudkowicz, E. Baxi, M. Benatar, J. P. Taylor, E. Rampersaud, G. Wu, J. Wuu, G. Lauria, F. Verde, I. Fogh, C. Tiloca, G. P. Comi, G. Soraru, C. Cereda, P. Corcia, H. Laaksovirta, L. Myllykangas, L. Jansson, M. Valori, J. Ealing, H. Hamdalla, S. Rollinson, S. Pickering-Brown, R. W. Orrell, K. C. Sidle, A. Malaspina, J. Hardy, A. B. Singleton, J. O. Johnson, S. Arepalli, P. C. Sapp, D. McKenna-Yasek, M. Polak, S. Asress, S. Al-Sarraj, A. King, C. Troakes, C. Vance, J. de Belleroche, F. Baas, Alma Ten Asbroek, J. L. Munoz-Blanco, D. G. Hernandez, J. Ding, J. R. Gibbs, S. W. Scholz, M. K. Floeter, R. H. Campbell, F. Landi, R. Bowser, S. M. Pulst, J. M. Ravits, D. J. L. MacGowan, J. Kirby, E. P. Pioro, R. Pamphlett, J. Broach, G. Gerhard, T. L. Dunckley, C. B. Brady, N. W. Kowall, J. C. Troncoso, I. Le Ber, K. Mouzat, S. Lumbroso, T. D. Heiman-Patterson, F. Kamel, L. Van Den Bosch, R. H. Baloh, T. M. Strom, T. Meitinger, A. Shatunov, K. R. Van Eijk, M. de Carvalho, M. Kooyman, B. Middelkoop, M. Moisse, R. L. McLaughlin, M. A. Van Es, M. Weber, K. B. Boylan, M. Van Blitterswijk, R. Rademakers, K. E. Morrison, A. N. Basak, J. S. Mora, V. E. Drory, P. J. Shaw, M. R. Turner, K. Talbot, O. Hardiman, K. L. Williams, J. A. Fifita, G. A. Nicholson, I. P. Blair, G. A. Rouleau, J. Esteban-Perez, A. Garcia-Redondo, A. Al-Chalabi, E. Rogaeva, L. Zinman, L. W. Ostrow, N. J. Maragakis, J. D. Rothstein, Z. Simmons, J. Cooper-Knock, A. Brice, S. A. Goutman, E. L. Feldman, S. B. Gibson, F. Taroni, A. Ratti, C. Gellera, P. Van Damme, W. Robberecht, P. Fratta, M. Sabatelli, C. Lunetta, A. C. Ludolph, P. M. Andersen, J. H. Weishaupt, W. Camu, J. Q. Trojanowski, V. M. Van Deerlin, R. H. Brown, Jr., L. H. van den Berg, J. H. Veldink, M. B. Harms, J. D. Glass, D. J. Stone, P. Tienari, V. Silani, A. Chio, C. E. Shaw, B. J. Traynor, and J. E. Landers. 2018. 'Genome-wide Analyses Identify KIF5A as a Novel ALS Gene', *Neuron*, 97: 1268-83.e6.

Nielsen, M. S., P. Madsen, E. I. Christensen, A. Nykjaer, J. Gliemann, D. Kasper, R. Pohlmann, and C. M. Petersen. 2001. 'The sortilin cytoplasmic tail conveys Golgi-endosome transport and binds the VHS domain of the GGA2 sorting protein', *EMBO J*, 20: 2180-90.

Nikolac Perkovic, M., and N. Pivac. 2019. 'Genetic Markers of Alzheimer's Disease', *Adv Exp Med Biol*, 1192: 27-52.

Nishimura, A. L., M. Mitne-Neto, H. C. Silva, A. Richieri-Costa, S. Middleton, D. Cascio, F. Kok, J. R. Oliveira, T. Gillingwater, J. Webb, P. Skehel, and M. Zatz. 2004. 'A mutation in the vesicle-trafficking protein VAPB causes late-onset spinal muscular atrophy and amyotrophic lateral sclerosis', *Am J Hum Genet*, 75: 822-31.

Noda, T., and Y. Ohsumi. 1998. 'Tor, a phosphatidylinositol kinase homologue, controls autophagy in yeast', *J Biol Chem*, 273: 3963-6.

Nodera, H., N. Takamatsu, Y. Shimatani, A. Mori, K. Sato, M. Oda, Y. Terasawa, Y. Izumi, and R. Kaji. 2014. 'Thinning of cervical nerve roots and peripheral nerves in ALS as measured by sonography', *Clin Neurophysiol*, 125: 1906-11.

Nomura, T., S. Watanabe, K. Kaneko, K. Yamanaka, N. Nukina, and Y. Furukawa. 2014. 'Intranuclear aggregation of mutant FUS/TLS as a molecular pathomechanism of amyotrophic lateral sclerosis', *J Biol Chem*, 289: 1192-202.

Nonaka, T., M. Masuda-Suzukake, T. Arai, Y. Hasegawa, H. Akatsu, T. Obi, M. Yoshida, S. Murayama, D. M. Mann, H. Akiyama, and M. Hasegawa. 2013. 'Prion-like properties of pathological TDP-43 aggregates from diseased brains', *Cell Rep*, 4: 124-34.

Nordmann, M., M. Cabrera, A. Perz, C. Brocker, C. Ostrowicz, S. Engelbrecht-Vandre, and C. Ungermann. 2010. 'The Mon1-Ccz1 complex is the GEF of the late endosomal Rab7 homolog Ypt7', *Curr Biol*, 20: 1654-9.

Novarino, G., A. G. Fenstermaker, M. S. Zaki, M. Hofree, J. L. Silhavy, A. D. Heiberg, M. Abdellateef, B. Rosti, E. Scott, L. Mansour, A. Masri, H. Kayserili, J. Y. Al-Aama, G. M. H. Abdel-Salam, A. Karminejad, M. Kara, B. Kara, B. Bozorgmehri, T. Ben-Omran, F. Mojahedi, I. G. El Din Mahmoud, N. Bouslam, A. Bouhouche, A. Benomar, S. Hanein, L. Raymond, S. Forlani, M. Mascaro, L. Selim, N. Shehata, N. Al-Allawi, P. S. Bindu, M. Azam, M. Gunel, A. Caglayan, K. Bilguvar, A. Tolun, M. Y. Issa, J. Schroth, E. G. Spencer, R. O. Rosti, N. Akizu, K. K. Vaux, A. Johansen, A. A. Koh, H. Megahed, A. Durr, A. Brice, G. Stevanin, S. B. Gabriel, T. Ideker, and J. G. Gleeson. 2014. 'Exome sequencing links corticospinal motor neuron disease to common neurodegenerative disorders', *Science*, 343: 506-11.

Nuytemans, K., G. Bademci, V. Inchausti, A. Dressen, D. D. Kinnamon, A. Mehta, L. Wang, S. Zuchner, G. W. Beecham, E. R. Martin, W. K. Scott, and J. M. Vance. 2013. 'Whole exome sequencing of rare variants in EIF4G1 and VPS35 in Parkinson disease', *Neurology*, 80: 982-9.

O'Brien, R. J., and P. C. Wong. 2011. 'Amyloid precursor protein processing and Alzheimer's disease', *Annu Rev Neurosci*, 34: 185-204.

Oakes, J. A., M. C. Davies, and M. O. Collins. 2017. 'TBK1: a new player in ALS linking autophagy and neuroinflammation', *Mol Brain*, 10: 5.

Oakes, S. A., and F. R. Papa. 2015. 'The role of endoplasmic reticulum stress in human pathology', *Annu Rev Pathol*, 10: 173-94.

Offe, K., S. E. Dodson, J. T. Shoemaker, J. J. Fritz, M. Gearing, A. I. Levey, and J. J. Lah. 2006. 'The lipoprotein receptor LR11 regulates amyloid beta production and amyloid precursor protein traffic in endosomal compartments', *J Neurosci*, 26: 1596-603.

Ohya, T., M. Miaczynska, U. Coskun, B. Lommer, A. Runge, D. Drechsel, Y. Kalaidzidis, and M. Zerial. 2009. 'Reconstitution of Rab- and SNARE-dependent membrane fusion by synthetic endosomes', *Nature*, 459: 1091-7.

Okamoto, K., S. Hirai, M. Amari, M. Watanabe, and A. Sakurai. 1993. 'Bunina bodies in amyotrophic lateral sclerosis immunostained with rabbit anti-cystatin C serum', *Neurosci Lett*, 162: 125-8.

Okamoto, K., S. Hirai, M. Shoji, Y. Senoh, and T. Yamazaki. 1990. 'Axonal swellings in the corticospinal tracts in amyotrophic lateral sclerosis', *Acta Neuropathol*, 80: 222-6.

Okamoto, K., Y. Mizuno, and Y. Fujita. 2008. 'Bunina bodies in amyotrophic lateral sclerosis', *Neuropathology*, 28: 109-15.

Olivan, S., A. C. Calvo, A. Rando, M. J. Munoz, P. Zaragoza, and R. Osta. 2015. 'Comparative study of behavioural tests in the SOD1G93A mouse model of amyotrophic lateral sclerosis', *Exp Anim*, 64: 147-53.

Ollila, H. M., P. Soronen, K. Silander, O. M. Palo, T. Kieseppa, M. A. Kaunisto, J. Lonnqvist, L. Peltonen, T. Partonen, and T. Paunio. 2009. 'Findings from bipolar disorder genome-wide association studies replicate in a Finnish bipolar family-cohort', *Mol Psychiatry*, 14: 351-3.

Olmos-Serrano, J. L., H. J. Kang, W. A. Tyler, J. C. Silbereis, F. Cheng, Y. Zhu, M. Pletikos, L. Jankovic-Rapan, N. P. Cramer, Z. Galdzicki, J. Goodliffe, A. Peters, C. Sethares, I. Delalle, J. A. Golden, T. F. Haydar, and N. Sestan. 2016. 'Down Syndrome Developmental Brain

Transcriptome Reveals Defective Oligodendrocyte Differentiation and Myelination', *Neuron*, 89: 1208-22.

'OMIM Phenotypic Series - PS303350'. https://omim.org/phenotypicSeries/PS303350.

Orlacchio, A., C. Babalini, A. Borreca, C. Patrono, R. Massa, S. Basaran, R. P. Munhoz, E. A. Rogaeva, P. H. St George-Hyslop, G. Bernardi, and T. Kawarai. 2010. 'SPATACSIN mutations cause autosomal recessive juvenile amyotrophic lateral sclerosis', *Brain*, 133: 591-8.

Orsi, A., M. Razi, H. C. Dooley, D. Robinson, A. E. Weston, L. M. Collinson, and S. A. Tooze. 2012. 'Dynamic and transient interactions of Atg9 with autophagosomes, but not membrane integration, are required for autophagy', *Mol Biol Cell*, 23: 1860-73.

Ostrowski, L. A., A. C. Hall, and K. Mekhail. 2017. 'Ataxin-2: From RNA Control to Human Health and Disease', *Genes (Basel)*, 8.

Otsmane, B., J. Aebischer, A. Moumen, and C. Raoul. 2014. 'Cerebrospinal fluid-targeted delivery of neutralizing anti-IFNgamma antibody delays motor decline in an ALS mouse model', *Neuroreport*, 25: 49-54.

Oyanagi, K., M. Yamazaki, H. Takahashi, K. Watabe, M. Wada, T. Komori, T. Morita, and T. Mizutani. 2008. 'Spinal anterior horn cells in sporadic amyotrophic lateral sclerosis show ribosomal detachment from, and cisternal distention of the rough endoplasmic reticulum', *Neuropathol Appl Neurobiol*, 34: 650-8.

Paisan-Ruiz, C., P. A. Lewis, and A. B. Singleton. 2013. 'LRRK2: cause, risk, and mechanism', *J Parkinsons Dis*, 3: 85-103.

Palmisano, R., P. Golfi, P. Heimann, C. Shaw, C. Troakes, T. Schmitt-John, and J. W. Bartsch. 2011. 'Endosomal accumulation of APP in wobbler motor neurons reflects impaired vesicle trafficking: implications for human motor neuron disease', *BMC Neurosci*, 12: 24.

Panzeri, C., C. De Palma, A. Martinuzzi, A. Daga, G. De Polo, N. Bresolin, C. C. Miller, E. L. Tudor, E. Clementi, and M. T. Bassi. 2006. 'The first ALS2 missense mutation associated with JPLS reveals new aspects of alsin biological function', *Brain*, 129: 1710-9.

Papadeas, S. T., S. E. Kraig, C. O'Banion, A. C. Lepore, and N. J. Maragakis. 2011. 'Astrocytes carrying the superoxide dismutase 1 (SOD1G93A) mutation induce wild-type motor neuron degeneration in vivo', *Proc Natl Acad Sci U S A*, 108: 17803-8.

Parkinson, N., P. G. Ince, M. O. Smith, R. Highley, G. Skibinski, P. M. Andersen, K. E. Morrison, H. S. Pall, O. Hardiman, J. Collinge, P. J. Shaw, and E. M. Fisher. 2006. 'ALS phenotypes with mutations in CHMP2B (charged multivesicular body protein 2B)', *Neurology*, 67: 1074-7.

Parvathy, S., I. Hussain, E. H. Karran, A. J. Turner, and N. M. Hooper. 1999. 'Cleavage of Alzheimer's amyloid precursor protein by alpha-secretase occurs at the surface of neuronal cells', *Biochemistry*, 38: 9728-34.

Pashkova, N., L. Gakhar, S. C. Winistorfer, A. B. Sunshine, M. Rich, M. J. Dunham, L. Yu, and R. C. Piper. 2013. 'The yeast Alix homolog Bro1 functions as a ubiquitin receptor for protein sorting into multivesicular endosomes', *Dev Cell*, 25: 520-33.

Pasinelli, P., and R. H. Brown. 2006. 'Molecular biology of amyotrophic lateral sclerosis: insights from genetics', *Nat Rev Neurosci*, 7: 710-23.

Pasqualato, S., F. Senic-Matuglia, L. Renault, B. Goud, J. Salamero, and J. Cherfils. 2004. 'The structural GDP/GTP cycle of Rab11 reveals a novel interface involved in the dynamics of recycling endosomes', *J Biol Chem*, 279: 11480-8.

Pearse, B. M. 1975. 'Coated vesicles from pig brain: purification and biochemical characterization', *J Mol Biol*, 97: 93-8.

Perez-Victoria, F. J., G. Abascal-Palacios, I. Tascon, A. Kajava, J. G. Magadan, E. P. Pioro, J. S. Bonifacino, and A. Hierro. 2010. 'Structural basis for the wobbler mouse neurodegenerative disorder caused by mutation in the Vps54 subunit of the GARP complex', *Proc Natl Acad Sci U S A*, 107: 12860-5.

Perez-Victoria, F. J., G. A. Mardones, and J. S. Bonifacino. 2008. 'Requirement of the human GARP complex for mannose 6-phosphate-receptor-dependent sorting of cathepsin D to lysosomes', *Mol Biol Cell*, 19: 2350-62.

Perini, E. D., R. Schaefer, M. Stoter, Y. Kalaidzidis, and M. Zerial. 2014. 'Mammalian CORVET is required for fusion and conversion of distinct early endosome subpopulations', *Traffic*, 15: 1366-89.

Peviani, M., M. Tortarolo, E. Battaglia, R. Piva, and C. Bendotti. 2014. 'Specific induction of Akt3 in spinal cord motor neurons is neuroprotective in a mouse model of familial amyotrophic lateral sclerosis', *Mol Neurobiol*, 49: 136-48.

Phatnani, H. P., P. Guarnieri, B. A. Friedman, M. A. Carrasco, M. Muratet, S. O'Keeffe, C. Nwakeze, F. Pauli-Behn, K. M. Newberry, S. K. Meadows, J. C. Tapia, R. M. Myers, and T. Maniatis. 2013. 'Intricate interplay between astrocytes and motor neurons in ALS', *Proc Natl Acad Sci U S A*, 110: E756-65.

Phillips-Krawczak, C. A., A. Singla, P. Starokadomskyy, Z. Deng, D. G. Osborne, H. Li, C. J. Dick, T. S. Gomez, M. Koenecke, J. S. Zhang, H. Dai, L. F. Sifuentes-Dominguez, L. N. Geng, S. H. Kaufmann, M. Y. Hein, M. Wallis, J. McGaughran, J. Gecz, Bv Sluis, D. D. Billadeau, and E. Burstein. 2015. 'COMMD1 is linked to the WASH complex and regulates endosomal trafficking of the copper transporter ATP7A', *Mol Biol Cell*, 26: 91-103.

Philtjens, S., S. Van Mossevelde, J. van der Zee, E. Wauters, L. Dillen, M. Vandenbulcke, R. Vandenberghe, A. Ivanoiu, A. Sieben, C. Willems, L. Benussi, R. Ghidoni, G. Binetti, B. Borroni, A. Padovani, P. Pastor, M. Diez-Fairen, M. Aguilar, A. de Mendonca, G. Miltenberger-Miltenyi, I. Hernandez, M. Boada, A. Ruiz, B. Nacmias, S. Sorbi, M. R. Almeida, I. Santana, J. Clarimon, A. Lleo, G. B. Frisoni, R. Sanchez-Valle, A. Llado, E. Gomez-Tortosa, E. Gelpi, M. Van den Broeck, K. Peeters, P. Cras, P. P. De Deyn, S. Engelborghs, M. Cruts, and C. Van Broeckhoven. 2018. 'Rare nonsynonymous variants in SORT1 are associated with increased risk for frontotemporal dementia', *Neurobiol Aging*, 66: 181.e3-81.e10.

Piao, Y. S., K. Wakabayashi, A. Kakita, M. Yamada, S. Hayashi, T. Morita, F. Ikuta, K. Oyanagi, and H. Takahashi. 2003. 'Neuropathology with clinical correlations of sporadic amyotrophic lateral sclerosis: 102 autopsy cases examined between 1962 and 2000', *Brain Pathol*, 13: 10-22.

Pires, R., B. Hartlieb, L. Signor, G. Schoehn, S. Lata, M. Roessle, C. Moriscot, S. Popov, A. Hinz, M. Jamin, V. Boyer, R. Sadoul, E. Forest, D. I. Svergun, H. G. Gottlinger, and W. Weissenhorn. 2009. 'A crescent-shaped ALIX dimer targets ESCRT-III CHMP4 filaments', *Structure*, 17: 843-56.

Polymenidou, M., C. Lagier-Tourenne, K. R. Hutt, S. C. Huelga, J. Moran, T. Y. Liang, S. C. Ling, E. Sun, E. Wancewicz, C. Mazur, H. Kordasiewicz, Y. Sedaghat, J. P. Donohue, L. Shiue, C. F. Bennett, G. W. Yeo, and D. W. Cleveland. 2011. 'Long pre-mRNA depletion and RNA missplicing contribute to neuronal vulnerability from loss of TDP-43', *Nat Neurosci*, 14: 459-68.

Posor, Y., M. Eichhorn-Gruenig, D. Puchkov, J. Schoneberg, A. Ullrich, A. Lampe, R. Muller, S. Zarbakhsh, F. Gulluni, E. Hirsch, M. Krauss, C. Schultz, J. Schmoranzer, F. Noe, and V. Haucke. 2013. 'Spatiotemporal control of endocytosis by phosphatidylinositol-3,4-bisphosphate', *Nature*, 499: 233-7.

Postuma, R. B., D. Berg, M. Stern, W. Poewe, C. W. Olanow, W. Oertel, J. Obeso, K. Marek, I. Litvan, A. E. Lang, G. Halliday, C. G. Goetz, T. Gasser, B. Dubois, P. Chan, B. R. Bloem, C. H. Adler, and G. Deuschl. 2015. 'MDS clinical diagnostic criteria for Parkinson's disease', *Mov Disord*, 30: 1591-601.

Poteryaev, D., S. Datta, K. Ackema, M. Zerial, and A. Spang. 2010. 'Identification of the switch in early-to-late endosome transition', *Cell*, 141: 497-508.

Poteryaev, D., H. Fares, B. Bowerman, and A. Spang. 2007. 'Caenorhabditis elegans SAND-1 is essential for RAB-7 function in endosomal traffic', *EMBO J*, 26: 301-12.

Prasad, A., V. Bharathi, V. Sivalingam, A. Girdhar, and B. K. Patel. 2019. 'Molecular Mechanisms of TDP-43 Misfolding and Pathology in Amyotrophic Lateral Sclerosis', *Front Mol Neurosci*, 12: 25.

Priya, A., I. V. Kalaidzidis, Y. Kalaidzidis, D. Lambright, and S. Datta. 2015. 'Molecular insights into Rab7-mediated endosomal recruitment of core retromer: deciphering the role of Vps26 and Vps35', *Traffic*, 16: 68-84.

Priya, A., J. Sugatha, S. Parveen, S. Lacas-Gervais, P. Raj, J. Gilleron, and S. Datta. 2017. 'Essential and selective role of SNX12 in transport of endocytic and retrograde cargo', *J Cell Sci*, 130: 2707-21.

Prudencio, M., K. R. Jansen-West, W. C. Lee, T. F. Gendron, Y. J. Zhang, Y. F. Xu, J. Gass, C. Stuani, C. Stetler, R. Rademakers, D. W. Dickson, E. Buratti, and L. Petrucelli. 2012. 'Misregulation of human sortilin splicing leads to the generation of a nonfunctional progranulin receptor', *Proc Natl Acad Sci U S A*, 109: 21510-5.

Puri, C., M. Renna, C. F. Bento, K. Moreau, and D. C. Rubinsztein. 2013. 'Diverse autophagosome membrane sources coalesce in recycling endosomes', *Cell*, 154: 1285-99.

Qian, K., H. Huang, A. Peterson, B. Hu, N. J. Maragakis, G. L. Ming, H. Chen, and S. C. Zhang. 2017. 'Sporadic ALS Astrocytes Induce Neuronal Degeneration In Vivo', *Stem Cell Reports*, 8: 843-55.

Raiborg, C., K. G. Bache, D. J. Gillooly, I. H. Madshus, E. Stang, and H. Stenmark. 2002. 'Hrs sorts ubiquitinated proteins into clathrin-coated microdomains of early endosomes', *Nat Cell Biol*, 4: 394-8.

Raiborg, C., B. Bremnes, A. Mehlum, D. J. Gillooly, A. D'Arrigo, E. Stang, and H. Stenmark. 2001. 'FYVE and coiled-coil domains determine the specific localisation of Hrs to early endosomes', *J Cell Sci*, 114: 2255-63.

Raiborg, C., and H. Stenmark. 2009. 'The ESCRT machinery in endosomal sorting of ubiquitylated membrane proteins', *Nature*, 458: 445-52.

Rajagopalan, V., Z. Liu, D. Allexandre, L. Zhang, X. F. Wang, E. P. Pioro, and G. H. Yue. 2013. 'Brain white matter shape changes in amyotrophic lateral sclerosis (ALS): a fractal dimension study', *PLoS One*, 8: e73614.

Raposo, G., and W. Stoorvogel. 2013. 'Extracellular vesicles: exosomes, microvesicles, and friends', *J Cell Biol*, 200: 373-83.

Ravikumar, B., K. Moreau, L. Jahreiss, C. Puri, and D. C. Rubinsztein. 2010. 'Plasma membrane contributes to the formation of pre-autophagosomal structures', *Nat Cell Biol*, 12: 747-57.

Re, D. B., V. Le Verche, C. Yu, M. W. Amoroso, K. A. Politi, S. Phani, B. Ikiz, L. Hoffmann, M. Koolen, T. Nagata, D. Papadimitriou, P. Nagy, H. Mitsumoto, S. Kariya, H. Wichterle, C. E. Henderson, and S. Przedborski. 2014. 'Necroptosis drives motor neuron death in models of both sporadic and familial ALS', *Neuron*, 81: 1001-08.

Reitz, C. 2018. 'Retromer Dysfunction and Neurodegenerative Disease', *Curr Genomics*, 19: 279-88.

Reitz, C., G. Tosto, B. Vardarajan, E. Rogaeva, M. Ghani, R. S. Rogers, C. Conrad, J. L. Haines, M. A. Pericak-Vance, M. D. Fallin, T. Foroud, L. A. Farrer, G. D. Schellenberg, P. S. George-Hyslop, and R. Mayeux. 2013. 'Independent and epistatic effects of variants in VPS10-d receptors on Alzheimer disease risk and processing of the amyloid precursor protein (APP)', *Transl Psychiatry*, 3: e256.

Ren, M., G. Xu, J. Zeng, C. De Lemos-Chiarandini, M. Adesnik, and D. D. Sabatini. 1998. 'Hydrolysis of GTP on rab11 is required for the direct delivery of transferrin from the pericentriolar recycling compartment to the cell surface but not from sorting endosomes', *Proc Natl Acad Sci U S A*, 95: 6187-92.

Ren, X., and J. H. Hurley. 2010. 'VHS domains of ESCRT-0 cooperate in high-avidity binding to polyubiquitinated cargo', *EMBO J*, 29: 1045-54.

Renton, A. E., A. Chio, and B. J. Traynor. 2014. 'State of play in amyotrophic lateral sclerosis genetics', *Nat Neurosci*, 17: 17-23.

Renton, A. E., E. Majounie, A. Waite, J. Simon-Sanchez, S. Rollinson, J. R. Gibbs, J. C. Schymick, H. Laaksovirta, J. C. van Swieten, L. Myllykangas, H. Kalimo, A. Paetau, Y. Abramzon, A. M. Remes, A. Kaganovich, S. W. Scholz, J. Duckworth, J. Ding, D. W. Harmer, D. G. Hernandez, J. O. Johnson, K. Mok, M. Ryten, D. Trabzuni, R. J. Guerreiro, R. W. Orrell, J. Neal, A. Murray, J. Pearson, I. E. Jansen, D. Sondervan, H. Seelaar, D. Blake, K. Young, N. Halliwell, J. B. Callister, G. Toulson, A. Richardson, A. Gerhard, J. Snowden, D. Mann, D. Neary, M. A. Nalls, T. Peuralinna, L. Jansson, V. M. Isoviita, A. L. Kaivorinne, M. Holtta-Vuori, E. Ikonen, R. Sulkava, M. Benatar, J. Wuu, A. Chio, G. Restagno, G. Borghero, M. Sabatelli, D. Heckerman, E. Rogaeva, L. Zinman, J. D. Rothstein, M. Sendtner, C. Drepper, E. E. Eichler, C. Alkan, Z. Abdullaev, S. D. Pack, A. Dutra, E. Pak, J. Hardy, A. Singleton, N. M. Williams, P. Heutink, S. Pickering-Brown, H. R. Morris, P. J. Tienari, and B. J. Traynor. 2011. 'A hexanucleotide repeat expansion in C9ORF72 is the cause of chromosome 9p21-linked ALS-FTD', *Neuron*, 72: 257-68.

Rink, J., E. Ghigo, Y. Kalaidzidis, and M. Zerial. 2005. 'Rab conversion as a mechanism of progression from early to late endosomes', *Cell*, 122: 735-49.

Robinson, F. L., and J. E. Dixon. 2006. 'Myotubularin phosphatases: policing 3-phosphoinositides', *Trends Cell Biol*, 16: 403-12.

Robinson, J. L., F. Geser, A. Stieber, M. Umoh, L. K. Kwong, V. M. Van Deerlin, V. M. Lee, and J. Q. Trojanowski. 2013. 'TDP-43 skeins show properties of amyloid in a subset of ALS cases', *Acta Neuropathol*, 125: 121-31.

Robinson, M. B. 1998. 'The family of sodium-dependent glutamate transporters: a focus on the GLT-1/EAAT2 subtype', *Neurochem Int*, 33: 479-91.

Roccatagliata, L., L. Bonzano, G. Mancardi, C. Canepa, and C. Caponnetto. 2009. 'Detection of motor cortex thinning and corticospinal tract involvement by quantitative MRI in amyotrophic lateral sclerosis', *Amyotroph Lateral Scler*, 10: 47-52.

Rogaeva, E., Y. Meng, J. H. Lee, Y. Gu, T. Kawarai, F. Zou, T. Katayama, C. T. Baldwin, R. Cheng, H. Hasegawa, F. Chen, N. Shibata, K. L. Lunetta, R. Pardossi-Piquard, C. Bohm,

Y. Wakutani, L. A. Cupples, K. T. Cuenco, R. C. Green, L. Pinessi, I. Rainero, S. Sorbi, A. Bruni, R. Duara, R. P. Friedland, R. Inzelberg, W. Hampe, H. Bujo, Y. Q. Song, O. M. Andersen, T. E. Willnow, N. Graff-Radford, R. C. Petersen, D. Dickson, S. D. Der, P. E. Fraser, G. Schmitt-Ulms, S. Younkin, R. Mayeux, L. A. Farrer, and P. St George-Hyslop. 2007. 'The neuronal sortilin-related receptor SORL1 is genetically associated with Alzheimer disease', *Nat Genet*, 39: 168-77.

Roizen, N. J., and D. Patterson. 2003. 'Down's syndrome', *Lancet*, 361: 1281-9.

Rojas, F., N. Cortes, S. Abarzua, A. Dyrda, and B. van Zundert. 2014. 'Astrocytes expressing mutant SOD1 and TDP43 trigger motoneuron death that is mediated via sodium channels and nitroxidative stress', *Front Cell Neurosci*, 8: 24.

Rojas, R., S. Kametaka, C. R. Haft, and J. S. Bonifacino. 2007. 'Interchangeable but essential functions of SNX1 and SNX2 in the association of retromer with endosomes and the trafficking of mannose 6-phosphate receptors', *Mol Cell Biol*, 27: 1112-24.

Rojas, R., T. van Vlijmen, G. A. Mardones, Y. Prabhu, A. L. Rojas, S. Mohammed, A. J. Heck, G. Raposo, P. van der Sluijs, and J. S. Bonifacino. 2008. 'Regulation of retromer recruitment to endosomes by sequential action of Rab5 and Rab7', *J Cell Biol*, 183: 513-26.

Roland, J. T., A. K. Kenworthy, J. Peranen, S. Caplan, and J. R. Goldenring. 2007. 'Myosin Vb interacts with Rab8a on a tubular network containing EHD1 and EHD3', *Mol Biol Cell*, 18: 2828-37.

Ropers, F., E. Derivery, H. Hu, M. Garshasbi, M. Karbasiyan, M. Herold, G. Nurnberg, R. Ullmann, A. Gautreau, K. Sperling, R. Varon, and A. Rajab. 2011. 'Identification of a novel candidate gene for non-syndromic autosomal recessive intellectual disability: the WASH complex member SWIP', *Hum Mol Genet*, 20: 2585-90.

Rosen, D. R., T. Siddique, D. Patterson, D. A. Figlewicz, P. Sapp, A. Hentati, D. Donaldson, J. Goto, J. P. O'Regan, H. X. Deng, and et al. 1993. 'Mutations in Cu/Zn superoxide dismutase gene are associated with familial amyotrophic lateral sclerosis', *Nature*, 362: 59-62.

Rossi, A., Z. Kontarakis, C. Gerri, H. Nolte, S. Holper, M. Kruger, and D. Y. Stainier. 2015. 'Genetic compensation induced by deleterious mutations but not gene knockdowns', *Nature*, 524: 230-3.

Row, P. E., I. A. Prior, J. McCullough, M. J. Clague, and S. Urbe. 2006. 'The ubiquitin isopeptidase UBPY regulates endosomal ubiquitin dynamics and is essential for receptor down-regulation', *J Biol Chem*, 281: 12618-24.

Rowland, L. P., and N. A. Shneider. 2001. 'Amyotrophic lateral sclerosis', *N Engl J Med*, 344: 1688-700.

Roybon, L., N. J. Lamas, A. D. Garcia, E. J. Yang, R. Sattler, V. J. Lewis, Y. A. Kim, C. A. Kachel, J. D. Rothstein, S. Przedborski, H. Wichterle, and C. E. Henderson. 2013. 'Human stem cell-derived spinal cord astrocytes with defined mature or reactive phenotypes', *Cell Rep*, 4: 1035-48.

Rudnick, N. D., C. J. Griffey, P. Guarnieri, V. Gerbino, X. Wang, J. A. Piersaint, J. C. Tapia, M. M. Rich, and T. Maniatis. 2017. 'Distinct roles for motor neuron autophagy early and late in the SOD1(G93A) mouse model of ALS', *Proc Natl Acad Sci U S A*, 114: E8294-e303.

Ruscher, K., and T. Wieloch. 2015. 'The involvement of the sigma-1 receptor in neurodegeneration and neurorestoration', *J Pharmacol Sci*, 127: 30-5.

Rusten, T. E., and H. Stenmark. 2009. 'How do ESCRT proteins control autophagy?', *J Cell Sci*, 122: 2179-83.

Ryu, H. H., M. H. Jun, K. J. Min, D. J. Jang, Y. S. Lee, H. K. Kim, and J. A. Lee. 2014. 'Autophagy regulates amyotrophic lateral sclerosis-linked fused in sarcoma-positive stress granules in neurons', *Neurobiol Aging*, 35: 2822-31.

Saberi, S., J. E. Stauffer, D. J. Schulte, and J. Ravits. 2015. 'Neuropathology of Amyotrophic Lateral Sclerosis and Its Variants', *Neurol Clin*, 33: 855-76.

Sachse, M., S. Urbe, V. Oorschot, G. J. Strous, and J. Klumperman. 2002. 'Bilayered clathrin coats on endosomal vacuoles are involved in protein sorting toward lysosomes', *Mol Biol Cell*, 13: 1313-28.

'Safety and efficacy of edaravone in well defined patients with amyotrophic lateral sclerosis: a randomised, double-blind, placebo-controlled trial'. 2017. *Lancet Neurol*, 16: 505-12.

Saksena, S., J. Wahlman, D. Teis, A. E. Johnson, and S. D. Emr. 2009. 'Functional reconstitution of ESCRT-III assembly and disassembly', *Cell*, 136: 97-109.

San Gil, R., L. Ooi, J. J. Yerbury, and H. Ecroyd. 2017. 'The heat shock response in neurons and astroglia and its role in neurodegenerative diseases', *Mol Neurodegener*, 12: 65.

Sanhueza, M., A. Chai, C. Smith, B. A. McCray, T. I. Simpson, J. P. Taylor, and G. Pennetta. 2015. 'Network analyses reveal novel aspects of ALS pathogenesis', *PLoS Genet*, 11: e1005107.

Sapp, P. C., B. A. Hosler, D. McKenna-Yasek, W. Chin, A. Gann, H. Genise, J. Gorenstein, M. Huang, W. Sailer, M. Scheffler, M. Valesky, J. L. Haines, M. Pericak-Vance, T. Siddique, H. R. Horvitz, and R. H. Brown, Jr. 2003. 'Identification of two novel loci for dominantly inherited familial amyotrophic lateral sclerosis', *Am J Hum Genet*, 73: 397-403.

Sasaki, S., and M. Iwata. 2007. 'Mitochondrial alterations in the spinal cord of patients with sporadic amyotrophic lateral sclerosis', *J Neuropathol Exp Neurol*, 66: 10-6.

Saxena, S., E. Cabuy, and P. Caroni. 2009. 'A role for motoneuron subtype-selective ER stress in disease manifestations of FALS mice', *Nat Neurosci*, 12: 627-36.

Scekic-Zahirovic, J., O. Sendscheid, H. El Oussini, M. Jambeau, Y. Sun, S. Mersmann, M. Wagner, S. Dieterle, J. Sinniger, S. Dirrig-Grosch, K. Drenner, M. C. Birling, J. Qiu, Y. Zhou, H. Li, X. D. Fu, C. Rouaux, T. Shelkovnikova, A. Witting, A. C. Ludolph, F. Kiefer, E. Storkebaum, C. Lagier-Tourenne, and L. Dupuis. 2016. 'Toxic gain of function from mutant FUS protein is crucial to trigger cell autonomous motor neuron loss', *EMBO J*, 35: 1077-97.

Schafer, I. B., G. G. Hesketh, N. A. Bright, S. R. Gray, P. R. Pryor, P. R. Evans, J. P. Luzio, and D. J. Owen. 2012. 'The binding of Varp to VAMP7 traps VAMP7 in a closed, fusogenically inactive conformation', *Nat Struct Mol Biol*, 19: 1300-9.

Schiffer, D., S. Cordera, P. Cavalla, and A. Migheli. 1996. 'Reactive astrogliosis of the spinal cord in amyotrophic lateral sclerosis', *J Neurol Sci*, 139 Suppl: 27-33.

Schlossman, D. M., S. L. Schmid, W. A. Braell, and J. E. Rothman. 1984. 'An enzyme that removes clathrin coats: purification of an uncoating ATPase', *J Cell Biol*, 99: 723-33.

Schmitt-John, T., C. Drepper, A. Mussmann, P. Hahn, M. Kuhlmann, C. Thiel, M. Hafner, A. Lengeling, P. Heimann, J. M. Jones, M. H. Meisler, and H. Jockusch. 2005. 'Mutation of Vps54 causes motor neuron disease and defective spermiogenesis in the wobbler mouse', *Nat Genet*, 37: 1213-5.

Schroder, M., and R. J. Kaufman. 2005. 'The mammalian unfolded protein response', *Annu Rev Biochem*, 74: 739-89.

Schwenk, B. M., H. Hartmann, A. Serdaroglu, M. H. Schludi, D. Hornburg, F. Meissner, D. Orozco, A. Colombo, S. Tahirovic, M. Michaelsen, F. Schreiber, S. Haupt, M. Peitz, O.

Brustle, C. Kupper, T. Klopstock, M. Otto, A. C. Ludolph, T. Arzberger, P. H. Kuhn, and D. Edbauer. 2016. 'TDP-43 loss of function inhibits endosomal trafficking and alters trophic signaling in neurons', *EMBO J*, 35: 2350-70.

Schwenk, F., U. Baron, and K. Rajewsky. 1995. 'A cre-transgenic mouse strain for the ubiquitous deletion of loxP-flanked gene segments including deletion in germ cells', *Nucleic Acids Res*, 23: 5080-1.

Scotter, E. L., H. J. Chen, and C. E. Shaw. 2015. 'TDP-43 Proteinopathy and ALS: Insights into Disease Mechanisms and Therapeutic Targets', *Neurotherapeutics*, 12: 352-63.

Seaman, M. N. 2005. 'Recycle your receptors with retromer', *Trends Cell Biol*, 15: 68-75.

Seaman, M. N., M. E. Harbour, D. Tattersall, E. Read, and N. Bright. 2009. 'Membrane recruitment of the cargo-selective retromer subcomplex is catalysed by the small GTPase Rab7 and inhibited by the Rab-GAP TBC1D5', *J Cell Sci*, 122: 2371-82.

Seaman, M. N. J., A. S. Mukadam, and S. Y. Breusegem. 2018. 'Inhibition of TBC1D5 activates Rab7a and can enhance the function of the retromer cargo-selective complex', *J Cell Sci*, 131.

Seaman, M. N., E. G. Marcusson, J. L. Cereghino, and S. D. Emr. 1997. 'Endosome to Golgi retrieval of the vacuolar protein sorting receptor, Vps10p, requires the function of the VPS29, VPS30, and VPS35 gene products', *J Cell Biol*, 137: 79-92.

Seaman, MNj, and C. L. Freeman. 2014. 'Analysis of the Retromer complex-WASH complex interaction illuminates new avenues to explore in Parkinson disease', *Commun Integr Biol*, 7: e29483.

Sen, I., A. Nalini, N. B. Joshi, and P. G. Joshi. 2005. 'Cerebrospinal fluid from amyotrophic lateral sclerosis patients preferentially elevates intracellular calcium and toxicity in motor neurons via AMPA/kainate receptor', *J Neurol Sci*, 235: 45-54.

Sevlever, D., P. Jiang, and S. H. Yen. 2008. 'Cathepsin D is the main lysosomal enzyme involved in the degradation of alpha-synuclein and generation of its carboxy-terminally truncated species', *Biochemistry*, 47: 9678-87.

Shan, X., P. M. Chiang, D. L. Price, and P. C. Wong. 2010. 'Altered distributions of Gemini of coiled bodies and mitochondria in motor neurons of TDP-43 transgenic mice', *Proc Natl Acad Sci U S A*, 107: 16325-30.

Sharma, A., A. K. Lyashchenko, L. Lu, S. E. Nasrabady, M. Elmaleh, M. Mendelsohn, A. Nemes, J. C. Tapia, G. Z. Mentis, and N. A. Shneider. 2016. 'ALS-associated mutant FUS induces selective motor neuron degeneration through toxic gain of function', *Nat Commun*, 7: 10465.

Sharma, M., J. P. Ioannidis, J. O. Aasly, G. Annesi, A. Brice, L. Bertram, M. Bozi, M. Barcikowska, D. Crosiers, C. E. Clarke, M. F. Facheris, M. Farrer, G. Garraux, S. Gispert, G. Auburger, C. Vilarino-Guell, G. M. Hadjigeorgiou, A. A. Hicks, N. Hattori, B. S. Jeon, Z. Jamrozik, A. Krygowska-Wajs, S. Lesage, C. M. Lill, J. J. Lin, T. Lynch, P. Lichtner, A. E. Lang, C. Libioulle, M. Murata, V. Mok, B. Jasinska-Myga, G. D. Mellick, K. E. Morrison, T. Meitnger, A. Zimprich, G. Opala, P. P. Pramstaller, I. Pichler, S. S. Park, A. Quattrone, E. Rogaeva, O. A. Ross, L. Stefanis, J. D. Stockton, W. Satake, P. A. Silburn, T. M. Strom, J. Theuns, E. K. Tan, T. Toda, H. Tomiyama, R. J. Uitti, C. Van Broeckhoven, K. Wirdefeldt, Z. Wszolek, G. Xiromerisiou, H. S. Yomono, K. C. Yueh, Y. Zhao, T. Gasser, D. Maraganore, and R. Kruger. 2012. 'A multi-centre clinico-genetic analysis of the VPS35 gene in Parkinson disease indicates reduced penetrance for disease-associated variants', *J Med Genet*, 49: 721-6.

Shaw, P. J., P. G. Ince, G. Falkous, and D. Mantle. 1995. 'Oxidative damage to protein in sporadic motor neuron disease spinal cord', *Ann Neurol*, 38: 691-5.

Shen, W. C., H. Y. Li, G. C. Chen, Y. Chern, and P. H. Tu. 2015. 'Mutations in the ubiquitin-binding domain of OPTN/optineurin interfere with autophagy-mediated degradation of misfolded proteins by a dominant-negative mechanism', *Autophagy*, 11: 685-700.

Sher, R. B., T. D. Heiman-Patterson, E. A. Blankenhorn, J. Jiang, G. Alexander, J. S. Deitch, and G. A. Cox. 2014. 'A major QTL on mouse chromosome 17 resulting in lifespan variability in SOD1-G93A transgenic mouse models of amyotrophic lateral sclerosis', *Amyotroph Lateral Scler Frontotemporal Degener*, 15: 588-600.

Shi, Y., S. Lin, K. A. Staats, Y. Li, W. H. Chang, S. T. Hung, E. Hendricks, G. R. Linares, Y. Wang, E. Y. Son, X. Wen, K. Kisler, B. Wilkinson, L. Menendez, T. Sugawara, P. Woolwine, M. Huang, M. J. Cowan, B. Ge, N. Koutsodendris, K. P. Sandor, J. Komberg, V. R. Vangoor, K. Senthilkumar, V. Hennes, C. Seah, A. R. Nelson, T. Y. Cheng, S. J. Lee, P. R. August, J. A. Chen, N. Wisniewski, V. Hanson-Smith, T. G. Belgard, A. Zhang, M. Coba, C. Grunseich, M. E. Ward, L. H. van den Berg, R. J. Pasterkamp, D. Trotti, B. V. Zlokovic, and J. K. Ichida. 2018. 'Haploinsufficiency leads to neurodegeneration in C9ORF72 ALS/FTD human induced motor neurons', *Nat Med*, 24: 313-25.

Shibata, N., A. Hirano, M. Kobayashi, S. Sasaki, T. Kato, S. Matsumoto, Z. Shiozawa, T. Komori, A. Ikemoto, T. Umahara, and et al. 1994. 'Cu/Zn superoxide dismutase-like immunoreactivity in Lewy body-like inclusions of sporadic amyotrophic lateral sclerosis', *Neurosci Lett*, 179: 149-52.

Shibata, N., R. Nagai, K. Uchida, S. Horiuchi, S. Yamada, A. Hirano, M. Kawaguchi, T. Yamamoto, S. Sasaki, and M. Kobayashi. 2001. 'Morphological evidence for lipid peroxidation and protein glycoxidation in spinal cords from sporadic amyotrophic lateral sclerosis patients', *Brain Res*, 917: 97-104.

Shiga, A., T. Ishihara, A. Miyashita, M. Kuwabara, T. Kato, N. Watanabe, A. Yamahira, C. Kondo, A. Yokoseki, M. Takahashi, R. Kuwano, A. Kakita, M. Nishizawa, H. Takahashi, and O. Onodera. 2012. 'Alteration of POLDIP3 splicing associated with loss of function of TDP-43 in tissues affected with ALS', *PLoS One*, 7: e43120.

Shin, H. W., M. Hayashi, S. Christoforidis, S. Lacas-Gervais, S. Hoepfner, M. R. Wenk, J. Modregger, S. Uttenweiler-Joseph, M. Wilm, A. Nystuen, W. N. Frankel, M. Solimena, P. De Camilli, and M. Zerial. 2005. 'An enzymatic cascade of Rab5 effectors regulates phosphoinositide turnover in the endocytic pathway', *J Cell Biol*, 170: 607-18.

Shurtleff, M. J., M. M. Temoche-Diaz, K. V. Karfilis, S. Ri, and R. Schekman. 2016. 'Y-box protein 1 is required to sort microRNAs into exosomes in cells and in a cell-free reaction', *Elife*, 5.

Siklos, L., J. Engelhardt, Y. Harati, R. G. Smith, F. Joo, and S. H. Appel. 1996. 'Ultrastructural evidence for altered calcium in motor nerve terminals in amyotropic lateral sclerosis', *Ann Neurol*, 39: 203-16.

Simon-Sanchez, J., E. G. Dopper, P. E. Cohn-Hokke, R. K. Hukema, N. Nicolaou, H. Seelaar, J. R. de Graaf, I. de Koning, N. M. van Schoor, D. J. Deeg, M. Smits, J. Raaphorst, L. H. van den Berg, H. J. Schelhaas, C. E. De Die-Smulders, D. Majoor-Krakauer, A. J. Rozemuller, R. Willemsen, Y. A. Pijnenburg, P. Heutink, and J. C. van Swieten. 2012. 'The clinical and pathological phenotype of C9ORF72 hexanucleotide repeat expansions', *Brain*, 135: 723-35.

Simon, D. K., C. M. Tanner, and P. Brundin. 2020. 'Parkinson Disease Epidemiology, Pathology, Genetics, and Pathophysiology', *Clin Geriatr Med*, 36: 1-12.

Simonetti, B., C. M. Danson, K. J. Heesom, and P. J. Cullen. 2017. 'Sequence-dependent cargo recognition by SNX-BARs mediates retromer-independent transport of CI-MPR', *J Cell Biol*, 216: 3695-712.

Simunovic, M., J. B. Manneville, H. F. Renard, E. Evergren, K. Raghunathan, D. Bhatia, A. K. Kenworthy, G. A. Voth, J. Prost, H. T. McMahon, L. Johannes, P. Bassereau, and A. Callan-Jones. 2017. 'Friction Mediates Scission of Tubular Membranes Scaffolded by BAR Proteins', *Cell*, 170: 172-84.e11.

Sisodia, S. S. 1992. 'Beta-amyloid precursor protein cleavage by a membrane-bound protease', *Proc Natl Acad Sci U S A*, 89: 6075-9.

Slagsvold, T., R. Aasland, S. Hirano, K. G. Bache, C. Raiborg, D. Trambaiolo, S. Wakatsuki, and H. Stenmark. 2005. 'Eap45 in mammalian ESCRT-II binds ubiquitin via a phosphoinositide-interacting GLUE domain', *J Biol Chem*, 280: 19600-6.

Small, S. A., K. Kent, A. Pierce, C. Leung, M. S. Kang, H. Okada, L. Honig, J. P. Vonsattel, and T. W. Kim. 2005. 'Model-guided microarray implicates the retromer complex in Alzheimer's disease', *Ann Neurol*, 58: 909-19.

Small, S. A., and G. A. Petsko. 2015. 'Retromer in Alzheimer disease, Parkinson disease and other neurological disorders', *Nat Rev Neurosci*, 16: 126-32.

Smethurst, P., J. Newcombe, C. Troakes, R. Simone, Y. R. Chen, R. Patani, and K. Sidle. 2016. 'In vitro prion-like behaviour of TDP-43 in ALS', *Neurobiol Dis*, 96: 236-47.

Smith, B. N., N. Ticozzi, C. Fallini, A. S. Gkazi, S. Topp, K. P. Kenna, E. L. Scotter, J. Kost, P. Keagle, J. W. Miller, D. Calini, C. Vance, E. W. Danielson, C. Troakes, C. Tiloca, S. Al-Sarraj, E. A. Lewis, A. King, C. Colombrita, V. Pensato, B. Castellotti, J. de Belleroche, F. Baas, A. L. ten Asbroek, P. C. Sapp, D. McKenna-Yasek, R. L. McLaughlin, M. Polak, S. Asress, J. Esteban-Perez, J. L. Munoz-Blanco, M. Simpson, W. van Rheenen, F. P. Diekstra, G. Lauria, S. Duga, S. Corti, C. Cereda, L. Corrado, G. Soraru, K. E. Morrison, K. L. Williams, G. A. Nicholson, I. P. Blair, P. A. Dion, C. S. Leblond, G. A. Rouleau, O. Hardiman, J. H. Veldink, L. H. van den Berg, A. Al-Chalabi, H. Pall, P. J. Shaw, M. R. Turner, K. Talbot, F. Taroni, A. Garcia-Redondo, Z. Wu, J. D. Glass, C. Gellera, A. Ratti, R. H. Brown, Jr., V. Silani, C. E. Shaw, and J. E. Landers. 2014. 'Exome-wide rare variant analysis identifies TUBA4A mutations associated with familial ALS', *Neuron*, 84: 324-31.

Smith, B. N., S. D. Topp, C. Fallini, H. Shibata, H. J. Chen, C. Troakes, A. King, N. Ticozzi, K. P. Kenna, A. Soragia-Gkazi, J. W. Miller, A. Sato, D. M. Dias, M. Jeon, C. Vance, C. H. Wong, M. de Majo, W. Kattuah, J. C. Mitchell, E. L. Scotter, N. W. Parkin, P. C. Sapp, M. Nolan, P. J. Nestor, M. Simpson, M. Weale, M. Lek, F. Baas, J. M. Vianney de Jong, Alma Ten Asbroek, A. G. Redondo, J. Esteban-Perez, C. Tiloca, F. Verde, S. Duga, N. Leigh, H. Pall, K. E. Morrison, A. Al-Chalabi, P. J. Shaw, J. Kirby, M. R. Turner, K. Talbot, O. Hardiman, J. D. Glass, J. De Belleroche, M. Maki, S. E. Moss, C. Miller, C. Gellera, A. Ratti, S. Al-Sarraj, R. H. Brown, Jr., V. Silani, J. E. Landers, and C. E. Shaw. 2017. 'Mutations in the vesicular trafficking protein annexin A11 are associated with amyotrophic lateral sclerosis', *Sci Transl Med*, 9.

Smith, R. G., Y. K. Henry, M. P. Mattson, and S. H. Appel. 1998. 'Presence of 4-hydroxynonenal in cerebrospinal fluid of patients with sporadic amyotrophic lateral sclerosis', *Ann Neurol*, 44: 696-9.

Sobue, G., Y. Matsuoka, E. Mukai, T. Takayanagi, I. Sobue, and Y. Hashizume. 1981. 'Spinal and cranial motor nerve roots in amyotrophic lateral sclerosis and X-linked recessive bulbospinal muscular atrophy: morphometric and teased-fiber study', *Acta Neuropathol*, 55: 227-35.

Soldati, T., and M. Schliwa. 2006. 'Powering membrane traffic in endocytosis and recycling', *Nat Rev Mol Cell Biol*, 7: 897-908.

Spang, A. 2016. 'Membrane Tethering Complexes in the Endosomal System', *Front Cell Dev Biol*, 4: 35.

Sreedharan, J., I. P. Blair, V. B. Tripathi, X. Hu, C. Vance, B. Rogelj, S. Ackerley, J. C. Durnall, K. L. Williams, E. Buratti, F. Baralle, J. de Belleroche, J. D. Mitchell, P. N. Leigh, A. Al-Chalabi, C. C. Miller, G. Nicholson, and C. E. Shaw. 2008. 'TDP-43 mutations in familial and sporadic amyotrophic lateral sclerosis', *Science*, 319: 1668-72.

Sreedharan, J., and R. H. Brown, Jr. 2013. 'Amyotrophic lateral sclerosis: Problems and prospects', *Ann Neurol*, 74: 309-16.

Stanga, S., L. Brambilla, B. Tasiaux, A. H. Dang, A. Ivanoiu, J. N. Octave, D. Rossi, V. van Pesch, and P. Kienlen-Campard. 2018. 'A Role for GDNF and Soluble APP as Biomarkers of Amyotrophic Lateral Sclerosis Pathophysiology', *Front Neurol*, 9: 384.

Starai, V. J., Y. Jun, and W. Wickner. 2007. 'Excess vacuolar SNAREs drive lysis and Rab bypass fusion', *Proc Natl Acad Sci U S A*, 104: 13551-8.

Steele, J. C., J. C. Richardson, and J. Olszewski. 1964. 'PROGRESSIVE SUPRANUCLEAR PALSY. A HETEROGENEOUS DEGENERATION INVOLVING THE BRAIN STEM, BASAL GANGLIA AND CEREBELLUM WITH VERTICAL GAZE AND PSEUDOBULBAR PALSY, NUCHAL DYSTONIA AND DEMENTIA', *Arch Neurol*, 10: 333-59.

Stefanis, L. 2012. 'alpha-Synuclein in Parkinson's disease', *Cold Spring Harb Perspect Med*, 2: a009399.

Steinacker, P., L. Fang, J. Kuhle, A. Petzold, H. Tumani, A. C. Ludolph, M. Otto, and J. Brettschneider. 2011. 'Soluble beta-amyloid precursor protein is related to disease progression in amyotrophic lateral sclerosis', *PLoS One*, 6: e23600.

Steinberg, F., M. Gallon, M. Winfield, E. C. Thomas, A. J. Bell, K. J. Heesom, J. M. Tavare, and P. J. Cullen. 2013. 'A global analysis of SNX27-retromer assembly and cargo specificity reveals a function in glucose and metal ion transport', *Nat Cell Biol*, 15: 461-71.

Steinberg, F., K. J. Heesom, M. D. Bass, and P. J. Cullen. 2012. 'SNX17 protects integrins from degradation by sorting between lysosomal and recycling pathways', *J Cell Biol*, 197: 219-30.

Stenmark, H., R. Aasland, B. H. Toh, and A. D'Arrigo. 1996. 'Endosomal localization of the autoantigen EEA1 is mediated by a zinc-binding FYVE finger', *J Biol Chem*, 271: 24048-54.

Stephenson, Jodie, and Sandra Amor. 2017. 'Modelling amyotrophic lateral sclerosis in mice', *Drug Discovery Today: Disease Models*, 25-26: 35-44.

Stimpson, H. E., C. P. Toret, A. T. Cheng, B. S. Pauly, and D. G. Drubin. 2009. 'Early-arriving Syp1p and Ede1p function in endocytic site placement and formation in budding yeast', *Mol Biol Cell*, 20: 4640-51.

Stoica, R., K. J. De Vos, S. Paillusson, S. Mueller, R. M. Sancho, K. F. Lau, G. Vizcay-Barrena, W. L. Lin, Y. F. Xu, J. Lewis, D. W. Dickson, L. Petrucelli, J. C. Mitchell, C. E. Shaw, and C. C. Miller. 2014. 'ER-mitochondria associations are regulated by the VAPB-

PTPIP51 interaction and are disrupted by ALS/FTD-associated TDP-43', *Nat Commun*, 5: 3996.

Sudhof, T. C., and J. E. Rothman. 2009. 'Membrane fusion: grappling with SNARE and SM proteins', *Science*, 323: 474-7.

Sugiura, A., G. L. McLelland, E. A. Fon, and H. M. McBride. 2014. 'A new pathway for mitochondrial quality control: mitochondrial-derived vesicles', *EMBO J*, 33: 2142-56.

Sullivan, C. P., A. G. Jay, E. C. Stack, M. Pakaluk, E. Wadlinger, R. E. Fine, J. M. Wells, and P. J. Morin. 2011. 'Retromer disruption promotes amyloidogenic APP processing', *Neurobiol Dis*, 43: 338-45.

Sumi, H., S. Kato, Y. Mochimaru, H. Fujimura, M. Etoh, and S. Sakoda. 2009. 'Nuclear TAR DNA binding protein 43 expression in spinal cord neurons correlates with the clinical course in amyotrophic lateral sclerosis', *J Neuropathol Exp Neurol*, 68: 37-47.

Sundaramoorthy, V., A. K. Walker, V. Tan, J. A. Fifita, E. P. McCann, K. L. Williams, I. P. Blair, G. J. Guillemin, M. A. Farg, and J. D. Atkin. 2015. 'Defects in optineurin- and myosin VI-mediated cellular trafficking in amyotrophic lateral sclerosis', *Hum Mol Genet*, 24: 3830-46.

Suzuki, H., K. Kanekura, T. P. Levine, K. Kohno, V. M. Olkkonen, S. Aiso, and M. Matsuoka. 2009. 'ALS-linked P56S-VAPB, an aggregated loss-of-function mutant of VAPB, predisposes motor neurons to ER stress-related death by inducing aggregation of co-expressed wild-type VAPB', *J Neurochem*, 108: 973-85.

Swaminathan, S., A. Y. Amerik, and M. Hochstrasser. 1999. 'The Doa4 deubiquitinating enzyme is required for ubiquitin homeostasis in yeast', *Mol Biol Cell*, 10: 2583-94.

Swinnen, B., and W. Robberecht. 2014. 'The phenotypic variability of amyotrophic lateral sclerosis', *Nat Rev Neurol*, 10: 661-70.

Tagami, M., F. Kimura, H. Nakajima, S. Ishida, S. Fujiwara, Y. Doi, T. Hosokawa, K. Yamane, K. Unoda, T. Hirose, H. Tani, S. Ota, T. Ito, M. Sugino, K. Shinoda, and T. Hanafusa. 2014. 'Tracheostomy and invasive ventilation in Japanese ALS patients: decision-making and survival analysis: 1990-2010', *J Neurol Sci*, 344: 158-64.

Takahashi, H., J. R. Mayers, L. Wang, J. M. Edwardson, and A. Audhya. 2015. 'Hrs and STAM function synergistically to bind ubiquitin-modified cargoes in vitro', *Biophys J*, 108: 76-84.

Takahashi, M., K. M. Weidenheim, D. W. Dickson, and H. Ksiezak-Reding. 2002. 'Morphological and biochemical correlations of abnormal tau filaments in progressive supranuclear palsy', *J Neuropathol Exp Neurol*, 61: 33-45.

Takahashi, Y., Y. Fukuda, J. Yoshimura, A. Toyoda, K. Kurppa, H. Moritoyo, V. V. Belzil, P. A. Dion, K. Higasa, K. Doi, H. Ishiura, J. Mitsui, H. Date, B. Ahsan, T. Matsukawa, Y. Ichikawa, T. Moritoyo, M. Ikoma, T. Hashimoto, F. Kimura, S. Murayama, O. Onodera, M. Nishizawa, M. Yoshida, N. Atsuta, G. Sobue, J. A. Fifita, K. L. Williams, I. P. Blair, G. A. Nicholson, P. Gonzalez-Perez, R. H. Brown, Jr., M. Nomoto, K. Elenius, G. A. Rouleau, A. Fujiyama, S. Morishita, J. Goto, and S. Tsuji. 2013. 'ERBB4 mutations that disrupt the neuregulin-ErbB4 pathway cause amyotrophic lateral sclerosis type 19', *Am J Hum Genet*, 93: 900-5.

Takahashi, Y., H. He, Z. Tang, T. Hattori, Y. Liu, M. M. Young, J. M. Serfass, L. Chen, M. Gebru, C. Chen, C. A. Wills, J. M. Atkinson, H. Chen, T. Abraham, and H. G. Wang. 2018. 'An autophagy assay reveals the ESCRT-III component CHMP2A as a regulator of phagophore closure', *Nat Commun*, 9: 2855.

Takats, S., K. Pircs, P. Nagy, A. Varga, M. Karpati, K. Hegedus, H. Kramer, A. L. Kovacs, M. Sass, and G. Juhasz. 2014. 'Interaction of the HOPS complex with Syntaxin 17 mediates autophagosome clearance in Drosophila', *Mol Biol Cell*, 25: 1338-54.

Takuma, H., S. Kwak, T. Yoshizawa, and I. Kanazawa. 1999. 'Reduction of GluR2 RNA editing, a molecular change that increases calcium influx through AMPA receptors, selective in the spinal ventral gray of patients with amyotrophic lateral sclerosis', *Ann Neurol*, 46: 806-15.

Tang, F. L., J. R. Erion, Y. Tian, W. Liu, D. M. Yin, J. Ye, B. Tang, L. Mei, and W. C. Xiong. 2015. 'VPS35 in Dopamine Neurons Is Required for Endosome-to-Golgi Retrieval of Lamp2a, a Receptor of Chaperone-Mediated Autophagy That Is Critical for alpha-Synuclein Degradation and Prevention of Pathogenesis of Parkinson's Disease', *J Neurosci*, 35: 10613-28.

Tang, F. L., W. Liu, J. X. Hu, J. R. Erion, J. Ye, L. Mei, and W. C. Xiong. 2015. 'VPS35 Deficiency or Mutation Causes Dopaminergic Neuronal Loss by Impairing Mitochondrial Fusion and Function', *Cell Rep*, 12: 1631-43.

Tann, J. Y., L. W. Wong, S. Sajikumar, and C. F. Ibanez. 2019. 'Abnormal TDP-43 function impairs activity-dependent BDNF secretion, synaptic plasticity, and cognitive behavior through altered Sortilin splicing', *EMBO J*, 38.

Tartaglia, M. C., A. Rowe, K. Findlater, J. B. Orange, G. Grace, and M. J. Strong. 2007. 'Differentiation between primary lateral sclerosis and amyotrophic lateral sclerosis: examination of symptoms and signs at disease onset and during follow-up', *Arch Neurol*, 64: 232-6.

Tateno, M., H. Sadakata, M. Tanaka, S. Itohara, R. M. Shin, M. Miura, M. Masuda, T. Aosaki, M. Urushitani, H. Misawa, and R. Takahashi. 2004. 'Calcium-permeable AMPA receptors promote misfolding of mutant SOD1 protein and development of amyotrophic lateral sclerosis in a transgenic mouse model', *Hum Mol Genet*, 13: 2183-96.

Taylor, J. P., R. H. Brown, Jr., and D. W. Cleveland. 2016. 'Decoding ALS: from genes to mechanism', *Nature*, 539: 197-206.

Taylor, M. J., D. Perrais, and C. J. Merrifield. 2011. 'A high precision survey of the molecular dynamics of mammalian clathrin-mediated endocytosis', *PLoS Biol*, 9: e1000604.

Teasdale, R. D., and B. M. Collins. 2012. 'Insights into the PX (phox-homology) domain and SNX (sorting nexin) protein families: structures, functions and roles in disease', *Biochem J*, 441: 39-59.

Teis, D., S. Saksena, and S. D. Emr. 2008. 'Ordered assembly of the ESCRT-III complex on endosomes is required to sequester cargo during MVB formation', *Dev Cell*, 15: 578-89.

Teis, D., S. Saksena, B. L. Judson, and S. D. Emr. 2010. 'ESCRT-II coordinates the assembly of ESCRT-III filaments for cargo sorting and multivesicular body vesicle formation', *EMBO J*, 29: 871-83.

Temkin, P., B. Lauffer, S. Jager, P. Cimermancic, N. J. Krogan, and M. von Zastrow. 2011. 'SNX27 mediates retromer tubule entry and endosome-to-plasma membrane trafficking of signalling receptors', *Nat Cell Biol*, 13: 715-21.

Temkin, P., W. Morishita, D. Goswami, K. Arendt, L. Chen, and R. Malenka. 2017. 'The Retromer Supports AMPA Receptor Trafficking During LTP', *Neuron*, 94: 74-82.e5.

Teo, H., D. J. Gill, J. Sun, O. Perisic, D. B. Veprintsev, Y. Vallis, S. D. Emr, and R. L. Williams. 2006. 'ESCRT-I core and ESCRT-II GLUE domain structures reveal role for GLUE in linking to ESCRT-I and membranes', *Cell*, 125: 99-111.

Teo, H., O. Perisic, B. Gonzalez, and R. L. Williams. 2004. 'ESCRT-II, an endosome-associated complex required for protein sorting: crystal structure and interactions with ESCRT-III and membranes', *Dev Cell*, 7: 559-69.

Thomsen, G. M., G. Gowing, J. Latter, M. Chen, J. P. Vit, K. Staggenborg, P. Avalos, M. Alkaslasi, L. Ferraiuolo, S. Likhite, B. K. Kaspar, and C. N. Svendsen. 2014. 'Delayed disease onset and extended survival in the SOD1G93A rat model of amyotrophic lateral sclerosis after suppression of mutant SOD1 in the motor cortex', *J Neurosci*, 34: 15587-600.

Tian, Y., F. L. Tang, X. Sun, L. Wen, L. Mei, B. S. Tang, and W. C. Xiong. 2015. 'VPS35-deficiency results in an impaired AMPA receptor trafficking and decreased dendritic spine maturation', *Mol Brain*, 8: 70.

Tobisawa, S., Y. Hozumi, S. Arawaka, S. Koyama, M. Wada, M. Nagai, M. Aoki, Y. Itoyama, K. Goto, and T. Kato. 2003. 'Mutant SOD1 linked to familial amyotrophic lateral sclerosis, but not wild-type SOD1, induces ER stress in COS7 cells and transgenic mice', *Biochem Biophys Res Commun*, 303: 496-503.

Toh, W. H., P. Z. C. Chia, M. I. Hossain, and P. A. Gleeson. 2018. 'GGA1 regulates signal-dependent sorting of BACE1 to recycling endosomes, which moderates Abeta production', *Mol Biol Cell*, 29: 191-208.

Tong, J., C. Huang, F. Bi, Q. Wu, B. Huang, X. Liu, F. Li, H. Zhou, and X. G. Xia. 2013. 'Expression of ALS-linked TDP-43 mutant in astrocytes causes non-cell-autonomous motor neuron death in rats', *EMBO J*, 32: 1917-26.

Topp, J. D., N. W. Gray, R. D. Gerard, and B. F. Horazdovsky. 2004. 'Alsin is a Rab5 and Rac1 guanine nucleotide exchange factor', *J Biol Chem*, 279: 24612-23.

Trancikova, A., E. Tsika, and D. J. Moore. 2012. 'Mitochondrial dysfunction in genetic animal models of Parkinson's disease', *Antioxid Redox Signal*, 16: 896-919.

Traub, L. M. 2009. 'Tickets to ride: selecting cargo for clathrin-regulated internalization', *Nat Rev Mol Cell Biol*, 10: 583-96.

Tsika, E., L. Glauser, R. Moser, A. Fiser, G. Daniel, U. M. Sheerin, A. Lees, J. C. Troncoso, P. A. Lewis, R. Bandopadhyay, B. L. Schneider, and D. J. Moore. 2014. 'Parkinson's disease-linked mutations in VPS35 induce dopaminergic neurodegeneration', *Hum Mol Genet*, 23: 4621-38.

Tsuchiya, K., M. Sano, H. Shiotsu, H. Akiyama, S. Watabiki, K. Taki, H. Kondo, I. Nakano, and K. Ikeda. 2004. 'Sporadic amyotrophic lateral sclerosis of long duration mimicking spinal progressive muscular atrophy exists: additional autopsy case with a clinical course of 19 years', *Neuropathology*, 24: 228-35.

Tumbarello, D. A., B. J. Waxse, S. D. Arden, N. A. Bright, J. Kendrick-Jones, and F. Buss. 2012. 'Autophagy receptors link myosin VI to autophagosomes to mediate Tom1-dependent autophagosome maturation and fusion with the lysosome', *Nat Cell Biol*, 14: 1024-35.

Turner, B. J., and K. Talbot. 2008. 'Transgenics, toxicity and therapeutics in rodent models of mutant SOD1-mediated familial ALS', *Prog Neurobiol*, 85: 94-134.

Umasankar, P. K., S. Sanker, J. R. Thieman, S. Chakraborty, B. Wendland, M. Tsang, and L. M. Traub. 2012. 'Distinct and separable activities of the endocytic clathrin-coat components Fcho1/2 and AP-2 in developmental patterning', *Nat Cell Biol*, 14: 488-501.

Ungewickell, E. 1985. 'The 70-kd mammalian heat shock proteins are structurally and functionally related to the uncoating protein that releases clathrin triskelia from coated vesicles', *EMBO J*, 4: 3385-91.

Vaccaro, A., A. Tauffenberger, D. Aggad, G. Rouleau, P. Drapeau, and J. A. Parker. 2012. 'Mutant TDP-43 and FUS cause age-dependent paralysis and neurodegeneration in C. elegans', *PLoS One*, 7: e31321.

Vagnozzi, A. N., J. G. Li, J. Chiu, R. Razmpour, R. Warfield, S. H. Ramirez, and D. Pratico. 2019. 'VPS35 regulates tau phosphorylation and neuropathology in tauopathy', *Mol Psychiatry*.

Valdmanis, P. N., I. A. Meijer, A. Reynolds, A. Lei, P. MacLeod, D. Schlesinger, M. Zatz, E. Reid, P. A. Dion, P. Drapeau, and G. A. Rouleau. 2007. 'Mutations in the KIAA0196 gene at the SPG8 locus cause hereditary spastic paraplegia', *Am J Hum Genet*, 80: 152-61.

Van Damme, P., E. Bogaert, M. Dewil, N. Hersmus, D. Kiraly, W. Scheveneels, I. Bockx, D. Braeken, N. Verpoorten, K. Verhoeven, V. Timmerman, P. Herijgers, G. Callewaert, P. Carmeliet, L. Van Den Bosch, and W. Robberecht. 2007. 'Astrocytes regulate GluR2 expression in motor neurons and their vulnerability to excitotoxicity', *Proc Natl Acad Sci U S A*, 104: 14825-30.

Van Deerlin, V. M., J. B. Leverenz, L. M. Bekris, T. D. Bird, W. Yuan, L. B. Elman, D. Clay, E. M. Wood, A. S. Chen-Plotkin, M. Martinez-Lage, E. Steinbart, L. McCluskey, M. Grossman, M. Neumann, I. L. Wu, W. S. Yang, R. Kalb, D. R. Galasko, T. J. Montine, J. Q. Trojanowski, V. M. Lee, G. D. Schellenberg, and C. E. Yu. 2008. 'TARDBP mutations in amyotrophic lateral sclerosis with TDP-43 neuropathology: a genetic and histopathological analysis', *Lancet Neurol*, 7: 409-16.

Van Den Bosch, L., W. Vandenberghe, H. Klaassen, E. Van Houtte, and W. Robberecht. 2000. 'Ca(2+)-permeable AMPA receptors and selective vulnerability of motor neurons', *J Neurol Sci*, 180: 29-34.

van Rheenen, W., A. Shatunov, A. M. Dekker, R. L. McLaughlin, F. P. Diekstra, S. L. Pulit, R. A. van der Spek, U. Vosa, S. de Jong, M. R. Robinson, J. Yang, I. Fogh, P. T. van Doormaal, G. H. Tazelaar, M. Koppers, A. M. Blokhuis, W. Sproviero, A. R. Jones, K. P. Kenna, K. R. van Eijk, O. Harschnitz, R. D. Schellevis, W. J. Brands, J. Medic, A. Menelaou, A. Vajda, N. Ticozzi, K. Lin, B. Rogelj, K. Vrabec, M. Ravnik-Glavac, B. Koritnik, J. Zidar, L. Leonardis, L. D. Groselj, S. Millecamps, F. Salachas, V. Meininger, M. de Carvalho, S. Pinto, J. S. Mora, R. Rojas-Garcia, M. Polak, S. Chandran, S. Colville, R. Swingler, K. E. Morrison, P. J. Shaw, J. Hardy, R. W. Orrell, A. Pittman, K. Sidle, P. Fratta, A. Malaspina, S. Topp, S. Petri, S. Abdulla, C. Drepper, M. Sendtner, T. Meyer, R. A. Ophoff, K. A. Staats, M. Wiedau-Pazos, C. Lomen-Hoerth, V. M. Van Deerlin, J. Q. Trojanowski, L. Elman, L. McCluskey, A. N. Basak, C. Tunca, H. Hamzeiy, Y. Parman, T. Meitinger, P. Lichtner, M. Radivojkov-Blagojevic, C. R. Andres, C. Maurel, G. Bensimon, B. Landwehrmeyer, A. Brice, C. A. Payan, S. Saker-Delye, A. Durr, N. W. Wood, L. Tittmann, W. Lieb, A. Franke, M. Rietschel, S. Cichon, M. M. Nothen, P. Amouyel, C. Tzourio, J. F. Dartigues, A. G. Uitterlinden, F. Rivadeneira, K. Estrada, A. Hofman, C. Curtis, H. M. Blauw, A. J. van der Kooi, M. de Visser, A. Goris, M. Weber, C. E. Shaw, B. N. Smith, O. Pansarasa, C. Cereda, R. Del Bo, G. P. Comi, S. D'Alfonso, C. Bertolin, G. Soraru, L. Mazzini, V. Pensato, C. Gellera, C. Tiloca, A. Ratti, A. Calvo, C. Moglia, M. Brunetti, S. Arcuti, R. Capozzo, C. Zecca, C. Lunetta, S. Penco, N. Riva, A. Padovani, M. Filosto, B. Muller, R. J. Stuit, I. Blair, K. Zhang, E. P. McCann, J. A. Fifita, G. A. Nicholson, D. B. Rowe, R. Pamphlett, M. C. Kiernan, J. Grosskreutz, O. W. Witte, T. Ringer, T. Prell, B. Stubendorff, I. Kurth, C. A. Hubner, P. N. Leigh, F. Casale, A. Chio, E. Beghi, E. Pupillo, R. Tortelli, G. Logroscino, J. Powell, A. C. Ludolph, J. H. Weishaupt, W. Robberecht, P. Van Damme, L. Franke, T. H. Pers, R. H. Brown, J. D. Glass, J. E.

Landers, O. Hardiman, P. M. Andersen, P. Corcia, P. Vourc'h, V. Silani, N. R. Wray, P. M. Visscher, P. I. de Bakker, M. A. van Es, R. J. Pasterkamp, C. M. Lewis, G. Breen, A. Al-Chalabi, L. H. van den Berg, and J. H. Veldink. 2016. 'Genome-wide association analyses identify new risk variants and the genetic architecture of amyotrophic lateral sclerosis', *Nat Genet*, 48: 1043-8.

van Zundert, B., M. H. Peuscher, M. Hynynen, A. Chen, R. L. Neve, R. H. Brown, Jr., M. Constantine-Paton, and M. C. Bellingham. 2008. 'Neonatal neuronal circuitry shows hyperexcitable disturbance in a mouse model of the adult-onset neurodegenerative disease amyotrophic lateral sclerosis', *J Neurosci*, 28: 10864-74.

Vance, C., B. Rogelj, T. Hortobagyi, K. J. De Vos, A. L. Nishimura, J. Sreedharan, X. Hu, B. Smith, D. Ruddy, P. Wright, J. Ganesalingam, K. L. Williams, V. Tripathi, S. Al-Saraj, A. Al-Chalabi, P. N. Leigh, I. P. Blair, G. Nicholson, J. de Belleroche, J. M. Gallo, C. C. Miller, and C. E. Shaw. 2009. 'Mutations in FUS, an RNA processing protein, cause familial amyotrophic lateral sclerosis type 6', *Science*, 323: 1208-11.

Vande Velde, C., K. K. McDonald, Y. Boukhedimi, M. McAlonis-Downes, C. S. Lobsiger, S. Bel Hadj, A. Zandona, J. P. Julien, S. B. Shah, and D. W. Cleveland. 2011. 'Misfolded SOD1 associated with motor neuron mitochondria alters mitochondrial shape and distribution prior to clinical onset', *PLoS One*, 6: e22031.

Vardarajan, B. N., S. Y. Bruesegem, M. E. Harbour, R. Inzelberg, R. Friedland, P. St George-Hyslop, M. N. Seaman, and L. A. Farrer. 2012. 'Identification of Alzheimer disease-associated variants in genes that regulate retromer function', *Neurobiol Aging*, 33: 2231.e15-31.e30.

Vardarajan, B. N., Y. Zhang, J. H. Lee, R. Cheng, C. Bohm, M. Ghani, C. Reitz, D. Reyes-Dumeyer, Y. Shen, E. Rogaeva, P. St George-Hyslop, and R. Mayeux. 2015. 'Coding mutations in SORL1 and Alzheimer disease', *Ann Neurol*, 77: 215-27.

Vargas, M. R., M. Pehar, P. Cassina, J. S. Beckman, and L. Barbeito. 2006. 'Increased glutathione biosynthesis by Nrf2 activation in astrocytes prevents p75NTR-dependent motor neuron apoptosis', *J Neurochem*, 97: 687-96.

Varnai, P., B. Thyagarajan, T. Rohacs, and T. Balla. 2006. 'Rapidly inducible changes in phosphatidylinositol 4,5-bisphosphate levels influence multiple regulatory functions of the lipid in intact living cells', *J Cell Biol*, 175: 377-82.

Vergne, I., E. Roberts, R. A. Elmaoued, V. Tosch, M. A. Delgado, T. Proikas-Cezanne, J. Laporte, and V. Deretic. 2009. 'Control of autophagy initiation by phosphoinositide 3-phosphatase Jumpy', *EMBO J*, 28: 2244-58.

Verhoeven, K., P. De Jonghe, K. Coen, N. Verpoorten, M. Auer-Grumbach, J. M. Kwon, D. FitzPatrick, E. Schmedding, E. De Vriendt, A. Jacobs, V. Van Gerwen, K. Wagner, H. P. Hartung, and V. Timmerman. 2003. 'Mutations in the small GTP-ase late endosomal protein RAB7 cause Charcot-Marie-Tooth type 2B neuropathy', *Am J Hum Genet*, 72: 722-7.

Verstraeten, A., E. Wauters, D. Crosiers, B. Meeus, E. Corsmit, E. Elinck, M. Mattheijssens, K. Peeters, P. Cras, B. Pickut, R. Vandenberghe, S. Engelborghs, P. P. De Deyn, C. Van Broeckhoven, and J. Theuns. 2012. 'Contribution of VPS35 genetic variability to LBD in the Flanders-Belgian population', *Neurobiol Aging*, 33: 1844.e11-3.

Vetter, I. R., and A. Wittinghofer. 2001. 'The guanine nucleotide-binding switch in three dimensions', *Science*, 294: 1299-304.

Vilarino-Guell, C., C. Wider, O. A. Ross, J. C. Dachsel, J. M. Kachergus, S. J. Lincoln, A. I. Soto-Ortolaza, S. A. Cobb, G. J. Wilhoite, J. A. Bacon, B. Behrouz, H. L. Melrose, E. Hentati, A. Puschmann, D. M. Evans, E. Conibear, W. W. Wasserman, J. O. Aasly, P. R. Burkhard, R. Djaldetti, J. Ghika, F. Hentati, A. Krygowska-Wajs, T. Lynch, E. Melamed, A. Rajput, A. H. Rajput, A. Solida, R. M. Wu, R. J. Uitti, Z. K. Wszolek, F. Vingerhoets, and M. J. Farrer. 2011. 'VPS35 mutations in Parkinson disease', *Am J Hum Genet*, 89: 162-7.

Visser, J., R. M. van den Berg-Vos, H. Franssen, L. H. van den Berg, J. H. Wokke, J. M. de Jong, R. Holman, R. J. de Haan, and M. de Visser. 2007. 'Disease course and prognostic factors of progressive muscular atrophy', *Arch Neurol*, 64: 522-8.

von Schwedler, U. K., M. Stuchell, B. Muller, D. M. Ward, H. Y. Chung, E. Morita, H. E. Wang, T. Davis, G. P. He, D. M. Cimbora, A. Scott, H. G. Krausslich, J. Kaplan, S. G. Morham, and W. I. Sundquist. 2003. 'The protein network of HIV budding', *Cell*, 114: 701-13.

Vucic, S., and M. C. Kiernan. 2013. 'Utility of transcranial magnetic stimulation in delineating amyotrophic lateral sclerosis pathophysiology', *Handb Clin Neurol*, 116: 561-75.

Walker, A. K., K. Y. Soo, V. Sundaramoorthy, S. Parakh, Y. Ma, M. A. Farg, R. H. Wallace, P. J. Crouch, B. J. Turner, M. K. Horne, and J. D. Atkin. 2013. 'ALS-associated TDP-43 induces endoplasmic reticulum stress, which drives cytoplasmic TDP-43 accumulation and stress granule formation', *PLoS One*, 8: e81170.

Walter, P., and D. Ron. 2011. 'The unfolded protein response: from stress pathway to homeostatic regulation', *Science*, 334: 1081-6.

Wan, C., B. Borgeson, S. Phanse, F. Tu, K. Drew, G. Clark, X. Xiong, O. Kagan, J. Kwan, A. Bezginov, K. Chessman, S. Pal, G. Cromar, O. Papoulas, Z. Ni, D. R. Boutz, S. Stoilova, P. C. Havugimana, X. Guo, R. H. Malty, M. Sarov, J. Greenblatt, M. Babu, W. B. Derry, E. R. Tillier, J. B. Wallingford, J. Parkinson, E. M. Marcotte, and A. Emili. 2015. 'Panorama of ancient metazoan macromolecular complexes', *Nature*, 525: 339-44.

Wandinger-Ness, A., and M. Zerial. 2014. 'Rab proteins and the compartmentalization of the endosomal system', *Cold Spring Harb Perspect Biol*, 6: a022616.

Wang, C. L., F. L. Tang, Y. Peng, C. Y. Shen, L. Mei, and W. C. Xiong. 2012. 'VPS35 regulates developing mouse hippocampal neuronal morphogenesis by promoting retrograde trafficking of BACE1', *Biol Open*, 1: 1248-57.

Wang, C., M. Niu, Z. Zhou, X. Zheng, L. Zhang, Y. Tian, X. Yu, G. Bu, H. Xu, Q. Ma, and Y. W. Zhang. 2016. 'VPS35 regulates cell surface recycling and signaling of dopamine receptor D1', *Neurobiol Aging*, 46: 22-31.

Wang, M., and R. J. Kaufman. 2014. 'The impact of the endoplasmic reticulum protein-folding environment on cancer development', *Nat Rev Cancer*, 14: 581-97.

Wang, W., L. Li, W. L. Lin, D. W. Dickson, L. Petrucelli, T. Zhang, and X. Wang. 2013. 'The ALS disease-associated mutant TDP-43 impairs mitochondrial dynamics and function in motor neurons', *Hum Mol Genet*, 22: 4706-19.

Wang, W., L. Wang, J. Lu, S. L. Siedlak, H. Fujioka, J. Liang, S. Jiang, X. Ma, Z. Jiang, E. L. da Rocha, M. Sheng, H. Choi, P. H. Lerou, H. Li, and X. Wang. 2016. 'The inhibition of TDP-43 mitochondrial localization blocks its neuronal toxicity', *Nat Med*, 22: 869-78.

Wang, W., X. Wang, H. Fujioka, C. Hoppel, A. L. Whone, M. A. Caldwell, P. J. Cullen, J. Liu, and X. Zhu. 2016. 'Parkinson's disease-associated mutant VPS35 causes mitochondrial dysfunction by recycling DLP1 complexes', *Nat Med*, 22: 54-63.

Wang, X., T. Huang, Y. Zhao, Q. Zheng, R. C. Thompson, G. Bu, Y. W. Zhang, W. Hong, and H. Xu. 2014. 'Sorting nexin 27 regulates Abeta production through modulating gamma-secretase activity', *Cell Rep*, 9: 1023-33.

Wang, X., Y. Zhao, X. Zhang, H. Badie, Y. Zhou, Y. Mu, L. S. Loo, L. Cai, R. C. Thompson, B. Yang, Y. Chen, P. F. Johnson, C. Wu, G. Bu, W. C. Mobley, D. Zhang, F. H. Gage, B. Ranscht, Y. W. Zhang, S. A. Lipton, W. Hong, and H. Xu. 2013. 'Loss of sorting nexin 27 contributes to excitatory synaptic dysfunction by modulating glutamate receptor recycling in Down's syndrome', *Nat Med*, 19: 473-80.

Wang, X., S. Zhou, X. Ding, M. Ma, J. Zhang, Y. Zhou, E. Wu, and J. Teng. 2015. 'Activation of ER Stress and Autophagy Induced by TDP-43 A315T as Pathogenic Mechanism and the Corresponding Histological Changes in Skin as Potential Biomarker for ALS with the Mutation', *Int J Biol Sci*, 11: 1140-9.

Wang, Y., M. Cella, K. Mallinson, J. D. Ulrich, K. L. Young, M. L. Robinette, S. Gilfillan, G. M. Krishnan, S. Sudhakar, B. H. Zinselmeyer, D. M. Holtzman, J. R. Cirrito, and M. Colonna. 2015. 'TREM2 lipid sensing sustains the microglial response in an Alzheimer's disease model', *Cell*, 160: 1061-71.

Wang, Z., G. Miao, X. Xue, X. Guo, C. Yuan, Z. Wang, G. Zhang, Y. Chen, D. Feng, J. Hu, and H. Zhang. 2016. 'The Vici Syndrome Protein EPG5 Is a Rab7 Effector that Determines the Fusion Specificity of Autophagosomes with Late Endosomes/Lysosomes', *Mol Cell*, 63: 781-95.

Warita, H., Y. Manabe, T. Murakami, M. Shiote, Y. Shiro, T. Hayashi, I. Nagano, M. Shoji, and K. Abe. 2002. 'Tardive decrease of astrocytic glutamate transporter protein in transgenic mice with ALS-linked mutant SOD1', *Neurol Res*, 24: 577-81.

Wassmer, T., N. Attar, M. Harterink, J. R. van Weering, C. J. Traer, J. Oakley, B. Goud, D. J. Stephens, P. Verkade, H. C. Korswagen, and P. J. Cullen. 2009. 'The retromer coat complex coordinates endosomal sorting and dynein-mediated transport, with carrier recognition by the trans-Golgi network', *Dev Cell*, 17: 110-22.

Wen, L., F. L. Tang, Y. Hong, S. W. Luo, C. L. Wang, W. He, C. Shen, J. U. Jung, F. Xiong, D. H. Lee, Q. G. Zhang, D. Brann, T. W. Kim, R. Yan, L. Mei, and W. C. Xiong. 2011. 'VPS35 haploinsufficiency increases Alzheimer's disease neuropathology', *J Cell Biol*, 195: 765-79.

Westrate, L. M., J. A. Drocco, K. R. Martin, W. S. Hlavacek, and J. P. MacKeigan. 2014. 'Mitochondrial morphological features are associated with fission and fusion events', *PLoS One*, 9: e95265.

Wichterle, H., I. Lieberam, J. A. Porter, and T. M. Jessell. 2002. 'Directed differentiation of embryonic stem cells into motor neurons', *Cell*, 110: 385-97.

Wild, P., H. Farhan, D. G. McEwan, S. Wagner, V. V. Rogov, N. R. Brady, B. Richter, J. Korac, O. Waidmann, C. Choudhary, V. Dotsch, D. Bumann, and I. Dikic. 2011. 'Phosphorylation of the autophagy receptor optineurin restricts Salmonella growth', *Science*, 333: 228-33.

Williams, E. T., L. Glauser, E. Tsika, H. Jiang, S. Islam, and D. J. Moore. 2018. 'Parkin mediates the ubiquitination of VPS35 and modulates retromer-dependent endosomal sorting', *Hum Mol Genet*, 27: 3189-205.

Williams, K. L., S. Topp, S. Yang, B. Smith, J. A. Fifita, S. T. Warraich, K. Y. Zhang, N. Farrawell, C. Vance, X. Hu, A. Chesi, C. S. Leblond, A. Lee, S. L. Rayner, V. Sundaramoorthy, C. Dobson-Stone, M. P. Molloy, M. van Blitterswijk, D. W. Dickson, R. C. Petersen, N. R. Graff-Radford, B. F. Boeve, M. E. Murray, C. Pottier, E. Don, C. Winnick, E. P. McCann,

A. Hogan, H. Daoud, A. Levert, P. A. Dion, J. Mitsui, H. Ishiura, Y. Takahashi, J. Goto, J. Kost, C. Gellera, A. S. Gkazi, J. Miller, J. Stockton, W. S. Brooks, K. Boundy, M. Polak, J. L. Munoz-Blanco, J. Esteban-Perez, A. Rabano, O. Hardiman, K. E. Morrison, N. Ticozzi, V. Silani, J. de Belleroche, J. D. Glass, J. B. Kwok, G. J. Guillemin, R. S. Chung, S. Tsuji, R. H. Brown, Jr., A. Garcia-Redondo, R. Rademakers, J. E. Landers, A. D. Gitler, G. A. Rouleau, N. J. Cole, J. J. Yerbury, J. D. Atkin, C. E. Shaw, G. A. Nicholson, and I. P. Blair. 2016. 'CCNF mutations in amyotrophic lateral sclerosis and frontotemporal dementia', *Nat Commun*, 7: 11253.

Williams, R. E., and S. E. Mole. 2012. 'New nomenclature and classification scheme for the neuronal ceroid lipofuscinoses', *Neurology*, 79: 183-91.

Williams, T. L., N. C. Day, P. G. Ince, R. K. Kamboj, and P. J. Shaw. 1997. 'Calcium-permeable alpha-amino-3-hydroxy-5-methyl-4-isoxazole propionic acid receptors: a molecular determinant of selective vulnerability in amyotrophic lateral sclerosis', *Ann Neurol*, 42: 200-7.

Willnow, T. E., C. M. Petersen, and A. Nykjaer. 2008. 'VPS10P-domain receptors - regulators of neuronal viability and function', *Nat Rev Neurosci*, 9: 899-909.

Winklhofer, K. F. 2014. 'Parkin and mitochondrial quality control: toward assembling the puzzle', *Trends Cell Biol*, 24: 332-41.

Winklhofer, K. F., and C. Haass. 2010. 'Mitochondrial dysfunction in Parkinson's disease', *Biochim Biophys Acta*, 1802: 29-44.

Winton, M. J., L. M. Igaz, M. M. Wong, L. K. Kwong, J. Q. Trojanowski, and V. M. Lee. 2008. 'Disturbance of nuclear and cytoplasmic TAR DNA-binding protein (TDP-43) induces disease-like redistribution, sequestration, and aggregate formation', *J Biol Chem*, 283: 13302-9.

Winton, M. J., V. M. Van Deerlin, L. K. Kwong, W. Yuan, E. M. Wood, C. E. Yu, G. D. Schellenberg, R. Rademakers, R. Caselli, A. Karydas, J. Q. Trojanowski, B. L. Miller, and V. M. Lee. 2008. 'A90V TDP-43 variant results in the aberrant localization of TDP-43 in vitro', *FEBS Lett*, 582: 2252-6.

Wu, C. H., C. Fallini, N. Ticozzi, P. J. Keagle, P. C. Sapp, K. Piotrowska, P. Lowe, M. Koppers, D. McKenna-Yasek, D. M. Baron, J. E. Kost, P. Gonzalez-Perez, A. D. Fox, J. Adams, F. Taroni, C. Tiloca, A. L. Leclerc, S. C. Chafe, D. Mangroo, M. J. Moore, J. A. Zitzewitz, Z. S. Xu, L. H. van den Berg, J. D. Glass, G. Siciliano, E. T. Cirulli, D. B. Goldstein, F. Salachas, V. Meininger, W. Rossoll, A. Ratti, C. Gellera, D. A. Bosco, G. J. Bassell, V. Silani, V. E. Drory, R. H. Brown, Jr., and J. E. Landers. 2012. 'Mutations in the profilin 1 gene cause familial amyotrophic lateral sclerosis', *Nature*, 488: 499-503.

Wu, J. W., M. Herman, L. Liu, S. Simoes, C. M. Acker, H. Figueroa, J. I. Steinberg, M. Margittai, R. Kayed, C. Zurzolo, G. Di Paolo, and K. E. Duff. 2013. 'Small misfolded Tau species are internalized via bulk endocytosis and anterogradely and retrogradely transported in neurons', *J Biol Chem*, 288: 1856-70.

Wu, P., D. Zhou, Y. Wang, W. Lin, A. Sun, H. Wei, Y. Fang, X. Cong, and Y. Jiang. 2019. 'Identification and validation of alternative splicing isoforms as novel biomarker candidates in hepatocellular carcinoma', *Oncol Rep*, 41: 1929-37.

Wurmser, A. E., and S. D. Emr. 1998. 'Phosphoinositide signaling and turnover: PtdIns(3)P, a regulator of membrane traffic, is transported to the vacuole and degraded by a process that requires lumenal vacuolar hydrolase activities', *EMBO J*, 17: 4930-42.

Xiao, Q., W. Zhao, D. R. Beers, A. A. Yen, W. Xie, J. S. Henkel, and S. H. Appel. 2007. 'Mutant SOD1(G93A) microglia are more neurotoxic relative to wild-type microglia', *J Neurochem*, 102: 2008-19.

Xu, Y., H. Hortsman, L. Seet, S. H. Wong, and W. Hong. 2001. 'SNX3 regulates endosomal function through its PX-domain-mediated interaction with PtdIns(3)P', *Nat Cell Biol*, 3: 658-66.

Yamanaka, K., S. Boillee, E. A. Roberts, M. L. Garcia, M. McAlonis-Downes, O. R. Mikse, D. W. Cleveland, and L. S. Goldstein. 2008. 'Mutant SOD1 in cell types other than motor neurons and oligodendrocytes accelerates onset of disease in ALS mice', *Proc Natl Acad Sci U S A*, 105: 7594-9.

Yamasaki, S., P. Ivanov, G. F. Hu, and P. Anderson. 2009. 'Angiogenin cleaves tRNA and promotes stress-induced translational repression', *J Cell Biol*, 185: 35-42.

Yamashita, Y., K. Kojima, T. Tsukahara, H. Agawa, K. Yamada, Y. Amano, N. Kurotori, N. Tanaka, K. Sugamura, and T. Takeshita. 2008. 'Ubiquitin-independent binding of Hrs mediates endosomal sorting of the interleukin-2 receptor beta-chain', *J Cell Sci*, 121: 1727-38.

Yanase, S., A. Onodera, P. Tedesco, T. E. Johnson, and N. Ishii. 2009. 'SOD-1 deletions in Caenorhabditis elegans alter the localization of intracellular reactive oxygen species and show molecular compensation', *J Gerontol A Biol Sci Med Sci*, 64: 530-9.

Yang, Y., A. Hentati, H. X. Deng, O. Dabbagh, T. Sasaki, M. Hirano, W. Y. Hung, K. Ouahchi, J. Yan, A. C. Azim, N. Cole, G. Gascon, A. Yagmour, M. Ben-Hamida, M. Pericak-Vance, F. Hentati, and T. Siddique. 2001. 'The gene encoding alsin, a protein with three guanine-nucleotide exchange factor domains, is mutated in a form of recessive amyotrophic lateral sclerosis', *Nat Genet*, 29: 160-5.

Yang, Z., A. Jakymiw, M. R. Wood, T. Eystathioy, R. L. Rubin, M. J. Fritzler, and E. K. Chan. 2004. 'GW182 is critical for the stability of GW bodies expressed during the cell cycle and cell proliferation', *J Cell Sci*, 117: 5567-78.

Ye, S. Y., J. E. Apple, X. Ren, F. L. Tang, L. L. Yao, Y. G. Wang, L. Mei, Y. G. Zhou, and W. C. Xiong. 2019. 'Microglial VPS35 deficiency regulates microglial polarization and decreases ischemic stroke-induced damage in the cortex', *J Neuroinflammation*, 16: 235.

Yin, J., X. Liu, Q. He, L. Zhou, Z. Yuan, and S. Zhao. 2016. 'Vps35-dependent recycling of Trem2 regulates microglial function', *Traffic*, 17: 1286-96.

Yoon, J. C., A. Ng, B. H. Kim, A. Bianco, R. J. Xavier, and S. J. Elledge. 2010. 'Wnt signaling regulates mitochondrial physiology and insulin sensitivity', *Genes Dev*, 24: 1507-18.

Young, J. E., L. K. Fong, H. Frankowski, G. A. Petsko, S. A. Small, and L. S. B. Goldstein. 2018. 'Stabilizing the Retromer Complex in a Human Stem Cell Model of Alzheimer's Disease Reduces TAU Phosphorylation Independently of Amyloid Precursor Protein', *Stem Cell Reports*, 10: 1046-58.

Yu, A., Y. Shibata, B. Shah, B. Calamini, D. C. Lo, and R. I. Morimoto. 2014. 'Protein aggregation can inhibit clathrin-mediated endocytosis by chaperone competition', *Proc Natl Acad Sci U S A*, 111: E1481-90.

Yu, I. M., and F. M. Hughson. 2010. 'Tethering factors as organizers of intracellular vesicular traffic', *Annu Rev Cell Dev Biol*, 26: 137-56.

Yu, S., and T. J. Melia. 2017. 'The coordination of membrane fission and fusion at the end of autophagosome maturation', *Curr Opin Cell Biol*, 47: 92-98.

Zavodszky, E., M. N. Seaman, K. Moreau, M. Jimenez-Sanchez, S. Y. Breusegem, M. E. Harbour, and D. C. Rubinsztein. 2014. 'Mutation in VPS35 associated with Parkinson's disease impairs WASH complex association and inhibits autophagy', *Nat Commun*, 5: 3828.

Zhang, F., A. L. Strom, K. Fukada, S. Lee, L. J. Hayward, and H. Zhu. 2007. 'Interaction between familial amyotrophic lateral sclerosis (ALS)-linked SOD1 mutants and the dynein complex', *J Biol Chem*, 282: 16691-9.

Zhang, H., T. Huang, Y. Hong, W. Yang, X. Zhang, H. Luo, H. Xu, and X. Wang. 2018. 'The Retromer Complex and Sorting Nexins in Neurodegenerative Diseases', *Front Aging Neurosci*, 10: 79.

Zhang, P., Y. Wu, T. Y. Belenkaya, and X. Lin. 2011. 'SNX3 controls Wingless/Wnt secretion through regulating retromer-dependent recycling of Wntless', *Cell Res*, 21: 1677-90.

Zhang, X., L. Wang, B. Lak, J. Li, E. Jokitalo, and Y. Wang. 2018. 'GRASP55 Senses Glucose Deprivation through O-GlcNAcylation to Promote Autophagosome-Lysosome Fusion', *Dev Cell*, 45: 245-61.e6.

Zhang, Z., S. Nie, and L. Chen. 2018. 'Targeting prion-like protein spreading in neurodegenerative diseases', *Neural Regen Res*, 13: 1875-78.

Zhao, Y. G., Y. Chen, G. Miao, H. Zhao, W. Qu, D. Li, Z. Wang, N. Liu, L. Li, S. Chen, P. Liu, D. Feng, and H. Zhang. 2017. 'The ER-Localized Transmembrane Protein EPG-3/VMP1 Regulates SERCA Activity to Control ER-Isolation Membrane Contacts for Autophagosome Formation', *Mol Cell*, 67: 974-89.e6.

Zhao, Y. G., N. Liu, G. Miao, Y. Chen, H. Zhao, and H. Zhang. 2018. 'The ER Contact Proteins VAPA/B Interact with Multiple Autophagy Proteins to Modulate Autophagosome Biogenesis', *Curr Biol*, 28: 1234-45.e4.

Zhao, Y. G., and H. Zhang. 2018. 'Formation and maturation of autophagosomes in higher eukaryotes: a social network', *Curr Opin Cell Biol*, 53: 29-36.

Zhao, Y. G., and H. Zhang. 2019. 'Autophagosome maturation: An epic journey from the ER to lysosomes', *J Cell Biol*, 218: 757-70.

Zhao, Y., G. Perera, J. Takahashi-Fujigasaki, D. C. Mash, J. P. G. Vonsattel, A. Uchino, K. Hasegawa, R. Jeremy Nichols, J. L. Holton, S. Murayama, N. Dzamko, and G. M. Halliday. 2018. 'Reduced LRRK2 in association with retromer dysfunction in post-mortem brain tissue from LRRK2 mutation carriers', *Brain*, 141: 486-95.

Zheng, H., and E. H. Koo. 2011. 'Biology and pathophysiology of the amyloid precursor protein', *Mol Neurodegener*, 6: 27.

Zhou, L., W. Wang, C. Hoppel, J. Liu, and X. Zhu. 2017. 'Parkinson's disease-associated pathogenic VPS35 mutation causes complex I deficits', *Biochim Biophys Acta Mol Basis Dis*, 1863: 2791-95.

Zimprich, A., A. Benet-Pages, W. Struhal, E. Graf, S. H. Eck, M. N. Offman, D. Haubenberger, S. Spielberger, E. C. Schulte, P. Lichtner, S. C. Rossle, N. Klopp, E. Wolf, K. Seppi, W. Pirker, S. Presslauer, B. Mollenhauer, R. Katzenschlager, T. Foki, C. Hotzy, E. Reinthaler, A. Harutyunyan, R. Kralovics, A. Peters, F. Zimprich, T. Brucke, W. Poewe, E. Auff, C. Trenkwalder, B. Rost, G. Ransmayr, J. Winkelmann, T. Meitinger, and T. M. Strom. 2011. 'A mutation in VPS35, encoding a subunit of the retromer complex, causes late-onset Parkinson disease', *Am J Hum Genet*, 89: 168-75.

Zolov, S. N., D. Bridges, Y. Zhang, W. W. Lee, E. Riehle, R. Verma, G. M. Lenk, K. Converso-Baran, T. Weide, R. L. Albin, A. R. Saltiel, M. H. Meisler, M. W. Russell, and L. S.

Weisman. 2012. 'In vivo, Pikfyve generates PI(3,5)P2, which serves as both a signaling lipid and the major precursor for PI5P', *Proc Natl Acad Sci U S A*, 109: 17472-7.

Zoncu, R., R. M. Perera, D. M. Balkin, M. Pirruccello, D. Toomre, and P. De Camilli. 2009. 'A phosphoinositide switch controls the maturation and signaling properties of APPL endosomes', *Cell*, 136: 1110-21.

Zoncu, R., R. M. Perera, R. Sebastian, F. Nakatsu, H. Chen, T. Balla, G. Ayala, D. Toomre, and P. V. De Camilli. 2007. 'Loss of endocytic clathrin-coated pits upon acute depletion of phosphatidylinositol 4,5-bisphosphate', *Proc Natl Acad Sci U S A*, 104: 3793-8.

Zwiegers, P., G. Lee, and C. A. Shaw. 2014. 'Reduction in hSOD1 copy number significantly impacts ALS phenotype presentation in G37R (line 29) mice: implications for the assessment of putative therapeutic agents', *J Negat Results Biomed*, 13: 14.